Multiscale Mollifier Technique in Poroelasticity With an Introduction to Thermal Aspects

DISSERTATION
zur Erlangung des Grades eines Doktors
der Naturwissenschaften

vorgelegt von
Bianca Kretz, M. Sc.

eingereicht bei der Naturwissenschaftlich-Technischen Fakultät
der Universität Siegen
Siegen 2022

gedruckt auf Papier nach DIN ISO 9706

Betreuer und erster Gutachter
Prof. Dr. Volker Michel
Universität Siegen

Zweiter Gutachter
Prof. Dr. Willi Freeden
Technische Universität Kaiserlautern

Tag der mündlichen Prüfung
26. September 2022

Danksagung

Hiermit möchte ich mich bei allen bedanken, die mich während meiner Promotion untersützt haben.

Besonderer Dank gilt hierbei meinem Betreuer Prof. Dr. Volker Michel für seine Untersützung in den letzten 6 Jahren und seinen Einsatz, dass ich die Dissertation fertigstellen konnte. Seine Anregungen und wertvollen Kommentare in vielen interessanten Diskussionen haben mich hierbei immer ein Stück weiter zum Ziel geführt.

Prof. Dr. Willi Freeden danke ich für sein Interesse an meiner Arbeit und die Möglichkeit mit anderen Wissenschaftlern im Rahmen eines Forschungsprojektes zu diskutieren. Prof. Dr. Mathias Bauer danke ich für die Gelegenheit in diesem Projekt mitzuarbeiten. Des Weiteren gilt mein Dank Dr. Matthias Augustin und Dr. Christian Blick für ihre Unterstützung und die geduldige Beantwortung meiner vielen Rückfragen.

Ebenso möchte ich den aktuellen und auch ehemaligen Mitgliedern der Arbeitsgruppe Geomathematik für ihr Interesse an meiner Arbeit und die vielen Diskussionen danken. Insbesondere gebührt mein Dank Dr. Naomi Schneider für ihre Unterstützung und Denkanstöße während unserer gemeinsamen Zeit.

Desweiteren danke ich meiner Familie, meinem Freund und meinen engeren Freunden.

Ohne euch alle wäre diese Arbeit nicht möglich gewesen.

Der Universität Siegen bin ich für die finanzielle Unterstützung und die Möglichkeit den HORUS- und OMNI-Cluster zu nutzen dankbar.

Zusammenfassung

Die Poroelastizität zählt zu einer Disziplin in den Materialwissenschaften und beschreibt die Wechselwirkung zwischen einer Materialverschiebung und dem Porendruck. Daher ist dieser Zusammenhang überall dort interessant, wo ein poröses Medium und eine Flüssigkeit eine Rolle spielen und einen gegenseitigen Effekt aufeinander haben. Dies ist in vielen Anwendungen der Fall und wir konzentrieren uns auf die Geothermie. Das ist ein wichtiger Aspekt beim Reservoirmanagement, den man berücksichtigen sollte, denn der Austausch von Wasser in einem Reservoir mehrere Kilometer unterhalb der Erdoberfläche hat einen Einfluss auf das umgebende Gestein und umgekehrt.
Die zugrundeliegenden physikalischen Prozesse können mit Hilfe von partiellen Differentialgleichungen beschrieben werden, den sogenannten quasistatischen Gleichungen der Poroelastizität (QEP).
Unser Ziel ist eine Multiskalenzerlegung der Komponenten Verschiebung und Porendruck. Dies ermöglicht es uns, zugrundeliegende Strukturen in den verschiedenen Zerlegungsskalen zu sehen, die im Gesamtbild nicht gesehen werden können. Wir möchten Trennflächen herausarbeiten und aus den Daten mehr Details erhalten.
Zunächst beginnen wir im allgemeineren Kontext der Thermoporoelastizität, die die Poroelastizität mit thermischen Effekten verbindet. Nach der Herleitung der Fundamentallösungen reduzieren wir das Ganze zur Poroelastizität. Wir konstruieren physikalisch begründete Skalierungsfunktionen mit der Hilfe einer Mollifier-Regularisierung der entsprechenden Fundamentallösungen. Hierbei haben wir einen genaueren Blick darauf, dass die Skalierungsfunktionen die notwendigen theoretischen Eigenschaften einer approximativen Identität erfüllen. Des Weiteren zeigen wir numerische Experimente mit synthetischen Daten, die die Anwendbarkeit unserer konstruierten Funktionen unterstreichen.

Abstract

Poroelasticity is part of material research discipline and describes the interaction between solids deformation and the pore pressure. Therefore, this is anywhere interesting where a porous medium and a fluid come into play and have an effect on each other. This is the case in many applications and we want to focus on geothermics. It is important to consider this aspect in reservoir management since the replacement of the water in the reservoir some kilometers below the Earth's surface has an effect on the surrounding material and vice versa.
The underlying physical processes can be described by partial differential equations, called the quasistatic equations of poroelasticity (QEP).
Our aim is to do a multiscale decomposition of the components given by displacement and pore pressure. This enables us to see underlying structures in the different decomposition scales that cannot be seen in the whole data. We want to detect interfaces and extract more details of the data.
First, we start in a more general setting, that is thermoporoelasticity which relates poroelasticity to thermal effects. After the derivation of fundamental solutions, we reduce the setting to poroelasticity. We construct physically motivated scaling functions with the help of a mollifier regularization of the appropriate fundamental solutions. Here we have a closer look that the scaling functions fulfill the necessary theoretical requirements of an approximate identity. Further, we present numerical experiments with synthetic data, which show the applicability of our constructed functions.

Contents

List of Figures **ix**

List of Tables **xiii**

1. Introduction **1**
1.1. Poroelasticity in a geothermal background 1
1.2. Layout of the Work 4

I. Mathematical Basics 7

2. Preliminaries **9**
2.1. Notation 9
2.2. Special Functions and Function Spaces 11
2.3. Theoretical Aspects of Constrained Optimization Problems 16

3. Differential Equations **19**
3.1. Basics 19
3.2. Some Known Classic Differential Equations 21
3.3. Fundamental Solutions 21

4. Multiscale Approach **25**
4.1. Scaling Functions and Wavelets 25
4.2. Scale and Detail Spaces 28

5. Cubature on Lattice Points **29**
5.1. Lattices 29
5.2. Lattice Point Summation Formulas 33

II. Physical Background 37

6. Thermoporoelasticity **39**
6.1. Overview 39
6.2. Physical Background and Mathematical Derivation of the Equations 40
6.3. Fundamental Solutions 44
6.3.1. Biot Decomposition 45
6.3.2. Continuous Heat Source 46

6.3.3. Continuous Fluid Source 49
6.3.4. Continuous Fluid and Heat Dipole 50
6.3.5. Continuous Force 50

7. Non-dimensionalization and reduction to poroelasticity 57
7.1. Equations of Thermoporoelasticity in Dimensionless Form 57
7.2. Governing Equations in Poroelasticity 58
7.3. Fundamental Solutions in Poroelasticity 59

III. Multiscale Decorrelation for Poroelasticity 63

8. Regularized Fundamental Solutions 65
8.1. Laplace and Generalization 65
8.2. Mollification of the Fundamental Solution Tensor 69
8.2.1. p^{St} 71
8.2.2. $\boldsymbol{u}^{\mathrm{CN}}$ 75
8.2.3. p^{Si} 80
8.2.4. u^{Si} 84
8.2.5. Summary 92
8.3. Source Scaling Functions and Wavelets 93
8.4. Theoretical Aspects of the Decorrelation 105

9. Numerical Experiments 121
9.1. Cubature Formulas for Scaling Functions 121
9.2. Test Datasets 131
9.3. Pictures 132

IV. Summary 151

10. Conclusion and Outlook 153

Bibliography 157

List of Figures

5.1. Example of a lattice in $\mathbb{R}^2$ and its corresponding fundamental cell $\mathcal{F}_\Lambda$. 30

7.1. Connection between the QEP and other known differential equations. 59

8.1. The Laplace fundamental solution $G(\Delta; r)$ (dashed black) and its potential scaling function $G_\tau(\Delta; \|x\|)$ for $\tau = 1$ (red), $\tau = 0.5$ (blue) and $\tau = 0.25$ (green). 66
8.2. The source scaling function $\Phi_\tau(\|x\|)$ in the Laplace case for $\tau = 1$ (red), $\tau = 0.5$ (blue) and $\tau = 0.25$ (green). 67
8.3. Flowchart showing the process of obtaining the relevant scaling functions and wavelets in the case of poroelasticity. The left-hand side indicates the design of the scaling functions and the right-hand side the construction of the corresponding wavelets. 70
8.4. The first component of the fundamental solution p^{St} with its singularity in the zero point. 71
8.5. The first component of the regularized fundamental solution $p^{\mathrm{St}}_{\tau_j}$ for selected parameters j. 72
8.6. The wavelets for the first component of $p^{\mathrm{St}}_{\mathrm{Wav},\tau_j}$ for selected parameters j. 73
8.7. Two of the four components of the fundamental solution tensor $\boldsymbol{u}^{\mathrm{CN}}$ with its singularity in the zero point. 76
8.8. The regularized fundamental solution $u^{\mathrm{CN}}_{11,\tau_j}$ forseveral parameters j. 76
8.9. The regularized fundamental solution $u^{\mathrm{CN}}_{12,\tau_j}$ for selected parameters j. 77
8.10. The wavelet for $u^{\mathrm{CN}}_{11,\mathrm{Wav},\tau_j}$ for selected parameters j. 77
8.11. The wavelet for $u^{\mathrm{CN}}_{12,\mathrm{Wav},\tau_j}$ for several parameters j. 78
8.12. The fundamental solution p^{Si} in space for two fixed times. 80
8.13. The fundamental solution p^{Si} for two different fixed points over time. 81
8.14. The regularized fundamental solution $p^{\mathrm{Si}}_{\tau_j}$ for a fixed time in space respectively for two different fixed spatial points over the time and selected parameters j. 82
8.15. The wavelet function $p^{\mathrm{Si}}_{\mathrm{Wav},\tau_j}$ for a fixed time in space respectively for two fixed spatial points over time for $j = 1$. 83
8.16. The first component of the fundamental solution u^{Si} for the time point $t = 0.05$. 85

8.17. The first component of the regularized fundamental solution $u_{\tau_j}^{\mathrm{Si}}$ for a fixed time in space respectively for two fixed spatial points over the time for $j = 1$. 86
8.18. The wavelet function for u_1^{Si} for two fixed times over the space respectively for one fixed point over the time for $j = 1$. 87
8.19. The source scaling function $\Phi_{11,\tau}$ for several parameters j. 101
8.20. The source scaling functions $\Phi_{12,\tau}$, $\Phi_{13,\tau}^{(1)}$ and $\Phi_{13,\tau}^{(2)}$ for $j = 1$. 101
8.21. The source scaling function $\Phi_{31,\tau}$ for a fixed time over the space respectively for a fixed point over time for selected parameters j. . 101
8.22. The source scaling function $\Phi_{33,\tau}$ for two fixed times in space respectively for a fixed point in space over the time for selected parameters j. 102
8.23. The source wavelet function $\Psi_{11,\tau}$ for selected parameters j. 102
8.24. The source wavelet functions $\Psi_{12,\tau}$, $\Psi_{13,\tau}^{(1)}$ and $\Psi_{13,\tau}^{(2)}$ for $j = 1$. 103
8.25. The source wavelet function $\Psi_{31,\tau}$ for two fixed times over space respectively for a fixed point in space over the time for selected parameters j. 103
8.26. The source wavelet function $\Psi_{33,\tau}$ for two fixed times over space respectively for a fixed point in space over the time for selected parameters j. 104

9.1. Data sets for the displacement component and the pore pressure given for the multiscale modeling for the fixed time $t = 1$. 132
9.2. Multiscale approximation of the data u_1 by convolution of the source scaling function (tensor) $\left\{\Phi_{\tau_j}\right\}_{j\in\mathbb{N}}$ (scale-space) and the source wavelet (tensor) $\left\{\Psi_{\tau_j}\right\}_{j\in\mathbb{N}}$ (detail-space) with the data f. 138
9.3. Multiscale approximation of the data u_1 by convolution of the source scaling function (tensor) $\left\{\Phi_{\tau_j}\right\}_{j\in\mathbb{N}}$ (scale-space) and the source wavelet (tensor) $\left\{\Psi_{\tau_j}\right\}_{j\in\mathbb{N}}$ (detail-space) with the data f. 139
9.4. Multiscale approximation of the data u_1 by convolution of the source scaling function (tensor) $\left\{\Phi_{\tau_j}\right\}_{j\in\mathbb{N}}$ (scale-space) and the source wavelet (tensor) $\left\{\Psi_{\tau_j}\right\}_{j\in\mathbb{N}}$ (detail-space) with the data f. 140
9.5. Multiscale approximation of the data u_2 by convolution of the source scaling function (tensor) $\left\{\Phi_{\tau_j}\right\}_{j\in\mathbb{N}}$ (scale-space) and the source wavelet (tensor) $\left\{\Psi_{\tau_j}\right\}_{j\in\mathbb{N}}$ (detail-space) with the data f. 141
9.6. Multiscale approximation of the data u_2 by convolution of the source scaling function (tensor) $\left\{\Phi_{\tau_j}\right\}_{j\in\mathbb{N}}$ (scale-space) and the source wavelet (tensor) $\left\{\Psi_{\tau_j}\right\}_{j\in\mathbb{N}}$ (detail-space) with the data f. 142
9.7. Multiscale approximation of the data u_2 by convolution of the source scaling function (tensor) $\left\{\Phi_{\tau_j}\right\}_{j\in\mathbb{N}}$ (scale-space) and the source wavelet (tensor) $\left\{\Psi_{\tau_j}\right\}_{j\in\mathbb{N}}$ (detail-space) with the data f. 143

9.8. Single parts of the application of the low-pass filter $\left(\mathcal{P}_{\Phi_{\tau_j}}[f]\right)_1$ at scale $j = 1$. 144
9.9. Single parts of the application of the low-pass filter $\left(\mathcal{P}_{\Phi_{\tau_j}}[f]\right)_1$ at scale $j = 3$. 145
9.10. Multiscale approximation of the data p by convolution of the source scaling function (tensor) $\left\{\Phi_{\tau_j}\right\}_{j\in\mathbb{N}}$ (scale-space) and the source wavelet (tensor) $\left\{\Psi_{\tau_j}\right\}_{j\in\mathbb{N}}$ (detail-space) with the data f. 146
9.11. Multiscale approximation of the data p by convolution of the source scaling function (tensor) $\left\{\Phi_{\tau_j}\right\}_{j\in\mathbb{N}}$ (scale-space) and the source wavelet (tensor) $\left\{\Psi_{\tau_j}\right\}_{j\in\mathbb{N}}$ (detail-space) with the data f. 147
9.12. Single parts of the application of the low-pass filter $\left(\mathcal{P}_{\Phi_{\tau_j}}[f]\right)_1$ at scale $j = 1$ without cutting off the boundary. 148
9.13. Single parts of the application of the low-pass filter $\left(\mathcal{P}_{\Phi_{\tau_j}}[f]\right)_1$ at scale $j = 3$ without cutting off the boundary. 149
9.14. Multiscale approximation of the data p by convolution of the source scaling function (tensor) $\left\{\Phi_{\tau_j}\right\}_{j\in\mathbb{N}}$ (scale-space) and the source wavelet (tensor) $\left\{\Psi_{\tau_j}\right\}_{j\in\mathbb{N}}$ (detail-space) with the data f. 150

List of Tables

6.1. Table with the main material constants for thermoporoelasticity. . . 40

9.1. RMSE for the plot area. 136
9.2. RMSE for the whole area without the boundary. 137

1. Introduction

1.1. Poroelasticity in a geothermal background

To understand why poroelasticity is important in geothermal research, we have to explain what is meant by poroelasticity. Briefly speaking, it is part of the material research discipline and describes the interaction between the solids deformation and the pore pressure of a fluid. This theory is an extension of the classical elasticity theory and goes back to Biot in the 1930s. These processes play an important role in geothermics, since aquifers can essentially be described as poroelastic (see for example [83, 147] for considerations of poroelasticity in reservoirs). Additionally, the consideration of thermal effects can be taken into account which is then called thermoporoelasticity. We can think of several influences of the components solids deformation, pore pressure and temperature: Changes in the pore pressure or extraction of fluid can cause a deformation of the solid right up to formation of fissures (which can cause land subsidence and seismic events) and temperature increase or decrease. Solid deformation influences the pore pressure and surely the temperature since compressing a material increases the temperature. Temperature variation can cause solid deformation and have effects on the pore pressure, for example by increasing the temperature, the fluid expands. One more aspect to mention is the influence of the reinjected fluid which is colder than the extracted fluid. It is important to consider these things when talking about reservoir management which can be in the drilling and in the exploitation phase. Up to now the reservoir management has a subordinate role in Germany in the operational phase but can be more and more important with essentially longer operational phases (see [30]).
Still, there are many more aspects and physical processes to consider in a geothermal project. The Geomathematics Group at the University of Kaiserslautern suggested a model (graphic illustration given in [10]) to show the different tasks in the field of geothermal energy, which bases on the four mainstays potential methods, seismic exploration, transport processes and stress field. Since there is many literature given to these four aspects, we want to give a few examples to show how many various scientists from different disciplines are concerned with these topics (in particular geothermics).
For potential methods (where the focus is here broader) we refer for example to the literature given by [57, 63, 65, 69, 76, 92, 114, 117–119, 121, 131, 138, 141] and in the case of seismics to [36, 53, 55, 95, 100, 122].

Under the aspect of transport processes (see for example [38]), the topics fluid flow [7, 14, 125, 132], heat flow [29, 109, 126, 129, 143], transport of chemical material [12, 56, 145] and transport of tracers [84, 130, 153] are summarized.
The topic of stress field contains poroelasticity [9, 28, 32, 33, 80, 99, 148], thermoelasticity [3, 8, 13, 42, 96, 102, 124, 139, 155], fracture mechanics [4, 87, 127, 133, 157], seismic waves [2, 31, 51, 146, 154] and microseismicity [47, 54, 113, 134].
We focus on the topic poroelasticity where our aim is to construct physically relevant wavelets by applying a mollifier technique. In general, mollifiers are auxiliary functions that are smooth. The convolution of a non-smooth function with mollifiers generates a sequence of smooth functions which act as approximations of the non-smooth function. The beginnings of mollifiers can be dated back to Friedrichs in 1944 (see [79]). In the general theory of inverse problems, mollifiers can be found in [48, 49, 106, 107] in connection with operator solutions. In this case the problem is assumed to be too ill-posed to be solved with known regularization methods. More applications of mollifiers are given by [52] for the construction of mollified finite element approximants, [91] for spherical deconvolutions, [98] for optimization problems, [137] for the Laplace transform, [136] for vector tomography, [149] for the solution of nonlinear systems of differential equations and [144] for the recovery of piecewise analytic functions. These papers depict some of the topics where mollifiers occur and do not raise a claim to be complete.
The theory of wavelets begins, to be precise, with the work of Haar (see [89]) and the Haar wavelets can be seen as the most simple wavelets. In general, there are many approaches to construct wavelets which we want to recover here in short. The similarity between all approaches is the construction of wavelets as basis functions for multiscale analysis. The main topics of wavelets are for example covered by [35, 43, 108, 110]. Besides the Haar wavelet as a wavelet on the real line, we can mention for example the Daubechies wavelet (see [43]) and the Meyer wavelet (see [115]). For wavelets on the sphere, there exist several possibilities for the construction. One ansatz to mention here is the tensor product ansatz [40] and another one as a more abstract ansatz with a group-theoretic approach is given in [5, 6]. Moreover, [93, 104, 123, 128, 142, 151] consider certain kernel wavelets. Another approach are the frequency reflected wavelets, for example given in [64, 74, 78, 152]. The constructions based on potential theoretic concepts, for example layer potentials, are presented in [62, 67, 82]. Some wavelet methods come from boundary integral equations [68, 90, 101]. In [105, 116] the construction under the aspect of localization has been done.
A survey on several multiresolution analyses can be found in [37].
More concepts about wavelets are considered in [39, 41, 45, 46, 70, 85, 88, 150].
For a more detailed literary overview about wavelets, we refer for example to [73] or [117]. The former contains also a classification regarding the geomathematical applications.
The key idea of the new approach (see for example [61] whose idea goes to back to [75]) is the construction of mollifier wavelets which have geophysical relevance

due to the connection to the differential equation and their fundamental solution. They should generate the decomposition of geophysical quantities. In the case of the gravitational potential, the potential wavelets use the density as input data to reconstruct the gravitational potential as the target data. Other wavelets (called source wavelets) for the decomposition of the gravitational potential or the density can be obtained by application of the associated operator on the potential wavelets. Outgoing from the usage in geothermal energy, the benefits of a wavelet approximation should be checked for signals with a relevance for the geothermal exploration.
Since this new approach of a multiscale mollifier technique was discussed for many other physical issues, we want to give an overview about the existing literature which concentrates on the multiscale mollifier technique, which we want to apply to poroelasticity. We group the existing literature by its application, that means gravimetry, magnetometry and seismics. We start with the case of gravimetry: In [59, 60, 119] (see also the references therein) the mollifier method has been elaborated and realized. For a similar technique in the case of migration results via the Helmholtz equation, we refer to [11, 27]. More discussions about the new approach are given in [21] for the acoustic wave equation, in [22] for the static Cauchy-Navier equation and [23] for the elasto-oscillatory Cauchy-Navier equation. For the application in magnetometry, the reader is referred to the most recent publications [24, 59].
In this thesis, we introduce the aspect of decorrelation in poroelasticity by applying a multiscale mollifier technique that means we transfer this method to the aspect of the stress field in geothermal reservoirs. Our starting points are the quasi-static equations of poroelasticity (QEP) (here in homogeneous form) given by

$$-\frac{\lambda+\mu}{\mu}\nabla_x(\nabla_x\cdot u)-\nabla_x^2 u+\alpha\nabla_x p=0, \tag{1.1}$$

$$\partial_t(c_0\mu p+\alpha(\nabla_x\cdot u))-\nabla_x^2 p=0. \tag{1.2}$$

They interrelate the dependencies between the main components displacement u and pore pressure p in a chosen porous medium defined by the material constants $\lambda, \mu, \alpha, c_0$. We construct in a first step scaling functions by mollifying the fundamental solution tensor belonging to the QEP with a scaling parameter. Secondly, we generate the corresponding wavelets by subtracting two consecutive scaling functions. After the application of the poroelastic differential operator on them, we get our desired scaling functions and wavelets that are necessary for the decorrelation of our data.

These scaling functions are given in the tensor $\mathbf{\Phi}_{\tau_j}$ and fulfill the property of an approximate identity which is a convolution with the given vector-valued data f

$$\lim_{j\to\infty} \int_{\mathcal{B}} \mathbf{\Phi}_{\tau_j}(x-y)\, f(y)\, \mathrm{d}y = f(x). \tag{1.3}$$

This is the main theoretical result in our thesis and the foundation for the convolution with the data. The scaling functions can be understood as the low-pass filters and their localization can be controlled with the scale parameter. This leads us to an approximation of the data at that given point. The wavelets are the band-pass filters and provide us with the necessary detail information. With the help of this outcome, we can show the decomposition ability of our functions with some synthetic test data.

1.2. Layout of the Work

The main goal of this thesis is to construct physically motivated source scaling functions and wavelets to do a decorrelation of poroelastic data. This work consists of three parts which discuss the mathematical basics, the physical background and the multiscale decorrelation in poroelasticity. In Part I, we introduce the general background and concepts which form the basis of this thesis. We start with the introduction of the necessary notation and special functions and function spaces we need, here especially the exponential integral, the Gauss error function and integrals, where the exponential function is linked with polynomials, are very important for us. Afterwards, we have a short overview on constrained optimization problems. We continue with classical partial differential equations and take a closer look at the Dirac distribution. The general concept of scaling functions and wavelets will be presented before we go over to the basic theory of lattices and lattice point summation formulas.
Part II deals with the physical background and the derivation of the partial differential equations and their fundamental solutions. The main physical laws are presented to gain the partial differential equations in thermoporoelasticity. With the help of a decomposition scheme, the fundamental solutions are derived very shortly. To come back to an easier setting, we want to neglect the thermal effects and reduce the equations to the quasistatic equations of poroelasticity (QEP). With the appropriate fundamental solutions, we conclude this part.
Based on the fundamental solutions in poroelasticity from the previous part, we construct in Part III mollifier regularizations for them, because they have singularities. This is done with the help of a Taylor expansion up to order 1. Applying the poroelastic differential operator on the modified fundamental solutions, we get our desired source scaling functions and wavelets. To fulfill the theoretical properties of an approximate identity, we have to do little modifications on some of the functions. This part completes with the numerical experiments. Therefore, we have to think about suitable cubature formulas with the help of the lattice

point summation formulas. Then we present the convolution pictures and additionally a relative root mean square error to show the ability of the constructed source scaling functions and wavelets.

Part I.

Mathematical Basics

2. Preliminaries

In the following, we introduce the required basic notations, which we use throughout this thesis.

2.1. Notation

We denote the non-negative integers by $\mathbb{N}$, the integers by $\mathbb{Z}$, the real numbers by $\mathbb{R}$ and the complex numbers by $\mathbb{C}$. Please note that $\mathbb{N}$, in our case, includes the zero. For every real number x, the floor function $\lfloor \cdot \rfloor$ is the largest integer n with $n \leq x$. The n-dimensional real vector space is defined as

$$\underbrace{\mathbb{R} \times \cdots \times \mathbb{R}}_{n\text{-times}} = \mathbb{R}^n, \quad n \in \mathbb{N} \setminus \{0\}. \tag{2.1}$$

We define the inner product $x \cdot y$ of two elements $x = (x_1, x_2, \ldots, x_n)^{\mathrm{T}} \in \mathbb{R}^n$, $y = (y_1, y_2, \ldots, y_n)^{\mathrm{T}} \in \mathbb{R}^n$ as

$$x \cdot y \coloneqq \sum_{i=1}^{n} x_i y_i \tag{2.2}$$

and the induced norm $\|x\|$ is

$$\|x\| \coloneqq \sqrt{x \cdot x} = \sqrt{\sum_{i=1}^{n} x_i^2}. \tag{2.3}$$

The closed ball $\mathbb{B}_r^n(x)$ with center $x \in \mathbb{R}^n$ and radius $r > 0$ is the following set

$$\mathbb{B}_r^n(x) \coloneqq \{y \in \mathbb{R}^n \big| \|x - y\| \leq r\}. \tag{2.4}$$

Furthermore, the sphere $\mathbb{S}_r^{n-1}(x)$ in $\mathbb{R}^n$ with radius r and center $x \in \mathbb{R}^n$ is defined by

$$\mathbb{S}_r^{n-1}(x) \coloneqq \{y \in \mathbb{R}^n \big| \|x - y\| = r\}. \tag{2.5}$$

For brevity, we write $\mathbb{B}_r(x)$ instead of $\mathbb{B}_r^2(x)$ and $\mathbb{S}^{n-1}(x)$ instead of $\mathbb{S}_1^{n-1}(x)$ throughout this thesis. Every point $x \neq 0 \in \mathbb{R}^n$ has a representation in polar coordinates with a uniquely determined ξ, that means

$$x = r\xi, \quad r = \|x\| = \sqrt{x_1^2 + \cdots + x_n^2}, \quad \xi \in \mathbb{S}^{n-1}, \quad r > 0. \tag{2.6}$$

In the following, we want to define the gradient, the divergence and the Laplace operator of a function. Therefore, we need an open subset of $\mathbb{R}^n$ called $\mathcal{B}$, whose boundary is denoted by $\partial\mathcal{B}$ and $\overline{\mathcal{B}} = \partial\mathcal{B} \cup \mathcal{B}$ is the closure. If $\mathcal{B}$ is open and connected, it is called a region. We call a bounded region regular, if $\partial\mathcal{B}$ is an orientable piecewise smooth Lipschitzian manifold of dimension $n-1$ (see [58]). For a regular region $\mathcal{B}$ the volume of $\mathcal{B}$ is given by

$$\mathrm{vol}(\mathcal{B}) \coloneqq \|\mathcal{B}\| \coloneqq \int_{\mathcal{B}} \mathrm{d}x. \tag{2.7}$$

Especially in the case of a ball $\mathbb{B}_r^n(x)$ and a sphere $\mathbb{S}_1^{n-1}(x)$, we have for the volume of the ball and the area of the sphere the following (see for example [120])

$$\|\mathbb{B}_r^n(x)\| = \frac{\pi^{\frac{n}{2}}}{\Gamma\left(\frac{n}{2}+1\right)} r^n, \tag{2.8}$$

$$\|\mathbb{S}_r^{n-1}(x)\| = 2\frac{\pi^{\frac{n}{2}}}{\Gamma\left(\frac{n}{2}\right)} r^{n-1}, \tag{2.9}$$

where Γ represents the Gamma function given by the following definition (see for example [65]).

Definition 2.1.1. *The function $x \mapsto \Gamma(x)$, $x > 0$ defined by*

$$\Gamma(x) = \int_0^\infty e^{-t} t^{x-1} \,\mathrm{d}t \tag{2.10}$$

is called the Gamma function.

For the following definitions, we assume that we have a region $\mathcal{B}$ in $\mathbb{R}^n$. The gradient of a differentiable scalar function $F : \mathcal{B} \to \mathbb{R}$ at $x \in \mathcal{B}$ (notation: $\nabla_x F(x)$) is given by

$$\nabla_x F(x) \coloneqq \left(\frac{\partial F}{\partial x_1}(x), \ldots, \frac{\partial F}{\partial x_n}(x)\right)^{\mathrm{T}}. \tag{2.11}$$

Let $f = (f_1, \ldots, f_n)^{\mathrm{T}}$ be a vectorial function, which is differentiable in $x \in \mathcal{B}$. We define the divergence $\mathrm{div}_x(f)$ by

$$\mathrm{div}_x(f)(x) \coloneqq \nabla_x \cdot f(x) = \sum_{i=1}^n \frac{\partial}{\partial x_i} f_i(x). \tag{2.12}$$

Please note that for a tensor-valued function $\boldsymbol{f}$, the divergence is defined row-wise, that means

$$(\nabla_x \cdot \boldsymbol{f})_i = \left(\sum_{j=1}^n \frac{\partial}{\partial x_j} f_j\right)_i, \tag{2.13}$$

where f_j is the j-th row of $\boldsymbol{f}$. If we now assume that F is twice differentiable in $x \in \mathcal{B}$, we can define the Laplace operator Δ of F in $\mathbb{R}^n$ at $x \in \mathcal{B}$ by

$$\Delta_x F(x) \coloneqq \nabla_x^2 F(x) \coloneqq \nabla_x \cdot \nabla_x F(x) = \sum_{i=1}^{n} \frac{\partial^2}{\partial x_i^2} F(x). \tag{2.14}$$

In the case of vectorial and tensorial functions, we apply the Laplace operator componentwise. Furthermore, we have to define the Kronecker Delta by

$$\delta_{nm} \coloneqq \begin{cases} 1, & n = m, \\ 0, & n \neq m, \end{cases} \tag{2.15}$$

for $n, m \in \mathbb{N}$. Please note that we use boldfaced letters for tensors of order 2 and higher.

2.2. Special Functions and Function Spaces

In this section, we want to introduce the function spaces (see for example [64, 117]) we need throughout this thesis and the well-known exponential integral (see also [1, 86, 94]). The exponential integral is necessary on the one hand for the fundamental solutions for thermoporoelasticity and on the other hand for our theory of decorrelation. We start with the exponential integral and go over to some more special functions and specific integrals that we need.

Definition 2.2.1. *The exponential integral is defined as the following integral*

$$\mathrm{Ei}(x) \coloneqq -\int_{-x}^{\infty} \frac{e^{-t}}{t}\,\mathrm{d}t = \int_{-\infty}^{x} \frac{e^{t}}{t}\,\mathrm{d}t, \quad x > 0 \tag{2.16}$$

and has to be understood in the sense of the Cauchy principal value. Furthermore, we have the following characterization as an alternative

$$\mathrm{Ei}(x) = C + \ln|x| + \sum_{k=1}^{\infty} \frac{x^k}{k \cdot k!}, \quad \forall x \in \mathbb{R} \setminus \{0\} \tag{2.17}$$

with C as the Euler constant. Hence we have

$$\mathrm{Ei}(-t) \cdot t^k \to 0 \text{ for } t \to 0 \text{ for } k \geq 1, \tag{2.18}$$

since $x \cdot \ln|x| \to 0$ $(x \to 0)$, which we need later for some limit considerations. Closely related is the following function

$$\mathrm{E}_1(x) \coloneqq \int_{x}^{\infty} \frac{e^{-t}}{t}\,\mathrm{d}t = \int_{1}^{\infty} \frac{e^{-xt}}{t}\,\mathrm{d}t, \quad x > 0. \tag{2.19}$$

Please note that for positive values of x, we may extend (2.19) in the sense that $-\mathrm{E}_1(x) = \mathrm{Ei}(-x)$. We also define

$$\mathrm{E}_0(x) = \int_1^\infty e^{-tx}\,\mathrm{d}t = \frac{e^{-x}}{x}, \quad x > 0. \tag{2.20}$$

The following relation between $E_1(x)$ and $E_0(x)$ holds true (see [86])

$$E_1'(x) = -E_0(x). \tag{2.21}$$

Furthermore, we need the error function (also called Gauss error function).

Definition 2.2.2. *The error function is defined by*

$$\mathrm{erf}(x) \coloneqq \frac{2}{\sqrt{\pi}} \int_0^x e^{-\tau^2}\,\mathrm{d}\tau. \tag{2.22}$$

Please note that we use the error function for real arguments.

For the proof of the theory of the decorrelation, there are some integrals related to the exponential function, that we use several times.

Lemma 2.2.3. *The following integrals are helpful for us (see [86]):*

$$\int \exp\left(-\frac{\tau^2}{4C_2t}\right)\,\mathrm{d}t = \frac{\tau^2 \mathrm{Ei}\left(-\frac{\tau^2}{4C_2t}\right)}{4C_2} + t \cdot \exp\left(-\frac{\tau^2}{4C_2t}\right) \tag{2.23}$$

$$\int \exp\left(-\frac{\tau^2}{4C_2t}\right) \cdot \frac{1}{t}\,\mathrm{d}t = -\mathrm{Ei}\left(-\frac{\tau^2}{4C_2t}\right) \tag{2.24}$$

$$\int \exp\left(-\frac{\tau^2}{4C_2t}\right) \cdot \frac{1}{t^2}\,\mathrm{d}t = \frac{4C_2 \exp\left(-\frac{\tau^2}{4C_2t}\right)}{\tau^2} \tag{2.25}$$

$$\int \exp\left(-\frac{\tau^2}{4C_2t}\right) \cdot \frac{1}{t^3}\,\mathrm{d}t = \frac{4C_2 \exp\left(-\frac{\tau^2}{4C_2t}\right)(4C_2t + \tau^2)}{t\tau^4} \tag{2.26}$$

$$\int \exp\left(-\frac{\tau^2}{4C_2t}\right) \cdot \frac{1}{t^4}\,\mathrm{d}t = \frac{4C_2 \exp\left(-\frac{\tau^2}{4C_2t}\right)(32C_2^2t^2 + 8C_2t\tau^2 + \tau^4)}{t^2\tau^6}. \tag{2.27}$$

Proof. We can easily verify these integrals by differentiation (see also Definition 2.2.1), that means

$$\begin{aligned}
&\frac{\partial}{\partial t}\left(\frac{\tau^2 \mathrm{Ei}\left(-\frac{\tau^2}{4C_2 t}\right)}{4C_2} + t\cdot\exp\left(-\frac{\tau^2}{4C_2 t}\right)\right)\\
&\quad= \frac{\tau^2}{4C_2}\cdot\frac{\exp\left(-\frac{\tau^2}{4C_2 t}\right)}{-\frac{\tau^2}{4C_2 t}}\cdot\frac{\tau^2}{4C_2 t^2} + \exp\left(-\frac{\tau^2}{4C_2 t}\right) + t\cdot\exp\left(-\frac{\tau^2}{4C_2 t}\right)\cdot\frac{\tau^2}{4C_2 t^2}\\
&\quad= \exp\left(-\frac{\tau^2}{4C_2 t}\right)\left(-\frac{\tau^2}{4C_2 t} + 1 + \frac{\tau^2}{4C_2 t}\right)\\
&\quad= \exp\left(-\frac{\tau^2}{4C_2 t}\right), \qquad (2.28)
\end{aligned}$$

$$\frac{\partial}{\partial t}\left(-\mathrm{Ei}\left(-\frac{\tau^2}{4C_2 t}\right)\right) = \frac{-\exp\left(-\frac{\tau^2}{4C_2 t}\right)}{-\frac{\tau^2}{4C_2 t}}\cdot\frac{\tau^2}{4C_2 t^2} = \exp\left(-\frac{\tau^2}{4C_2 t}\right)\cdot\frac{1}{t}, \qquad (2.29)$$

$$\frac{\partial}{\partial t}\left(\frac{4C_2}{\tau^2}\exp\left(-\frac{\tau^2}{4C_2 t}\right)\right) = \frac{4C_2}{\tau^2}\exp\left(-\frac{\tau^2}{4C_2 t}\right)\cdot\frac{\tau^2}{4C_2 t^2} = \exp\left(-\frac{\tau^2}{4C_2 t}\right)\cdot\frac{1}{t^2}, \qquad (2.30)$$

$$\begin{aligned}
&\frac{\partial}{\partial t}\left(4C_2\exp\left(-\frac{\tau^2}{4C_2 t}\right)\left(\frac{4C_2}{\tau^4} + \frac{1}{t\tau^2}\right)\right)\\
&\quad= 4C_2\exp\left(-\frac{\tau^2}{4C_2 t}\right)\cdot\frac{\tau^2}{4C_2 t^2}\left(\frac{4C_2}{\tau^4} + \frac{1}{t\tau^2}\right) + 4C_2\exp\left(-\frac{\tau^2}{4C_2 t}\right)\cdot\left(-\frac{1}{\tau^2 t^2}\right)\\
&\quad= \exp\left(-\frac{\tau^2}{4C_2 t}\right)\cdot\frac{1}{t^3}, \qquad (2.31)
\end{aligned}$$

$$\begin{aligned}
&\frac{\partial}{\partial t}\left(\frac{4C_2}{\tau^6}\exp\left(-\frac{\tau^2}{4C_2 t}\right)\left(32C_2^2 + \frac{8C_2\tau^2}{t} + \frac{\tau^4}{t^2}\right)\right)\\
&\quad= \frac{4C_2}{\tau^6}\exp\left(-\frac{\tau^2}{4C_2 t}\right)\cdot\frac{\tau^2}{4C_2 t^2}\left(32C_2^2 + \frac{8C_2\tau^2}{t} + \frac{\tau^4}{t^2}\right)\\
&\qquad+ \frac{4C_2}{\tau^6}\exp\left(-\frac{\tau^2}{4C_2 t}\right)\left(-\frac{8C_2\tau^2}{t^2} - \frac{2\tau^4}{t^3}\right)\\
&\quad= \frac{4C_2}{\tau^6}\exp\left(-\frac{\tau^2}{4C_2 t}\right)\left(\frac{8C_2\tau^2}{t^2} + \frac{2\tau^4}{t^3} + \frac{\tau^6}{4C_2 t^4} - \frac{8C_2\tau^2}{t^2} - \frac{2\tau^4}{t^3}\right)\\
&\quad= \exp\left(-\frac{\tau^2}{4C_2 t}\right)\cdot\frac{1}{t^4}. \qquad (2.32)
\end{aligned}$$

□

We use these integrals mostly in combination with the particular interval $[0, T]$. Therefore, we have a look at the integrals again with these interval boundaries. Please note that in our case the constant C_2 is a combination of positive material parameters and always > 0.

Remark 2.2.4. *For the case of an integral $\int_0^T$ we obtain for the previous integrals with $C_2 > 0$*

$$\begin{aligned}\int_0^T \exp\left(-\frac{\tau^2}{4C_2 t}\right)\,\mathrm{d}t &= \frac{\tau^2}{4C_2}\mathrm{Ei}\left(-\frac{\tau^2}{4C_2 T}\right) + T\exp\left(-\frac{\tau^2}{4C_2 T}\right)\\ &\quad - \lim_{b\to 0^+}\left[\frac{\tau^2}{4C_2}\mathrm{Ei}\left(-\frac{\tau^2}{4C_2 b}\right) + b\exp\left(-\frac{\tau^2}{4C_2 b}\right)\right]\\ &= \frac{\tau^2}{4C_2}\mathrm{Ei}\left(-\frac{\tau^2}{4C_2 T}\right) + T\exp\left(-\frac{\tau^2}{4C_2 T}\right), \end{aligned} \tag{2.33}$$

$$\int_0^T \exp\left(-\frac{\tau^2}{4C_2 t}\right)\cdot\frac{1}{t}\,\mathrm{d}t = -\mathrm{Ei}\left(-\frac{\tau^2}{4C_2 T}\right) + \lim_{b\to 0^+}\mathrm{Ei}\left(-\frac{\tau^2}{4C_2 b}\right) = -\mathrm{Ei}\left(-\frac{\tau^2}{4C_2 T}\right), \tag{2.34}$$

$$\int_0^T \exp\left(-\frac{\tau^2}{4C_2 t}\right)\cdot\frac{1}{t^2}\,\mathrm{d}t = \frac{4C_2\exp\left(-\frac{\tau^2}{4C_2 T}\right)}{\tau^2}, \tag{2.35}$$

$$\int_0^T \exp\left(-\frac{\tau^2}{4C_2 t}\right)\cdot\frac{1}{t^3}\,\mathrm{d}t = \frac{4C_2\exp\left(-\frac{\tau^2}{4C_2 T}\right)(\tau^2 + 4C_2 T)}{T\tau^4}, \tag{2.36}$$

$$\int_0^T \exp\left(-\frac{\tau^2}{4C_2 t}\right)\cdot\frac{1}{t^4}\,\mathrm{d}t = \frac{4C_2\exp\left(-\frac{\tau^2}{4C_2 T}\right)(32C_2^2T^2 + 8C_2T\tau^2 + \tau^4)}{T^2\tau^6}. \tag{2.37}$$

Now we go over to the function spaces and start with the definition of a compact support.

Definition 2.2.5. *We assume that we have an open set $\mathcal{B} \subset \mathbb{R}^n$ and a given function $F : \mathcal{B} \to \mathbb{R}$. We say the function F has compact support if there is a compact set $\mathcal{G} \subset \mathcal{B}$ such that*

$$\mathrm{supp}(F) = \overline{\{x \in \mathcal{B} \big| F(x) \neq 0\}} \subset \mathcal{G}. \tag{2.38}$$

Assume that we have an open subset $X \subset \mathbb{R}^n$. The class $\mathrm{C}^{(k)}(X)$ denotes the set of all functions, which are k-times continuously differentiable for $k \geq 0$. The case $k = -1$ denotes the piecewise continuous functions. For $k = 0$ we simply write $\mathrm{C}(X)$ instead of $\mathrm{C}^{(0)}(X)$. Furthermore, we set

$$\mathrm{C}^{(\infty)}(X) = \bigcap \mathrm{C}^{(k)}(X), \tag{2.39}$$

where the intersection is taken for all finite k. Especially $\mathrm{C}_0^{(k)}(X)$ denotes the space of all $u \in \mathrm{C}^k(k)(X)$ with compact support. Furthermore, assume that we have a region $\mathcal{B}$ in $\mathbb{R}^n$. Then we define the space $\mathcal{L}^p(\mathcal{B})$ by all measurable functions $F : \mathcal{B} \to \mathbb{R}$, that satisfy

$$\int_{\mathcal{B}} \|F(x)\|^p\,\mathrm{d}x < +\infty, \quad 1 \leq p < +\infty. \tag{2.40}$$

In analogy the space $\mathcal{N}^p(\mathcal{B})$ is

$$\mathcal{N}^p(\mathcal{B}) \coloneqq \left\{ F : \mathcal{B} \to \mathbb{R} \text{ measurable} \;\middle|\; \int_{\mathcal{B}} \|F(x)\|^p \,\mathrm{d}x = 0 \right\},\ 1 \leq p < +\infty. \tag{2.41}$$

With these definitions and the concept of equivalence classes, we can define

$$\mathrm{L}^p(\mathcal{B}) \coloneqq \mathcal{L}^p(\mathcal{B})/_{\mathcal{N}^p(\mathcal{B})}, \tag{2.42}$$

which is together with the norm

$$\|F\|_{\mathrm{L}^p(\mathcal{B})} \coloneqq \left(\int_{\mathcal{B}} \|F(x)\|^p \,\mathrm{d}x \right)^{1/p}, \quad 1 \leq p \leq \infty, \tag{2.43}$$

a normed space. Note that for $1 \leq q \leq p < +\infty$ it holds true that $\mathrm{L}^p(\mathcal{B}) \subset \mathrm{L}^q(\mathcal{B})$, if $\mathcal{B}$ is bounded. For the case $p = 2$, we have the function space $\mathrm{L}^2(\mathcal{B})$ with the inner product $\langle \cdot, \cdot \rangle_{\mathrm{L}^2(\mathcal{B})}$ defined by

$$\langle F, G \rangle_{\mathrm{L}^2(\mathcal{B})} = \int_{\mathcal{B}} F(x) G(x) \,\mathrm{d}x, \quad F, G \in \mathrm{L}^2(\mathcal{B}), \tag{2.44}$$

which is a Hilbert space. For a continuous function $F \in \mathrm{C}(\mathcal{B})$, we define

$$\|F\|_\infty \coloneqq \|F\|_{\mathrm{C}(\mathcal{B})} \coloneqq \sup_{x \in \mathcal{B}} |F(x)| \,. \tag{2.45}$$

Since $\mathrm{C}(\mathcal{B})$ is a pre-Hilbert space with the topology $\langle \cdot, \cdot \rangle_{\mathrm{L}^2(\mathcal{B})}$, we have for every $F \in \mathrm{C}(\mathcal{B})$ the following estimate for the norm

$$\|F\|_{\mathrm{L}^2(\mathcal{B})} \leq \sqrt{\|\mathcal{B}\|}\, \|F\|_{\mathrm{C}(\mathcal{B})}. \tag{2.46}$$

With this, we get that $\mathrm{L}^2(\mathcal{B})$ is the completion of $\mathrm{C}(\mathcal{B})$ with respect to $\|\cdot\|_{\mathrm{L}^2(\mathcal{B})}$, that means

$$\mathrm{L}^2(\mathcal{B}) = \overline{\mathrm{C}(\mathcal{B})}^{\|\cdot\|_{\mathrm{L}^2(\mathcal{B})}}. \tag{2.47}$$

A last very important point to define, is the convolution of two functions, which we will use later and plays an important role in this thesis.

Definition 2.2.6. *Let a measurable set $D \subset \mathbb{R}^n$ and $\Phi \in \mathrm{L}^2(D \times D),\ F \in \mathrm{L}^2(D)$ be given. We define the convolution of Φ and F (characterized by $*$) by*

$$(\Phi * F)(x) \coloneqq \int_D \Phi(x, y) F(y) \,\mathrm{d}y, \quad x \in D. \tag{2.48}$$

We can show that the convolution is always defined in $\mathrm{L}^2(D)$ by the use of the Cauchy-Schwarz inequality

$$\begin{aligned} \|\Phi * F\|^2_{\mathrm{L}^2(D)} &= \int_D \left(\int_D \Phi(x, y) F(y) \,\mathrm{d}y \right)^2 \mathrm{d}x \\ &\leq \int_D \int_D \Phi(x, y)^2 \,\mathrm{d}y \int_D F(y)^2 \,\mathrm{d}y \,\mathrm{d}x \\ &= \|\Phi\|^2_{\mathrm{L}^2(D \times D)} \|F\|^2_{\mathrm{L}^2(D)}. \end{aligned} \tag{2.49}$$

2.3. Theoretical Aspects of Constrained Optimization Problems

The following aspects of constrained optimization problems are briefly summarized and are obtained from [81]. We consider an optimization problem of the following form

$$\text{find } \min f(x) \tag{2.50}$$
$$\text{under the constraints } g_i(x) \leq 0, \quad i = 1, \ldots, m, \tag{2.51}$$
$$h_j(x) = 0, \quad j = 1, \ldots, p, \tag{2.52}$$

where the objective function $f : \mathbb{R}^n \to \mathbb{R}$ and the functions describing the constraints $g_i : \mathbb{R}^n \to \mathbb{R}$ and $h_j : \mathbb{R}^n \to \mathbb{R}$ are assumed to be continuously differentiable. For solving this optimization problem, the following Lagrange function plays an important role.

Definition 2.3.1. *The Lagrange function L of a constrained optimization problem is a mapping $L : \mathbb{R}^n \times \mathbb{R}^m \times \mathbb{R}^p \to \mathbb{R}$ given by*

$$L(x, \lambda, \mu) := f(x) + \sum_{i=1}^{m} \lambda_i g_i(x) + \sum_{j=1}^{p} \mu_j h_j(x). \tag{2.53}$$

With the help of the Lagrange function, we want to define the so called Karush-Kuhn-Tucker conditions (KKT conditions).

Definition 2.3.2. *We consider the optimization problem* (2.50)-(2.52) *with continuously differentiable functions f, g and h.*

(i) We call the conditions

$$\nabla_x L(x, \lambda, \mu) = 0, \tag{2.54}$$
$$h(x) = 0, \tag{2.55}$$
$$\lambda \geq 0, \ g(x) \leq 0, \ \lambda^{\mathrm{T}} g(x) = 0 \tag{2.56}$$

the KKT conditions of the optimization problem. Here

$$\nabla_x L(x, \lambda, \mu) = \nabla f(x) + \sum_{i=1}^{m} \lambda_i \nabla g_i(x) + \sum_{j=1}^{p} \mu_j \nabla h_j(x) \tag{2.57}$$

is the gradient of the Lagrange function L concerning the x-variable.

(ii) Each vector $(x^*, \lambda^*, \mu^*) \in \mathbb{R}^n \times \mathbb{R}^m \times \mathbb{R}^p$, which fulfills the KKT conditions, is called a Karush-Kuhn-Tucker point (KKT point) of the optimization problem. We call the components of λ^* and μ^* the Lagrange multipliers.

In a last step, we have to establish a connection between local minima of the optimization problem (2.50)-(2.52) and the corresponding KKT conditions given in (2.54)-(2.56). Therefore, we want to have a look at the KKT conditions under the Abadie constraint qualification (Abadie CQ). We first define the constraint qualification of Abadie.

Definition 2.3.3. *Let the optimization problem* (2.50)-(2.52) *be given. An admissible point x of the optimization problem satisfies the constraint qualification of Abadie if $\mathcal{T}_X(x) = \mathcal{T}_{\text{lin}}(x)$ holds true.*

Here we have the tangential cone of $X \subset \mathbb{R}^n$ in x given by

$$\mathcal{T}_X(x) \coloneqq \{d \in \mathbb{R}^n \mid \exists \{x_k\} \subseteq X \; \exists t_k \downarrow 0 : x_k \to x \text{ and } (x_k - x)/t_k \to d\} \tag{2.58}$$

with sequences $\{x_k\} \subseteq X$ and $\{t_k\} \subseteq \mathbb{R}$. Furthermore, we have the linearized tangential cone of X in x defined by

$$\mathcal{T}_{\text{lin}}(x) \coloneqq \left\{d \in \mathbb{R}^n \mid \nabla g_i(x)^{\mathrm{T}} d \leq 0 \; (i \in I(x)), \nabla h_j(x)^{\mathrm{T}} d = 0 \; (j = 1, \ldots, p)\right\}, \tag{2.59}$$

with the set of the active inequality restrictions in x

$$I(x) \coloneqq \{i \in \{1, \ldots, m\} \, | g_i(x) = 0\} \tag{2.60}$$

and the admissible set X given by

$$X \coloneqq \{x \in \mathbb{R}^n | g_i(x) \leq 0 \; (i = 1, \ldots, m), h_j(x) = 0 \; (j = 1, \ldots, p)\}. \tag{2.61}$$

With this definition, we can go over to this important theorem for the interrelation of KKT points and local minima.

Theorem 2.3.4. *Assume that we have a local minimum x^* of the optimization problem* (2.50)-(2.52) *given which fulfills Abadie CQ. In that case there exist Lagrange multipliers $\lambda^* \in \mathbb{R}^m$ and $\mu^* \in \mathbb{R}^p$ such that the triple (x^*, λ^*, μ^*) is a KKT point of* (2.50)-(2.52).

There are some more constraint qualifications, especially for non-linear restrictions, namely the constraint qualification of Mangasarian-Fromovitz (MFCQ) or linear independence (LICQ). For details see [81].

3. Differential Equations

This chapter deals with a general introduction into partial differential equations (PDEs). After the introduction of the classification of PDEs, we continue with some known PDEs, where we can see similarities to the later introduced equations of poroelasticity. We end up with a short introduction of fundamental solutions and present the fundamental solutions of the known PDEs from above. We are mainly guided by [50, 94, 103].

3.1. Basics

Our aim in this section is to give an overview of the classification of partial differential equations corresponding the order and the properties ellipticity, parabolicity and hyperbolicity. Assume we have an open subset U of $\mathbb{R}^n$ and an element $x = (x_1, x_2, \ldots, x_n)$. The following equation is called a partial differential equation (PDE) of order k for $u(x)$ in U:

$$F\left(D^k u(x), D^{k-1}u(x), \ldots, Du(x), u(x), x\right) = 0, \quad x \in U, \tag{3.1}$$

where we use the usual multi-index notation (here $\nu \in \mathbb{N}_0^n$)

$$D^\nu := \frac{\partial^{\nu_1}}{\partial x_1^{\nu_1}} \cdots \frac{\partial^{\nu_n}}{\partial x_n^{\nu_n}} = \frac{\partial^{|\nu|}}{\partial x_1^{\nu_1} \cdots \partial x_n^{\nu_n}}, \quad |\nu| = \sum_{i=1}^{n} \nu_i. \tag{3.2}$$

Here $|\nu|$ is the order of the derivative and we denote the set of all derivatives of the function u of order k by $(D^k u)(x) = \{(D^\nu)(x) : |\nu| = k\}$. The mapping $F : \mathbb{R}^{n^k} \times \mathbb{R}^{n^{k-1}} \times \cdots \times \mathbb{R}^n \times \mathbb{R} \times U \to \mathbb{R}$ is known and $u : U \to \mathbb{R}$ is unknown. The PDE is of order k that means there is at least one derivative with order k and none with higher order. Since we only handle with linear PDEs, we can write (3.1) in the following way:

$$\sum_{|\nu| \le k} a_\nu(x) D^\nu u(x) = f(x), \quad \nu \in \mathbb{N}^n. \tag{3.3}$$

The PDE is called homogeneous if $f \equiv 0$. In the following, we present the three main categories of partial differential operators and start with the elliptic one.

Definition 3.1.1 (Elliptic PDE). *Assume we have an open and bounded subset $U \subset \mathbb{R}^n$, $u : \overline{U} \to \mathbb{R}$ and L a second-order linear operator of the form*

$$Lu = \sum_{i,j=1}^{n} a_{ij}(x)\partial_{x_i}\partial_{x_j}u(x) + \sum_{i=1}^{n} b_i(x)\partial_{x_i}u(x,t) + c(x)u(x). \tag{3.4}$$

The operator L is said to be uniformly elliptic if there exists a constant $M > 0$ such that

$$\sum_{i,j=1}^{n} a_{ij}(x)\xi_i\xi_j \geq M\|\xi\|^2 \tag{3.5}$$

for almost every $x \in U$ and all $\xi \in \mathbb{R}^n$.

The following two classes have also a time dependency and we continue with the second class, the parabolic PDEs.

Definition 3.1.2 (Parabolic PDE). *We have an open and bounded subset $U \subset \mathbb{R}^n$, $u : \overline{U} \times [0,T] \to \mathbb{R}$ and L a second-order linear operator with the form*

$$Lu = \sum_{i,j=1}^{n} a_{ij}(x,t)\partial_{x_i}\partial_{x_j}u(x,t) + \sum_{i=1}^{n} b_i(x,t)\partial_{x_i}u(x,t) + c(x,t)u(x,t) - \partial_t u(x,t). \tag{3.6}$$

The operator L is said to be uniformly elliptic if there exists a constant $M > 0$ such that

$$\sum_{i,j=1}^{n} a_{ij}(x,t)\xi_i\xi_j \geq M\|\xi\|^2 \tag{3.7}$$

for all $(x,t) \in U \times [0,T]$ and all $\xi \in \mathbb{R}^n$.

The last case to consider the case of the hyperbolic PDE.

Definition 3.1.3 (Hyperbolic PDE). *We have an open and bounded subset $U \subset \mathbb{R}^n$, $u : \overline{U} \times [0,T] \to \mathbb{R}$ and L a second-order linear operator with the form*

$$Lu = \sum_{i,j=1}^{n} a_{ij}(x,t)\partial_{x_i}\partial_{x_j}u(x,t) + \sum_{i=1}^{n} b_i(x,t)\partial_{x_i}u(x,t) + c(x,t)u(x,t) - \partial_t^2 u(x,t). \tag{3.8}$$

The operator L is said to be uniformly elliptic if there exists a constant $M > 0$ such that

$$\sum_{i,j=1}^{n} a_{ij}(x,t)\xi_i\xi_j \geq M\|\xi\|^2 \tag{3.9}$$

for all $(x,t) \in U \times [0,T]$ and all $\xi \in \mathbb{R}^n$.

The difference between the last two cases is only the fact that we have the second derivative with respect to the time in the hyperbolic case. Note that not every partial differential equation can be dedicated to one of the three classes above clearly.

3.2. Some Known Classic Differential Equations

In this section, we want to present some basic known partial differential equations and their belonging to one of the three classes defined above. At first we have a look at Laplace's equation defined by

$$\Delta u(x) = \nabla^2 u(x) = \sum_{i=1}^{n} \partial_{x_i}^2 u(x) = 0. \tag{3.10}$$

This is a linear, elliptic second-order partial differential equation. The next one to consider is the heat (or diffusion equation), which is known as

$$\partial_t u(x,t) - \Delta u(x,t) = 0. \tag{3.11}$$

Here we have a linear, parabolic differential equation of second order. The next interesting one for us is a system of partial differential equations, the equilibrium equations of linear elasticity (also Cauchy-Navier equations), which are given by

$$\mu \Delta u(x) + (\lambda + \mu) \nabla (\nabla \cdot u(x)) = 0. \tag{3.12}$$

Please note here that u is a vector-valued function and λ and μ are the so-called Lamé constants, which are material constants. We deal here with a linear elliptic partial differential equation. The last PDEs to mention here, are the Stokes equations (please note here, that they are a simplification of the Navier-Stokes equations), which are given by

$$-\mu \nabla^2 u(x) + \nabla p(x) = 0, \tag{3.13}$$

$$\nabla \cdot u = 0. \tag{3.14}$$

In the next chapter we will see several similarities between these basic PDEs and the governing equations of thermoporoelasticity and certainly poroelasticity.

3.3. Fundamental Solutions

Since we need the fundamental solutions for the construction of our desired functions for the decorrelation, this section presents the definition of a fundamental solution and shows the fundamental solutions for the four PDEs defined above (Laplace, heat, equilibrium and Stokes equations). First we have to define what a distribution and the Dirac measure are. Furthermore, we present some properties of them (see also [94, 97, 103]).

Definition 3.3.1. *Assume, we have an open set X in $\mathbb{R}^n$. We call a linear form u in X on $\mathrm{C}_0^{(\infty)}(X)$ a distribution if for every compact set $K \subset X$ there are constants C and k such that*

$$|u(\phi)| \leq C \sum_{|\nu| \leq k} \sup_{x \in K} \left| \partial^\nu \phi(x) \right|, \quad \phi \in \mathrm{C}_0^\infty(K). \tag{3.15}$$

We denote the set of all distributions in the open set X in $\mathbb{R}^n$ by $\mathcal{D}'(X)$. Let us continue with the Dirac measure.

Definition 3.3.2. *The Dirac distribution (or Dirac functional, Dirac measure, Delta distribution) δ_a at $a \in \mathbb{R}^n$ is a mapping defined as*

$$\delta_a : \mathrm{C}_0(\mathbb{R}) \to \mathbb{R} \tag{3.16}$$

$$\langle \delta_a, \phi \rangle \coloneqq \delta_a(\phi) = \phi(a), \tag{3.17}$$

that means the Dirac measure δ_a of a function ϕ is the evaluation of ϕ at the point a.

Furthermore, we need more properties of distributions especially of the Delta distribution for our convolutions later. The following features are useful for us.

Remark 3.3.3. *For an open set X in $\mathbb{R}^n$, $\phi \in \mathrm{C}_0^\infty(X)$ and $u \in \mathcal{D}'(X)$, we have*

$$(\partial_{x_k} u)\, \phi = -u\, (\partial_{x_k} \phi)\,. \tag{3.18}$$

Furthermore, we have especially for the Dirac distribution

$$\langle \delta', \phi \rangle = -\langle \delta, \phi' \rangle\,. \tag{3.19}$$

The following properties can be seen in the sense of an extension of the result above (formally speaking)

$$\langle -\delta', 1 \rangle = \left\langle \delta, \frac{\mathrm{d}}{\mathrm{d}x} 1 \right\rangle = \langle \delta, 0 \rangle = 0, \tag{3.20}$$

$$\langle -\delta', x \rangle = \left\langle \delta, \frac{\mathrm{d}}{\mathrm{d}x} x \right\rangle = \langle \delta, 1 \rangle = 1. \tag{3.21}$$

With this definition and properties, we can go on to the definition of a fundamental solution.

Definition 3.3.4. *We have a differential operator $P = \sum a_\nu \partial^\nu$ with constant coefficients and a distribution $E \in \mathcal{D}'(\mathbb{R}^n)$. We call E a fundamental solution of P if $PE = \delta_0$.*

Furthermore, we have to explain what we understand as a regular distribution, which is a subset of the set of distributions.

Definition 3.3.5. *We say that a distribution u is regular, if it is generated by a locally integrable function f, that means there exists a representation in the following way*

$$u_f(\phi) = \int_{\mathbb{R}^n} f(t)\phi(t)\, \mathrm{d}t \quad \textit{for all } \phi \in \mathrm{C}_0^\infty(\mathbb{R}^n). \tag{3.22}$$

So regular distributions can be represented by functions. Distributions that are not regular are called singular. The Delta distribution is an example for a singular

distribution, because there does not exist a locally integrable function that fulfills (3.22) (for the proof see [97]).
In a next step, we want to show the fundamental solutions of the four differential equations mentioned above. Let us start with Laplace's equation. The fundamental solution is given by

$$u(x) = \begin{cases} \frac{1}{2\pi} \ln \|x\|, & n = 2 \\ -\frac{1}{(n-2)\omega_n} \frac{1}{\|x\|^{n-2}}, & n > 2, \end{cases} \tag{3.23}$$

where $\omega_n = 2\pi^{n/2}\Gamma\left(\frac{n}{2}\right)^{-1}$, which is the area of the surface of the n-dimensional unit sphere and Γ is the Gamma function given in Definition 2.1.1. For more properties of the Gamma function or other representations like the functional equation see [65]. Continuing with the heat equation, we obtain

$$u(x,t) = \begin{cases} \dfrac{1}{(4\pi t)^{n/2}} e^{-\frac{\|x\|^2}{4t}}, & x \in \mathbb{R}^n,\ t > 0 \\ 0, & x \in \mathbb{R}^n,\ t < 0. \end{cases} \tag{3.24}$$

The next one is the tensor-valued fundamental solution of the equilibrium equation (also Cauchy-Navier equation)

$$u_{ik}(x) = \begin{cases} \frac{\lambda+\mu}{4\pi\mu(2\mu+\lambda)} \left[\left(\frac{\lambda+3\mu}{\lambda+\mu} \right) \ln(\|x\|)\delta_{ik} + \frac{x_i x_k}{\|x\|^2} \right], & n = 2, \\ \frac{\lambda+\mu}{8\pi\mu(2\mu+\lambda)\|x\|} \left[\left(\frac{\lambda+3\mu}{\lambda+\mu} \right) \delta_{ik} + \frac{x_i x_k}{\|x\|^2} \right], & n = 3. \end{cases} \tag{3.25}$$

At last, we have the fundamental solutions for the Stokes equations. They are also tensor- and vector-valued and given by

$$u_{ij}(x) = \frac{1}{8\pi\|x\|} \left(\delta_{ij} + \frac{x_i x_j}{\|x\|^2} \right), \tag{3.26}$$

$$p(x) = \frac{x}{4\pi\|x\|^2}. \tag{3.27}$$

With the definition and properties of distributions, we now have to come back to convolutions, especially we have to say something about convolutions with distributions. In general for $u \in \mathcal{D}'(\mathbb{R}^n)$ and $\phi \in \mathrm{C}_0^\infty(\mathbb{R}^n)$ their convolution is defined by

$$(u * \phi)(x) = u(\phi(x - \cdot)) \tag{3.28}$$

that means u is acting on $\phi(x-y)$ as a function on y. Furthermore, it holds true that the convolution $u * \phi \in \mathrm{C}^\infty(\mathbb{R}^n)$ fulfills the following with respect to the derivatives

$$\partial^\alpha (u * \phi) = (\partial^\alpha u) * \phi = u * (\partial^\alpha \phi). \tag{3.29}$$

With this property and Remark 3.3.3, we can have a look at distributions of the form $\phi(x)\delta_t$ or $\phi(x)\delta_t'$ with a distributional time dependent part (in our case the Delta distribution) and set the convolution of these (scaling) functions with the data given by f (assumed to be differentiable with respect to t) as

$$(\phi\delta_t * f) \coloneqq \int_{\mathbb{R}^2} \phi(x-y)\,(\delta_t f(y,\cdot))\ \mathrm{d}y = \int_{\mathbb{R}^2} \phi(x-y) f(y,t)\ \mathrm{d}y, \tag{3.30}$$

$$(\phi\delta_t' * f) \coloneqq \left(\phi\delta_t * \frac{\partial}{\partial t} f\right) = \int_{\mathbb{R}^2} \phi(x-y) \frac{\partial}{\partial t} f(y,t)\ \mathrm{d}y. \tag{3.31}$$

4. Multiscale Approach

This chapter deals with the definition of scaling functions and their wavelets. Furthermore, we define operators and spaces. A similar multiscale approach as stated here, was proposed in [75]. See also [21, 25] and the references therein.

4.1. Scaling Functions and Wavelets

In this section, we introduce the (scale discrete) scaling and wavelet functions, which build the basis for a multiscale approach. We start with the definition and the properties of a scaling function.

Definition 4.1.1. *We assume that we have a regular region $\mathcal{B}$ in $\mathbb{R}^n$. Furthermore, $\{\tau_j\}_{j\in\mathbb{N}}$, $\tau_j > 0$, is a strictly monotonically decreasing null sequence, that means*

$$\lim_{j\to\infty} \tau_j = 0. \tag{4.1}$$

The sequence $\{\Phi_{\tau_j}\}_{j\in\mathbb{N}}$, $\Phi_{\tau_j} : \mathbb{R} \to \mathbb{C}$ is called a scaling function if

$$\lim_{j\to\infty} \int_{\mathcal{B}} \Phi_{\tau_j}(x-y)\, F(y)\, \mathrm{d}y = \alpha(x) F(x) \tag{4.2}$$

holds true for all $x \in \overline{\mathcal{B}}$ and all $F \in \mathrm{C}(\overline{\mathcal{B}})$.

Especially, we notice that

$$\lim_{j\to\infty} \int_{\mathcal{B}} \Phi_{\tau_j}(x-y)\, \mathrm{d}y = \alpha(x) \tag{4.3}$$

holds true for all $x \in \mathcal{B}$ by inserting $F(x) = 1$. Here $\alpha(x)$ denotes the solid angle, which can in general be defined in the following way (see [63]).

Definition 4.1.2. *We have a region $\mathcal{G} \subset \mathbb{R}^3$. The solid angle $\alpha(x)$ can be defined by*

$$\alpha(x) = \int_{\partial\mathcal{B}} \frac{\partial}{\partial \nu_y} G(\Delta; \|x-y\|)\, \mathrm{d}y, \tag{4.4}$$

where $G(\Delta; \|x-y\|)$ is the fundamental solution of the Laplace operator Δ in $\mathbb{R}^q$ given by (see also (3.23) *for the fundamental solution in the case of a unit sphere)*

$$G(\Delta; \|x-y\|) = \begin{cases} \frac{1}{2\pi} \ln(\|x-y\|), & n = 2, \\ \frac{\|x-y\|^{2-n}}{(2-n)\|\mathbb{S}^{n-1}\|}, & n \geq 3, \end{cases} \tag{4.5}$$

and ν_y denotes the unit normal vector in y pointing into the space $\mathbb{R}^q \setminus \overline{\mathcal{B}}$.

In a 3-dimensional cube $\mathcal{B} = (-1,1)^3$, the solid angle $\alpha(x)$ correlates with the position of x in the cube that means

$$\alpha(x) = \begin{cases} 0, \text{ if } x \text{ is not an element of the cube } \mathcal{B} \text{ or of the boundary } \partial\mathcal{B}, \\ \frac{1}{8}, \text{ if } x \text{ is one of the eight corner points of } \partial\mathcal{B}, \\ \frac{1}{4}, \text{ if } x \text{ is on one of the four edges of } \partial\mathcal{B} \text{ but is not a corner point}, \\ \frac{1}{2}, \text{ if } x \text{ is on one of the six faces of } \partial\mathcal{B} \text{ but not on a corner or edge}, \\ 1, \text{ if } x \text{ is in the open cube } \mathcal{B}. \end{cases} \tag{4.6}$$

If we now assume that we have $x \in \mathcal{B}$, then $\alpha(x) = 1$ and we obtain for the convolution integral in the limit

$$\lim_{j\to\infty} \int_{\mathcal{B}} \Phi_{\tau_j}(x-y)\, F(y)\, \mathrm{d}y = F(x). \tag{4.7}$$

Please note that in our case the scale discrete scaling function Φ is a tensor with $\mathbf{\Phi} : \mathbb{R}^3 \to \mathbb{R}^{3\times 3}$ and the data function F is then vector-valued and approximated by $f : \overline{\mathcal{B}} \times \mathbb{R} \to \mathbb{R}^3$. Therefore, we have to extend this definition of a scaling function also due to the time and therefore modify the definition to the following (cf. [21] for a one dimensional time-variate case or [22] for a multidimensional case without a time component).

Definition 4.1.3. *Suppose that $\mathcal{B}$ is a regular region in $\mathbb{R}^3$, $f : \overline{\mathcal{B}} \times \mathbb{R} \to \mathbb{R}^3$ continuous and $\{\tau_j\}_{j\in\mathbb{N}},\ \tau_j > 0$ is a strictly monotonically decreasing sequence with*

$$\lim_{j\to\infty} \tau_j = 0. \tag{4.8}$$

The sequence $\{\mathbf{\Phi}_{\tau_j}\}_{j\in\mathbb{N}}$, $\mathbf{\Phi}_{\tau_j} : \mathbb{R}^3 \to \mathbb{R}^{3\times 3}$ is called a scaling function if

$$\lim_{j\to\infty} \int_{\mathcal{B}} \int_{\mathbb{R}} \mathbf{\Phi}_{\tau_j}(x-y, t-\theta) f(y,\theta)\, \mathrm{d}\theta\, \mathrm{d}y = f(x,t) \tag{4.9}$$

holds true for all $x \in \mathcal{B}$ and $t \in \mathbb{R}$.

Please note that we now assume $x \in \mathcal{B}$ instead of $x \in \overline{\mathcal{B}}$, which means that we can set $\alpha(x) = 1$.

Remark 4.1.4. *A possible sequence for τ_j can, for example, be $\tau_j = 2^{-j}$. This is the sequence which we will use later.*

In the following, we will use the tensor-valued varieties of the definition that means our scaling functions and wavelets are tensor-valued and the data function f is vector-valued. Please notice that they can always be replaced by a scalar-valued scaling function and data function instead. With the help of the scaling function, we can define the wavelet function.

Definition 4.1.5. *Assume that we have a scaling function $\{\mathbf{\Phi}_{\tau_j}\}_{j\in\mathbb{N}}$. Then we can define the wavelet function $\{\mathbf{\Psi}_{\tau_j}\}_{j\in\mathbb{N}}$, $\mathbf{\Psi}_{\tau_j} : \mathbb{R}^3 \to \mathbb{R}^{3\times 3}$ as the following*

$$\mathbf{\Psi}_{\tau_j} = \mathbf{\Phi}_{\tau_j} - \mathbf{\Phi}_{\tau_{j-1}}. \tag{4.10}$$

With this definition of the wavelet function, we can write a scaling function $\mathbf{\Phi}_{\tau_J}$ for $j \in \mathbb{N}$ as the following sum of wavelets.

Lemma 4.1.6. *Let $j,\ J \in \mathbb{N}$ with $j < J$ arbitrary. Then any $\mathbf{\Phi}_{\tau_J}$ of $\{\mathbf{\Phi}_{\tau_j}\}_{j\in\mathbb{N}}$ can be represented as*

$$\mathbf{\Phi}_{\tau_J} = \mathbf{\Phi}_{\tau_j} + \sum_{l=j+1}^{J} \mathbf{\Psi}_{\tau_l}. \tag{4.11}$$

With this representation of $\mathbf{\Phi}_{\tau_J}$, we can write the following convolution of a function $f \in \mathrm{C}(\overline{\mathcal{B}}, \mathbb{R}^3)$ in this way.

Theorem 4.1.7. *Our assumptions are as follows: We have a strictly monotonically decreasing sequence $\{\tau_j\}_{j\in\mathbb{N}}$, the scaling function $\{\mathbf{\Phi}_{\tau_j}\}_{j\in\mathbb{N}}$ and the corresponding wavelet $\{\mathbf{\Psi}_{\tau_j}\}_{j\in\mathbb{N}}$. Furthermore, $f \in \mathrm{C}(\overline{\mathcal{B}}, \mathbb{R}^3)$ with a regular region $\mathcal{B}$ and $j > j_0$ with $j, j_0 \in \mathbb{N}$. We get for all $x \in \mathcal{B}$*

$$\begin{aligned} f_{\tau_j}(x) &:= \int_{\mathcal{B}} \mathbf{\Phi}_{\tau_j}(x-y) f(y)\,\mathrm{d}y \\ &= \int_{\mathcal{B}} \mathbf{\Phi}_{\tau_{j_0}}(x-y) f(y)\,\mathrm{d}y + \sum_{l=j_0+1}^{j} \int_{\mathcal{B}} \mathbf{\Psi}_{\tau_l}(x-y) f(y)\,\mathrm{d}y \end{aligned} \tag{4.12}$$

and

$$\begin{aligned} f(x) &= \lim_{j\to\infty} f_{\tau_j}(x) \\ &= \lim_{j\to\infty} \int_{\mathcal{B}} \mathbf{\Phi}_{\tau_j}(x-y) f(y)\,\mathrm{d}y \\ &= \int_{\mathcal{B}} \mathbf{\Phi}_{\tau_{j_0}}(x-y) f(y)\,\mathrm{d}y + \sum_{l=j_0+1}^{\infty} \int_{\mathcal{B}} \mathbf{\Psi}_{\tau_l}(x-y) f(y)\,\mathrm{d}y. \end{aligned} \tag{4.13}$$

The convolution of a function f against the kernel $\mathbf{\Phi}_{\tau_j}$ as represented in (4.12) shows us the decomposition of the approximation of a function f into a low-pass part, which is the convolution of f against $\mathbf{\Phi}_{\tau_{j_0}}$, and several band-pass parts, which we get by the convolution of f with the wavelets $\mathbf{\Psi}_{\tau_l},\ l = j_0+1, \ldots, j$.

Remark 4.1.8. *Please note that in numerical uses, we will only calculate the convolution of the data with the scaling functions and obtain the convolution of the data with the wavelet by subtracting the convolution of two consecutive scaling functions.*

With this, we obtain the multiscale representation.

Corollary 4.1.9. *Again let $\{\mathbf{\Phi}_{\tau_j}\}_{j\in\mathbb{N}}$ be a scaling function and $\{\mathbf{\Psi}_{\tau_j}\}_{j\in\mathbb{N}}$ the wavelet belonging to it. The multiscale representation is then given by*

$$\int_{\mathcal{B}} \mathbf{\Phi}_{\tau_0}(x-y)f(y)\,\mathrm{d}y + \sum_{j=1}^{\infty}\int_{\mathcal{B}} \mathbf{\Psi}_{\tau_j}(x-y)f(y)\,\mathrm{d}y = f(x) \tag{4.14}$$

and holds true for all $x \in \mathcal{B}$ and $f \in \mathrm{C}(\overline{\mathcal{B}},\mathbb{R}^3)$.

4.2. Scale and Detail Spaces

We can define operators $\mathcal{P}_{\mathbf{\Phi}_{\tau_j}}$ in relation to the scaling function and $\mathcal{R}_{\mathbf{\Phi}_{\tau_j}}$ concerning the wavelet function as follows (see [77, 78])

$$\mathcal{P}_{\mathbf{\Phi}_{\tau_j}}[f] = \int_{\mathcal{B}} \mathbf{\Phi}_{\tau_j}(\cdot - y)f(y)\,\mathrm{d}y, \quad f \in \mathrm{C}(\overline{\mathcal{B}},\mathbb{R}^3), \tag{4.15}$$

$$\mathcal{R}_{\mathbf{\Phi}_{\tau_j}}[f] = \int_{\mathcal{B}} \mathbf{\Psi}_{\tau_j}(\cdot - y)f(y)\,\mathrm{d}y, \quad f \in \mathrm{C}(\overline{\mathcal{B}},\mathbb{R}^3). \tag{4.16}$$

Since the operator $\mathcal{P}_{\mathbf{\Phi}_{\tau_j}}$ is in connection with $\mathbf{\Phi}_{\tau_j}$ and $\mathcal{R}_{\mathbf{\Psi}_{\tau_j}}$ with $\mathbf{\Psi}_{\tau_j}$, they can be understood as the so called low-pass filter and band-pass-filter. With the help of these operators, we can define scale-spaces $\mathcal{V}_{\mathbf{\Phi}_{\tau_j}}$ and detail-spaces $\mathcal{W}_{\mathbf{\Phi}_{\tau_j}}$.

Definition 4.2.1. *We define the scale-spaces $\mathcal{V}_{\mathbf{\Phi}_{\tau_j}}$ and the detail-spaces $\mathcal{W}_{\mathbf{\Phi}_{\tau_j}}$ by*

$$\mathcal{V}_{\mathbf{\Phi}_{\tau_j}} = \mathcal{P}_{\mathbf{\Phi}_{\tau_j}}\left[\mathrm{C}(\overline{\mathcal{B}})\right] = \{\mathcal{P}_{\mathbf{\Phi}_{\tau_j}}[f] \big| f \in \mathrm{C}(\overline{\mathcal{B}},\mathbb{R}^3)\}, \tag{4.17}$$

$$\mathcal{W}_{\mathbf{\Phi}_{\tau_j}} = \mathcal{R}_{\mathbf{\Phi}_{\tau_j}}\left[\mathrm{C}(\overline{\mathcal{B}})\right] = \{\mathcal{R}_{\mathbf{\Psi}_{\tau_j}}[f] \big| f \in \mathrm{C}(\overline{\mathcal{B}},\mathbb{R}^3)\}. \tag{4.18}$$

By writing

$$\mathcal{P}_{\mathbf{\Phi}_{\tau_{j+1}}}[f] = \mathcal{P}_{\mathbf{\Phi}_{\tau_j}}[f] + \mathcal{R}_{\mathbf{\Phi}_{\tau_{j+1}}}[f], \quad j \in \mathbb{N}, \tag{4.19}$$

we can conclude (see also Definition 4.1.5)

$$\mathcal{V}_{\mathbf{\Phi}_{\tau_j}} = \mathcal{V}_{\mathbf{\Phi}_{\tau_j}} + \mathcal{W}_{\mathbf{\Phi}_{\tau_{j+1}}}. \tag{4.20}$$

5. Cubature on Lattice Points

We introduce the most important results that we need for the calculation of our convolution integrals, that means volume integrals over regular regions. Therefore we want to adopt suitable cubature formulas which we obtain from [58]. More precisely, we are interested in the Poisson summation formula in the formulation of Gauß-Weierstraß summability. We show here a very compressed version of [58] referring to the condensed version given in [21]. For more information about integration and cubature methods from a geomathematical point of view see also [66].

5.1. Lattices

At the beginning it is important to define a lattice Λ in $\mathbb{R}^q$, its fundamental cell and the appropriate inverse lattice. With this, we go afterwards over to the so-called Λ-periodic functions and their function spaces.

Definition 5.1.1. *We have the space $\mathbb{R}^q$ and the basis $g_1, \ldots, g_q$. We call the set Λ of all points obtained by*

$$g = n_1 g_1 + \cdots + n_q g_q, \quad n_1, \ldots, n_q \in \mathbb{Z}, \tag{5.1}$$

a lattice in $\mathbb{R}^q$ regarding the basis $g_1, \ldots, g_q$. Furthermore, the half-open parallelotope $\mathcal{F}_\Lambda$ consists of the points $x \in \mathbb{R}^q$ given by

$$x = t_1 g_1 + \cdots + t_q g_q, \quad -\frac{1}{2} \leq t_i < \frac{1}{2}, \tag{5.2}$$

$i = 1, \ldots, q$ and is named the fundamental cell $\mathcal{F}_\Lambda$ of the lattice Λ.

In Figure 5.1 an example of a lattice with basis g_1, g_2 in $\mathbb{R}^2$ and its fundamental cell $\mathcal{F}_\Lambda$ is shown. Proceeding from this definition, we have for example that the unit vectors $e_1, \ldots, e_q$ form a basis of $\mathbb{Z}^q$.
The volume of a fundamental cell can be obtained by linear algebra in the following way (see for example [44])

$$\|\mathcal{F}_\Lambda\| = \int_{\mathcal{F}_\Lambda} \mathrm{d}x = \sqrt{\det\left((g_i \cdot g_j)_{i,j=1,\ldots,q}\right)}. \tag{5.3}$$

In the case that we have $\Lambda = \mathbb{Z}^q$, we get that the volume of the fundamental cell is given by $\|\mathcal{F}_\Lambda\| = 1$. Furthermore, we have the following properties.

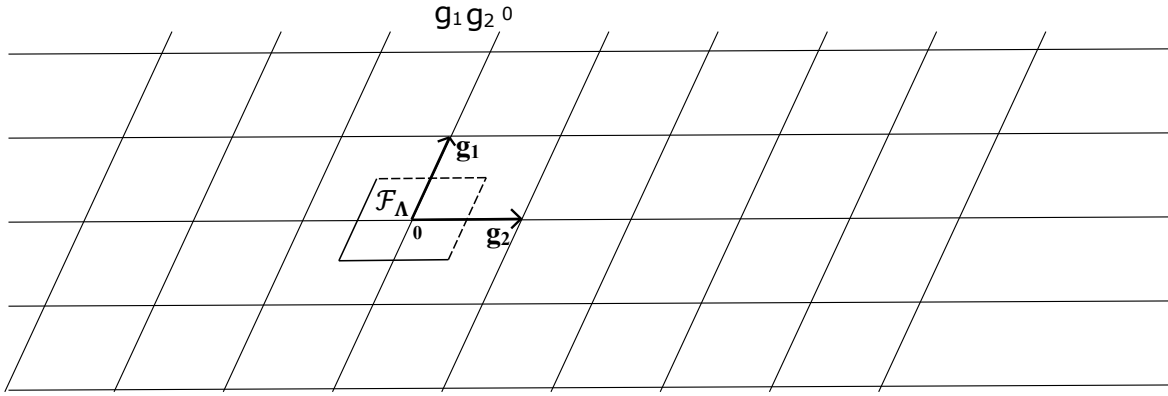

Figure 5.1.: Example of a lattice in $\mathbb{R}^2$ and its corresponding fundamental cell $\mathcal{F}_\Lambda$.

Remark 5.1.2. *For each $g \in \Lambda$ and $\mathcal{F}_\Lambda + \{g\} := \{y + g | y \in \mathcal{F}_\Lambda\}$, we obtain for the volume*

$$\|\mathcal{F}_\Lambda\| = \|\mathcal{F}_\Lambda + \{g\}\|. \tag{5.4}$$

With the property $(\mathcal{F}_\Lambda + \{g\}) \cap (\mathcal{F}_\Lambda + \{g'\}) = \emptyset$ for $g \neq g'$ and $g, g' \in \Lambda$, we can write the space $\mathbb{R}^q$ as

$$\mathbb{R}^q = \bigcup_{g \in \Lambda} (\mathcal{F}_\Lambda + \{g\}) = \bigcup_{g \in \Lambda} (\mathcal{F}_\Lambda - \{g\}). \tag{5.5}$$

For the definition of the inverse lattice, we have a look at the vectors $h_1, \ldots, h_q$, which should satisfy

$$h_j \cdot g_i = \delta_{ij}, \tag{5.6}$$

where δ_{ij} is the Kronecker Delta (see (2.15)). The existence of the vectors $h_1, \ldots, h_q$ is given due to the linear independency of the vectors $g_1, \ldots, g_q$.
The vectors $h_1, \ldots, h_q$ can be obtained with the following considerations and computations. We define the scalars γ_{ij} with the help of the inner product of the vectors $g_1, \ldots, g_q$ by

$$\gamma_{ij} = g_i \cdot g_j, \quad i, j = 1, \ldots, q. \tag{5.7}$$

We are interested in getting the scalars γ^{ij} by solving the linear equation system

$$\sum_{i=1}^{q} \gamma^{ij} \gamma_{jk} = \delta_{ik}. \tag{5.8}$$

With this we can calculate the vectors $h_j,\ j = 1, \ldots, q$ with the help of the vectors $g_k,\ k = 1, \ldots, q$ by

$$h_j = \sum_{k=1}^{q} \gamma^{jk} g_k. \tag{5.9}$$

They satisfy the equations

$$h_j \cdot g_i = \sum_{k=1}^{q} \gamma^{jk} g_k \cdot g_i = \sum_{k=1}^{q} \gamma^{jk} \gamma_{ki} = \delta_{ij}, \tag{5.10}$$

for $i, j = 1, \ldots, q$, which is the property we wanted. Moreover, we get

$$\begin{aligned} h_i \cdot h_j &= \sum_{k=1}^{q} \gamma^{ik} g_k \cdot \sum_{l=1}^{q} \gamma^{jl} g_l \\ &= \sum_{l=1}^{q} \gamma^{jl} \sum_{k=1}^{q} \gamma^{ik} \gamma_{kl} \\ &= \gamma^{ji}. \end{aligned} \tag{5.11}$$

With these preliminary considerations, we want to define the inverse lattice Λ^{-1}.

Definition 5.1.3. *The inverse (or dual) lattice Λ^{-1} of Λ is the lattice with basis $h_1, \ldots, h_q$ with the properties given in* (5.6).

Furthermore, the following properties between the lattice and the inverse lattice hold true

$$\Lambda = \left(\Lambda^{-1}\right)^{-1} \tag{5.12}$$

and

$$\left\|\mathcal{F}_{\Lambda}^{-1}\right\| = \left\|\mathcal{F}_{\Lambda}\right\|^{-1}. \tag{5.13}$$

In the last part of this section, we define Λ-periodic functions and their function spaces.

Definition 5.1.4. *Let a lattice $\Lambda \subset \mathbb{R}^q$ be given. We call a function $\Phi : \mathbb{R}^q \to \mathbb{C}$ Λ-periodic, if*

$$\Phi(x + g) = \Phi(x) \tag{5.14}$$

holds true for all $x \in \mathbb{R}^q$ and all $g \in \Lambda$.

We want to give an example for a Λ-periodic function.

Lemma 5.1.5. *Now assume that h is an element of the inverse lattice Λ^{-1}. The functions $\Phi_h : \mathbb{R}^q \to \mathbb{C}$ defined by*

$$\Phi_h(x) = \frac{1}{\sqrt{\|\mathcal{F}_{\Lambda}\|}} \exp\left(2\pi i h \cdot x\right), \quad x \in \mathbb{R}^q, \tag{5.15}$$

are Λ-periodic.

Furthermore, we can define the following spaces in connection with Λ-periodic functions.

Definition 5.1.6. *The space $\mathrm{C}_\Lambda^{(k)}(\mathbb{R}^q)$ denotes the set of all functions $F \in \mathrm{C}^{(k)}(\mathbb{R}^q)$ with $0 \leq k \leq \infty$ that are Λ-periodic. By $\mathcal{L}_\Lambda^p(\mathbb{R}^q)$ we denote the space of all $F : \mathbb{R}^q \to \mathbb{C}$ that are $\Lambda - periodic$ and Lebesgue-measurable on $\mathcal{F}_\Lambda$ with*

$$\|F\|_{\mathrm{L}_\Lambda^p(\mathbb{R}^q)} = \left(\int_{\mathcal{F}_\Lambda} |F(x)|^p \, \mathrm{d}x \right)^{\frac{1}{p}} < \infty, \quad 1 \leq p < \infty. \tag{5.16}$$

Furthermore, we define the null space $\mathcal{N}_\Lambda^p(\mathbb{R}^q)$ by

$$\mathcal{N}_\Lambda^p(\mathbb{R}^q) \coloneqq \left\{ F \in \mathcal{L}_\Lambda^p(\mathbb{R}^q) \middle| \int_{\mathcal{F}_\Lambda} |F(x)|^p \, \mathrm{d}x = 0 \right\} \quad 1 \leq p < \infty. \tag{5.17}$$

With the concept of equivalence classes and the two definitions above, we can define the space $\mathrm{L}_\Lambda^p(\mathbb{R}^q)$ by

$$\mathrm{L}_\Lambda^p(\mathbb{R}^q) \coloneqq \mathcal{L}_\Lambda^p(\mathbb{R}^q) /_{\mathcal{N}_\Lambda^p(\mathbb{R}^q)}. \tag{5.18}$$

Furthermore, we have that $\mathrm{C}_\Lambda^{(k)}(\mathbb{R}^q) \subset \mathrm{L}_\Lambda^p(\mathbb{R}^q)$ holds true and that $\mathrm{L}_\Lambda^2(\mathbb{R}^q)$ is the completion of $\mathrm{C}_\Lambda^{(k)}(\mathbb{R}^q)$ with respect to the norm $\|\cdot\|_{\mathrm{L}_\Lambda^2(\mathbb{R}^q)}$, that means

$$\mathrm{L}_\Lambda^2(\mathbb{R}^q) = \overline{\mathrm{C}_\Lambda^{(k)}(\mathbb{R}^q)}^{\|\cdot\|_{\mathrm{L}_\Lambda^2(\mathbb{R}^q)}}. \tag{5.19}$$

We see that the system $\{\Phi_h\}_{h \in \Lambda^{-1}}$ from above is orthonormal with respect to the $\mathrm{L}_\Lambda^p(\mathbb{R}^q)$-inner product for $h, h' \in \Lambda^{-1}$:

$$(\Phi_h, \Phi_{h'})_{\mathrm{L}_\Lambda^p(\mathbb{R}^q)} = \int_{\mathcal{F}_\Lambda} \Phi_h(x) \overline{\Phi_{h'}(x)} \, \mathrm{d}x = \delta_{hh'}. \tag{5.20}$$

We continue with the Laplace operator Δ_x and the eigenvalue λ of the lattice Λ.

Definition 5.1.7. *If we have a non-trivial solution U of the given differential equation $(\Delta_x + \lambda)U(x) = 0$, that satisfies the condition $U(x + g) = U(x)$ for all $g \in \Lambda$ and all $x \in \mathbb{R}^q$, we call λ an eigenvalue of the lattice Λ with respect to the Laplace operator Δ_x. We say that U is the eigenfunction of the lattice Λ regarding the eigenvalue λ and the operator Δ_x.*

We get the following connection of the definition to the function Φ_h from above.

Lemma 5.1.8. *The function $\Phi_h(x)$ (see Lemma 5.1.5) is called an eigenfunction of the lattice Λ regarding the Laplace operator Δ_x and the eigenvalue $\Delta^\wedge(h) = 4\pi^2 \|h\|^2$.*

The functions Φ_h are the only eigenfunctions of the lattice and the scalars $\Delta^\wedge(h)$ are the only eigenvalues of Δ with respect to the lattice Λ. We get that the system $\{\Phi_h\}_{h\in\Lambda^{-1}}$ is closed and complete in the pre-Hilbert space $(\mathrm{C}_\Lambda^{(0)}(\mathbb{R}^q), \|\cdot\|_{\mathrm{L}^2_\Lambda(\mathbb{R}^q)})$ and also in the Hilbert space $(\mathrm{L}^2_\Lambda(\mathbb{R}^q), \|\cdot\|_{\mathrm{L}^2_\Lambda(\mathbb{R}^q)})$. Furthermore, we get for $F \in \mathrm{L}^2_\Lambda(\mathbb{R}^q)$ the following

$$\lim_{N\to\infty} \left\| F - \sum_{\substack{\|h\|\le N \\ h\in\Lambda^{-1}}} F^\wedge_\Lambda(h)\Phi_h \right\|_{\mathrm{L}^2_\Lambda(\mathbb{R}^q)} = 0, \tag{5.21}$$

where we have the respective Fourier coefficients $F^\wedge_\Lambda(h)$ given by

$$F^\wedge_\Lambda(h) = \int_{\mathcal{F}_\Lambda} F(x)\overline{\Phi_h(x)}\,\mathrm{d}x, \quad h \in \Lambda^{-1}. \tag{5.22}$$

That means each $F \in \mathrm{L}^2_\Lambda(\mathbb{R}^q)$ can be represented by its Fourier series.

5.2. Lattice Point Summation Formulas

In this section, we have some preparations left on our way to the Poisson summation formula in Gauß-Weierstraß summability. In order to do this, we need the Poisson summation formula and the Theta function.
Please note that we write $\sum_{g\in\Lambda}$ instead of $\lim_{N\to\infty}\sum_{\substack{\|g\|\le N \\ g\in\Lambda}}$ for reasons of brevity.
We start with the introduction of two new spaces.

Definition 5.2.1. *We have $m \in \mathbb{N}$, $\varepsilon > 0$ and $\lambda \in \mathbb{R}$ given. The spaces $\mathrm{CP}_1^{(2m)}(\lambda, \mathbb{R}^q)$ and $\mathrm{CP}_2^{(2m)}(\varepsilon, \lambda, \mathbb{R}^q)$ are defined as below*

(i) The space of all functions $H \in \mathrm{C}^{(2m)}(\mathbb{R}^q)$ with the asymptotic relations

$$(\Delta_x + \lambda)^k H(x) = o\left(\|x\|^{1-q}\right), \quad \|x\| \to \infty, \tag{5.23}$$
$$\left\|\nabla_x(\Delta_x + \lambda)^k H(x)\right\| = o\left(\|x\|^{1-q}\right), \quad \|x\| \to \infty, \tag{5.24}$$

for $k = 0, \ldots, m-1$ is denoted by $\mathrm{CP}_1^{(2m)}(\lambda, \mathbb{R}^q)$.

(ii) By $\mathrm{CP}_2^{(2m)}(\varepsilon, \lambda, \mathbb{R}^q)$, the space of all functions $H \in \mathrm{C}^{(2m)}(\mathbb{R}^q)$ fulfilling

$$(\Delta_x + \lambda)^m H(x) = \mathcal{O}\left(\|x\|^{-(1+\varepsilon)}\right), \quad \|x\| \to \infty \tag{5.25}$$

is denoted.

The next theorem is the Poisson summation formula and obtained from [58] and is required for our desired summation formula.

Theorem 5.2.2. *Let a lattice Λ in the space $\mathbb{R}^q$ be given. Let us assume that for $\varepsilon > 0$ and $\lambda \in \mathbb{R}$ the function $F \in \mathrm{C}^{(2m)}(\mathbb{R}^q)$, $m > \frac{q}{2}$, fulfills the property that it is a member of class $\mathrm{CP}_1^{(2m)}(\lambda, \mathbb{R}^q) \cap \mathrm{CP}_2^{(2m)}(\varepsilon, \lambda, \mathbb{R}^q)$, then the following holds true*

$$\begin{aligned}\lim_{N\to\infty} &\left(\sum_{\substack{\|g\|\leq N \\ g\in\Lambda}} F(g) - \frac{1}{\sqrt{\|\mathcal{F}_\Lambda\|}} \sum_{\substack{(\Delta+\lambda)^\wedge(h)=0 \\ h\in\Lambda^{-1}}} \int_{\substack{\|x\|\leq N \\ x\in\mathbb{R}^q}} F(x)\overline{\Phi_h(x)}\,\mathrm{d}x \right) \\ &= \frac{1}{\sqrt{\|\mathcal{F}_\Lambda\|}} \sum_{\substack{(\Delta+\lambda)^\wedge(h)\neq 0 \\ h\in\Lambda^{-1}}} \int_{x\in\mathbb{R}^q} F(x)\overline{\Phi_h(x)}\,\mathrm{d}x. \end{aligned} \tag{5.26}$$

Moreover, if we have that the sum

$$\sum_{\substack{(\Delta+\lambda)^\wedge(h)=0 \\ h\in\Lambda^{-1}}} \int_{\substack{\|x\|\leq N \\ x\in\mathbb{R}^q}} F(x)\overline{\Phi_h(x)}\,\mathrm{d}x \tag{5.27}$$

converges for $N \to \infty$, we are able to conclude that

$$\begin{aligned}\sum_{g\in\Lambda} F(g) - &\frac{1}{\sqrt{\|\mathcal{F}_\Lambda\|}} \sum_{\substack{(\Delta+\lambda)^\wedge(h)=0 \\ h\in\Lambda^{-1}}} \int_{x\in\mathbb{R}^q} F(x)\overline{\Phi_h(x)}\,\mathrm{d}x \\ &= \frac{1}{\sqrt{\|\mathcal{F}_\Lambda\|}} \sum_{\substack{(\Delta+\lambda)^\wedge(h)\neq 0 \\ h\in\Lambda^{-1}}} \int_{\mathbb{R}^q} F(x)\overline{\Phi_h(x)}\,\mathrm{d}x. \end{aligned} \tag{5.28}$$

Now we come to the last component that we need for the development of the Poisson summation formula in Gauß-Weierstraß summability, which is the Theta function in $\mathbb{R}^q$ of degree 0 and its functional equation. Please note here that the Theta function of degree 0 is sufficient here for us. For a representation of the Theta function of degree n, see [58].

Definition 5.2.3. *Let arbitrary points $x, y \in \mathbb{R}^q$ and an arbitrary lattice Λ be given. We call $\vartheta^{(q)}(\cdot;\cdot,\cdot;\Lambda)$ with $\sigma \in \mathbb{C}$ and real part $\Re(\sigma) > 0$ given by*

$$\vartheta^{(q)}(\sigma; x, y; \Lambda) = \sum_{g\in\Lambda} \frac{\exp\left(-\pi\sigma\left\|g - x\right\|^2\right)}{\sqrt{4\pi}} \exp\left(2\pi i g \cdot y\right), \tag{5.29}$$

the Theta function of degree 0 and dimension q.

The Theta function is an example for a function that fulfills the property to be a member of class $\mathrm{CP}_1^{(2m)}(\lambda, \mathbb{R}^q) \cap \mathrm{CP}_2^{(2m)}(\varepsilon, \lambda, \mathbb{R}^q)$. We continue with the functional equation.

Theorem 5.2.4. *The Theta function $\vartheta^{(q)}(\cdot; x, y; \Lambda)$ is for all values $\sigma \in \mathbb{C}$ with real part $\Re(\sigma) > 0$ holomorphic and fulfills the following functional equation*

$$\vartheta^{(q)}(\sigma; x, y; \Lambda) = \frac{1}{\|\mathcal{F}_\Lambda\|} \exp(2\pi i x \cdot y)\sigma^{-\frac{q}{2}} \vartheta^{(q)}\left(\frac{1}{\sigma}; -y, x; \Lambda^{-1}\right) \quad \text{for all } x, y \in \mathbb{R}^q. \tag{5.30}$$

Starting with the functional equation, we can deduce the summation formula. This is done by multiplying the functional equation of the Theta function with a function $F \in \mathrm{C}(\overline{\mathcal{B}})$ and application of the Poisson summation formula (see Theorem 5.2.2). We do not show the derivation of the formula in detail. For a detailed proof, see [58]. The result is given in the next theorem.

Theorem 5.2.5. *Assume that $\mathcal{B}$ is a regular region in $\mathbb{R}^q$ and $F \in \mathrm{C}(\overline{\mathcal{B}})$. For all $x \in \mathbb{R}^q$ and all $\tau \in \mathbb{R}$ with $\tau > 0$, the series*

$$\sum_{h \in \Lambda^{-1}} \exp(-\tau\pi^2 h^2) \int_{\mathcal{B}} F(y)\overline{\Phi_h(y)} \, \mathrm{d}y \; \Phi_h(x) \tag{5.31}$$

converges. Furthermore, we have for all $x \in \mathbb{R}^q$ the summation formula

$$\sum_{\substack{g+x \in \overline{\mathcal{B}} \\ g \in \Lambda}} \alpha(g+x)F(g+x) = \lim_{\substack{\tau \to 0 \\ \tau > 0}} \sum_{h \in \Lambda^{-1}} \exp(-\tau\pi^2 h^2) \int_{\mathcal{B}} F(y)\overline{\Phi_h(y)} \, \mathrm{d}y \; \Phi_h(x). \tag{5.32}$$

We want to simplify the theorem by setting $x = 0$ and separate the term belonging to $h = 0$ and get the following.

Corollary 5.2.6. *For an arbitrary lattice Λ in $\mathbb{R}^q$, a regular region $\mathcal{B} \subset \mathbb{R}$ and a function $F \in \mathrm{C}(\overline{\mathcal{B}})$, we get*

$$\begin{aligned}\sum_{\substack{g \in \overline{\mathcal{B}} \\ g \in \Lambda}} \alpha(g)F(g) = \frac{1}{\|\mathcal{F}_\Lambda\|} \int_{\mathcal{B}} F(y) \, \mathrm{d}y \\ + \frac{1}{\|\mathcal{F}_\Lambda\|} \lim_{\substack{\tau \to 0 \\ \tau > 0}} \sum_{\substack{h \neq 0 \\ h \in \Lambda^{-1}}} \exp(-\tau\pi^2 h^2) \int_{\mathcal{B}} F(y) \exp(-2\pi i h \cdot y) \, \mathrm{d}y.\end{aligned} \tag{5.33}$$

Now let us have a look at the second term on the right-hand side, that means the second line of the equation above. In the limit, this term vanishes, if the mesh size and also the area of the fundamental cell tend to zero due to the Riemann integrability of the function $F \in \mathrm{C}(\overline{\mathcal{B}})$. With this knowledge, we can deduce the following cubature formula

$$\int_{\mathcal{B}} F(y) \, \mathrm{d}y \approx \|\mathcal{F}_\Lambda\| \sum_{\substack{g \in \overline{\mathcal{B}} \\ g \in \Lambda}} \alpha(g)F(g). \tag{5.34}$$

There are some things left to say: This summation formula will only give good results if the support of the integrand is large enough, that means covers enough data points. Since our source scaling functions have a shrinking support for the limit $\tau \to 0+$, it is necessary to do a little modification of the summation formula that we get good results also for the case with a small support. This is done analogously to the modification in [21]. For further details see Section 9.1.

Part II.

Physical Background

6. Thermoporoelasticity

In this chapter, we want to give a short overview of the term thermoporoelasticity and what is meant by this. We continue with the derivation of the governing equations of thermoporoelasticity before we derive the fundamental solutions. We are guided by [33].

6.1. Overview

We start with a short description of what is meant by poroelasticity. This term describes the connection between a solid and the pore pressure for example in a geothermal reservoir and its interaction on each other. That means for example solid deformation can change the pore pressure and also a variation in the pore pressure has an effect on the solid. In this case the temperature is assumed to be constant. Thermoporoelasticity connects poroelasticity with thermal effects. Since thermal effects play an important role in geothermal reservoirs, it is necessary to have a look at poroelastic effects that are linked with thermal ones. The temperature can change for example by deformation of the solid itself but also by heat conduction, for example by injecting a colder fluid than extracted before. Furthermore, deformation of the solid can cause temperature changes. For the description of the thermoporoelastic behavior of such a setting, several material constants for the solid and fluid are necessary. For an overview (listed in the order as they appear in the derivation of the equations below) of the symbol and the corresponding quantity, see Table 6.1. Please note that there are many more material constants that we do not explain here in detail, because they can be expressed with the ones above. There exist relations between the thermoporoelastic constants. An important one for the Biot-Willis constant α is

$$\alpha = \left(1 - \frac{K}{K_\mathrm{s}}\right). \tag{6.1}$$

Another one is the connection to the well-known Lamé constants, where we have

$$\mu = G, \quad \lambda = K - \frac{2}{3}G. \tag{6.2}$$

For further relations between the constants and the other constants, that exist, we refer to [33]. For the derivation of the partial differential equations in thermoporoelasticity, we need 9 of these constants, which can for example be the following $\{G, K, M, \alpha, \alpha_d, \beta_e, m_d, \kappa, \kappa_T\}$. For the theory of poroelasticity later, only 4 constants are necessary, for example $\{G, K, \alpha, B\}$.

Symbol	Quantity
G	shear modulus
K	drained bulk modulus
α_{d}	drained thermoelastic effective stress coefficient
K_{s}	bulk modulus of the solid
α	Biot-Willis constant
κ	permeability coefficient
M	Biot modulus
β_{e}	coefficient for volumetric thermal expansion for variation in fluid content at constant frame volume
κ_{T}	thermal conductivity
m_{d}	drained thermoelastic constitutive constant
B	Skempton pore pressure coefficient
β_{d}	drained coefficient of volumetric thermal expansion for porous medium frame

Table 6.1.: Table with the main material constants for thermoporoelasticity.

6.2. Physical Background and Mathematical Derivation of the Equations

In this section the main idea and the most important physical laws for the derivation of the partial differential equations for the thermally coupled model of thermoporoelasticity are shown. Later the simplification to the uncoupled model is presented.
The first constitutive equations and a consistent theory for the three-dimensional linear poroelasticity without thermal effects go back to Biot (see [15–17, 20]) and furthermore for thermoelasticity see [19].
In thermoporoelasticity, we have a look at a combination of both. In general, there exist three models, the complete, the coupled and the uncoupled model. The detailed derivation for the three models can be found in [33] and also for the uncoupled model see [139]. We show here briefly the way to get the governing equations of the thermally coupled model and afterwards to the uncoupled model. For that reason, the Navier equation, the fluid diffusion equation and the thermal diffusion equation are used. Note that in the following the displacement u, the pore pressure p and the temperature T are the unknown variables. It is possible to express the equations with the set of unknown variables displacement, pore pressure and temperature $\{u, p, T\}$ in equations with the unknown variables stress-strain-tensor, variation in fluid content and entropy $\{\sigma_{ij}, \zeta, s\}$, which depend on $\{u, p, T\}$. In some cases it is easier to switch between the variables. It is also possible to have combinations of these six as unknown variables, that means one can choose, if u or σ_{ij} for the displacement component, p or ζ for the pressure component and T or s for the temperature component.

Beginning with the variables u, p and T, the variables σ_{ij}, ζ and s are defined in the following way:

$$\sigma_{ij} = \left(K - \frac{2G}{3}\right)\delta_{ij}e + 2Ge_{ij} - \alpha\delta_{ij} - \alpha_{\mathrm{d}}\delta_{ij}T, \tag{6.3}$$

$$\zeta = \alpha e + \frac{p}{M} - \beta_{\mathrm{e}}T, \tag{6.4}$$

$$s = \alpha_{\mathrm{d}}e - \beta_{\mathrm{e}}p + m_{\mathrm{d}}T. \tag{6.5}$$

Here e_{ij} is the infinitesimal or total (Cauchy) strain tensor which is given by

$$\boldsymbol{e}_{ij} = \frac{1}{2}\left(\frac{\partial u_i}{\partial x_j} + \frac{\partial u_j}{\partial x_i}\right) = \frac{1}{2}\left(\partial_{x_j}u_i + \partial_{x_i}u_j\right) \tag{6.6}$$

and e the total volumetric strain

$$e = \sum_{i=1}^{3}\boldsymbol{e}_{ii} = \sum_{i=1}^{3}\partial_{x_i}u_i = \nabla\cdot u. \tag{6.7}$$

We see that e and e_{ij} depend on the variable u. The following notation is used for a better readability

$$u_{i,j} = \frac{\partial}{\partial x_j}u_i. \tag{6.8}$$

There are three main physical laws that lead us to the partial diferential equations and that we have a look at successively. We start with the force equilibrium equation.

Navier-type equation/Force equilibrium equation

For an isotropic material, the stress-strain relation in general can with the help of the shear and drained bulk modulus be written as

$$\sigma_{ij} = 2G\boldsymbol{e}_{ij} + \left(K - \frac{2G}{3}\right)\delta_{ij}e. \tag{6.9}$$

Taking into account the pressure and the temperature, the stress-strain-temperature relation is given by

$$\sigma_{ij} = 2G\boldsymbol{e}_{ij} + \left(K - \frac{2G}{3}\right)\delta_{ij}e - \alpha_{\mathrm{d}}\delta_{ij}T - \alpha\delta_{ij}p, \tag{6.10}$$

where σ_{ij} is the Cauchy stress tensor in the porous medium. The static equilibrium equation is written as

$$\sum_{j=1}^{3}\sigma_{ij,j} = 0, \tag{6.11}$$

since there are no body forces and inertia effect. Also the thermal effect has no influence on the force equilibrium. Putting (6.10) in (6.11) and considering (6.6) yields

$$\begin{aligned}
&\left(K-\frac{2G}{3}\right)\sum_{j=1}^{3}\delta_{ij}\partial_{x_j}e+2G\sum_{j=1}^{3}\partial_{x_j}\boldsymbol{e}_{ij}-\alpha\sum_{j=1}^{3}\delta_{ij}\partial_{x_j}p-\alpha_{\mathrm{d}}\sum_{j=1}^{3}\delta_{ij}\partial_{x_j}T=0\\
\Leftrightarrow&\left(K-\frac{2G}{3}\right)\nabla(\nabla\cdot u)+2G\frac{1}{2}\left(\sum_{j=1}^{3}\partial_{x_jx_j}u_i+\sum_{j=1}^{3}\partial_{x_ix_j}u_j\right)-\alpha\nabla p-\alpha_{\mathrm{d}}\nabla T=0\\
\Leftrightarrow&\left(K-\frac{2G}{3}\right)\nabla(\nabla\cdot u)+G\left(\nabla^2u+\nabla(\nabla\cdot u)\right)-\alpha\nabla p-\alpha_{\mathrm{d}}\nabla T=0\\
\Leftrightarrow&\left(K+\frac{G}{3}\right)\nabla(\nabla\cdot u)+G\nabla^2u-\alpha\nabla p-\alpha_{\mathrm{d}}\nabla T=0,
\end{aligned}\tag{6.12}$$

which is the first equation of thermoporoelasticity. We continue with the equation for the main equation that concerns the behavior of the fluid.

Fluid diffusion equation

For the derivation of the fluid diffusion equation, first the fluid mass balance equation

$$\frac{\partial\zeta}{\partial t}+\nabla\cdot q=0\tag{6.13}$$

and Darcy's law (which describes the flow of a fluid through a porous medium)

$$q=-\kappa\nabla p\tag{6.14}$$

are combined to get

$$\frac{\partial\zeta}{\partial t}-\kappa\nabla^2p=0.\tag{6.15}$$

In this case, q is the specific flux and ζ the variation in fluid content. The variable ζ in the equation above can be eliminated with the help of (6.4) to obtain

$$\frac{\partial p}{\partial t}-\kappa M\nabla^2p=-\alpha M\frac{\partial e}{\partial t}+\beta_{\mathrm{e}}M\frac{\partial T}{\partial t}.\tag{6.16}$$

This is a pore pressure diffusion equation and the second equation, which can also be written as

$$\frac{\partial p}{\partial t}-\kappa M\nabla^2p=-\alpha M\frac{\partial(\nabla\cdot u)}{\partial t}+\beta_{\mathrm{e}}M\frac{\partial T}{\partial t}.\tag{6.17}$$

We continue with the last equation, which effects the thermal behavior.

Thermal diffusion equation
The thermal diffusion equation is based on the thermal energy balance and also Fourier's law. The linearized version of the thermal energy conservation equation is

$$\mathcal{T}_0 \frac{\partial s}{\partial t} + \nabla \cdot \mathfrak{q} = 0, \tag{6.18}$$

where s is the entropy, $\mathfrak{q}$ the so-called heat flux vector and $\mathcal{T}_0$ the reference absolute temperature. Together with Fourier's law (which describes the rate of heat transfer in a material), the heat flux vector can be replaced by

$$\mathfrak{q} = -k_{\mathrm{T}} \nabla T \tag{6.19}$$

and the following equation is obtained

$$\frac{\partial s}{\partial t} - \frac{k_{\mathrm{T}}}{\mathcal{T}_0} \nabla^2 T = 0. \tag{6.20}$$

By substituting $s = \alpha_{\mathrm{d}} e - \beta_{\mathrm{e}} p + m_{\mathrm{d}} T$ (see (6.5)), the diffusion equation for temperature is obtained

$$\alpha_{\mathrm{d}} \frac{\partial e}{\partial t} - \beta_{\mathrm{e}} \frac{\partial p}{\partial t} + m_{\mathrm{d}} \frac{\partial T}{\partial t} - \frac{k_{\mathrm{T}}}{\mathcal{T}_0} \nabla^2 T = 0. \tag{6.21}$$

Dividing this equation by m_{d}, setting $\frac{k_{\mathrm{T}}}{\mathcal{T}_0 m_{\mathrm{d}}} = \kappa_{\mathrm{T}}$ and replacing e, the third governing equation of thermoporoelasticity is obtained:

$$\frac{\partial T}{\partial t} - \kappa_{\mathrm{T}} \nabla^2 T = -\frac{\alpha_{\mathrm{d}}}{m_{\mathrm{d}}} \frac{\partial (\nabla \cdot u)}{\partial t} + \frac{\beta_{\mathrm{e}}}{m_{\mathrm{d}}} \frac{\partial p}{\partial t}. \tag{6.22}$$

The equations (6.12), (6.17) and (6.22) are the governing equations for the coupled model in thermoporoelasticity. The unknown variables are u, p and T. The set of 9 independent material constants consists of $\{G, K, M, \alpha, \alpha_{\mathrm{d}}, \beta_{\mathrm{e}}, m_{\mathrm{d}}, \kappa, \kappa_{\mathrm{T}}\}$. Now we have a look at the derivation of the uncoupled equations, which is done by the following considerations. In the coupled equations there exists a poroelastic and a thermoelastic coupling. Poroelastic coupling means that pore pressure can generate solid deformation and solid deformation can cause pore pressure (called the Skempton effect). This poroelastic coupling can be ignored (see [156]) if

$$\alpha B \ll 1 \tag{6.23}$$

holds true. Based on the materials given in [33], this condition is not satisfied and therefore the poroelastic coupling cannot be ignored. The thermoelastic coupling on the contrary can be disregarded if

$$\frac{K \beta_{\mathrm{d}}^2}{m_{\mathrm{d}}} \ll 1. \tag{6.24}$$

For the materials deep sea clay, rock salt, Berea sandstone and Westerly granite given in [33] this coupling coefficient is 1.7×10^{-6}, 4.6×10^{-2}, 2.7×10^{-5} and 1.8×10^{-3}. That means in most cases the thermoelastic coupling is weak and can be ignored. This uncoupling of the thermoelastic effect is achieved by taking $m_d \to \infty$ and the thermal diffusion equation (6.22) reduces to

$$\frac{\partial T}{\partial t} - \kappa_{\mathrm{T}} \nabla^2 T = 0. \tag{6.25}$$

In this case the constant m_{d} is not longer necessary and the independent material constants reduce to 8. The governing equations for the uncoupled model in thermoporoelasticity are

$$\left(K + \frac{G}{3}\right) \nabla(\nabla \cdot u) + G\nabla^2 u = \alpha \nabla p + \alpha_{\mathrm{d}} \nabla T \tag{6.26}$$

$$\frac{\partial p}{\partial t} - \kappa M \nabla^2 p = -\alpha M \frac{\partial(\nabla \cdot u)}{\partial t} + \beta_{\mathrm{e}} M \frac{\partial T}{\partial t} \tag{6.27}$$

$$\frac{\partial T}{\partial t} - \kappa_{\mathrm{T}} \nabla^2 T = 0. \tag{6.28}$$

The temperature equation (6.28) is a homogeneous heat equation for T and can be solved independently from the other two. The equation for the pore pressure (6.27) is an inhomogeneous heat equation, where its right-hand side depends on u and T. Equation (6.26) (for u) is an inhomogeneous Navier-type equation, which is subjected on p and T.

6.3. Fundamental Solutions

Fundamental solutions for the partial differential equations in porothermoelasticity are derived in [33] for the coupled equations, where this subsection is guided by it. The idea is to show the main concept and strategy how such fundamental solutions can be constructed. We write down the fundamental solutions for the unknown u, p and T in detail in contrast to [33], where not all components are presented explicitly. For the determination of the fundamental solutions first singular forcing terms for displacement, pore pressure and temperature are needed. In this case F_i is the concentrated force, γ the fluid source and γ_T the heat source. Another possible way to get fundamental solutions is the integral transform technique (see [140]).

With these forces the equilibrium equations (6.11), the fluid mass balance (6.13) and the thermal energy balance (6.18) can be rewritten as

$$\sum_{j=1}^{3} \sigma_{ij,j} = -F_i, \tag{6.29}$$

$$\frac{\partial \zeta}{\partial t} + \sum_{i=1}^{3} q_{i,i} = \gamma, \tag{6.30}$$

$$\mathcal{T}_0 \frac{\partial s}{\partial t} + \sum_{i=1}^{3} \mathfrak{q}_{i,i} = \gamma_T. \tag{6.31}$$

Note that we now switch here from the unknown variables $\{u, p, T\}$ to $\{u, \zeta, s\}$ in the equations derived before that means we now express $\{u, p, T\}$ from the equations above in terms of $\{u, \zeta, s\}$ and obtain (see [33] for a detailed derivation)

$$G \sum_{j=1}^{3} u_{i,jj} + \left(K_\mathrm{b} + \frac{G}{3} \right) \sum_{j=1}^{3} u_{j,ji} - \alpha_\mathrm{b} M \zeta_{,i} - \frac{\alpha_\mathrm{u}}{m_\mathrm{u}} s_{,i} = -F_i, \tag{6.32}$$

$$\frac{\partial \zeta}{\partial t} - c_\mathrm{c} \nabla^2 \zeta - \frac{c_\mathrm{c} \beta_\mathrm{g}}{m_\mathrm{d}} \nabla^2 s = \frac{3 M \alpha_\mathrm{b} \kappa}{3K_\mathrm{b} + 4G} \sum_{i=1}^{3} F_{i,i} + \gamma, \tag{6.33}$$

$$\frac{\partial s}{\partial t} - c_\mathrm{b} \nabla^2 s - M c_\mathrm{b} \beta_\mathrm{h} \nabla^2 \zeta = \frac{3 m_\mathrm{d} \alpha_\mathrm{u} \kappa_\mathrm{T}}{m_\mathrm{u}(3K_\mathrm{b} + 4G)} \sum_{i=1}^{3} F_{i,i} + \frac{\gamma_T}{\mathcal{T}_0}. \tag{6.34}$$

Some new obtained constants here are combinations of the well-known constants from above and are introduced as an abbreviation here for the sake of readability. The relations between the new and the old constants can be found very detailed in [33]. In this setting (6.32) depends on all unknowns but (6.33) and (6.34) are independent of u and uncoupled from the Navier equation that means can be solved independently from (6.32). This is easier for the derivation of the fundamental solutions. We can get back to p and T with the help of the following formulas (see [33] for details)

$$p = M \left(-\alpha_\mathrm{b} e + \frac{m_\mathrm{d}}{m_\mathrm{u}} \zeta + \frac{\beta_\mathrm{e}}{m_\mathrm{u}} s \right), \tag{6.35}$$

$$T = \frac{1}{m_\mathrm{u}} \left(s - \alpha_\mathrm{u} e + m \beta_\mathrm{e} \zeta \right), \tag{6.36}$$

which are obtained by rearrangement of (6.4) and (6.5).

6.3.1. Biot Decomposition

We have a look at the fundamental solutions in the two-dimensional case. For the derivation of the fundamental solutions, a variable decomposition, which was

first suggested by Biot (see [18]) in poroelasticity, is applied to further decouple the equations (6.32)-(6.34). This decomposition holds true for all different types of forcing terms and is very important for us to calculate the u_i in the different cases

$$u_i = u_i^0 + \frac{\eta_\mathrm{b} M}{G}\Phi_{,i} + \frac{\eta_\mathrm{u}}{m_\mathrm{u} G}\Psi_{,i}. \tag{6.37}$$

Here Φ and Ψ are potentials fulfilling

$$\zeta = \nabla^2\Phi, \tag{6.38}$$
$$s = \nabla^2\Psi. \tag{6.39}$$

The main idea is to solve the equations first for the unknown $\{u_i^0, \Psi, \Phi\}$. Then we obtain u_i, ζ and s with the help of (6.37), (6.38) and (6.39). In the end we can use (6.35) and (6.36) for the determination of p and T or use directly the following equations for p and T in dependency on the defined potentials (obtained from [33])

$$p = \frac{1}{S_\mathrm{c}}\nabla^2\Phi + \frac{\beta_\mathrm{g}}{m_\mathrm{d} S_\mathrm{c}}\nabla^2\Psi + \frac{\eta_\mathrm{b} M}{G} g_1, \tag{6.40}$$
$$T = \frac{\beta_\mathrm{h} M}{S_\mathrm{b}}\nabla^2\Phi + \frac{1}{S_\mathrm{b}}\nabla^2\Psi + \frac{\eta_\mathrm{u}}{m_\mathrm{u} G} g_1, \tag{6.41}$$

where

$$g_{1k} = \frac{1}{2\pi}\frac{x_k}{r^2} \tag{6.42}$$

and the new constants depend on the well-known constants and are introduced for a better readability. In the following, we will consider several scenarios of source functions to obtain the components of the fundamental solution matrix as it is done in [33]

6.3.2. Continuous Heat Source

We start with the heat source, that means γ_T is represented as a point heat source located at x, which corresponds to the following singular forcing distribution

$$\gamma_T = \delta_x H(t-\tau);\ \gamma = F_i = 0. \tag{6.43}$$

In this case the corresponding fundamental solutions and quantities have the superscript $\cdot^{\mathrm{hsc}}$ and the potentials Φ and Ψ are given by (see [33])

$$\Phi^{\mathrm{hsc}} = \frac{\beta_{\mathrm{g}}}{2\pi\mathcal{T}_0 m_{\mathrm{d}} c_{\mathrm{b}}(\mu_1^2-\mu_2^2)}\left[\frac{1}{2}t\exp\left(-\frac{\mu_1^2 r^2}{4t}\right)-\frac{1}{8}(\mu_1^2 r^2+4t)\mathrm{E}_1\left(\frac{\mu_1^2 r^2}{4t}\right)\right.$$
$$\left.-\frac{1}{2}t\exp\left(-\frac{\mu_2^2 r^2}{4t}\right)+\frac{1}{8}(\mu_2^2 r^2+4t)\mathrm{E}_1\left(\frac{\mu_2^2 r^2}{4t}\right)\right], \tag{6.44}$$

$$\Psi_1^{\mathrm{hsc}} = -\frac{m_{\mathrm{d}}}{\beta_{\mathrm{g}}}\Phi^{\mathrm{hsc}}, \tag{6.45}$$

$$\Psi_2^{\mathrm{hsc}} = \frac{1}{2\pi\mathcal{T}_0 c_{\mathrm{b}} c_{\mathrm{c}}(\mu_1^2-\mu_2^2)}\left[\frac{1}{2\mu_1^2}t\exp\left(-\frac{\mu_1^2 r^2}{4t}\right)-\frac{1}{8\mu_1^2}(\mu_1^2 r^2+4t)\mathrm{E}_1\left(\frac{\mu_1^2 r^2}{4t}\right)\right.$$
$$\left.-\frac{1}{2\mu_2^2}t\exp\left(-\frac{\mu_2^2 r^2}{4t}\right)+\frac{1}{8\mu_2^2}(\mu_2^2 r^2+4t)\mathrm{E}_1\left(\frac{\mu_1^2 r^2}{4t}\right)\right], \tag{6.46}$$

$$\Psi^{\mathrm{hsc}} = \Psi_1^{\mathrm{hsc}} + \Psi_2^{\mathrm{hsc}}. \tag{6.47}$$

The detailed derivation for Φ and Ψ can be found in [33], where also a Laplace transform is used. We obtain for p and T (see also [33])

$$p^{\mathrm{hsc}}(r,t) = -\frac{\beta_{\mathrm{g}}}{4\pi\mathcal{T}_0 m_{\mathrm{d}} S_{\mathrm{c}} c_{\mathrm{b}} c_{\mathrm{c}}(\mu_1^2-\mu_2^2)}\left[\mathrm{E}_1\left(\frac{\mu_1^2 r^2}{4t}\right)-\mathrm{E}_1\left(\frac{\mu_2^2 r^2}{4t}\right)\right], \tag{6.48}$$

$$T^{\mathrm{hsc}}(r,t) = \frac{c_{\mathrm{c}}\mu_1^2(m_{\mathrm{d}}-M\beta_{\mathrm{g}}\beta_{\mathrm{h}})-m_{\mathrm{d}}}{4\pi\mathcal{T}_0 c_{\mathrm{c}} c_{\mathrm{b}} m_{\mathrm{d}} S_{\mathrm{b}}(\mu_1^2-\mu_2^2)}\mathrm{E}_1\left(\frac{\mu_1^2 r^2}{4t}\right)$$
$$-\frac{c_{\mathrm{c}}\mu_2^2(m_{\mathrm{d}}-M\beta_{\mathrm{g}}\beta_{\mathrm{h}})-m_{\mathrm{d}}}{4\pi\mathcal{T}_0 c_{\mathrm{c}} c_{\mathrm{b}} m_{\mathrm{d}} S_{\mathrm{b}}(\mu_1^2-\mu_2^2)}\mathrm{E}_1\left(\frac{\mu_2^2 r^2}{4t}\right). \tag{6.49}$$

We calculate the displacement, which obtained with the relations (see (6.37))

$$u_i = u_i^0 + \frac{\eta_{\mathrm{b}} M}{G}\Phi_{,i} + \frac{\eta_{\mathrm{u}}}{m_{\mathrm{u}} G}\Psi_{,i}, \tag{6.50}$$

$$u_i^0 = 0, \tag{6.51}$$

resulting from the decomposition and the assumptions in (6.43). To get the fundamental solution u_i, the derivative with respect to x_i of $\mathrm{E}_1(\cdot)$ has to be determined. This is (see the properties of the exponential integral in (2.21) and (2.20))

$$\frac{\partial}{\partial x_i}\mathrm{E}_1\left(\frac{\mu_1^2 r^2}{4t}\right) = -\mathrm{E}_0\left(\frac{\mu_1^2 r^2}{4t}\right)\cdot\frac{\mu_1^2 x_i}{2t}$$
$$= \frac{-\mu_1^2 x_i}{2t}\cdot\frac{4t}{\mu_1^2 r^2}\exp\left(-\frac{\mu_1^2 r^2}{4t}\right)$$
$$= \frac{-2x_i}{r^2}\exp\left(-\frac{\mu_1^2 r^2}{4t}\right). \tag{6.52}$$

For a better readability, we summarize the fractions of constants in front of Φ and Ψ in two new constants given by

$$K_1 := \frac{\beta_\mathrm{g}}{2\pi\mathcal{T}_0 m_\mathrm{d} c_\mathrm{b}(\mu_1^2-\mu_2^2)}, \tag{6.53}$$

$$K_2 := \frac{1}{2\pi\mathcal{T}_0 c_\mathrm{b} c_\mathrm{c}(\mu_1^2-\mu_2^2)}, \tag{6.54}$$

and first calculate the derivative of the term of Φ^hsc equipped with μ_1 and use (6.52)

$$\begin{aligned}
&\frac{\partial}{\partial x_i}\left[\frac{1}{2}t\exp\left(-\frac{\mu_1^2r^2}{4t}\right)-\frac{1}{8}(\mu_1^2r^2+4t)\mathrm{E}_1\left(\frac{\mu_1^2r^2}{4t}\right)\right]\\
&\quad=\frac{1}{2}t\exp\left(-\frac{\mu_1^2r^2}{4t}\right)\cdot\left(\frac{-2x_i\mu_1^2}{4t}\right)-\frac{1}{8}\mu_1^2 2x_i\mathrm{E}_1\left(\frac{\mu_1^2r^2}{4t}\right)\\
&\qquad+\frac{1}{8}(\mu_1^2r^2+4t)\frac{2x_i}{r^2}\exp\left(-\frac{\mu_1^2r^2}{4t}\right)\\
&\quad=-\frac{x_i\mu_1^2}{4}\exp\left(-\frac{\mu_1^2r^2}{4t}\right)-\frac{1}{4}x_i\mu_1^2\mathrm{E}_1\left(\frac{\mu_1^2r^2}{4t}\right)+\frac{1}{4}x_i\exp\left(-\frac{\mu_1^2r^2}{4t}\right)\left(\mu_1^2+\frac{4t}{r^2}\right)\\
&\quad=-\frac{x_i\mu_1^2}{4}\mathrm{E}_1\left(\frac{\mu_1^2r^2}{4t}\right)+\frac{x_it}{r^2}\exp\left(-\frac{\mu_1^2r^2}{4t}\right).
\end{aligned}\tag{6.55}$$

The term provided with μ_2 and the derivative of Ψ_2^hsc can be derived in analogy due to the similarity of both terms. We get for u_i^hsc

$$\begin{aligned}
u_i^\mathrm{hsc} &\overset{(6.50)}{=} \frac{\eta_\mathrm{b}M}{G}\Phi^\mathrm{hsc}_{,i}+\frac{\eta_\mathrm{u}}{m_\mathrm{u}G}\Psi^\mathrm{hsc}_{,i}\\
&= \frac{\eta_\mathrm{b}M}{G}\frac{\partial}{\partial x_i}\Phi^\mathrm{hsc}+\frac{\eta_\mathrm{u}}{m_\mathrm{u}G}\frac{\partial}{\partial x_i}\Psi^\mathrm{hsc}\\
&\overset{(6.45),(6.47)}{=} \frac{\eta_\mathrm{b}M}{G}\frac{\partial}{\partial x_i}\Phi^\mathrm{hsc}+\frac{\eta_\mathrm{u}}{m_\mathrm{u}G}\frac{\partial}{\partial x_i}\left(\frac{-m_d}{\beta_g}\Phi^\mathrm{hsc}+\Psi_2^\mathrm{hsc}\right)\\
&\overset{(6.55)}{=} \left(\frac{\eta_\mathrm{b}M}{G}-\frac{m_\mathrm{d}\eta_\mathrm{u}}{\beta_\mathrm{g}m_\mathrm{u}G}\right)K_1\left[-\frac{x_i\mu_1^2}{4}\mathrm{E}_1\left(\frac{\mu_1^2r^2}{4t}\right)+\frac{x_it}{r^2}\exp\left(-\frac{\mu_1^2r^2}{4t}\right)\right.\\
&\qquad\left.+\frac{x_i\mu_2^2}{4}\mathrm{E}_1\left(\frac{\mu_2^2r^2}{4t}\right)-\frac{x_it}{r^2}\exp\left(-\frac{\mu_2^2r^2}{4t}\right)\right]\\
&\quad+\frac{\eta_\mathrm{u}}{m_\mathrm{u}G}K_2\left[-\frac{x_i}{4}\mathrm{E}_1\left(\frac{\mu_1^2r^2}{4t}\right)+\frac{x_it}{r^2\mu_1^2}\exp\left(-\frac{\mu_1^2r^2}{4t}\right)\right.\\
&\qquad\left.+\frac{x_i}{4}\mathrm{E}_1\left(\frac{\mu_2^2r^2}{4t}\right)-\frac{x_it}{r^2\mu_2^2}\exp\left(-\frac{\mu_2^2r^2}{4t}\right)\right].
\end{aligned}\tag{6.56}$$

6.3.3. Continuous Fluid Source

For the continuous fluid source the following assumptions have to be made in analogy to the continuous heat source before

$$\gamma = \delta_x H(t-\tau);\ \gamma_T = F_i = 0. \tag{6.57}$$

Due to the symmetry between ζ and s in (6.33) and (6.34), we obtain (see [33])

$$\begin{aligned}\Psi^{\mathrm{fsc}} = \frac{M\beta_{\mathrm{h}}}{2\pi c_{\mathrm{c}}(\mu_1^2-\mu_2^2)}\Bigg[&\frac{1}{2}t\exp\left(-\frac{\mu_1^2 r^2}{4t}\right) - \frac{1}{8}(\mu_1^2 r^2+4t)\mathrm{E}_1\left(\frac{\mu_1^2 r^2}{4t}\right)\\ &- \frac{1}{2}t\exp\left(-\frac{\mu_2^2 r^2}{4t}\right) + \frac{1}{8}(\mu_2^2 r^2+4t)\mathrm{E}_1\left(\frac{\mu_2^2 r^2}{4t}\right)\Bigg],\end{aligned} \tag{6.58}$$

$$\Phi_1^{\mathrm{fsc}} = -\frac{1}{M\beta_{\mathrm{h}}}\Psi^{\mathrm{fsc}}, \tag{6.59}$$

$$\begin{aligned}\Phi_2^{\mathrm{fsc}} = \frac{1}{2\pi c_{\mathrm{b}}c_{\mathrm{c}}(\mu_1^2-\mu_2^2)}\Bigg[&\frac{1}{2\mu_1^2}t\exp\left(-\frac{\mu_1^2 r^2}{4t}\right) - \frac{1}{8\mu_1^2}(\mu_1^2 r^2+4t)\mathrm{E}_1\left(\frac{\mu_1^2 r^2}{4t}\right)\\ &- \frac{1}{2\mu_2^2}t\exp\left(-\frac{\mu_2^2 r^2}{4t}\right) + \frac{1}{8\mu_2^2}(\mu_2^2 r^2+4t)\mathrm{E}_1\left(\frac{\mu_2^2 r^2}{4t}\right)\Bigg],\end{aligned} \tag{6.60}$$

$$\Phi^{\mathrm{fsc}} = \Phi_1^{\mathrm{fsc}} + \Phi_2^{\mathrm{fsc}} \tag{6.61}$$

$$T^{\mathrm{fsc}} = -\frac{M\beta_{\mathrm{h}}}{4\pi S_{\mathrm{b}}c_{\mathrm{b}}c_{\mathrm{c}}}(\mu_1^2-\mu_2^2)\left[\mathrm{E}_1\left(\frac{\mu_1^2 r^2}{4t}\right) - \mathrm{E}_1\left(\frac{\mu_2^2 r^2}{4t}\right)\right], \tag{6.62}$$

$$\begin{aligned}p^{\mathrm{fsc}} = &\frac{c_{\mathrm{b}}\mu_1^2(m_{\mathrm{d}}-M\beta_{\mathrm{g}}\beta_{\mathrm{h}})-m_{\mathrm{d}}}{4\pi c_{\mathrm{b}}c_{\mathrm{c}}m_{\mathrm{d}}S_{\mathrm{c}}(\mu_1^2-\mu_2^2)}\mathrm{E}_1\left(\frac{\mu_1^2 r^2}{4t}\right)\\ &- \frac{c_{\mathrm{b}}\mu_2^2(m_{\mathrm{d}}-M\beta_{\mathrm{g}}\beta_{\mathrm{h}})-m_{\mathrm{d}}}{4\pi c_{\mathrm{b}}c_{\mathrm{c}}m_{\mathrm{d}}S_{\mathrm{c}}(\mu_1^2-\mu_2^2)}\mathrm{E}_1\left(\frac{\mu_2^2 r^2}{4t}\right),\end{aligned} \tag{6.63}$$

where we can also see the symmetry between ζ and s compared to (6.48), (6.49) and (6.44)-(6.47). Please note that these fundamental solutions only differ from those corresponding to the continuous heat source by substituting the following: $\Phi \leftrightarrow \Psi$, $c_b \leftrightarrow c_c$, $\beta_g \leftrightarrow \beta_h$, $m_d \leftrightarrow \frac{1}{M}$, $S_b \leftrightarrow S_c$ and omitting $\mathcal{T}_0$. The case hsc deals with the heat source and needs therefore a reference temperature. We define the following constants

$$K_3 \coloneqq \frac{M\beta_{\mathrm{h}}}{2\pi c_{\mathrm{c}}(\mu_1^2-\mu_2^2)} \tag{6.64}$$

$$K_4 \coloneqq \frac{1}{2\pi c_{\mathrm{b}}c_{\mathrm{c}}(\mu_1^2-\mu_2^2)} \tag{6.65}$$

and determine the displacement vector with the help of the considerations in the case of the continuous heat source

$$\begin{aligned}
u_i^{\mathrm{fsc}} &= \frac{\eta_{\mathrm{b}} M}{G}\Phi_{,i}^{\mathrm{fsc}} + \frac{\eta_{\mathrm{u}}}{m_{\mathrm{u}} G}\Psi_{,i}^{\mathrm{fsc}} \\
&= \frac{\eta_{\mathrm{b}} M}{G}\frac{\partial}{\partial x_i}\Phi^{\mathrm{fsc}} + \frac{\eta_{\mathrm{u}}}{m_{\mathrm{u}} G}\frac{\partial}{\partial x_i}\Psi^{\mathrm{fsc}} \\
&\overset{(6.55)}{=} \left(\frac{\eta_{\mathrm{u}}}{m_{\mathrm{u}} G} - \frac{\eta_{\mathrm{b}}}{\beta_{\mathrm{h}} G}\right) K_3 \left[-\frac{x_i \mu_1^2}{4}\mathrm{E}_1\left(\frac{\mu_1^2 r^2}{4t}\right) + \frac{x_i t}{r^2}\exp\left(-\frac{\mu_1^2 r^2}{4t}\right)\right. \\
&\qquad \left. + \frac{x_i \mu_2^2}{4}\mathrm{E}_1\left(\frac{\mu_2^2 r^2}{4t}\right) - \frac{x_i t}{r^2}\exp\left(-\frac{\mu_2^2 r^2}{4t}\right)\right] \\
&\quad + \frac{\eta_{\mathrm{b}} M}{G} K_4 \left[-\frac{x_i}{4}\mathrm{E}_1\left(\frac{\mu_1^2 r^2}{4t}\right) + \frac{x_i t}{r^2 \mu_1^2}\exp\left(-\frac{\mu_1^2 r^2}{4t}\right)\right. \\
&\qquad \left. + \frac{x_i}{4}\mathrm{E}_1\left(\frac{\mu_2^2 r^2}{4t}\right) - \frac{x_i t}{r^2 \mu_2^2}\exp\left(-\frac{\mu_2^2 r^2}{4t}\right)\right].
\end{aligned} \tag{6.66}$$

The following interrelations are obtained

$$\Psi^{\mathrm{fsc}} = \frac{K_3}{K_1}\Phi^{\mathrm{hsc}}, \tag{6.67}$$

$$\Phi_1^{\mathrm{fsc}} = -\frac{1}{M\beta_{\mathrm{h}}}\Psi^{\mathrm{fsc}} = -\frac{1}{M\beta_{\mathrm{h}}}\cdot\frac{K_3}{K_1}\Phi^{\mathrm{hsc}}, \tag{6.68}$$

$$\Phi_2^{\mathrm{fsc}} = \frac{K_4}{K_2}\Psi_2^{\mathrm{hsc}}. \tag{6.69}$$

With this, the fundamental solutions with superscript $\cdot^{\mathrm{fsc}}$ can be expressed with those with $\cdot^{\mathrm{hsc}}$.

6.3.4. Continuous Fluid and Heat Dipole

We obtain the dipole solution (a solution of source and sink pushed together) by differentiating the source solution with a negative sign, that means

$$\Phi_i^{\mathrm{hpc}} = -\Phi_{,i}^{\mathrm{hsc}}, \qquad \Psi_i^{\mathrm{hpc}} = -\Psi_{,i}^{\mathrm{hsc}}, \tag{6.70}$$

$$\Phi_i^{\mathrm{fpc}} = -\Phi_{,i}^{\mathrm{fsc}}, \qquad \Psi_i^{\mathrm{fpc}} = -\Psi_{,i}^{\mathrm{fsc}}. \tag{6.71}$$

This is necessary for the last case of the continuous force.

6.3.5. Continuous Force

The last case to consider is the continuous force given by the last combination

$$F_{ik} = \delta_{ik}\delta_x H(t-\tau); \gamma = \gamma_T = 0. \tag{6.72}$$

In this case the following fundamental solutions terms can in a first step be affiliated to some known from the continuous heat source (hsc) and continuous fluid source (fsc) and in a second step the terms of $\cdot^{\mathrm{fsc}}$ attributed to terms in $\cdot^{\mathrm{hsc}}$ (see (6.67),(6.68),(6.69)). Note that in the derivation of these fundamental solutions many derivatives and Laplace operators have to be applied and therefore, we try to reduce the terms to a minimum of different functions (here we reduce to Φ^{hsc} and Ψ_2^{hsc}). It holds true:

$$\begin{aligned}
\Phi_k^{\mathrm{Fc}} &= -\frac{\eta_{\mathrm{b}} M\kappa}{G}\Phi_k^{\mathrm{fpc}} - \frac{\eta_{\mathrm{u}} m_{\mathrm{d}}\kappa_{\mathrm{T}}}{m_{\mathrm{u}} G}\Phi_k^{\mathrm{hpc}} \\
&\overset{(6.70),(6.71)}{=} \frac{\eta_{\mathrm{b}} M\kappa}{G}\Phi_{,k}^{\mathrm{fsc}} + \frac{\eta_{\mathrm{u}} m_{\mathrm{d}}\kappa_{\mathrm{T}}}{m_{\mathrm{u}} G}\Phi_{,k}^{\mathrm{hsc}} \\
&\overset{(6.68)}{=} \frac{\eta_{\mathrm{b}} M\kappa}{G}\cdot\frac{K_4}{K_2}\Psi_{2,k}^{\mathrm{hsc}} + \left(\frac{\eta_{\mathrm{b}} M\kappa}{G}\cdot\left(\frac{-1}{M\beta_{\mathrm{h}}}\right)\cdot\frac{K_3}{K_1} + \frac{\eta_{\mathrm{u}} m_{\mathrm{d}}\kappa_{\mathrm{T}}}{m_{\mathrm{u}} G}\right)\Phi_{,k}^{\mathrm{hsc}} \\
&= \frac{\eta_{\mathrm{b}} M\kappa}{G}\cdot\frac{K_4}{K_2}\Psi_{2,k}^{\mathrm{hsc}} + \left(-\frac{\eta_{\mathrm{b}}\kappa}{G\beta_{\mathrm{h}}}\cdot\frac{K_3}{K_1} + \frac{\eta_{\mathrm{u}} m_{\mathrm{d}}\kappa_{\mathrm{T}}}{m_{\mathrm{u}} G}\right)\Phi_{,k}^{\mathrm{hsc}}, \qquad (6.73)\\
\Psi_k^{\mathrm{Fc}} &= -\frac{\eta_{\mathrm{b}} M\kappa}{G}\Psi_k^{\mathrm{fpc}} - \frac{\eta_{\mathrm{u}} m_{\mathrm{d}}\kappa_{\mathrm{T}}}{m_{\mathrm{u}} G}\Psi_k^{\mathrm{hpc}} \\
&\overset{(6.70),(6.71)}{=} \frac{\eta_{\mathrm{b}} M\kappa}{G}\Psi_{,k}^{fsc} + \frac{\eta_{\mathrm{u}} m_{\mathrm{d}}\kappa_{\mathrm{T}}}{m_{\mathrm{u}} G}\Psi_{,k}^{\mathrm{hsc}} \\
&\overset{(6.68)}{=} \frac{\eta_{\mathrm{b}} M\kappa}{G}\cdot\frac{K_3}{K_1}\Phi_{,k}^{\mathrm{hsc}} + \frac{\eta_{\mathrm{u}} m_{\mathrm{d}}\kappa_{\mathrm{T}}}{m_{\mathrm{u}} G}\Psi_{,k}^{\mathrm{hsc}} \\
&\overset{(6.45),(6.47)}{=} \left(\frac{\eta_{\mathrm{b}} M\kappa}{G}\cdot\frac{K_3}{K_1} - \frac{\eta_{\mathrm{u}} m_{\mathrm{d}}\kappa_{\mathrm{T}}}{m_{\mathrm{u}} G}\frac{m_{\mathrm{d}}}{\beta_{\mathrm{g}}}\right)\Phi_{,k}^{\mathrm{hsc}} + \frac{\eta_{\mathrm{u}} m_{\mathrm{d}}\kappa_{\mathrm{T}}}{m_{\mathrm{u}} G}\Psi_{2,k}^{\mathrm{hsc}}. \qquad (6.74)
\end{aligned}$$

For a better readability for the calculation of the components p^{Fc}, T^{Fc} and u^{Fc}, we define again constants

$$K_5 := -\frac{\eta_{\mathrm{b}}\kappa}{G\beta_{\mathrm{h}}}\cdot\frac{K_3}{K_1} + \frac{\eta_{\mathrm{u}} m_{\mathrm{d}}\kappa_{\mathrm{T}}}{m_{\mathrm{u}} G}, \qquad K_6 := \frac{\eta_{\mathrm{b}} M\kappa}{G}\cdot\frac{K_4}{K_2}, \qquad (6.75)$$

$$K_7 := \frac{\eta_{\mathrm{b}} M\kappa}{G}\cdot\frac{K_3}{K_1} - \frac{\eta_{\mathrm{u}} m_{\mathrm{d}}\kappa_{\mathrm{T}}}{m_{\mathrm{u}} G}\frac{m_{\mathrm{d}}}{\beta_{\mathrm{g}}}, \qquad K_8 := \frac{\eta_{\mathrm{u}} m_d\kappa_{\mathrm{T}}}{m_{\mathrm{u}} G}, \qquad (6.76)$$

and get

$$\Phi_k^{\mathrm{Fc}} = K_5\Phi_{,k}^{\mathrm{hsc}} + K_6\Psi_{2,k}^{\mathrm{hsc}}, \qquad (6.77)$$

$$\Psi_k^{\mathrm{Fc}} = K_7\Phi_{,k}^{\mathrm{hsc}} + K_8\Psi_{2,k}^{\mathrm{hsc}}. \qquad (6.78)$$

It is obtained (see (6.55))

$$\nabla_x \Phi^{\mathrm{hsc}} = K_1 \begin{pmatrix} x_1 \\ x_2 \end{pmatrix} \left[-\frac{\mu_1^2}{4} \mathrm{E}_1 \left(\frac{\mu_1^2 r^2}{4t} \right) + \frac{t}{r^2} \exp\left(-\frac{\mu_1^2 r^2}{4t} \right) + \frac{\mu_2^2}{4} \mathrm{E}_1 \left(\frac{\mu_2^2 r^2}{4t} \right) - \frac{t}{r^2} \exp\left(-\frac{\mu_2^2 r^2}{4t} \right) \right], \tag{6.79}$$

$$\nabla_x \Psi_2^{\mathrm{hsc}} = K_2 \begin{pmatrix} x_1 \\ x_2 \end{pmatrix} \left[-\frac{1}{4} \mathrm{E}_1 \left(\frac{\mu_1^2 r^2}{4t} \right) + \frac{t}{r^2 \mu_1^2} \exp\left(-\frac{\mu_1^2 r^2}{4t} \right) + \frac{1}{4} \mathrm{E}_1 \left(\frac{\mu_2^2 r^2}{4t} \right) - \frac{t}{r^2 \mu_2^2} \exp\left(-\frac{\mu_2^2 r^2}{4t} \right) \right]. \tag{6.80}$$

With (which is a fundamental solution in elasticity and given by [33])

$$u_{ik}^0 = \frac{1}{16\pi G(1-\nu_{\mathrm{b}})} \frac{1}{r} \left[\frac{x_i x_k}{r^2} + (3 - 4\nu_{\mathrm{b}}) \delta_{ik} \right], \tag{6.81}$$

we obtain the fundamental solution by

$$u_{ik}^{\mathrm{Fc}} = u_{ik}^0 + \frac{\eta_{\mathrm{b}} M}{G} \Phi_{k,i}^{\mathrm{Fc}} + \frac{\eta_{\mathrm{u}}}{m_{\mathrm{u}} G} \Psi_{k,i}^{\mathrm{Fc}}. \tag{6.82}$$

To obtain p_k and T_k, we use (6.40), (6.41) and (6.42). For the determination of the complete fundamental solutions, we have to apply the differential operator and the Laplacian on Φ_k^{Fc} and Ψ_k^{Fc} respectively on (6.79) and (6.80). First we consider the derivative with respect to x_1 and x_2 for the following part with μ_1 of (6.79). The other cases are obtained due to symmetry.

$$\begin{aligned}
&\frac{\partial}{\partial x_1} \left[\frac{-\mu_1^2 x_1}{4} \mathrm{E}_1 \left(\frac{\mu_1^2 r^2}{4t} \right) + \frac{x_1 t}{r^2} \exp\left(-\frac{\mu_1^2 r^2}{4t} \right) \right] \\
&\quad = -\frac{\mu_1^2}{4} \mathrm{E}_1 \left(\frac{\mu_1^2 r^2}{4t} \right) + \frac{\mu_1^2 x_1}{4} \cdot \frac{2x_1}{r^2} \exp\left(-\frac{\mu_1^2 r^2}{4t} \right) \\
&\qquad + \frac{t(x_2^2 - x_1^2)}{r^4} \exp\left(-\frac{\mu_1^2 r^2}{4t} \right) + \frac{x_1 t}{r^2} \exp\left(-\frac{\mu_1^2 r^2}{4t} \right) \cdot \left(-\frac{\mu_1^2 x_1}{2t} \right) \\
&\quad = -\frac{\mu_1^2}{4} \mathrm{E}_1 \left(\frac{\mu_1^2 r^2}{4t} \right) + \frac{\mu_1^2 x_1^2}{2r^2} \exp\left(-\frac{\mu_1^2 r^2}{4t} \right) \\
&\qquad + \frac{t(x_2^2 - x_1^2)}{r^4} \exp\left(-\frac{\mu_1^2 r^2}{4t} \right) - \frac{\mu_1^2 x_1^2}{2r^2} \exp\left(-\frac{\mu_1^2 r^2}{4t} \right) \\
&\quad = -\frac{\mu_1^2}{4} \mathrm{E}_1 \left(\frac{\mu_1^2 r^2}{4t} \right) + \frac{t(x_2^2 - x_1^2)}{r^4} \exp\left(-\frac{\mu_1^2 r^2}{4t} \right),
\end{aligned} \tag{6.83}$$

$$
\begin{aligned}
&\frac{\partial}{\partial x_2}\left[\frac{-\mu_1^2 x_1}{4}\mathrm{E}_1\left(\frac{\mu_1^2 r^2}{4t}\right)+\frac{x_1 t}{r^2}\exp\left(-\frac{\mu_1^2 r^2}{4t}\right)\right]\\
&\quad=\frac{\mu_1^2 x_1}{4}\cdot\frac{2x_2}{r^2}\exp\left(-\frac{\mu_1^2 r^2}{4t}\right)-\frac{2x_1x_2t}{r^4}\exp\left(-\frac{\mu_1^2 r^2}{4t}\right)\\
&\qquad+\frac{x_1 t}{r^2}\exp\left(-\frac{\mu_1^2 r^2}{4t}\right)\cdot\left(-\frac{\mu_1^2 x_2}{2t}\right)\\
&\quad=\frac{\mu_1^2 x_1 x_2}{2r^2}\exp\left(-\frac{\mu_1^2 r^2}{4t}\right)-\frac{2x_1x_2t}{r^4}\exp\left(-\frac{\mu_1^2 r^2}{4t}\right)-\frac{\mu_1^2 x_1x_2}{2r^2}\exp\left(-\frac{\mu_1^2 r^2}{4t}\right)\\
&\quad=-\frac{2x_1x_2t}{r^4}\exp\left(-\frac{\mu_1^2 r^2}{4t}\right). \qquad (6.84)
\end{aligned}
$$

We get

$$
\begin{aligned}
(6.79)_{1,1}&=K_1\left[-\frac{\mu_1^2}{4}\mathrm{E}_1\left(\frac{\mu_1^2 r^2}{4t}\right)+\frac{t(x_2^2-x_1^2)}{r^4}\exp\left(-\frac{\mu_1^2 r^2}{4t}\right)\right.\\
&\qquad\left.+\frac{\mu_2^2}{4}\mathrm{E}_1\left(\frac{\mu_1^2 r^2}{4t}\right)-\frac{t(x_2^2-x_1^2)}{r^4}\exp\left(-\frac{\mu_2^2 r^2}{4t}\right)\right], \qquad (6.85)\\
(6.79)_{1,2}&=K_1\left[-\frac{2x_1x_2t}{r^4}\exp\left(-\frac{\mu_1^2 r^2}{4t}\right)+\frac{2x_1x_2t}{r^4}\exp\left(-\frac{\mu_2^2 r^2}{4t}\right)\right], \qquad (6.86)\\
(6.79)_{2,1}&=K_1\left[-\frac{2x_1x_2t}{r^4}\exp\left(-\frac{\mu_1^2 r^2}{4t}\right)+\frac{2x_1x_2t}{r^4}\exp\left(-\frac{\mu_2^2 r^2}{4t}\right)\right], \qquad (6.87)\\
(6.79)_{2,2}&=K_1\left[-\frac{\mu_1^2}{4}\mathrm{E}_1\left(\frac{\mu_1^2 r^2}{4t}\right)+\frac{t(x_1^2-x_2^2)}{r^4}\exp\left(-\frac{\mu_1^2 r^2}{4t}\right)\right.\\
&\qquad\left.+\frac{\mu_2^2}{4}\mathrm{E}_1\left(\frac{\mu_1^2 r^2}{4t}\right)-\frac{t(x_1^2-x_2^2)}{r^4}\exp\left(-\frac{\mu_2^2 r^2}{4t}\right)\right]. \qquad (6.88)
\end{aligned}
$$

We obtain in general

$$
\begin{aligned}
(6.79)_{i,k}&=K_1\left[-\frac{\mu_1^2}{4}\mathrm{E}_1\left(\frac{\mu_1^2 r^2}{4t}\right)\delta_{ik}+\frac{t(r^2\delta_{ik}-2x_ix_k)}{r^4}\exp\left(-\frac{\mu_1^2 r^2}{4t}\right)\right.\\
&\qquad\left.+\frac{\mu_2^2}{4}\mathrm{E}_1\left(\frac{\mu_2^2 r^2}{4t}\right)\delta_{ik}-\frac{t(r^2\delta_{ik}-2x_ix_k)}{r^4}\exp\left(-\frac{\mu_2^2 r^2}{4t}\right)\right]. \qquad (6.89)
\end{aligned}
$$

Please note that we only have here the term of (6.79) with the μ_1-factor in front because the other one is the same with different signs.

Furthermore, we have some of the second derivatives required for the Laplacian. We get

$$\begin{aligned}
(6.79)^{\mu_1}_{1,11} &= K_1 \left[\frac{\mu_1^2}{4} \frac{2x_1}{r^2} \exp\left(-\frac{\mu_1^2 r^2}{4t}\right) + t \cdot \frac{2x_1^3 - 6x_1 x_2^2}{r^6} \exp\left(-\frac{\mu_1^2 r^2}{4t}\right) \right. \\
&\quad \left. + t \cdot \frac{x_2^2 - x_1^2}{r^4} \exp\left(-\frac{\mu_1^2 r^2}{4t}\right) \cdot \left(-\frac{\mu_1^2 x_1}{2t}\right) \right] \\
&= K_1 \left[\frac{\mu_1^2 x_1}{2r^2} \exp\left(-\frac{\mu_1^2 r^2}{4t}\right) + t \frac{2x_1^3 - 6x_1 x_2^2}{r^6} \exp\left(-\frac{\mu_1^2 r^2}{4t}\right) \right. \\
&\quad \left. - \exp\left(-\frac{\mu_1^2 r^2}{4t}\right) \frac{(x_2^2 - x_1^2) x_1 \mu_1^2}{2r^4} \right] \\
&= K_1 \left[\frac{\mu_1^2 x_1 (x_1^2 + x_2^2)}{r^4} \exp\left(-\frac{\mu_1^2 r^2}{4t}\right) + t \frac{2x_1^3 - 6x_1 x_2^2}{r^6} \exp\left(-\frac{\mu_1^2 r^2}{4t}\right) \right. \\
&\quad \left. - \exp\left(-\frac{\mu_1^2 r^2}{4t}\right) \frac{(x_2^2 - x_1^2) x_1 \mu_1^2}{2r^4} \right] \\
&= K_1 \left[\frac{\mu_1^2 x_1 (2x_1^2 + 2x_2^2 - x_2^2 + x_1^2)}{2r^4} \exp\left(-\frac{\mu_1^2 r^2}{4t}\right) \right. \\
&\quad \left. + t \frac{2x_1^3 - 6x_1 x_2^2}{r^6} \exp\left(-\frac{\mu_1^2 r^2}{4t}\right) \right] \\
&= K_1 \left[\frac{\mu_1^2 x_1 (3x_1^2 + x_2^2)}{r^4} \exp\left(-\frac{\mu_1^2 r^2}{4t}\right) + t \frac{2x_1^3 - 6x_1 x_2^2}{r^6} \exp\left(-\frac{\mu_1^2 r^2}{4t}\right) \right]
\end{aligned} \tag{6.90}$$

and

$$\begin{aligned}
(6.79)^{\mu_1}_{1,22} &= K_1 \left[-\frac{2x_1 t r^4 - 2x_1 x_2 t \cdot 2r^2 \cdot 2x_2}{r^8} \exp\left(-\frac{\mu_1^2 r^2}{4t}\right) \right. \\
&\quad \left. - \frac{2x_1 x_2 t}{r^4} \exp\left(-\frac{\mu_1^2 r^2}{4t}\right) \cdot \left(-\frac{\mu_1^2 x_2}{2t}\right) \right] \\
&= K_1 \left[-t \frac{2x_1 r^2 - 8x_1 x_2^2}{r^6} \exp\left(-\frac{\mu_1^2 r^2}{4t}\right) + \frac{\mu_1^2 x_1 x_2^2}{r^4} \exp\left(-\frac{\mu_1^2 r^2}{4t}\right) \right] \\
&= K_1 \left[-t \frac{2x_1^3 + 2x_1 x_2^2 - 8x_1 x_2^2}{r^6} \exp\left(-\frac{\mu_1^2 r^2}{4t}\right) + \frac{\mu_1^2 x_1 x_2^2}{r^4} \exp\left(-\frac{\mu_1^2 r^2}{4t}\right) \right] \\
&= K_1 \left[-t \frac{2x_1^3 - 6x_1 x_2^2}{r^6} \exp\left(-\frac{\mu_1^2 r^2}{4t}\right) + \frac{\mu_1^2 x_1 x_2^2}{r^4} \exp\left(-\frac{\mu_1^2 r^2}{4t}\right) \right].
\end{aligned} \tag{6.91}$$

The corresponding second derivatives of the second component are derived due to the symmetry. Furthermore, second derivatives of (6.80) are the same as (6.79) divided by the factor μ_1^2 for the first term and divided by μ_2^2 for the second term.

We get for the Laplacian for the first component and the term with μ_1

$$\begin{aligned}\nabla^2(6.79)^{\mu_1} &= (6.90) + (6.91)\\ &= K_1\mu_1^2\frac{x_1(3x_1^2+x_2^2+x_2^2)}{r^4}\exp\left(-\frac{\mu_1^2r^2}{4t}\right)\\ &= K_1\mu_1^2\frac{x_1(3x_1^2+2x_2^2)}{r^4}\exp\left(-\frac{\mu_1^2r^2}{4t}\right).\end{aligned} \tag{6.92}$$

All in all, we obtain for the thermoporoelastic components u, p and T with the help of (6.92) and together with (6.40), (6.41), (6.42), (6.77) and (6.78)

$$\begin{aligned}p_k^{\mathrm{Fc}} &= \frac{1}{S_{\mathrm{c}}}\nabla^2\Phi_k^{\mathrm{Fc}} + \frac{\beta_{\mathrm{g}}}{m_{\mathrm{d}}S_{\mathrm{c}}}\nabla^2\Psi_k^{\mathrm{Fc}} + \frac{\eta_{\mathrm{b}}M}{G}g_{1k}\\ &= \frac{1}{S_{\mathrm{c}}}\nabla^2\left(K_5\Phi_{,k}^{\mathrm{hsc}} + K_6\Psi_{2,k}^{\mathrm{hsc}}\right) + \frac{\beta_{\mathrm{g}}}{m_{\mathrm{d}}S_{\mathrm{c}}}\nabla^2\left(K_7\Phi_{,k}^{\mathrm{hsc}} + K_8\Psi_{2,k}^{\mathrm{hsc}}\right)\\ &\quad + \frac{\eta_{\mathrm{b}}M}{G}\frac{1}{2\pi}\frac{x_k}{r^2}\\ &= \left(\frac{1}{S_{\mathrm{c}}}K_5 + \frac{\beta_{\mathrm{g}}}{m_{\mathrm{d}}S_{\mathrm{c}}}K_7\right)\nabla^2\Phi_{,k}^{\mathrm{hsc}} + \left(\frac{1}{S_{\mathrm{c}}}K_6 + \frac{\beta_{\mathrm{g}}}{m_{\mathrm{d}}S_{\mathrm{c}}}K_8\right)\nabla^2\Psi_{2,k}^{\mathrm{hsc}} + \frac{\eta_{\mathrm{b}}M}{G}\frac{1}{2\pi}\frac{x_k}{r^2}\\ &= \left(\frac{1}{S_{\mathrm{c}}}K_5 + \frac{\beta_{\mathrm{g}}}{m_{\mathrm{d}}S_{\mathrm{c}}}K_7\right)K_1x_k(x_k^2+2r^2)\left[\frac{\mu_1^2}{r^4}\exp\left(-\frac{\mu_1^2r^2}{4t}\right) - \frac{\mu_2^2}{r^4}\exp\left(-\frac{\mu_2^2r^2}{4t}\right)\right]\\ &\quad + \left(\frac{1}{S_{\mathrm{c}}}K_6 + \frac{\beta_{\mathrm{g}}}{m_{\mathrm{d}}S_{\mathrm{c}}}K_8\right)K_2x_k(x_k^2+2r^2)\left[\frac{1}{r^4}\exp\left(-\frac{\mu_1^2r^2}{4t}\right) - \frac{1}{r^4}\exp\left(-\frac{\mu_2^2r^2}{4t}\right)\right]\\ &\quad + x_k\frac{\eta_{\mathrm{b}}M}{G}\frac{1}{2\pi}\frac{1}{r^2}\end{aligned} \tag{6.93}$$

and

$$\begin{aligned}T_k^{\mathrm{Fc}} &= \frac{\beta_{\mathrm{h}}M}{S_{\mathrm{b}}}\nabla^2\Phi_k^{\mathrm{Fc}} + \frac{1}{S_{\mathrm{b}}}\nabla^2\Psi_k^{\mathrm{Fc}} + \frac{\eta_{\mathrm{u}}}{m_{\mathrm{u}}G}g_{1k}\\ &= \frac{\beta_{\mathrm{h}}M}{S_{\mathrm{b}}}\nabla^2\left(K_5\Phi_{,k}^{\mathrm{hsc}} + K_6\Psi_{2,k}^{\mathrm{hsc}}\right) + \frac{1}{S_{\mathrm{b}}}\nabla^2\left(K_7\Phi_{,k}^{\mathrm{hsc}} + K_8\Psi_{2,k}^{\mathrm{hsc}}\right)\\ &\quad + \frac{\eta_{\mathrm{u}}}{m_{\mathrm{u}}G}\frac{1}{2\pi}\frac{x_k}{r^2}\\ &= \left(\frac{\beta_{\mathrm{h}}M}{S_{\mathrm{b}}}K_5 + \frac{1}{S_{\mathrm{b}}}K_7\right)\nabla^2\Phi_{,k}^{\mathrm{hsc}} + \left(\frac{\beta_{\mathrm{h}}M}{S_{\mathrm{b}}}K_6 + \frac{1}{S_{\mathrm{b}}}K_8\right)\nabla^2\Psi_{2,k}^{\mathrm{hsc}} + \frac{\eta_{\mathrm{u}}}{m_{\mathrm{u}}G}\frac{1}{2\pi}\frac{x_k}{r^2}\\ &= \left(\frac{\beta_{\mathrm{h}}M}{S_{\mathrm{b}}}K_5 + \frac{1}{S_{\mathrm{b}}}K_7\right)K_1x_k(x_k^2+2r^2)\left[\frac{\mu_1^2}{r^4}\exp\left(-\frac{\mu_1^2r^2}{4t}\right) - \frac{\mu_2^2}{r^4}\exp\left(-\frac{\mu_2^2r^2}{4t}\right)\right]\\ &\quad + \left(\frac{\beta_{\mathrm{h}}M}{S_{\mathrm{b}}}K_6 + \frac{1}{S_{\mathrm{b}}}K_8\right)K_2x_k(x_k^2+2r^2)\left[\frac{1}{r^4}\exp\left(-\frac{\mu_1^2r^2}{4t}\right) - \frac{1}{r^4}\exp\left(-\frac{\mu_2^2r^2}{4t}\right)\right]\\ &\quad + x_k\frac{\eta_{\mathrm{u}}}{m_{\mathrm{u}}G}\frac{1}{2\pi}\frac{1}{r^2}.\end{aligned} \tag{6.94}$$

Furthermore, we obtain with (6.82), (6.81), (6.77), (6.78) and (6.89)

$$\begin{aligned}
u_{ik}^{\mathrm{Fc}} &= u_{ik}^{0} + \frac{\eta_{\mathrm{b}} M}{G}\Phi_{k,i}^{\mathrm{Fc}} + \frac{\eta_{\mathrm{u}}}{m_{\mathrm{u}} G}\Psi_{k,i}^{\mathrm{Fc}} \\
&= \frac{1}{16\pi G(1-\nu_{\mathrm{b}})}\frac{1}{r}\left[\frac{x_i x_k}{r^2} + (3-4\nu_{\mathrm{b}})\delta_{ik}\right] \\
&\quad + \frac{\eta_{\mathrm{b}} M}{G}\left(K_5\left(\Phi_{,k}^{hsc}\right)_{,i} + K_6\left(\Psi_{2,k}^{hsc}\right)_{,i}\right) + \frac{\eta_{\mathrm{u}}}{m_{\mathrm{u}} G}\left(K_7\left(\Phi_{,k}^{hsc}\right)_{,i} + K_8\left(\Psi_{2,k}^{hsc}\right)_{,i}\right) \\
&= \frac{1}{16\pi G(1-\nu_{\mathrm{b}})}\frac{1}{r}\left[\frac{x_i x_k}{r^2} + (3-4\nu_{\mathrm{b}})\delta_{ik}\right] \\
&\quad + \left(\frac{\eta_{\mathrm{b}} M}{G}K_5 + \frac{\eta_{\mathrm{u}}}{m_{\mathrm{u}} G}K_7\right)\left(\Phi_{,k}^{hsc}\right)_{,i} + \left(\frac{\eta_{\mathrm{b}} M}{G}K_6 + \frac{\eta_{\mathrm{u}}}{m_{\mathrm{u}} G}K_8\right)\left(\Psi_{2,k}^{hsc}\right)_{,i} \\
&= \frac{1}{16\pi G(1-\nu_{\mathrm{b}})}\frac{1}{r}\left[\frac{x_i x_k}{r^2} + (3-4\nu_{\mathrm{b}})\delta_{ik}\right] \\
&\quad + \left(\frac{\eta_{\mathrm{b}} M}{G}K_5 + \frac{\eta_{\mathrm{u}}}{m_{\mathrm{u}} G}K_7\right) K_1\left[-\frac{\mu_1^2}{4}\mathrm{E}_1\left(\frac{\mu_1^2 r^2}{4t}\right)\delta_{ik} + \frac{t(\delta_{ik}r^2 - 2x_i x_k)}{r^4}\right. \\
&\quad \left.\times \exp\left(-\frac{\mu_1^2 r^2}{4t}\right) + \frac{\mu_2^2}{4}\mathrm{E}_1\left(\frac{\mu_2^2 r^2}{4t}\right)\delta_{ik} - \frac{t(r^2\delta_{ik} - 2x_i x_k)}{r^4}\exp\left(-\frac{\mu_2^2 r^2}{4t}\right)\right] \\
&\quad + \left(\frac{\eta_{\mathrm{b}} M}{G}K_6 + \frac{\eta_{\mathrm{u}}}{m_{\mathrm{u}} G}K_8\right) K_2\left[-\frac{1}{4}\mathrm{E}_1\left(\frac{\mu_1^2 r^2}{4t}\right)\delta_{ik} + \frac{t(\delta_{ik}r^2 - 2x_i x_k)}{r^4\mu_1^2}\right. \\
&\quad \left.\times \exp\left(-\frac{\mu_1^2 r^2}{4t}\right) + \frac{1}{4}\mathrm{E}_1\left(\frac{\mu_2^2 r^2}{4t}\right)\delta_{ik} - \frac{t(r^2\delta_{ik} - 2x_i x_k)}{r^4\mu_2^2}\exp\left(-\frac{\mu_2^2 r^2}{4t}\right)\right].
\end{aligned} \tag{6.95}$$

All in all, the fundamental solutions can be written as a fundamental solution tensor given by

$$G(x,t) = \begin{pmatrix} u_{11}^{\mathrm{Fc}} & u_{12}^{\mathrm{Fc}} & p_1^{\mathrm{Fc}} & T_1^{\mathrm{Fc}} \\ u_{21}^{\mathrm{Fc}} & u_{22}^{\mathrm{Fc}} & p_2^{\mathrm{Fc}} & T_2^{\mathrm{Fc}} \\ u_1^{\mathrm{fsc}} & u_2^{\mathrm{fsc}} & p^{\mathrm{fsc}} & T^{\mathrm{fsc}} \\ u_1^{\mathrm{hsc}} & u_2^{\mathrm{hsc}} & p^{\mathrm{hsc}} & T^{\mathrm{hsc}} \end{pmatrix} = \begin{pmatrix} u_{ik}^{\mathrm{Fc}} & p_k^{\mathrm{Fc}} & T_k^{\mathrm{Fc}} \\ \left(u_k^{\mathrm{fsc}}\right)^T & p^{\mathrm{fsc}} & T^{\mathrm{fsc}} \\ \left(u_k^{\mathrm{hsc}}\right)^T & p^{\mathrm{hsc}} & T^{\mathrm{hsc}} \end{pmatrix}. \tag{6.96}$$

7. Non-dimensionalization and reduction to poroelasticity

In this section, the dimensionless form of the governing equations of thermoporoelasticity are derived. Then, with these equations, we go over to the quasi-static equations of poroelasticity, where we also depict the appropriate fundamental solutions. We need these fundamental solutions afterwards for the construction of the scaling functions and wavelets for the decorrelation process.

7.1. Equations of Thermoporoelasticity in Dimensionless Form

The governing equations from the section above for the coupled case are given by

$$\left(K + \frac{G}{3}\right) \nabla(\nabla \cdot u) + G\nabla^2 u - \alpha \nabla p - \alpha_d \nabla T = 0, \tag{7.1}$$

$$\frac{\partial p}{\partial t} - \kappa M \nabla^2 p + \alpha M \frac{\partial(\nabla \cdot u)}{\partial t} - \beta_e M \frac{\partial T}{\partial t} = 0, \tag{7.2}$$

$$\frac{\partial T}{\partial t} - \kappa_T \nabla^2 T + \frac{\alpha_d}{m_d} \frac{\partial(\nabla \cdot u)}{\partial t} - \frac{\beta_e}{m_d} \frac{\partial p}{\partial t} = 0. \tag{7.3}$$

For the non-dimensionalization we define u_0 and t_0 as a characteristic length- and timescale and define

$$\check{x} = \frac{x}{x_0}, \quad \check{t} = \frac{t}{t_0}, \tag{7.4}$$

$$\check{u} = \frac{u}{x_0}, \quad \check{p} = \frac{p}{\mu}, \quad \check{T} = T \cdot \beta_e. \tag{7.5}$$

Please note that the entities marked with a $\check{}$ are dimensionless and x_0, μ and β_e are necessary constants to non-dimensionalize u, p and T. We start by inserting (7.4) and (7.5) in (7.1) and get

$$G\frac{x_0}{x_0^2}\nabla_{\check{x}}^2 \check{u} + \left(K + \frac{G}{3}\right) \frac{x_0}{x_0^2} \nabla_{\check{x}} (\nabla_{\check{x}} \cdot \check{u}) - \alpha \frac{\mu}{x_0} \nabla_{\check{x}} \check{p} - \alpha_d \frac{1}{\beta_e x_0} \nabla_{\check{x}} \check{T} = 0 \quad \left| \left(: \frac{\mu}{x_0} \right) \right.$$

$$\Leftrightarrow \quad \frac{G}{\mu}\nabla_{\check{x}}^2 \check{u} + \frac{\left(K + \frac{G}{3}\right)}{\mu} \nabla_{\check{x}} (\nabla_{\check{x}} \cdot \check{u}) - \alpha \nabla \check{p} - \frac{\alpha_d}{\beta_e \mu} \nabla_{\check{x}} \check{T} = 0. \tag{7.6}$$

Following the same way for (7.2) and (7.3) and choosing $t_0 = \frac{x_0^2}{\kappa\mu}$, we obtain

$$\begin{aligned}
\frac{\mu}{t_0}\frac{\partial \check{p}}{\partial \check{t}} - \kappa M \frac{\mu}{x_0^2}\nabla_{\check{x}}\check{p} + \alpha M \frac{1}{t_0}\frac{\partial\left(\nabla_{\check{x}}\cdot\check{u}\right)}{\partial \check{t}} - \beta_e M \frac{\partial \check{T}}{\partial \check{t}}\frac{1}{\beta_e t_0} = 0 \;\Big|\cdot \frac{t_0}{M} \\
\Leftrightarrow \frac{\mu}{M}\frac{\partial \check{p}}{\partial \check{t}} - \kappa\mu\frac{t_0}{x_0^2}\nabla_{\check{x}}^2\check{p} + \alpha\frac{\partial\left(\nabla_{\check{x}}\cdot\check{u}\right)}{\partial \check{t}} - \frac{\partial \check{T}}{\partial \check{t}} = 0 \\
\Leftrightarrow \frac{\mu}{M}\frac{\partial \check{p}}{\partial \check{t}} - \nabla_{\check{x}}^2\check{p} + \alpha\frac{\partial\left(\nabla_{\check{x}}\cdot\check{u}\right)}{\partial \check{t}} - \frac{\partial \check{T}}{\partial \check{t}} = 0, \qquad (7.7) \\
\frac{1}{t_0\beta_e}\frac{\partial \check{T}}{\partial \check{t}} - \kappa_T\frac{1}{x_0^2\beta_e}\nabla_{\check{x}}^2\check{T} + \frac{\alpha_d}{m_d}\frac{1}{t_0}\frac{\partial\left(\nabla_{\check{x}}\cdot\check{u}\right)}{\partial \check{t}} - \frac{\beta_e}{m_d}\cdot\frac{\mu}{t_0}\frac{\partial \check{p}}{\partial \check{t}} = 0 \;\Big|\cdot t_0\beta_e \\
\Leftrightarrow \frac{\partial \check{T}}{\partial \check{t}} - \frac{\kappa_T}{\kappa\mu}\nabla_{\check{x}}^2\check{T} + \frac{\alpha_d\beta_e}{m_d}\frac{\partial\left(\nabla_{\check{x}}\cdot\check{u}\right)}{\partial \check{t}} - \frac{\beta_e^2\mu}{m_d}\frac{\partial \check{p}}{\partial \check{t}} = 0. \qquad (7.8)
\end{aligned}$$

In the following, we omit the $\check{}$ for the sake of readability. From here on we always use the dimensionless quantities. Furthermore, we replace G and K by the more known Lamé constants λ and μ by the following rule: $G = \mu$ and $K = \lambda + \frac{2}{3}\mu$. Furthermore, we can write $1/M =: c_0$ as a specific storage coefficient (see [10]). We obtain the equations for thermoporoelasticity in dimensionless form:

$$\begin{aligned}
\nabla_x^2 u + \frac{\lambda+\mu}{\mu}\nabla_x\left(\nabla_x\cdot u\right) - \alpha\nabla p - \frac{\alpha_d}{\beta_e\mu}\nabla_x T = 0 \qquad (7.9) \\
c_0\mu\frac{\partial p}{\partial t} - \nabla_x^2 p + \alpha\frac{\partial\left(\nabla_x\cdot u\right)}{\partial t} - \frac{\partial T}{\partial t} = 0 \qquad (7.10) \\
\frac{\partial T}{\partial t} - \frac{\kappa_T}{\kappa\mu}\nabla_x^2 T + \frac{\alpha_d\beta_e}{m_d}\frac{\partial\left(\nabla_x\cdot u\right)}{\partial t} - \frac{\beta_e^2\mu}{m_d}\frac{\partial p}{\partial t} = 0. \qquad (7.11)
\end{aligned}$$

7.2. Governing Equations in Poroelasticity

Now we want to reduce the partial differential equations in thermoporoelasticity in dimensionless form to the case of poroelasticity. For this, we have to consider the equations (7.9)-(7.11) with a constant temperature. That means specifically that for a constant temperature T, the gradient $\nabla_x T$, the Laplacian $\nabla_x^2 T$ and the time derivative $\partial T/\partial t$ are zero and can be omitted. We obtain the dimensionless equations in poroelasticity by

$$\begin{aligned}
-\frac{\lambda+\mu}{\mu}\nabla_x(\nabla_x\cdot u) - \nabla_x^2 u + \alpha\nabla_x p = 0, \qquad (7.12) \\
\partial_t(c_0\mu p + \alpha(\nabla_x\cdot u)) - \nabla_x^2 p = 0. \qquad (7.13)
\end{aligned}$$

For the third equation (7.11), the following is left after setting the gradient and time derivative of T to zero

$$\frac{\alpha_d}{m_d}\frac{\partial(\nabla \cdot u)}{\partial t} - \frac{\beta_e \mu}{m_d}\frac{\partial p}{\partial t} = 0. \tag{7.14}$$

This equation is trivially true, because in the thermal uncoupled case, we mentioned that for this case the material constant m_d goes to infinity. With this assumption the terms on the left-hand side go to zero. That means for poroelasticity, the equations (7.12) and (7.13) are the governing equations, called the quasistatic equations of poroelasticity (briefly QEP). In Figure 7.1, the QEP are compared with the known differential equations from Section 3.2 (see also [72]), where we can see several similarities.

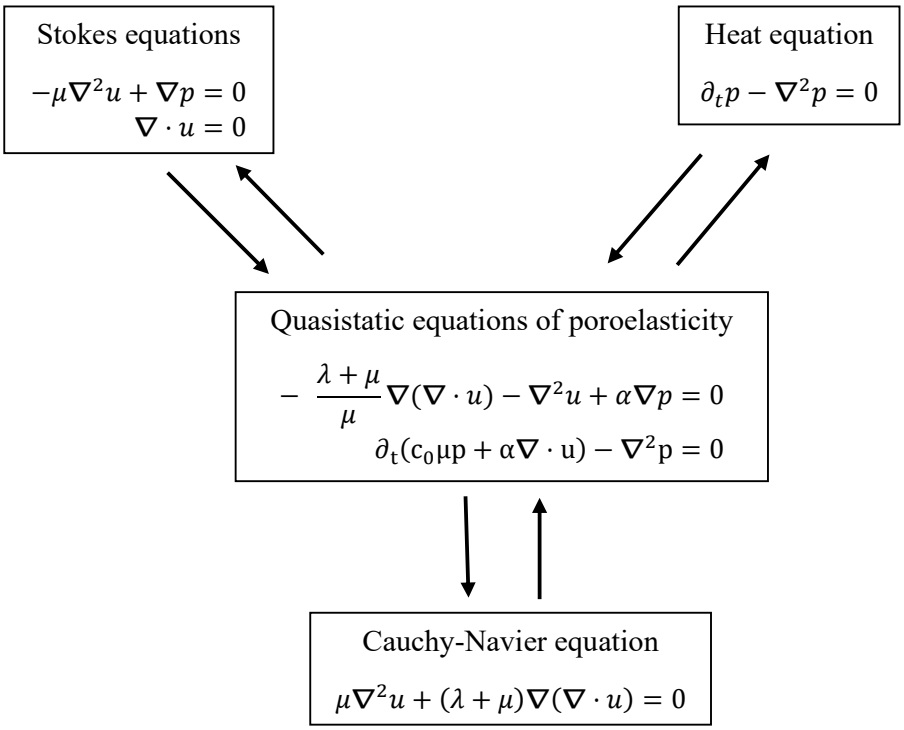

Figure 7.1.: Connection between the QEP and other known differential equations.

7.3. Fundamental Solutions in Poroelasticity

The QEP in dimensionless form are given by (see the considerations from above and [10])

$$-\frac{\lambda+\mu}{\mu}\nabla_x(\nabla_x \cdot u) - \nabla_x^2 u + \alpha\nabla_x p = f, \tag{7.15}$$

$$\partial_t(c_0 \mu p + \alpha(\nabla_x \cdot u)) - \nabla_x^2 p = h, \tag{7.16}$$

where we first have a look at the QEP in the inhomogeneous case following the way of [10]. Here f is the volume force and h results from the mass transport. With the help of the QEP, we define the poroelastic differential operator in the following way

$$L^{\mathrm{pe}}(u,p) = \begin{pmatrix} -\frac{\lambda+\mu}{\mu}\nabla_x(\nabla_x \cdot u) - \nabla_x^2 u + \alpha\nabla_x p \\ \partial_t(c_0\mu p + \alpha(\nabla_x \cdot u)) - \nabla_x^2 p \end{pmatrix}, \tag{7.17}$$

which we will use later for the construction of the source scaling functions. Please note that we only show here the basic idea of the derivation of the fundamental solutions again. A detailed proof for the dimensionless case can be found in [10] and cf. [34] for the non-dimensionless case. For the derivation of the fundamental solutions it is convenient to rearrange the QEP and express them in terms of the displacement u and the volumetric dimensionless fluid content change ζ, which depends on u and p, and is given by

$$\zeta \coloneqq c_0\mu p + \alpha(\nabla_x \cdot u). \tag{7.18}$$

This is similar to the derivation of the fundamental solutions in thermoporoelasticity. This trick has the advantage that the second equation in ζ is now uncoupled from u and leads us to the following

$$-\frac{c_0(\lambda+\mu)+\alpha^2}{c_0\mu}\nabla_x(\nabla_x \cdot u) - \nabla_x^2 u = f - \frac{\alpha}{c_0\mu}\nabla_x\zeta, \tag{7.19}$$

$$\partial_t\zeta - \frac{\lambda+2\mu}{c_0\mu(\lambda+2\mu)+\mu\alpha^2}\nabla_x^2\zeta = \frac{\alpha}{c_0(\lambda+2\mu)+\alpha^2}\nabla_x \cdot f + h. \tag{7.20}$$

That means we can solve (7.19) and (7.20) for u and ζ. In a next step, we can determine p from u and ζ by using the connection in (7.18). For the sake of readability there are the following abbreviations for some material constants which result from the determination of the fundamental solutions (see [10])

$$C_1 \coloneqq \frac{\alpha}{c_0(\lambda+2\mu)+\alpha^2}, \qquad C_2 \coloneqq \frac{\lambda+2\mu}{c_0\mu(\lambda+2\mu)+\mu\alpha^2}, \tag{7.21}$$

$$C_3 \coloneqq \frac{c_0(\lambda+3\mu)+\alpha^2}{2(c_0(\lambda+2\mu)+\alpha^2)}, \qquad C_4 \coloneqq \frac{c_0(\lambda+\mu)+\alpha^2}{c_0(\lambda+3\mu)+\alpha^2}. \tag{7.22}$$

Remark 7.3.1. *Please note that $C_1, C_2, C_3, C_4 > 0$ holds true for the constants because they consist of positive material constants. This is helpful for us later for the theoretical part.*

Remark 7.3.2. *For the graphic representation of the fundamental solutions and their regularized versions and wavelets, we use material constants from Berea sandstone (which are also used in [10]) which are given by*

$$\lambda = 4 \times 10^9, \quad \mu = 6 \times 10^9, \quad \alpha = 0.867, \quad c_0\mu = 0.461. \tag{7.23}$$

With the help of a so-called Biot decomposition, the fundamental solutions can be calculated (see [10, 33]). They are on the plane $\mathbb{R}^2$ given by

$$p^{\mathrm{Si}}(x,t) = \frac{1}{4\pi t}\exp\left(-\frac{\|x\|^2}{4C_2t}\right), \tag{7.24}$$

$$u^{\mathrm{Si}}(x,t) = C_1\frac{x}{2\pi\|x\|^2}\left(1-\exp\left(-\frac{\|x\|^2}{4C_2t}\right)\right), \tag{7.25}$$

$$p^{\mathrm{Fi}}(x,t) = C_1\frac{x}{2\pi\|x\|^2}\delta_t - C_1C_2\frac{2}{\pi}\frac{x}{(4C_2t)^2}\exp\left(-\frac{\|x\|^2}{4C_2t}\right), \tag{7.26}$$

$$\begin{aligned}\boldsymbol{u}^{\mathrm{Fi}}_{ki}(x,t) = {} & C_3\frac{1}{2\pi}\left(-\delta_{ki}\ln(\|x\|)+C_4\frac{x_ix_k}{\|x\|^2}\right)\delta_t \\ & + C_1^2\frac{1}{2\pi\|x\|^2}\left[\left(\delta_{ik}-\frac{2x_ix_k}{\|x\|^2}\right)\left(1-\exp\left(-\frac{\|x\|^2}{4C_2t}\right)\right)\right. \\ & \left.+\frac{2}{4C_2t}x_ix_k\exp\left(-\frac{\|x\|^2}{4C_2t}\right)\right].\end{aligned} \tag{7.27}$$

In the following, we consider the QEP from (7.12) and (7.13) with vanishing right-hand sides, that means $f \equiv 0$, $h \equiv 0$. Please note that we first go back to the equations with unknown u and ζ again for the homogeneous QEP for the determination of the fundamental solutions. With this assumption, (7.19) and (7.20) in u and ζ simplify to

$$-\frac{c_0(\lambda+\mu)+\alpha^2}{c_0\mu}\nabla_x(\nabla_x\cdot u) - \nabla_x^2 u = -\frac{\alpha}{c_0\mu}\nabla_x\zeta \tag{7.28}$$

$$\partial_t\zeta - C_2\nabla_x^2\zeta = 0. \tag{7.29}$$

We have the homogeneous heat equation (7.29) for ζ and an inhomogeneous Cauchy-Navier equation (7.28) for u. With the help of a Biot decomposition again, we get the alternative fundamental solution tensor $\boldsymbol{G}^{\mathrm{alt}}$ (for now in u and ζ) for (7.28) and (7.29) by

$$\boldsymbol{G}^{\mathrm{alt}}(x,t) = \begin{pmatrix}\boldsymbol{u}^{\mathrm{CN}}(x)\delta_t & 0\\ u^{\mathrm{Si}}(x,t) & G^{\mathrm{Heat}}(x,t)\end{pmatrix}. \tag{7.30}$$

That means the fundamental solutions in $\boldsymbol{G}^{\mathrm{alt}}$ belonging to u and ζ are an intermediate step to our fundamental solution tensor for (7.12) and (7.13) with $f \equiv h \equiv 0$. Getting back to the origin variables u and p means calculating then p from ζ and u (see (7.18) and [10]) and our fundamental solution tensor $\boldsymbol{G}$ in u and p reads

$$\boldsymbol{G}(x,t) = \begin{pmatrix}\boldsymbol{u}^{\mathrm{CN}}(x)\delta_t & p^{\mathrm{St}}(x)\delta_t\\ u^{\mathrm{Si}}(x,t) & p^{\mathrm{Si}}(x,t)\end{pmatrix} \tag{7.31}$$

with the following entries

$$p^{\mathrm{Si}}(x,t) = \frac{1}{4\pi t}\exp\left(-\frac{\|x\|^2}{4C_2 t}\right), \tag{7.32}$$

$$u^{\mathrm{Si}}(x,t) = C_1\frac{x}{2\pi\|x\|^2}\left(1-\exp\left(-\frac{\|x\|^2}{4C_2 t}\right)\right), \tag{7.33}$$

$$p^{\mathrm{St}}(x) = C_1\frac{x}{2\pi\|x\|^2}, \tag{7.34}$$

$$\boldsymbol{u}_{ki}^{\mathrm{CN}}(x) = C_3\frac{1}{2\pi}\left(-\delta_{ki}\ln(\|x\|)+C_4\frac{x_i x_k}{\|x\|^2}\right). \tag{7.35}$$

That means our differential operator (7.17) applied to the fundamental solution tensor yields the following

$$L^{\mathrm{pe}}(\boldsymbol{G}) = I\delta_x\delta_t, \tag{7.36}$$

where I is the identity matrix. Please note here that the application of the differential operator is applied row-wise like in the case of the divergence (see (2.13)). These fundamental solutions are on the one hand necessary for the method of fundamental solutions (briefly MFS, for more information about the MFS in poroelasticity see [10]) to approximate given data for u and p and on the other hand for the decorrelation of u and p at which we are aiming. Please note the similarity of some of them by comparison with the fundamental solutions for more known partial differential equations given in Section 3.3.

Part III.

Multiscale Decorrelation for Poroelasticity

8. Regularized Fundamental Solutions

This chapter starts with a short overview of the concept of decorrelation for the Laplace case and the construction of the relevant source scaling functions appropriate for the multiscale mollifier approach. The idea and the realization for this are given in [61] with more details. Furthermore, in [71] the method was worked out theoretically for gravimetry and the numerical realization was done in [21] and [26]. For more information see the mentioned literature in the introduction. With this knowledge, we go over to the construction of the appropriate functions in poroelasticity and present some theoretical results.

8.1. Laplace and Generalization

We now start with the Laplace equation and explain the approach of the mollifier fundamental solution and the corresponding potential and source scaling functions. The development of these two types of scaling functions is physically motivated and takes the Newton integral equation as a starting point. We have a body $\mathcal{B}$ and its gravitational potential V in its exterior $\mathbb{R}^3 \setminus \overline{\mathcal{B}}$ is given by

$$V(x) = \gamma \int_{\mathcal{B}} G(\Delta; \|x - y\|)\rho(y)\, \mathrm{d}y, \quad x \in \mathbb{R}^3 \setminus \mathcal{B}. \tag{8.1}$$

Here γ is the gravitational constant and ρ is the density function. Since the description here is very short, please see for example [21, 25, 61] for further details to this approach. For more general information on the Newton integral equation, we refer for example to [61, 63] and the references therein. Please note that we have a look at the 3-dimensional case whereas our fundamental solutions for poroelasticity below are 2-dimensional in the spatial part. The fundamental solution of the Laplace equation is in the 3-dimensional case given by (here we replaced $\|x\|$ by r)

$$G(\Delta; r) = -\frac{1}{4\pi r}. \tag{8.2}$$

In the next step, we want to avoid the singularity of the fundamental solution in $r = 0$ by applying a Taylor expansion for r in the zero point. This is also called a regularization or a mollification that means using these two phrases implies the

same procedure. First we set $r = \sqrt{u}$ and get for the expansion up to the linear term

$$\frac{1}{\sqrt{u}} = \frac{1}{\sqrt{u_0}} - \frac{1}{2u_0^{3/2}}(u - u_0) + \mathcal{O}\left((u - u_0)^2\right) \quad \text{as } u \to u_0. \tag{8.3}$$

Replacing u by $\|x\|^2$ and u_0 by τ^2 leads us to

$$\frac{1}{\|x\|} \approx \frac{1}{\tau} - \frac{1}{2\tau^3}(\|x\|^2 - \tau^2). \tag{8.4}$$

With this, we define our regularized fundamental solution as a mollification of G piecewise in the following way

$$G_\tau(\Delta; \|x\|) \coloneqq \begin{cases} -\frac{1}{4\pi\|x\|}, & \|x\| \geq \tau, \\ -\frac{1}{4\pi}\left(\frac{1}{\tau} - \frac{1}{2\tau^3}(\|x\|^2 - \tau^2)\right), & \|x\| < \tau. \end{cases} \tag{8.5}$$

We use for $\|x\| \geq \tau$ the fundamental solution itself and for $\|x\| < \tau$ the modified variety of it. This function G_τ is also called the "potential scaling function". For the Laplace case in Figure 8.1 the fundamental solution $G(\Delta; r)$ and $G_\tau(\Delta; \|x\|)$ for selected values of τ are shown. We see that the difference between the funda-

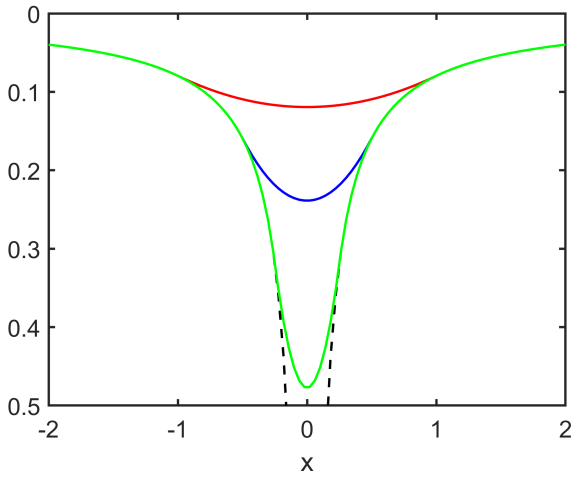

Figure 8.1.: The Laplace fundamental solution $G(\Delta; r)$ (dashed black) and its potential scaling function $G_\tau(\Delta; \|x\|)$ for $\tau = 1$ (red), $\tau = 0.5$ (blue) and $\tau = 0.25$ (green).

mental solution and the potential scaling function gets smaller with decreasing parameter τ.

Remark 8.1.1. *Please note that in [21, 25, 61] the Taylor mollification was done up to order n but this is not necessary here because we only want to show the main idea of the mollification.*

In a next step, we apply the Laplace operator on G_τ. The result is the so-called "source scaling function" Φ_τ and is given by

$$\begin{aligned}\Phi_\tau := \Delta G_\tau &= \Delta\left(-\frac{1}{4\pi}\left(\frac{1}{\tau} - \frac{1}{2\tau^3}(\|x\|^2 - \tau^2)\right)\right) \\ &= \frac{1}{4\pi}\frac{6}{2\tau^3} \\ &= \frac{3}{4\pi\tau^3}\end{aligned} \tag{8.6}$$

for $\|x\| < \tau$. In the case $\|x\| \geq \tau$, the application of the Laplace operator is the application on the fundamental solution itself and results in zero, because outside of the zero point, the fundamental solution is harmonic. Therefore the source scaling function has compact support. The source scaling function for selected parameters of τ can be seen in Figure 8.2. Due to the construction, we have a

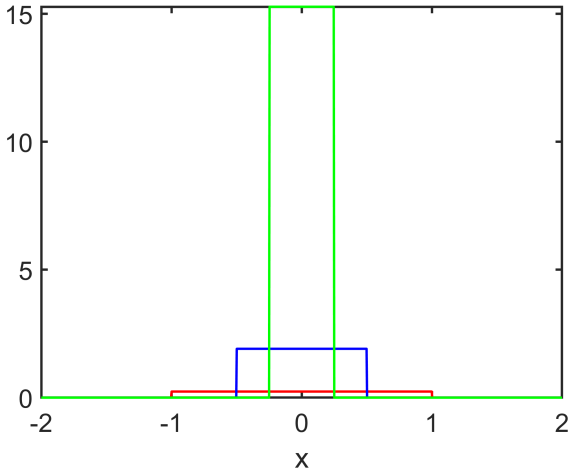

Figure 8.2.: The source scaling function $\Phi_\tau(\|x\|)$ in the Laplace case for $\tau = 1$ (red), $\tau = 0.5$ (blue) and $\tau = 0.25$ (green).

shrinking support of the source scaling function for a decreasing parameter τ. With the potential and source scaling functions, we can define the "τ-Newton potential functions" by

$$V_\tau(x) := \int_{\mathcal{B}} G_\tau(\Delta; \|x - y\|)\rho(y)\,\mathrm{d}y \tag{8.7}$$

and the "τ-Newton contrast functions" given by

$$\rho_\tau(x) = \int_{\mathcal{B}} \Phi_\tau(\|x - y\|)\rho(y)\,\mathrm{d}y. \tag{8.8}$$

The second convolution integral will later be the interesting one for us, because our aim in poroelasticity is to do a decorrelation of given data. Now we go over to a more general statement, which will be helpful for us later. We pursue the following ansatz for a more arbitrary function, where we can show that the mollification is in $\mathrm{C}^{(1)}$. First we start with a radially symmetric function. We want to regularize the radially symmetric function $f(\|x\|)$ with the help of a one-dimensional Taylor expansion up to the first order conform to the same principle as for the Laplace case. Please note our designations: We name the Taylor modified function itself with the index reg (for example f_{reg}) whereas the index τ denotes the composite function, that means the fundamental solution itself for $\|x\| \geq \tau$ and the Taylor modified variety for $\|x\| < \tau$ (for example f_τ). We have a look at a radially symmetric function in general and obtain by a Taylor expansion in u_0 for $f(\sqrt{u})$ for $\|x\| < \tau$

$$f_{\mathrm{reg}}(u) \coloneqq f(\sqrt{u_0}) + \left(\frac{\partial}{\partial u} f(\sqrt{u})\right)\Big|_{u=u_0} (u - u_0). \tag{8.9}$$

The substitutions $u = \|x\|^2$ and $u_0 = \tau^2$ yield

$$\begin{aligned} f_{\mathrm{reg}}(u) &= f(\tau) + \left(\frac{\partial}{\partial u} f(\sqrt{u})\right)\Big|_{u=\tau^2} (\|x\|^2 - \tau^2) \\ &= f(\tau) + \left(f'(\sqrt{u}) \cdot \frac{1}{2\sqrt{u}}\right)\Big|_{u=\tau^2} (\|x\|^2 - \tau^2) \\ &= f(\tau) + f'(\tau)\frac{1}{2\tau}(\|x\|^2 - \tau^2). \end{aligned} \tag{8.10}$$

We call the composite function f_τ the Taylor mollification of f, that means

$$f_\tau(x) \coloneqq \begin{cases} f(\|x\|), & \|x\| > \tau, \\ f(\tau) + f'(\tau)\frac{1}{2\tau}(\|x\|^2 - \tau^2), & \|x\| < \tau. \end{cases} \tag{8.11}$$

We want to show the $\mathrm{C}^{(1)}$ property of our function f_τ.

Lemma 8.1.2. *The Taylor mollification for the radially symmetric continuously differentiable function $f(\|x\|)$ given by*

$$f_\tau(x) \coloneqq \begin{cases} f(\|x\|), & \|x\| > \tau, \\ f(\tau) + f'(\tau)\frac{1}{2\tau}(\|x\|^2 - \tau^2), & \|x\| < \tau, \end{cases} \tag{8.12}$$

fulfills the property $\mathrm{C}^{(1)}$.

Proof. It is easy to see that f_τ is continuous at the transition point for $\|x\| = \tau$ if we insert this. We now want to show the same property for the gradient. We consider the gradient of f and f_{reg} and compare them for $\|x\| = \tau$:

$$\nabla_x f(\|x\|) = f'(\|x\|) \cdot \frac{x}{\|x\|}, \tag{8.13}$$

$$\nabla_x f_{\text{reg}}(x) = f'(\tau)\frac{x}{\tau}. \tag{8.14}$$

We can now see that they are equal if we insert $\tau = \|x\|$ in $\nabla_x f_{\text{reg}}$. □

With this we go over to the more general function F, which is not radially symmetric any more. We write F in the following way $F(x) = f(\|x\|)g(x_1)h(x_2)$ and only regularize the f-function. With the help of the regularization from above, we get

$$F_\tau(x) := \begin{cases} f(\|x\|)g(x_1)h(x_2), & \|x\| > \tau, \\ f_{\text{reg}}(\|x\|)g(x_1)h(x_2), & \|x\| < \tau. \end{cases} \tag{8.15}$$

We can show here again the $\mathrm{C}^{(1)}$- property in the following theorem.

Theorem 8.1.3. *Let f, g and h be continuously differentiable functions. The regularization for the function $F(x) = f(\|x\|)g(x_1)h(x_2)$ given by*

$$F_\tau(x) := \begin{cases} f(\|x\|)g(x_1)h(x_2), & \|x\| > \tau, \\ f_{\text{reg}}(\|x\|)g(x_1)h(x_2), & \|x\| < \tau, \end{cases} \tag{8.16}$$

is in $\mathrm{C}^{(1)}$.

Proof. The continuously differentiability of F_τ is given by the lemma above, because here we have a product of $\mathrm{C}^{(1)}$-functions. □

After this short introduction of the approach of mollified fundamental solutions, we go over to the QEP. Our aim is to apply the technique above to the fundamental solutions of the QEP and construct potential and source scaling functions in an analogous way. In the case of poroelasticity, we have a fundamental solution tensor and additionally some time dependent functions. Our main aim here is the decomposition of poroelastic data into their components via the application of low-pass and band-pass filter.

8.2. Mollification of the Fundamental Solution Tensor

In this section, we want to adopt the approach from the Laplace equation to our application poroelasticity and its appropriate fundamental solutions. For the development process of the physically relevant functions, we have a look at Figure 8.3 (scheme adopted from [21]) which is more detailed with the intermediate steps than the introduction for the Laplace case. In this overview, we can see the construction of the potential and source scaling functions resulting from the mollification of the fundamental solution (tensor) on the left-hand-side. On the

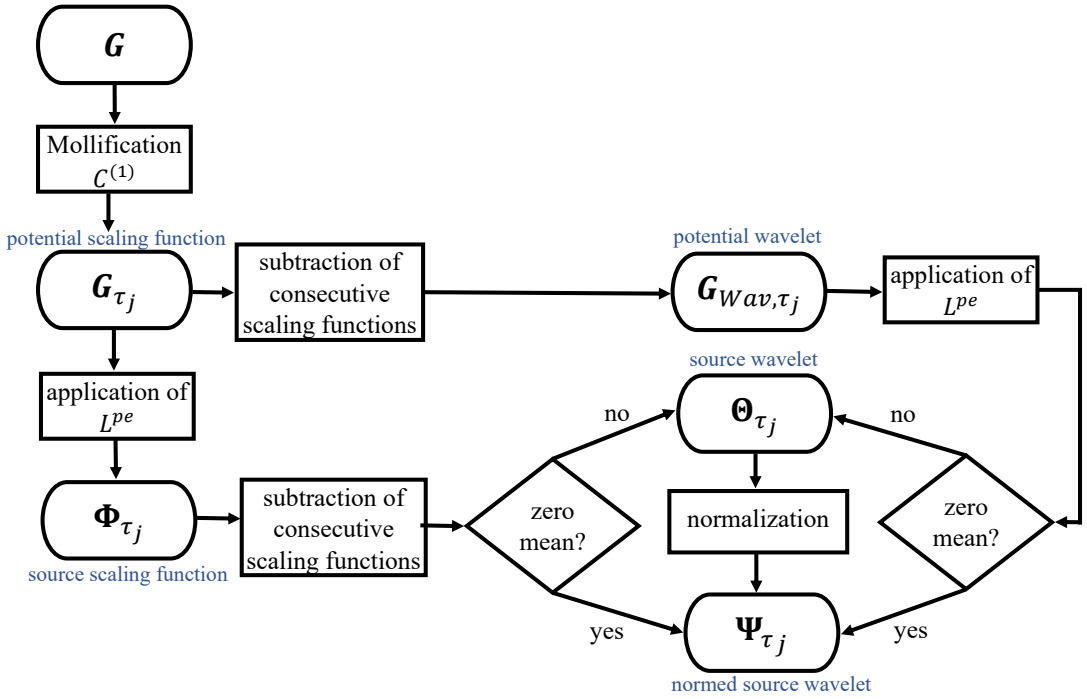

Figure 8.3.: Flowchart showing the process of obtaining the relevant scaling functions and wavelets in the case of poroelasticity. The left-hand side indicates the design of the scaling functions and the right-hand side the construction of the corresponding wavelets.

right-hand side, the resulting potential and normed source wavelets are shown. Depending on the application, one uses the potential scaling function in combination with the potential wavelet or the source scaling functions together with the normed source wavelets for the decorrelation. In our case, the latter combination is interesting for the multiscale decomposition of poroelastic data with the background that we want to uncover structures in the data that cannot be seen in the whole picture. For our decorrelation, we need the fundamental solutions, more precisely the fundamental solution tensor, from Section 7.3 and especially since the fundamental solutions have singularities, we want to mollify them (cf. for example [21] for Laplace's, Helmholtz' and d'Alembert's equation, [25] for Laplace's equation and [22] for the Cauchy-Navier equation and the references therein). In the following, we will have a look at each fundamental solution separately because they are too different in their form to consider them together. We use the same notation as before and name the Taylor modified function itself with the index reg (for example $p^{\mathrm{St}}_{1,\mathrm{reg}}$) and the index τ denotes the composite function, that means the fundamental solution itself for $\|x\| \geq \tau$ and the Taylor modified variety for $\|x\| < \tau$ (for example $p^{\mathrm{St}}_{1,\tau}$, see also (8.5) and Lemma 8.1.2 for the no-

tation). We follow the same principle as in the Laplace case and start with the fundamental solution p^{St}.

8.2.1. p^{St}

The fundamental solution

$$p^{\mathrm{St}}(x) = C_1 \frac{x}{2\pi \|x\|^2} \tag{8.17}$$

has a singularity for $x = (0, 0)$ (see also Figure 8.4), because the norm $\|x\|^2$ appears in the denominator.

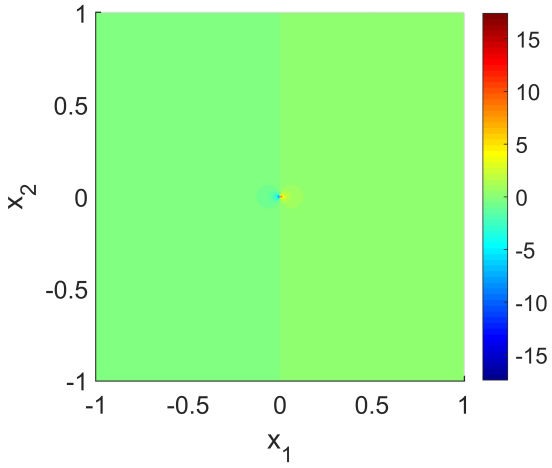

Figure 8.4.: The first component of the fundamental solution p^{St} with its singularity in the zero point.

For the regularization, we write p^{St} as a gradient in the following way

$$\frac{x}{\|x\|^2} = \frac{1}{2} \nabla_x \left(\ln \left(\|x\|^2 \right) \right). \tag{8.18}$$

Then we do a Taylor mollification of $\ln\left(\|x\|^2\right)$ and afterwards apply the gradient to it. Please note that we want to regularize p^{St} up to the linear Taylor term, that means we have to regularize the $\ln$-function above up to the quadratic term because of the application of the gradient then. With a Taylor expansion in u (we write $\|x\|^2 = u$) we get

$$\begin{aligned}
\frac{1}{2} \ln u &= \frac{1}{2} \left(\ln u_0 + \frac{1}{u_0}(u - u_0) - \frac{1}{2u_0^2}(u - u_0)^2 \right) + \mathcal{O}\left((u - u_0)^3\right) \\
&= \frac{1}{2} \left(\ln u_0 + \frac{u}{u_0} - 1 - \frac{u^2}{2u_0^2} + \frac{u}{u_0} - \frac{1}{2} \right) + \mathcal{O}\left((u - u_0)^3\right) \\
&= \frac{1}{2} \left(\ln u_0 + \frac{2u}{u_0} - \frac{3}{2} - \frac{u^2}{2u_0^2} \right) + \mathcal{O}\left((u - u_0)^3\right) \quad \text{as } u \to u_0.
\end{aligned} \tag{8.19}$$

Replacing u_0 by τ^2 and u by r^2 respectively $\|x\|^2$, we obtain for the regularized fundamental solution

$$p^{\mathrm{St}}_{\mathrm{reg}}(x) \coloneqq \frac{C_1}{2\pi} \cdot \frac{1}{2} \nabla_x \left(\ln \tau^2 + \frac{2\|x\|^2}{\tau^2} - \frac{3}{2} - \frac{\|x\|^4}{2\tau^4} \right). \tag{8.20}$$

We call τ here the regularization parameter (see also Section 8.1). Now we apply the gradient to the regularized function and get

$$\begin{aligned} \nabla_x \left(\frac{1}{2} \left(\ln \tau^2 + \frac{2\|x\|^2}{\tau^2} - \frac{3}{2} - \frac{\|x\|^4}{2\tau^4} \right) \right) &= \frac{1}{2} \left(\frac{2 \cdot 2x}{\tau^2} - \frac{2\|x\|^2 \cdot 2x}{2\tau^4} \right) \\ &= x \left(\frac{2}{\tau^2} - \frac{\|x\|^2}{\tau^4} \right). \end{aligned} \tag{8.21}$$

We obtain the regularized fundamental solution as a combination of the fundamental solution itself and the modified variety of it, that means

$$p^{\mathrm{St}}_{\tau}(x) \coloneqq \begin{cases} \frac{C_1}{2\pi} \frac{x}{\|x\|^2}, & \|x\| \geq \tau, \\ \frac{C_1}{2\pi} \frac{x}{\tau^2} \left(2 - \frac{\|x\|^2}{\tau^2} \right), & \|x\| < \tau. \end{cases} \tag{8.22}$$

Note that in the way we regularized the fundamental solution, the gradient of $p^{\mathrm{St}}_{\mathrm{reg}}$ and p^{St} correspond to each other at the transition for every (x_1, x_2) with $\|x\| = \tau$ (see Theorem 8.1.3 for the general case) and therefore $p^{\mathrm{St}}_{\tau} \in \mathrm{C}^{(1)}$. We choose $\{\tau_j\}_{j \in \mathbb{N}}$ as a positive, monotonically decreasing sequence with the property $\lim_{j \to \infty} \tau_j = 0$. We will choose $\tau_j = 2^{-j}$ (see also Definition 4.1.3 and Remark 4.1.4). Figure 8.5 shows the first component of the regularized fundamental solution for different parameters τ_j.

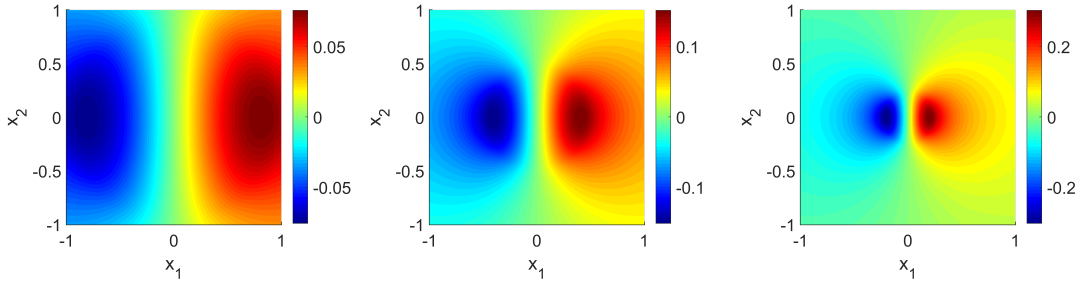

(a) $j = 0$ (b) $j = 1$ (c) $j = 2$

Figure 8.5.: The first component of the regularized fundamental solution $p^{\mathrm{St}}_{\tau_j}$ for selected parameters j.

The regularized fundamental solution approaches to the fundamental solution for increasing j.

The "τ_j-fundamental wavelet function " for p_τ^{St} is constructed in the following way

$$p_{\mathrm{Wav},\tau_j}^{\mathrm{St}} := p_{\tau_j}^{\mathrm{St}} - p_{\tau_{j-1}}^{\mathrm{St}}. \tag{8.23}$$

In Figure 8.6 the corresponding wavelets of the first component are shown.

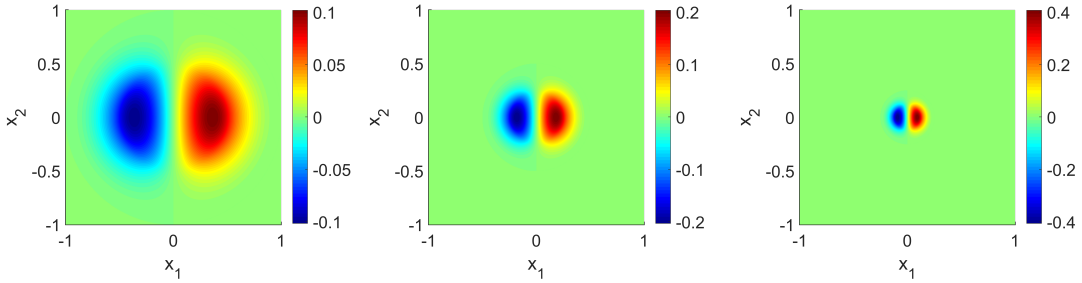

(a) $j = 1$ (b) $j = 2$ (c) $j = 3$

Figure 8.6.: The wavelets for the first component of $p_{\mathrm{Wav},\tau_j}^{\mathrm{St}}$ for selected parameters j.

Due to the construction of the wavelets, they have compact support. We can show that the regularized fundamental solution converges weakly to the fundamental solution for $\tau \to 0+$ (see Theorem 8.2.2 below). But first we want to have a look at the functions $L(x) = \frac{1}{\|x\|^2}$ and $N(x) = -\ln\|x\|$ and their Taylor mollifications, which we obtain by the same principle as in the case of Lemma 8.1.2 and p^{St} and are given by

$$\frac{1}{u} \approx \frac{1}{u_0} - \frac{1}{u_0^2}(u - u_0) = \frac{2}{u_0} - \frac{u}{u_0^2}, \tag{8.24}$$

$$-\ln\sqrt{u} \approx -\ln\sqrt{u_0} - \frac{1}{2u_0}(u - u_0) = -\ln\sqrt{u_0} - \frac{u}{2u_0} + \frac{1}{2}. \tag{8.25}$$

We replace again u by $\|x\|^2$ and u_0 by τ^2 and get for the Taylor mollification (that means the composite function)

$$L_\tau(x) := \begin{cases} \frac{1}{\|x\|^2}, & \|x\| \geq \tau, \\ \left(\frac{2}{\tau^2} - \frac{\|x\|^2}{\tau^4}\right), & \|x\| < \tau, \end{cases} \tag{8.26}$$

$$N_\tau(x) := \begin{cases} -\ln\|x\|, & \|x\| \geq \tau, \\ -\ln\tau - \frac{\|x\|^2}{2\tau^2} + \frac{1}{2}, & \|x\| < \tau. \end{cases} \tag{8.27}$$

We can show some properties of the functions above in the following lemma, which helps us for the theoretical results in this section.

Lemma 8.2.1. *For the mollifications of $L(x) = \frac{1}{\|x\|^2}$ and $N(x) = -\ln\|x\|$ given above, it holds true that $(L - L_\tau)(x) \geq 0$ and $(N - N_\tau)(x) \geq 0$ for all $x \in \mathbb{R}^2 \setminus \{0\}$.*

Proof. We have a look at the term $(L-L_\tau)(x) = \frac{1}{\|x\|^2} - \frac{2}{\tau^2} + \frac{\|x\|^2}{\tau^4}$ for $\|x\| < \tau$ because for $\|x\| \geq \tau$ the difference is zero. Due to the radially symmetry of the difference of the functions, we derive them with respect to $\|x\| = r$ and get

$$\begin{aligned} & \frac{\partial}{\partial r}(L - L_\tau)(x) = -\frac{2}{r^3} + \frac{2r}{\tau^4} \stackrel{!}{=} 0 \\ \Leftrightarrow \quad & \frac{2}{r^3} = \frac{2r}{\tau^4} \\ \Leftrightarrow \quad & r = \tau. \end{aligned} \tag{8.28}$$

We obtain the following estimate

$$r < \tau \;\Leftrightarrow\; 2r^4 < 2\tau^4 \;\Leftrightarrow\; \frac{2}{r^3} > \frac{2r}{\tau^4} \;\Leftrightarrow\; -\frac{2}{r^3} + \frac{2r}{\tau^4} < 0. \tag{8.29}$$

That means we have that $(L - L_\tau)(x)$ is a monotonically decreasing function with respect to $r = \|x\|$ and a zero value at $\|x\| = \tau$, which yields $(L - L_\tau)(x) \geq 0$. Now we have a look at the term $(N - N_\tau)(x) = -\ln\|x\| + \ln\tau + \frac{\|x\|^2}{2\tau^2} - \frac{1}{2}$ also for $\|x\| < \tau$ because otherwise it is zero due to the construction. We differentiate this term also for $\|x\| = r$ with respect to r and get

$$\begin{aligned} & \frac{\partial}{\partial r}(N - N_\tau)(x) = -\frac{1}{r} + \frac{r}{\tau^2} \stackrel{!}{=} 0 \\ \Leftrightarrow \quad & r^2 = \tau^2 \\ \Leftrightarrow \quad & r = \tau. \end{aligned} \tag{8.30}$$

An estimation gives us the following result

$$\begin{aligned} r < \tau \;\Leftrightarrow\; & \frac{r}{\tau^2} < \frac{\tau}{\tau^2} = \frac{1}{\tau} < \frac{1}{r} \\ \Leftrightarrow\; & -\frac{1}{r} + \frac{r}{\tau^2} < 0. \end{aligned} \tag{8.31}$$

With the same arguments as above, we get $(N - N_\tau)(x) \geq 0$. □

After this preparatory work, we can state the following theorem now.

Theorem 8.2.2. *We assume that $\mathcal{B}$ is a regular region in $\mathbb{R}^2$ and $f : \overline{\mathcal{B}} \to \mathbb{R}^2$ is continuous. Let $x \in \overline{\mathcal{B}}$, then we get*

$$\lim_{\substack{\tau \to 0 \\ \tau > 0}} \left| \int_{\mathcal{B}} \left(p_i^{\mathrm{St}}(x-y) - p_{i,\tau}^{\mathrm{St}}(x-y) \right) f_i(y) \, \mathrm{d}y \right| = 0, \quad i = 1, 2. \tag{8.32}$$

Proof. First we observe that due to the construction, the support of the difference of functions is $\mathbb{B}_\tau(x)$ for sufficiently small τ. We use the triangle inequality, drag the f-component outside of the integral with its maximum and obtain

$$\begin{aligned}
&\left| \int_{\mathbb{B}_\tau(x)\cap\overline{\mathcal{B}}} \left(p_i^{\mathrm{St}}(x-y) - p_{i,\tau}^{\mathrm{St}}(x-y)\right) f_i(y)\,\mathrm{d}y \right| \\
&\leq \max_{y\in\mathbb{B}_\tau(x)\cap\overline{\mathcal{B}}} |f_i(y)| \int_{\mathbb{B}_\tau(x)\cap\overline{\mathcal{B}}} \left|p_i^{\mathrm{St}}(x-y) - p_{i,\tau}^{\mathrm{St}}(x-y)\right| \mathrm{d}y \\
&\leq \max_{y\in\mathbb{B}_\tau(x)\cap\overline{\mathcal{B}}} |f_i(y)| \int_{\mathbb{B}_\tau(0)} \left|p_i^{\mathrm{St}}(y) - p_{i,\tau}^{\mathrm{St}}(y)\right| \mathrm{d}y, \quad i=1,2. \qquad (8.33)
\end{aligned}$$

Because of the symmetry of the functions, we only consider the first quadrant of the y-domain and show the proof for the first component of the difference $p_1^{\mathrm{St}} - p_{1,\tau}^{\mathrm{St}}$ by using polar coordinates. Due to Lemma 8.2.1, we can drop out the absolute value.

$$\begin{aligned}
&\lim_{\substack{\tau\to 0\\ \tau>0}} \int_{\substack{\mathbb{B}_\tau(0)\\ y_1,y_2>0}} \left|p_1^{\mathrm{St}}(y) - p_{1,\tau}^{\mathrm{St}}(y)\right| \,\mathrm{d}y \\
&\qquad = \frac{C_1}{2\pi} \lim_{\substack{\tau\to 0\\ \tau>0}} \int_{\substack{\mathbb{B}_\tau(0)\\ x,y>0}} \frac{y_1}{\|y\|^2} - \frac{y_1}{\tau^2}\left(2 - \frac{\|y\|^2}{\tau^2}\right) \,\mathrm{d}y \\
&\qquad = \frac{C_1}{2\pi} \lim_{\substack{\tau\to 0\\ \tau>0}} \int_0^\tau \int_0^{\frac{\pi}{2}} \left(\frac{r\cos\varphi}{r^2} - \frac{r\cos\varphi}{\tau^2}\left(2 - \frac{r^2}{\tau^2}\right)\right) r \,\mathrm{d}\varphi\,\mathrm{d}r \\
&\qquad = \frac{C_1}{2\pi} \lim_{\substack{\tau\to 0\\ \tau>0}} \int_0^\tau \int_0^{\frac{\pi}{2}} \left(\cos\varphi - 2\frac{r^2\cos\varphi}{\tau^2} + \frac{r^4\cos\varphi}{\tau^4}\right) \,\mathrm{d}\varphi\,\mathrm{d}r \\
&\qquad = \frac{C_1}{2\pi} \lim_{\substack{\tau\to 0\\ \tau>0}} \int_0^\tau \left(1 - 2\frac{r^2}{\tau^2} + \frac{r^4}{\tau^4}\right) \,\mathrm{d}r \\
&\qquad = \frac{C_1}{2\pi} \lim_{\substack{\tau\to 0\\ \tau>0}} \left(\tau - \frac{2}{3}\frac{\tau^3}{\tau^2} + \frac{1}{5}\frac{\tau^5}{\tau^4}\right) \\
&\qquad = 0, \qquad (8.34)
\end{aligned}$$

which finishes the proof. □

The theorem above was transferred from the concept of the Laplace equation. In the case of the Laplace equation, such an analogous theorem has a physical background and interpretation. In our case this theorem can be shown but has no direct physical interpretability and benefit at the moment. We continue with the second spatial-dependent function, which is a tensor with four entries and certain symmetry relations.

8.2.2. $\boldsymbol{u}^{\mathrm{CN}}$

Similar to the fundamental solution p^{St}, we have the problem with the singularity for $x = (0,0)$ (see also Figure 8.7).

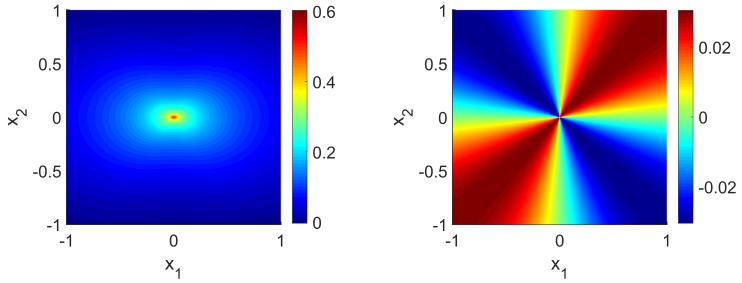

(a) u_{11}^{CN} (b) u_{12}^{CN}

Figure 8.7.: Two of the four components of the fundamental solution tensor $\boldsymbol{u}^{\mathrm{CN}}$ with its singularity in the zero point.

Because of the symmetry of the components of $\boldsymbol{u}^{\mathrm{CN}}$, we only show here two of the four components. For the mollification of the fundamental solutions we consider the main components $\ln\|x\|$ and $\frac{1}{\|x\|^2}$ (see Lemma 8.2.1) and obtain the regularized fundamental solution with a Taylor expansion up to the first order for the particular components of the tensor $\boldsymbol{u}^{\mathrm{CN}}$ by

$$u_{12,\tau}^{\mathrm{CN}}(x) := \frac{C_3C_4}{2\pi}x_1x_2\begin{cases}\frac{1}{\|x\|^2}, & \|x\| \geq \tau,\\ \frac{2}{\tau^2} - \frac{\|x\|^2}{\tau^4}, & \|x\| < \tau.\end{cases} \tag{8.35}$$

$$u_{kk,\tau}^{\mathrm{CN}}(x) := \begin{cases}\frac{C_3}{2\pi}\left(-\ln(\|x\|) + C_4\frac{x_k^2}{\|x\|^2}\right), & \|x\| \geq \tau,\\ \frac{C_3}{2\pi}\left(-\ln(\tau) - \frac{\|x\|^2}{2\tau^2} + \frac{1}{2} + C_4x_k^2\left(\frac{2}{\tau^2} - \frac{\|x\|^2}{\tau^4}\right)\right), & \|x\| < \tau.\end{cases} \tag{8.36}$$

We do not consider here the x_ix_k-term because for the regularization above the gradient is again equal at the transition for a point (x_1, x_2) with $\|x\| = \tau$, which was shown in general in Theorem 8.1.3.
Figures 8.8 and 8.9 show the regularized fundamental solutions $u_{11,\tau}^{\mathrm{CN}}$ and $u_{12,\tau}^{\mathrm{CN}}$ separated from each other.

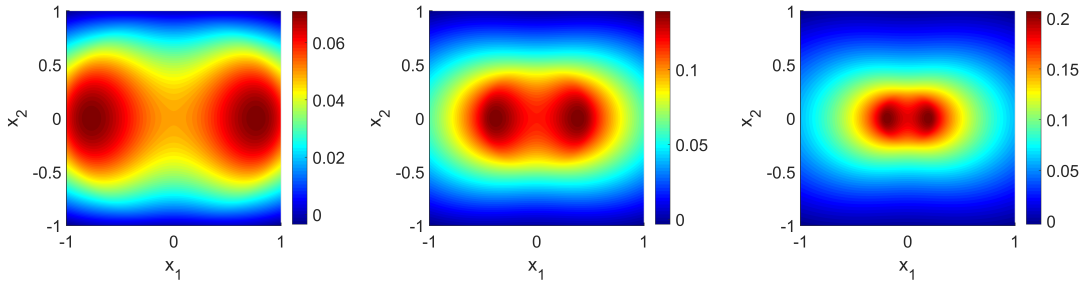

(a) $j = 0$ (b) $j = 1$ (c) $j = 2$

Figure 8.8.: The regularized fundamental solution $u_{11,\tau_j}^{\mathrm{CN}}$ forseveral parameters j.

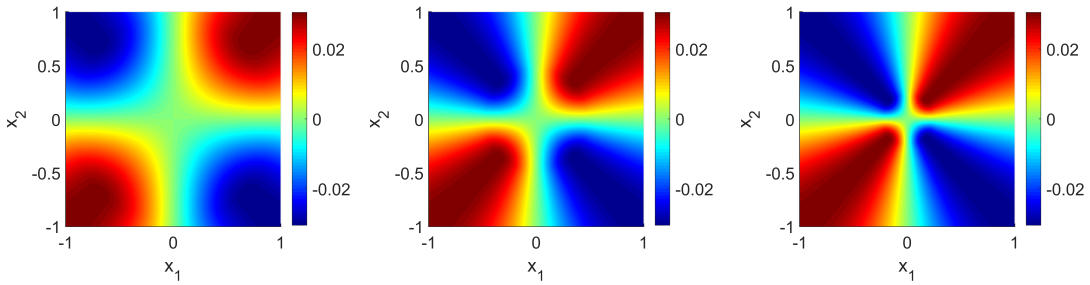

(a) $j = 0$ (b) $j = 1$ (c) $j = 2$

Figure 8.9.: The regularized fundamental solution $u^{\mathrm{CN}}_{12,\tau_j}$ for selected parameters j.

In analogy to the case of p^{St} and p^{St}_{τ}, we can see that the regularized fundamental solution approaches to the fundamental solution with decreasing τ.
The respective "τ_j-fundamental wavelet function" is constructed by

$$u^{\mathrm{CN}}_{ik,\mathrm{Wav},\tau_j} := u^{\mathrm{CN}}_{ik,\tau_j} - u^{\mathrm{CN}}_{ik,\tau_{j-1}}. \tag{8.37}$$

In Figures 8.10 and 8.11 the corresponding wavelets for each component are shown separately and we see the compact and shrinking support for increasing j.

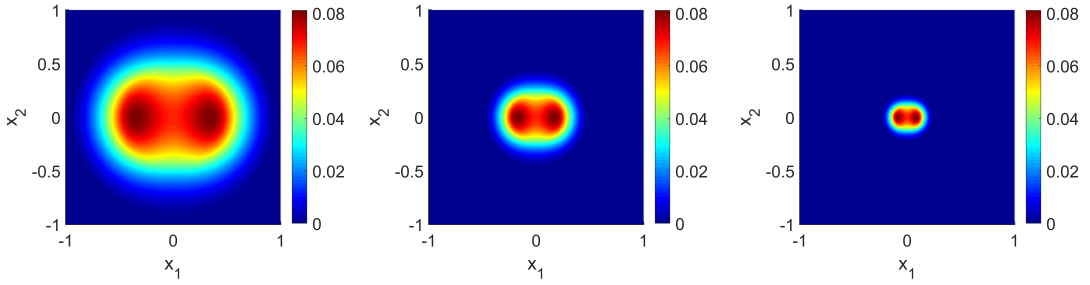

(a) $j = 1$ (b) $j = 2$ (c) $j = 3$

Figure 8.10.: The wavelet for $u^{\mathrm{CN}}_{11,\mathrm{Wav},\tau_j}$ for selected parameters j.

Now let us state the following theorem in analogy to the Laplace equation like we did it for the regularized fundamental solution above.

Theorem 8.2.3. *We have the same assumptions as above, that means $\mathcal{B}$ is a regular region in $\mathbb{R}^2$ and $f : \overline{\mathcal{B}} \to \mathbb{R}^2$ is continuous. Let $x \in \overline{\mathcal{B}}$, then we get*

$$\lim_{\substack{\tau \to 0 \\ \tau > 0}} \left| \int_{\mathcal{B}} \left(u^{\mathrm{CN}}_{ik}(x-y) - u^{\mathrm{CN}}_{ik,\tau}(x-y) \right) f_i(y) \, \mathrm{d}y \right| = 0 \tag{8.38}$$

for all $i, k = 1, 2$.

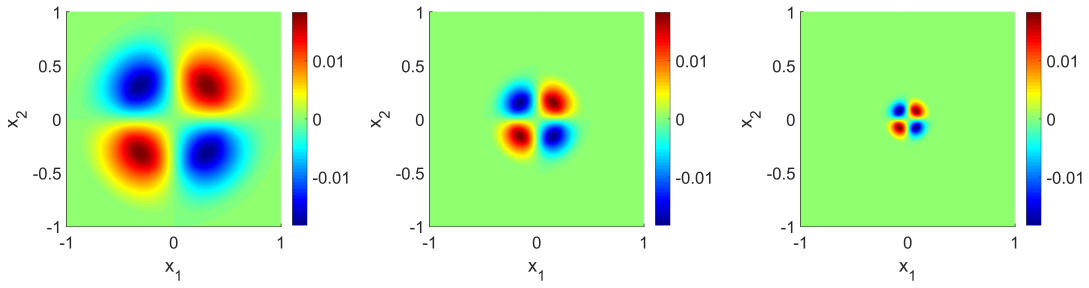

(a) $j = 1$ (b) $j = 2$ (c) $j = 3$

Figure 8.11.: The wavelet for $u^{\mathrm{CN}}_{12,\mathrm{Wav},\tau_j}$ for several parameters j.

Proof. We show this theorem for two of the four components of $\boldsymbol{u}^{\mathrm{CN}}$ and $\boldsymbol{u}^{\mathrm{CN}}_{\tau}$ because of their symmetry property. Using again the triangle inequality, the compact support $\mathbb{B}_\tau(x)$ of the difference of the functions for sufficiently small τ and the maximum of the data f like above, we obtain

$$\begin{aligned}&\left|\int_{\mathbb{B}_\tau(x)\cap\overline{\mathcal{B}}} \left(u^{\mathrm{CN}}_{ik}(x-y) - u^{\mathrm{CN}}_{ik,\tau}(x-y)\right) f_i(y)\,\mathrm{d}y\right| \\ &\leq \max_{y\in\mathbb{B}_\tau(x)\cap\overline{\mathcal{B}}} |f_i(y)| \int_{\mathbb{B}_\tau(0)} \left|u^{\mathrm{CN}}_{ik}(y) - u^{\mathrm{CN}}_{ik,\tau}(y)\right|\,\mathrm{d}y, \quad i,k=1,2. \end{aligned} \tag{8.39}$$

Now we have a look at the components separately and use polar coordinates. Please note that due to Lemma 8.2.1, we can drop out the absolute value in the integral, since C_3, C_4 are positive as a combination of positive material constants (see Remark 7.3.1). We obtain for the difference

$$\begin{aligned}&\lim_{\substack{\tau\to 0\\ \tau>0}} \int_{\mathbb{B}_\tau(0)} \left(u^{\mathrm{CN}}_{11}(y) - u^{\mathrm{CN}}_{11,\tau}(y)\right)\,\mathrm{d}y \\ &= \lim_{\substack{\tau\to 0\\ \tau>0}} \int_{\mathbb{B}_\tau(0)} \frac{C_3}{2\pi}\left(-\ln\|y\| + C_4\frac{y_1^2}{\|y\|^2} + \ln\tau + \frac{\|y\|^2}{2\tau^2} - \frac{1}{2} - C_4 y_1^2\left(\frac{2}{\tau^2} - \frac{\|y\|^2}{\tau^4}\right)\right)\,\mathrm{d}y. \end{aligned} \tag{8.40}$$

Splitting the integral in two separate terms, we get

$$\begin{aligned}&\lim_{\substack{\tau\to 0\\ \tau>0}} C_4 \int_{\mathbb{B}_\tau(0)} \left(\frac{y_1^2}{\|y\|^2} - y_1^2\left(\frac{2}{\tau^2} - \frac{\|y\|^2}{\tau^4}\right)\right)\,\mathrm{d}y \\ &\qquad = C_4 \lim_{\substack{\tau\to 0\\ \tau>0}} \int_0^\tau \int_0^{2\pi} \left(\cos^2\varphi - r^2\cos^2\varphi\left(\frac{2}{\tau^2} - \frac{r^2}{\tau^4}\right)\right) r\mathrm{d}r\,\mathrm{d}\varphi \\ &\qquad = C_4 \lim_{\substack{\tau\to 0\\ \tau>0}} \left(\frac{1}{2}\tau^2\cdot\frac{1}{2}\cdot 2\pi - \frac{1}{2}\cdot 2\pi\cdot\int_0^\tau \frac{2r^3}{\tau^2} - \frac{r^5}{\tau^4}\,\mathrm{d}r\right) \end{aligned}$$

$$= C_4 \lim_{\substack{\tau\to 0\\ \tau>0}} \left(\frac{1}{2}\tau^2\pi - \pi \cdot \left(\frac{1}{2}\frac{\tau^4}{\tau^2} - \frac{1}{6}\frac{\tau^6}{\tau^4} \right) \right)$$
$$= 0. \tag{8.41}$$

The part with the $\ln$-function and its regularization is left:

$$\lim_{\substack{\tau\to 0\\ \tau>0}} \int_{\mathbb{B}_\tau(0)} -\ln\|y\| + \ln\tau + \frac{\|y\|^2}{2\tau^2} - \frac{1}{2}\,\mathrm{d}y$$
$$= \lim_{\substack{\tau\to 0\\ \tau>0}} \int_0^\tau \int_0^{2\pi} \left(-\ln r + \ln\tau + \frac{r^2}{2\tau^2} - \frac{1}{2} \right) r\,\mathrm{d}\varphi\,\mathrm{d}r$$
$$= \lim_{\substack{\tau\to 0\\ \tau>0}} \left(2\pi \int_0^\tau -\ln r \cdot r + \ln\tau \cdot r + \frac{r^3}{2\tau^2} - \frac{1}{2}r\,\mathrm{d}r \right)$$
$$= \lim_{\substack{\tau\to 0\\ \tau>0}} 2\pi \left(-\frac{1}{4}r^2(2\ln r - 1) + \frac{1}{2}r^2\ln\tau + \frac{1}{4}\frac{r^4}{2\tau^2} - \frac{1}{4}r^2 \right)\Bigg|_0^\tau$$
$$= \lim_{\substack{\tau\to 0\\ \tau>0}} 2\pi \left(-\frac{1}{4}\tau^2(2\ln\tau - 1) + \frac{1}{2}\tau^2\ln\tau + \frac{1}{4}\frac{\tau^4}{2\tau^2} - \frac{1}{4}\tau^2 \right)$$
$$= 0. \tag{8.42}$$

Please note that due to l'Hospital's rule, it holds true that

$$\lim_{\substack{b\to 0\\ b>0}} b^2 \cdot \ln b = \lim_{\substack{b\to 0\\ b>0}} \frac{\ln b}{1/b^2} = \lim_{\substack{b\to 0\\ b>0}} \frac{1/b}{-2/b^3} = \lim_{\substack{b\to 0\\ b>0}} -\frac{1}{2}b^2 = 0. \tag{8.43}$$

At last, we consider the function $u_{12,\tau}^{\mathrm{CN}}$. Due to the symmetry, we only consider the function for $y_1, y_2 > 0$ and get subsequently with polar coordinates

$$\lim_{\substack{\tau\to 0\\ \tau>0}} \int_{\substack{\mathbb{B}_\tau(0)\\ y_1,y_2>0}} \left(u_{12}^{\mathrm{CN}}(y) - u_{12,\tau}^{\mathrm{CN}}(y) \right)\,\mathrm{d}y$$
$$= \lim_{\substack{\tau\to 0\\ \tau>0}} \frac{C_3C_4}{2\pi} \int_{\substack{\mathbb{B}_\tau(0)\\ y_1,y_2>0}} \frac{y_1y_2}{\|y\|^2} - y_1y_2\left(\frac{2}{\tau^2} - \frac{\|y\|^2}{\tau^4} \right)\,\mathrm{d}y$$
$$= \lim_{\substack{\tau\to 0\\ \tau>0}} \frac{C_3C_4}{2\pi} \int_0^\tau \int_0^{\pi/2} \frac{r^2\cos\varphi\sin\varphi}{r^2} \cdot r - r^2\cos\varphi\sin\varphi \left(\frac{2}{\tau^2} - \frac{r^2}{\tau^4} \right) \cdot r\,\mathrm{d}\varphi\,\mathrm{d}r$$
$$= \lim_{\substack{\tau\to 0\\ \tau>0}} \frac{C_3C_4}{2\pi} \left(\int_0^{\pi/2} \sin\varphi\cos\varphi\,\mathrm{d}\varphi \cdot \int_0^\tau r - \frac{2r^3}{\tau^2} + \frac{r^5}{\tau^4}\,\mathrm{d}r \right)$$
$$= \lim_{\substack{\tau\to 0\\ \tau>0}} \frac{C_3C_4}{2\pi} \left(\frac{1}{2} \cdot \left(\frac{1}{2}\tau^2 - \frac{1}{2}\tau^2 + \frac{1}{6}\tau^2 \right) \right)$$
$$= 0. \tag{8.44}$$

□

With this theorem, we have the same situation as with the analogous theorem for p^{St}: We do not have a practical benefit of it at the moment. Now we come to the last part of the fundamental solutions, which is location- and time-dependent. This is more challenging, because we have to check, if a spatial Taylor mollification is sufficient or additionally some Taylor expansion in the time-domain is necessary. Beforehand let us say: We tested several possibilities for the regularization of p^{Si} and u^{Si} and the one which we present here is the best-working for us.

8.2.3. p^{Si}

The fundamental solution p^{Si} depends on the space and the time and has a singularity for the time $t = 0$ combined with the point $x = (0, 0)$. Figure 8.12 shows the fundamental solution for two fixed times for the space and Figure 8.13 for two fixed points over time. (7.32) shows us that the fundamental solution is not defined respectively gets singular if $t = 0$ and $x = (0, 0)$. We can show with a concrete sequence for x and t that the limit does not exist for $x = (0, 0)$ and $t = 0$. We use the sequences $x^k = (1/k, 1/k)$ and $t^k = 1/k$. We get by inserting this in p^{Si}

$$\lim_{k\to\infty} \frac{1}{4\pi\frac{1}{k}} \exp\left(-\frac{\frac{2}{k^2}}{4C_2\frac{1}{k}}\right) = \lim_{k\to\infty} \frac{k}{4\pi} \exp\left(-\frac{1}{2C_2 k}\right) = \infty. \tag{8.45}$$

Therefore it is necessary to mollify it. We have the possibilities to do this regarding the space, the time or as a combination of both. Due to the fact that we want to keep the regularization as simple as possible, we do this with respect to the space, that means for a fixed t, we do a Taylor expansion for $\|x\|$ like in the cases above. This is also the most practicable ansatz. A pure regularization in time did not yield the necessary theoretical results. A combination of both is too complicated and we could not prove the necessary theoretical results. Furthermore, the last-mentioned variety is not necessary to achieve our theoretical results for the decorrelation. Definition 4.1.3 shows our required theoretical properties.

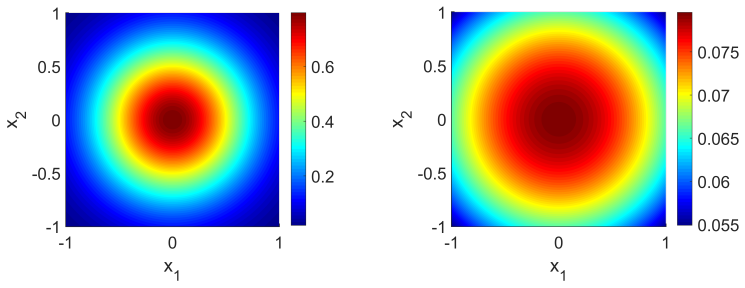

(a) $t = 0.1$ (b) $t = 1$

Figure 8.12.: The fundamental solution p^{Si} in space for two fixed times.

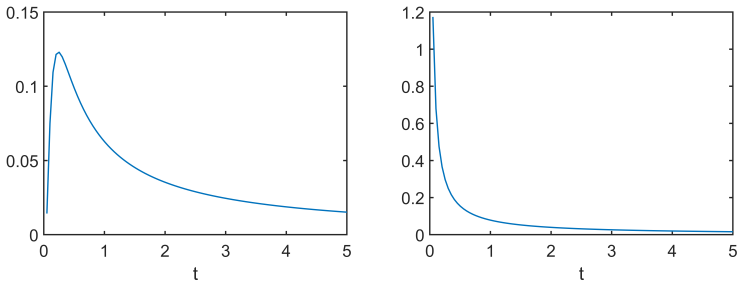

(a) $x = (0.8, 0.8)$ (b) $x = (0.2, 0.2)$

Figure 8.13.: The fundamental solution p^{Si} for two different fixed points over time.

As above, we make a Taylor expansion with respect to $\|x\|$ with the parameter τ similar to the cases above. Replacing $\|x\|^2$ by u and deriving p^{Si} with respect to u, we get

$$\frac{\partial}{\partial u} p^{\mathrm{Si}}(u,t) = \frac{\partial}{\partial u} \frac{1}{4\pi t} \exp\left(-\frac{u}{4C_2 t}\right) = \frac{-1}{16\pi C_2 t^2} \exp\left(-\frac{u}{4C_2 t}\right) \tag{8.46}$$

and the following Taylor expansion for $\|x\| < \tau$

$$\begin{aligned} p^{\mathrm{Si}}(u,t) &= p^{\mathrm{Si}}(u_0,t) + \frac{\partial}{\partial u} p^{\mathrm{Si}}(u_0,t)(u-u_0) + \mathcal{O}\left((u-u_0)^2\right) \\ &= \frac{1}{4\pi t} \exp\left(-\frac{u_0}{4C_2 t}\right) - \frac{1}{16\pi C_2 t^2} \exp\left(-\frac{u_0}{4C_2 t}\right)(u-u_0) + \mathcal{O}\left((u-u_0)^2\right) \\ &= \frac{1}{4\pi t} \exp\left(-\frac{u_0}{4C_2 t}\right)\left[1 - \frac{1}{4C_2 t}(u-u_0)\right] + \mathcal{O}\left((u-u_0)^2\right). \end{aligned} \tag{8.47}$$

Replacing $u = \|x\|^2$ and $u_0 = \tau^2$, we obtain for $\|x\| < \tau$ up to the linear term, the identity

$$p^{\mathrm{Si}}_{\mathrm{reg}}(x,t) \coloneqq \frac{1}{4\pi t} \exp\left(-\frac{\tau^2}{4C_2 t}\right)\left[1 - \frac{1}{4C_2 t}\left(\|x\|^2 - \tau^2\right)\right]. \tag{8.48}$$

With this we can define our mollified fundamental solution in the following way

$$p^{\mathrm{Si}}_{\tau}(x,t) \coloneqq \begin{cases} \frac{1}{4\pi t} \exp\left(-\frac{\|x\|^2}{4C_2 t}\right), & \|x\| \geq \tau \\ \frac{1}{4\pi t} \exp\left(-\frac{\tau^2}{4C_2 t}\right)\left[1 - \frac{1}{4C_2 t}\left(\|x\|^2 - \tau^2\right)\right], & \|x\| < \tau. \end{cases} \tag{8.49}$$

Figure 8.14 shows the regularized fundamental solution $p^{\mathrm{Si}}_{\tau}(x,t)$ for fixed positions in space respectively fixed times. Especially the case for $x = (0,0)$ can be presented since p^{Si}_{τ} is no longer singular for this point (see the mentioned figure).

In the following, we can prove that the limit for $x = (0,0)$ and $t = 0$ exists in general which we can see with the help of the consideration below. For this purpose, we have a look at the regularized part of the function and multiply the terms out to sort them in another way (terms with and without $\|x\|$). We can see that we get terms only with t-dependency and terms with t- and $\|x\|$-dependency that are separated. It follows

$$\begin{aligned}
\lim_{t\to 0+}\lim_{\|x\|\to 0} p_\tau^{\mathrm{Si}}(x,t) &= \lim_{t\to 0+}\lim_{\|x\|\to 0}\left(\frac{1}{4\pi t}\exp\left(-\frac{\tau^2}{4C_2 t}\right)\left[1-\frac{1}{4C_2 t}(\|x\|^2-\tau^2)\right]\right)\\
&= \lim_{t\to 0+}\lim_{\|x\|\to 0}\left[\frac{1}{4\pi t}\exp\left(-\frac{\tau^2}{4C_2 t}\right)\left(1+\frac{\tau^2}{4C_2 t}\right)\right]\\
&\quad - \lim_{t\to 0+}\lim_{\|x\|\to 0}\frac{1}{4\pi t}\exp\left(-\frac{\tau^2}{4C_2 t}\right)\frac{\|x\|^2}{4C_2 t}\\
&= \lim_{t\to 0+}\left[\frac{1}{4\pi t}\exp\left(-\frac{\tau^2}{4C_2 t}\right)\left(1+\frac{\tau^2}{4C_2 t}\right)\right]\\
&\quad - \lim_{t\to 0+}\frac{1}{16C_2\pi t^2}\exp\left(-\frac{\tau^2}{4C_2 t}\right)\cdot\lim_{\|x\|\to 0}\|x\|^2\\
&= 0
\end{aligned} \tag{8.50}$$

with the usual limit theorems since $1/t\cdot\exp(-\tau^2/(4C_2t))$ and $1/t^2\cdot\exp(-\tau^2/(4C_2t))$ tend to 0 for $t\to 0+$. Please note here that the order of the limits does not make a difference here.

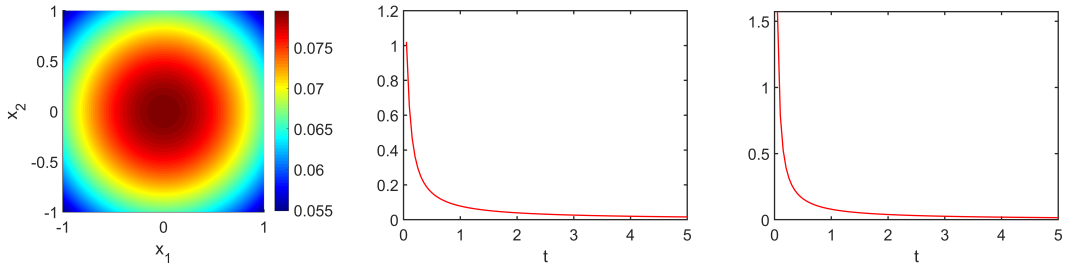

(a) $t = 1,\ j = 1.$ (b) $x = (0.2, 0.2),\ j = 1.$ (c) $x = (0,0),\ j = 3.$

Figure 8.14.: The regularized fundamental solution $p_{\tau_j}^{\mathrm{Si}}$ for a fixed time in space respectively for two different fixed spatial points over the time and selected parameters j.

The respective wavelet function is defined in analogy to the other wavelets. The "τ_j-fundamental wavelet function" is given by

$$p_{\mathrm{Wav},\tau_j}^{\mathrm{Si}} := p_{\mathrm{reg},\tau_j}^{\mathrm{Si}} - p_{\mathrm{reg},\tau_{j-1}}^{\mathrm{Si}}. \tag{8.51}$$

Figure 8.15 shows the corresponding wavelet functions.
For the theoretical part, we can show the following theorem.

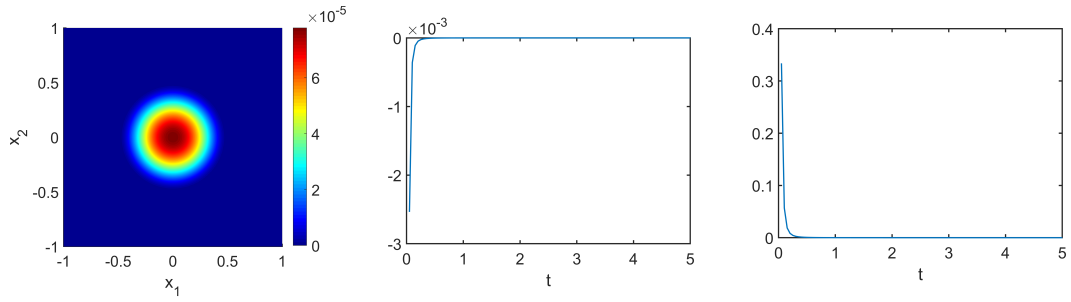

(a) $t = 1,\ j = 1.$ (b) $x = (0.2, 0.2),\ j = 1.$ (c) $x = (0, 0), j = 1.$

Figure 8.15.: The wavelet function $p^{\mathrm{Si}}_{\mathrm{Wav},\tau_j}$ for a fixed time in space respectively for two fixed spatial points over time for $j = 1$.

Theorem 8.2.4. *We assume that $\mathcal{B}$ is a regular region in $\mathbb{R}^2$ and $f : \overline{\mathcal{B}} \times \mathbb{R} \to \mathbb{R}$ is continuous and bounded. Let $x \in \overline{\mathcal{B}}$ and $t \in \mathbb{R}$, then we get*

$$\lim_{\substack{\tau \to 0 \\ \tau > 0}} \left| \int_{t-T}^{t} \int_{\mathcal{B}} \left(p^{\mathrm{Si}}(x - y, t - \theta) - p^{\mathrm{Si}}_{\tau}(x - y, t - \theta) \right) f(y, \theta) \, \mathrm{d}y \, \mathrm{d}\theta \right| = 0, \tag{8.52}$$

where $T > 0$ is the length of our considered time interval.

Proof. We have similar steps as in the proofs above. In a first step, we use the triangle inequality and drag the f-component outside of the integral with its supremum. Please observe that, due to the construction, the spatial support for a fixed t of the difference of functions is $\mathbb{B}_\tau(x)$ for sufficiently small τ. We obtain

$$\begin{aligned} &\left| \int_{t-T}^{t} \int_{\mathbb{B}_\tau(x) \cap \overline{\mathcal{B}}} \left(p^{\mathrm{Si}}(x - y, t - \theta) - p^{\mathrm{Si}}_{\tau}(x - y, t - \theta) \right) f(y, \theta) \, \mathrm{d}y \, \mathrm{d}\theta \right| \\ &\leq \sup_{y \in \mathbb{B}_\tau(x) \cap \overline{\mathcal{B}}, \theta \in \mathbb{R}} |f(y, \theta)| \int_{0}^{T} \int_{\mathbb{B}_\tau(0)} \left| p^{\mathrm{Si}}(y, \theta) - p^{\mathrm{Si}}_{\tau}(y, \theta) \right| \mathrm{d}y \, \mathrm{d}\theta. \end{aligned} \tag{8.53}$$

Note that we assumed that f is bounded. We can show that $p^{\mathrm{Si}} - p^{\mathrm{Si}}_{\tau} \geq 0$ holds true by showing that this difference is monotonically decreasing for $\|x\| = r$, where we assume that $t > 0$ holds true:

$$\begin{aligned} \frac{\partial}{\partial r} \left(p^{\mathrm{Si}} - p^{\mathrm{Si}}_{\tau} \right)(x, t) &= \frac{\partial}{\partial r} \frac{1}{4\pi t} \left[\exp\left(\frac{-r^2}{4C_2 t} \right) - \exp\left(\frac{-\tau^2}{4C_2 t} \right) \left(1 - \frac{1}{4C_2 t} (r^2 - \tau^2) \right) \right] \\ &= \frac{1}{4\pi t} \left[\exp\left(\frac{-r^2}{4C_2 t} \right) \cdot \left(\frac{-2r}{4C_2 t} \right) - \exp\left(\frac{-\tau^2}{4C_2 t} \right) \cdot \left(\frac{-1}{4C_2 t} \right) \cdot 2r \right] \\ &= \underbrace{\frac{1}{4\pi t}}_{>0} \cdot \underbrace{\left(\frac{-2r}{4C_2 t} \right)}_{<0} \underbrace{\left[\exp\left(\frac{-r^2}{4C_2 t} \right) - \exp\left(\frac{-\tau^2}{4C_2 t} \right) \right]}_{>0 \ (\text{for } r < \tau)} < 0. \end{aligned} \tag{8.54}$$

That means the difference is monotonically decreasing for $\|x\| = r$ and together with the evaluation at $\|x\| = \tau$ which has the value 0, we get that the difference of the functions is non-negative for all $t > 0$ because our consideration and estimation was independent of t. It holds true that $p_\tau^{\mathrm{Si}} \in \mathrm{C}^{(1)}(\mathbb{R}^2 \times \mathbb{R})$ due to the considerations in Theorem 8.1.3. That means we consider the integral above without the absolute value and get with polar coordinates (see also Remark 2.2.4 for the time integrals)

$$
\begin{aligned}
&\int_0^T \int_{\mathbb{B}_\tau(0)} \frac{1}{4\pi t} \exp\left(\frac{-\|x\|^2}{4C_2 t}\right) - \frac{1}{4\pi t} \exp\left(\frac{-\tau^2}{4C_2 t}\right) \left[1 - \frac{1}{4C_2 t}(\|x\|^2 - \tau^2)\right] \,\mathrm{d}x \,\mathrm{d}t \\
&= \int_0^T \int_0^{2\pi} \int_0^\tau \frac{r}{4\pi t} \exp\left(\frac{-r^2}{4C_2 t}\right) - \frac{r}{4\pi t} \exp\left(\frac{-\tau^2}{4C_2 t}\right) \left[1 - \frac{1}{4C_2 t}(r^2 - \tau^2)\right] \,\mathrm{d}r \,\mathrm{d}\varphi \,\mathrm{d}t \\
&= 2\pi \int_0^T \int_0^\tau \frac{r}{4\pi t} \exp\left(\frac{-r^2}{4C_2 t}\right) - \frac{1}{4\pi t} \exp\left(\frac{-\tau^2}{4C_2 t}\right) \left[r - \frac{r^3}{4C_2 t} + \frac{r\tau^2}{4C_2 t}\right] \,\mathrm{d}r \,\mathrm{d}t \\
&= 2\pi \cdot \frac{1}{2\pi} \int_0^T -C_2 \exp\left(\frac{-\tau^2}{4C_2 t}\right) + C_2 - \frac{1}{2t} \exp\left(\frac{-\tau^2}{4C_2 t}\right) \left[\frac{1}{2}\tau^2 - \frac{\tau^4}{16C_2 t} + \frac{\tau^4}{8C_2 t}\right] \,\mathrm{d}t \\
&= C_2 \left(T - \frac{\tau^2 \mathrm{Ei}\left(-\frac{\tau^2}{4C_2 T}\right)}{4C_2} - T \exp\left(\frac{-\tau^2}{4C_2 T}\right) \right) \\
&\quad + \mathrm{Ei}\left(-\frac{\tau^2}{4C_2 T}\right) \cdot \frac{\tau^2}{4} - \frac{\tau^4}{32C_2} \cdot \frac{4C_2 \exp\left(-\frac{\tau^2}{4C_2 T}\right)}{\tau^2} \\
&\to 0 \quad (\text{as } \tau \to 0+),
\end{aligned}
\tag{8.55}
$$

where we considered (2.18) and which completes the proof. □

We can now go over to the last function of the fundamental solution tensor.

8.2.4. u^{Si}

The fundamental solution u^{Si} has a singularity for $x = (0, 0)$ and for $t = 0$ (see also Figure 8.16). We can show this by using the sequences $x^k = (1/k, 1/k)$ and $t^k = 1/k^2$ and get

$$
\lim_{k\to\infty} \frac{C_1}{2\pi} \frac{k}{2} \left(1 - \underbrace{\exp\left(-\frac{2/k^2}{4C_2 \cdot 1/k^2}\right)}_{=\text{const.}\neq 1} \right) = \infty. \tag{8.56}
$$

We mollify it in the same way as p^{Si} only for the spatial component and do not consider the x-part like in the case of $\boldsymbol{u}^{\mathrm{CN}}$.

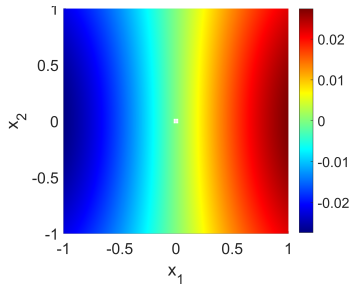

Figure 8.16.: The first component of the fundamental solution u^{Si} for the time point $t = 0.05$.

Replacing $\|x\|^2 = u$ and applying a Taylor expansion up to the linear term in u_0, we obtain

$$\frac{C_1}{2\pi} x \left[\frac{1}{u_0} \left(1 - \exp\left(-\frac{u_0}{4C_2 t} \right) \right) + \left(\frac{-1}{u_0^2} + \frac{1}{u_0} \frac{1}{4C_2 t} \exp\left(-\frac{u_0}{4C_2 t} \right) + \frac{1}{u_0^2} \exp\left(-\frac{u_0}{4C_2 t} \right) \right) (u - u_0) \right]. \tag{8.57}$$

Substituting $u = \|x\|^2$ and $u_0 = \tau^2$ for $\|x\| < \tau$, the mollified function reads

$$u_{\mathrm{reg}}^{\mathrm{Si}}(x,t) = \frac{C_1}{2\pi} x \left[\frac{1}{\tau^2} - \frac{1}{\tau^2} \exp\left(-\frac{\tau^2}{4C_2 t} \right) + \left(\frac{-1}{\tau^4} + \frac{1}{\tau^2} \frac{1}{4C_2 t} \exp\left(-\frac{\tau^2}{4C_2 t} \right) + \frac{1}{\tau^4} \exp\left(-\frac{\tau^2}{4C_2 t} \right) \right) (\|x\|^2 - \tau^2) \right]. \tag{8.58}$$

All in all, we get for our mollified fundamental solution

$$u_{\tau}^{\mathrm{Si}}(x,t) = \begin{cases} \frac{C_1}{2\pi} \frac{x}{\|x\|^2} \left(1 - \exp\left(-\frac{\|x\|^2}{4C_2 t} \right) \right), & \|x\| \geq \tau \\ \frac{C_1}{2\pi} x \left[\frac{1}{\tau^2} - \frac{1}{\tau^2} \exp\left(-\frac{\tau^2}{4C_2 t} \right) + \left(\frac{1}{\tau^2} \frac{1}{4C_2 t} \exp\left(-\frac{\tau^2}{4C_2 t} \right) \right. \right. & \\ \left. \left. -\frac{1}{\tau^4} + \frac{1}{\tau^4} \exp\left(-\frac{\tau^2}{4C_2 t} \right) \right) (\|x\|^2 - \tau^2) \right], & \|x\| < \tau. \end{cases} \tag{8.59}$$

Figure 8.17 shows $u_{\mathrm{reg},\tau}^{\mathrm{Si}}$ in space for a fixed time and for fixed points during the time interval.

We can show that the limit in $x = (0,0)$ and $t = 0$ exists for our regularized fundamental solution with the usual limit theorems.

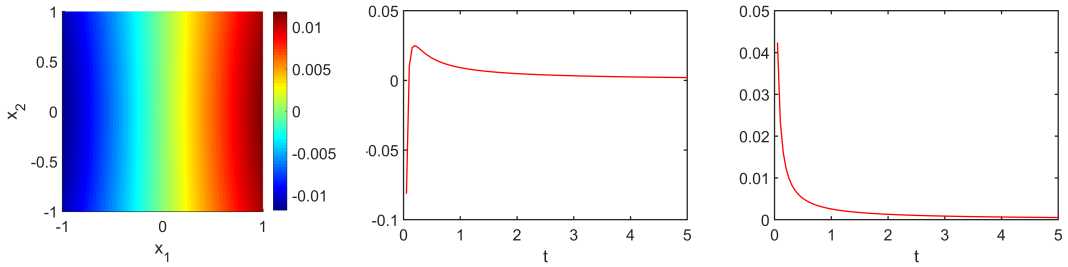

(a) $t = 1,\ j = 1.$ (b) $x = (0.8, 0.8),\ j = 1.$ (c) $x = (0.2, 0.2),\ j = 1.$

Figure 8.17.: The first component of the regularized fundamental solution $u^{\mathrm{Si}}_{\tau_j}$ for a fixed time in space respectively for two fixed spatial points over the time for $j = 1$.

First, we rearrange the terms of $u^{\mathrm{Si}}_{1,\tau}$ for a better clarity (we only consider the part of the function for $\|x\| < \tau$)

$$
\begin{aligned}
&\lim_{t\to 0+}\lim_{\|x\|\to 0} u^{\mathrm{Si}}_{1,\tau}(x,t)\\
&= \lim_{t\to 0+}\lim_{\|x\|\to 0} \frac{C_1}{2\pi} x_1 \left[\frac{1}{\tau^2}\left(1-\exp\left(-\frac{\tau^2}{4C_2t}\right)\right)\right.\\
&\quad \left.+\left(\frac{1}{\tau^2}\frac{1}{4C_2t}\exp\left(-\frac{\tau^2}{4C_2t}\right)+\frac{1}{\tau^4}\left(\exp\left(-\frac{\tau^2}{4C_2t}\right)-1\right)\right)\left(\|x\|^2-\tau^2\right)\right]\\
&= \lim_{t\to 0+}\lim_{\|x\|\to 0} \frac{C_1}{2\pi} x_1 \left[\frac{1}{\tau^2}\left(1-\exp\left(-\frac{\tau^2}{4C_2t}\right)\right)\right.\\
&\quad \left.+\left(-\frac{1}{4C_2t}\exp\left(-\frac{\tau^2}{4C_2t}\right)-\frac{1}{\tau^2}\left(\exp\left(-\frac{\tau^2}{4C_2t}\right)-1\right)\right)\right]\\
&\quad +\lim_{t\to 0+}\lim_{\|x\|\to 0} \frac{C_1}{2\pi} x_1\|x\|^2\left(\frac{1}{\tau^2}\frac{1}{4C_2t}\exp\left(-\frac{\tau^2}{4C_2t}\right)+\frac{1}{\tau^4}\left(\exp\left(-\frac{\tau^2}{4C_2t}\right)-1\right)\right)\\
&= \frac{C_1}{2\pi}\lim_{\|x\|\to 0} x_1 \cdot \lim_{t\to 0+}\left[\frac{1}{\tau^2}\left(1-\exp\left(-\frac{\tau^2}{4C_2t}\right)\right)\right.\\
&\quad \left.+\left(-\frac{1}{4C_2t}\exp\left(-\frac{\tau^2}{4C_2t}\right)-\frac{1}{\tau^2}\left(\exp\left(-\frac{\tau^2}{4C_2t}\right)-1\right)\right)\right]\\
&\quad +\frac{C_1}{2\pi}\lim_{\|x\|\to 0}\left(x_1\|x\|^2\right)\cdot\lim_{t\to 0+}\left(\frac{1}{\tau^2}\frac{1}{4C_2t}\exp\left(-\frac{\tau^2}{4C_2t}\right)+\frac{1}{\tau^4}\left(\exp\left(-\frac{\tau^2}{4C_2t}\right)-1\right)\right)\\
&= \frac{C_1}{2\pi}\cdot 0\cdot\frac{2}{\tau^2}+\frac{C_1}{2\pi}\cdot 0\cdot\left(-\frac{1}{\tau^4}\right)\\
&= 0
\end{aligned}
\tag{8.60}
$$

since $\exp(-\tau^2/(4C_2t))$ and $1/t\cdot\exp(-\tau^2/(4C_2t))$ tend to 0 for $t\to 0+$. This can be done analogously for the second component. Furthermore, our regularized fundamental solution u^{Si}_{τ} is of class $\mathrm{C}^{(1)}(\mathbb{R}^2)$ due to Theorem 8.1.3. In analogy

to the cases above, we can define the "τ_j-fundamental wavelet function" in the following way

$$u^{\mathrm{Si}}_{\mathrm{Wav},\tau_j} := u^{\mathrm{Si}}_{\tau_j} - u^{\mathrm{Si}}_{\tau_{j-1}}. \tag{8.61}$$

Figure 8.18 shows three different states of time and domain of the wavelet.

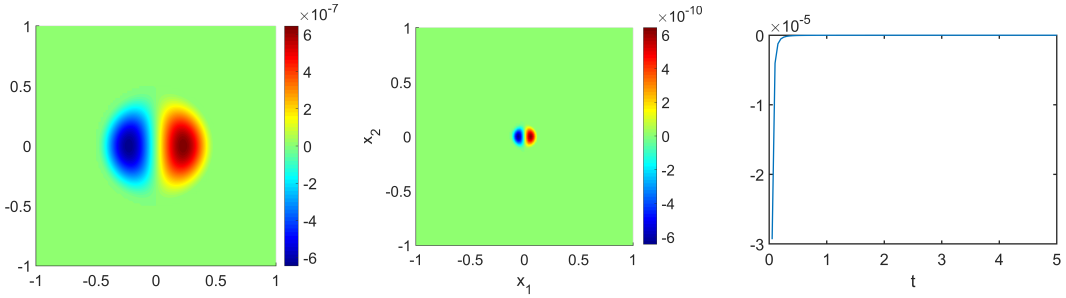

(a) $t = 1,\ j = 1.$ (b) $t = 1,\ j = 3.$ (c) $x = (0.2, 0.2)$ for $j = 1.$

Figure 8.18.: The wavelet function for u^{Si}_1 for two fixed times over the space respectively for one fixed point over the time for $j = 1$.

For the theoretical part, we consider again the following difference of the fundamental solution and its mollification.

Theorem 8.2.5. *We assume that $\mathcal{B}$ is a regular region in $\mathbb{R}^2$ and $f : \overline{\mathcal{B}} \times \mathbb{R} \to \mathbb{R}^2$ is continuous and bounded. Let $x \in \overline{\mathcal{B}}$ and $t \in \mathbb{R}$, then we get*

$$\lim_{\substack{\tau\to 0\\ \tau>0}} \left| \int_{t-T}^{t} \int_{\mathcal{B}} \left(u^{\mathrm{Si}}_i(x-y, t-\theta) - u^{\mathrm{Si}}_{i,\tau}(x-y, t-\theta) \right) f_i(y,\theta)\, \mathrm{d}y\, \mathrm{d}\theta \right| = 0, \quad i = 1, 2, \tag{8.62}$$

where $T > 0$ is the length of our considered time interval.

Proof. The steps are the same as for the p^{Si}-part. In a first step, we use the triangle inequality and drag the f-component outside of the integral with its supremum. Due to the construction, we have here that the support of the spatial component of the difference of functions is $\mathbb{B}_\tau(x)$ with the same arguments as above. We obtain

$$\begin{aligned} &\left| \int_{t-T}^{t} \int_{\mathbb{B}_\tau(x)\cap\overline{\mathcal{B}}} \left(u^{\mathrm{Si}}_i(x-y, t-\theta) - u^{\mathrm{Si}}_{i,\tau}(x-y, t-\theta) \right) f_i(y,\theta)\, \mathrm{d}y\, \mathrm{d}\theta \right| \\ &\leq \sup_{y\in\mathbb{B}_\tau(x)\cap\overline{\mathcal{B}},\theta\in\mathbb{R}} |f_i(y,\theta)| \int_0^T \int_{\mathbb{B}_\tau(0)} \left| u^{\mathrm{Si}}_i(y,\theta) - u^{\mathrm{Si}}_{i,\tau}(y,\theta) \right| \mathrm{d}y\, \mathrm{d}\theta. \end{aligned} \tag{8.63}$$

Please note that we show the next steps of this theorem without loss of generality for the first component of the difference. The second component is obtained due

to symmetric aspects. First, we consider the difference of $u_1^{\mathrm{Si}} - u_{1,\tau}^{\mathrm{Si}}$ without the factor $\frac{C_1}{2\pi}x_1$ for $\|x\| < \tau$ and get

$$\begin{aligned}&\frac{1}{\|x\|^2}\left(1-\exp\left(-\frac{\|x\|^2}{4C_2t}\right)\right)-\frac{1}{\tau^2}\left(1-\exp\left(-\frac{\tau^2}{4C_2t}\right)\right)\\&+\left(\frac{1}{\tau^2}\frac{1}{4C_2t}\exp\left(-\frac{\tau^2}{4C_2t}\right)+\frac{1}{\tau^4}\left(\exp\left(-\frac{\tau^2}{4C_2t}\right)-1\right)\right)(\tau^2-\|x\|^2).\end{aligned}\tag{8.64}$$

We have a look at the two lines separately and show that the first one is non-negative and the second one is non-positive. Let us start our considerations with the second line. The term $(\tau^2 - \|x\|^2)$ is positive since we have the case $\|x\| < \tau$. For the first term, we do the following conversions

$$\begin{aligned}&\frac{1}{\tau^2}\frac{1}{4C_2t}\exp\left(-\frac{\tau^2}{4C_2t}\right)+\frac{1}{\tau^4}\left(\exp\left(-\frac{\tau^2}{4C_2t}\right)-1\right)\\&=\frac{\tau^2\exp\left(-\frac{\tau^2}{4C_2t}\right)+4C_2t\exp\left(-\frac{\tau^2}{4C_2t}\right)-4C_2t}{4C_2t\tau^4}.\end{aligned}\tag{8.65}$$

Due to the fact that $\tau, t, C_2 > 0$ holds true, the denominator is non-negative and we have to take a closer look at the numerator, which we differentiate with respect to τ

$$\begin{aligned}&2\tau\exp\left(-\frac{\tau^2}{4C_2t}\right)+\tau^2\exp\left(-\frac{\tau^2}{4C_2t}\right)\cdot\left(-\frac{2\tau}{4C_2t}\right)+4C_2t\exp\left(-\frac{\tau^2}{4C_2t}\right)\cdot\left(-\frac{2\tau}{4C_2t}\right)\\&=\exp\left(-\frac{\tau^2}{4C_2t}\right)\cdot\left(-\frac{2\tau^3}{4C_2t}\right)<0,\end{aligned}\tag{8.66}$$

that means the numerator of (8.65) is monotonically deceasing with respect to τ and we can estimate it with its maximum for $\tau = 0$. Inserting this yields

$$\tau^2\exp\left(-\frac{\tau^2}{4C_2t}\right)+4C_2t\exp\left(-\frac{\tau^2}{4C_2t}\right)-4C_2t\leq 0+4C_2t-4C_2t=0.\tag{8.67}$$

Thus (8.65) is non-positive and therefore the second line of (8.64), too. We take a look at the first line of (8.64), set $c \coloneqq 4C_2t$ for the sake of readability and show that the function

$$\frac{1}{r^2}\left(1-\exp\left(-\frac{r^2}{4C_2t}\right)\right)\tag{8.68}$$

is monotonically decreasing. We consider the derivative with respect to r and get

$$\begin{aligned}&-\frac{2}{r^3}\left(1-\exp\left(-\frac{r^2}{c}\right)\right)+\frac{1}{r^2}\exp\left(-\frac{r^2}{c}\right)\frac{2r}{c}\\&=\frac{2}{cr^3}\left[-c+c\exp\left(-\frac{r^2}{c}\right)+r^2\exp\left(-\frac{r^2}{c}\right)\right],\end{aligned}\tag{8.69}$$

from which we want to show that it is negative. The first factor is positive and we have a closer look at the term in the brackets. We want to detect the maximum of it and derive it again with respect to r and get

$$\begin{aligned} & c\exp\left(-\frac{r^2}{c}\right)\cdot\left(-\frac{2r}{c}\right)+2r\exp\left(-\frac{r^2}{c}\right)+r^2\exp\left(-\frac{r^2}{c}\right)\cdot\left(-\frac{2r}{c}\right) \\ & =\exp\left(-\frac{r^2}{c}\right)\cdot\left(-\frac{2r^3}{c}\right). \end{aligned} \tag{8.70}$$

Possible roots are $r=0$ or $c=0$, whereas we want to consider the case $c=0$ later separately. For the case $r=0$, we can see directly from (8.70) that we have a conversion from positive to negative sign around $r=0$ which means that we have a maximum for $r=0$. We can estimate the squared brackets in (8.69) by

$$-c+c\exp\left(-\frac{r^2}{c}\right)+r^2\exp\left(-\frac{r^2}{c}\right)\leq -c+c+0=0 \tag{8.71}$$

and obtain that (8.69) is non-positive and therefore the function in (8.68) is monotonically decreasing and furthermore, the difference in the first line of (8.64) is non-negative. The case $c=0$ reflects the case $t=0$ and results in the function $1/r^2$ instead of (8.68), which is also monotonically decreasing.

Now we consider the absolute value of the difference as given in the original integral above and estimate with the triangle inequality. We can drop out the absolute value for the first term (except for the term x_1) since we showed that the first term is positive. For the second term, we can omit the absolute value by changing the sign in front of the term since the term in the absolute value is negative

$$\begin{aligned} & \left|u_1^{\mathrm{Si}}(x,t)-u_{1,\tau}^{\mathrm{Si}}(x,t)\right| \\ & \leq \frac{C_1}{2\pi}|x_1|\left|\frac{1}{\|x\|^2}\left(1-\exp\left(-\frac{\|x\|^2}{4C_2t}\right)\right)-\frac{1}{\tau^2}\left(1-\exp\left(-\frac{\tau^2}{4C_2t}\right)\right)\right| \\ & \quad +\frac{C_1}{2\pi}|x_1|\left|\left(\frac{1}{\tau^2}\frac{1}{4C_2t}\exp\left(-\frac{\tau^2}{4C_2t}\right)+\frac{1}{\tau^4}\left(\exp\left(-\frac{\tau^2}{4C_2t}\right)-1\right)\right)\right|\left|\tau^2-\|x\|^2\right| \\ & \leq \frac{C_1}{2\pi}|x_1|\left(\frac{1}{\|x\|^2}\left(1-\exp\left(-\frac{\|x\|^2}{4C_2t}\right)\right)-\frac{1}{\tau^2}\left(1-\exp\left(-\frac{\tau^2}{4C_2t}\right)\right)\right) \\ & \quad -\frac{C_1}{2\pi}|x_1|\left(\frac{1}{\tau^2}\frac{1}{4C_2t}\exp\left(-\frac{\tau^2}{4C_2t}\right)+\frac{1}{\tau^4}\left(\exp\left(-\frac{\tau^2}{4C_2t}\right)-1\right)\right)\left(\tau^2-\|x\|^2\right) \end{aligned} \tag{8.72}$$

That means we consider the integral above without the absolute value and get with polar coordinates for the case $x_1 > 0$:

$$\begin{aligned}
&\frac{C_1}{2\pi}\int_0^T \int_{\substack{\mathbb{B}_\tau(0),\\ x_1>0}} \frac{x_1}{\|x\|^2}\left(1-\exp\left(-\frac{\|x\|^2}{4C_2t}\right)\right)\\
&\quad - x_1\left[\frac{1}{\tau^2}\left(1-\exp\left(-\frac{\tau^2}{4C_2t}\right)\right)\right.\\
&\quad \left.-\left(-\frac{1}{\tau^4}\left(1-\exp\left(-\frac{\tau^2}{4C_2t}\right)\right)+\frac{1}{4C_2t}\frac{1}{\tau^2}\exp\left(-\frac{\tau^2}{4C_2t}\right)\right)\cdot(\|x\|^2-\tau^2)\right]\,\mathrm{d}x\,\mathrm{d}t\\
&=\frac{C_1}{2\pi}\int_{-\pi/2}^{\pi/2}\cos\varphi\,\mathrm{d}\varphi\\
&\quad\times\int_0^T\int_0^\tau \frac{r^2}{r^2}\left(1-\exp\left(-\frac{r^2}{4C_2t}\right)\right)\\
&\quad -\left[\frac{r^2}{\tau^2}\left(1-\exp\left(-\frac{\tau^2}{4C_2t}\right)\right)\right.\\
&\quad \left.-\left(-\frac{1}{\tau^4}\left(1-\exp\left(-\frac{\tau^2}{4C_2t}\right)\right)+\frac{1}{\tau^2}\frac{1}{4C_2t}\exp\left(-\frac{\tau^2}{4C_2t}\right)\right)(r^4-r^2\tau^2)\right]\,\mathrm{d}r\,\mathrm{d}t.
\end{aligned} \tag{8.73}$$

For the first integral, we get

$$\int_{-\pi/2}^{\pi/2}\cos\varphi\,\mathrm{d}\varphi = 2. \tag{8.74}$$

We have a look at the second line of the integral separately later. Now we come to the third and fourth line of the integral, which is integrated with respect to r and evaluated (see also Remark 2.2.4)

$$\begin{aligned}
&\int_0^T -\frac{1}{3}\frac{\tau^3}{\tau^2}\left(1-\exp\left(-\frac{\tau^2}{4C_2t}\right)\right)\\
&\quad+\left(\frac{1}{\tau^4}\left(1-\exp\left(-\frac{\tau^2}{4C_2t}\right)\right)-\frac{1}{\tau^2}\frac{1}{4C_2t}\exp\left(-\frac{\tau^2}{4C_2t}\right)\right)\frac{2}{15}\tau^5\,\mathrm{d}t\\
&=-\frac{1}{3}\tau\left(T-\frac{\tau^2\mathrm{Ei}\left(-\frac{\tau^2}{4C_2T}\right)}{4C_2}-T\exp\left(-\frac{\tau^2}{4C_2T}\right)\right)\\
&\quad+\left(\frac{1}{\tau^4}\left(T-\frac{\tau^2\mathrm{Ei}\left(-\frac{\tau^2}{4C_2T}\right)}{4C_2}-T\exp\left(-\frac{\tau^2}{4C_2T}\right)\right)\right.\\
&\qquad\left.-\frac{1}{\tau^2}\frac{1}{4C_2}\cdot\left(-\mathrm{Ei}\left(-\frac{\tau^2}{4C_2T}\right)\right)\right)\frac{2}{15}\tau^5\\
&\to 0\ (\tau\to 0+)
\end{aligned} \tag{8.75}$$

with the considerations from (2.18). Now we have the second line of the integral in (8.73) above left, which is

$$\begin{aligned}&\int_0^T \int_0^\tau 1 - \exp\left(-\frac{r^2}{4C_2 t}\right)\,\mathrm{d}r\,\mathrm{d}t\\ &= \int_0^T \tau - \frac{1}{2}\sqrt{\pi}\sqrt{4C_2 t}\,\operatorname{erf}\left(\frac{\tau}{\sqrt{4C_2 t}}\right)\,\mathrm{d}t.\end{aligned} \tag{8.76}$$

Here the first part with τ is also convergent to 0 for $\tau \to 0+$. Let us have a look at the second part, which is given by

$$\begin{aligned}&\int_0^T \sqrt{4C_2 t}\,\operatorname{erf}\left(\frac{\tau}{\sqrt{4C_2 t}}\right)\,\mathrm{d}t\\ &= \frac{2}{3}\left(\frac{\tau\left(\frac{\tau^2 \mathrm{Ei}\left(-\frac{\tau^2}{4C_2 T}\right)}{4C_2} + T\exp\left(-\frac{\tau^2}{4C_2 T}\right)\right)}{\sqrt{\pi}} + T\cdot\sqrt{4C_2 T}\operatorname{erf}\left(\frac{\tau}{\sqrt{4C_2 T}}\right)\right)\\ &\to 0\ (\tau \to 0+)\end{aligned} \tag{8.77}$$

with the help of (2.18). We can verify this primitive function easily by deriving (see also Definition 2.2.1 and (2.22))

$$\begin{aligned}&\frac{\partial}{\partial t}\left[\frac{2}{3}\left(\frac{\tau\left(\frac{\tau^2 \mathrm{Ei}\left(-\frac{\tau^2}{4C_2 t}\right)}{4C_2} + t\exp\left(-\frac{\tau^2}{4C_2 t}\right)\right)}{\sqrt{\pi}} + t\cdot\sqrt{4C_2 t}\,\operatorname{erf}\left(\frac{\tau}{\sqrt{4C_2 t}}\right)\right)\right]\\ &= \frac{2}{3}\left[\frac{\tau}{\sqrt{\pi}}\left(\frac{\tau^2}{4C_2}\exp\left(-\frac{\tau^2}{4C_2 t}\right)\cdot\left(\frac{-4C_2 t}{\tau^2}\right)\cdot\left(\frac{\tau^2}{4C_2 t^2}\right) + \exp\left(-\frac{\tau^2}{4C_2 t}\right)\right.\right.\\ &\quad \left. + t\exp\left(-\frac{\tau^2}{4C_2 t}\right)\cdot\frac{\tau^2}{4C_2 t^2}\right) + \sqrt{4C_2 t}\,\operatorname{erf}\left(\frac{\tau}{\sqrt{4C_2 t}}\right) + t\frac{4C_2}{2\sqrt{4C_2 t}}\operatorname{erf}\left(\frac{\tau}{\sqrt{4C_2 t}}\right)\\ &\quad \left. + t\sqrt{4C_2 t}\frac{2}{\sqrt{\pi}}\exp\left(-\frac{\tau^2}{4C_2 t}\right)\cdot\left(-\frac{\tau\cdot 4C_2}{2(4C_2 t)^{3/2}}\right)\right]\\ &= \frac{2}{3}\left[\frac{\tau}{\sqrt{\pi}}\left(-\frac{\tau^2}{4C_2 t}\exp\left(-\frac{\tau^2}{4C_2 t}\right) + \exp\left(-\frac{\tau^2}{4C_2 t}\right) + \frac{\tau^2}{4C_2 t}\exp\left(-\frac{\tau^2}{4C_2 t}\right)\right)\right.\\ &\quad \left. + \sqrt{4C_2 t}\,\operatorname{erf}\left(\frac{\tau}{\sqrt{4C_2 t}}\right) + \sqrt{C_2 t}\,\operatorname{erf}\left(\frac{\tau}{\sqrt{4C_2 t}}\right) - \frac{\tau}{\sqrt{\pi}}\exp\left(-\frac{\tau^2}{4C_2 t}\right)\right]\\ &= \frac{2}{3}\operatorname{erf}\left(\frac{\tau}{\sqrt{4C_2 t}}\right)\left(\sqrt{4C_2 t} + \frac{1}{2}\sqrt{4C_2 t}\right)\\ &= \sqrt{4C_2 t}\,\operatorname{erf}\left(\frac{\tau}{\sqrt{4C_2 t}}\right).\end{aligned} \tag{8.78}$$

This finishes the proof for u^{Si} and for all regularized fundamental solutions. □

8.2.5. Summary

The fundamental solutions $\boldsymbol{u}^{\mathrm{CN}}$, p^{St}, p^{Si} and u^{Si} have been regularized with respect to their spatial component $\|x\|$. Regularization with respect to the time was for u^{Si} and p^{Si} not useful due to the necessary theoretical properties for our decorrelation, that means the theoretical properties of the source scaling functions that we will construct in the next section. We need the properties of an approximate identity (see Definition 4.1.3). Thus the regularized fundamental solutions are an intermediate step to our desired source scaling functions. Since we did the construction with the Taylor expansion with the constant and linear term, our regularized functions are $\mathrm{C}^{(1)}$ due to Theorem 8.1.3. In the next section, we want to continue with the construction of our source scaling functions and wavelets, where we need our deduced mollified fundamental solutions.

8.3. Source Scaling Functions and Wavelets

Before we go over to the construction of the source scaling functions, we have to recall the connection between the fundamental solutions ans the poroelastic differential operator L^{pe}. If we understand the fundamental solutions of the QEP as a fundamental solution tensor, we can apply the poroelastic differential operator to the given tensor

$$\boldsymbol{G}(x,t) = \begin{pmatrix} u_{11}^{\mathrm{CN}}(x)\delta_t & u_{12}^{\mathrm{CN}}(x)\delta_t & p_1^{\mathrm{St}}(x)\delta_t \\ u_{21}^{\mathrm{CN}}(x)\delta_t & u_{22}^{\mathrm{CN}}(x)\delta_t & p_2^{\mathrm{St}}(x)\delta_t \\ u_1^{\mathrm{Si}}(x,t) & u_2^{\mathrm{Si}}(x,t) & p^{\mathrm{Si}}(x,t) \end{pmatrix} \tag{8.79}$$

in the following way and get (see (7.17))

$$L^{\mathrm{pe}}G = I\delta_x\delta_t, \tag{8.80}$$

where I is the identity matrix. This is the way how the fundamental solutions were constructed (see [10, 34] and the references therein). For the construction of the source scaling functions, we apply the differential operator L^{pe} now on G_τ, which is the tensor containing the regularized fundamental solutions, that means

$$\boldsymbol{G}_\tau(x,t) = \begin{pmatrix} u_{11,\tau}^{\mathrm{CN}}(x)\delta_t & u_{12,\tau}^{\mathrm{CN}}(x)\delta_t & p_{1,\tau}^{\mathrm{St}}(x)\delta_t \\ u_{21,\tau}^{\mathrm{CN}}(x)\delta_t & u_{22,\tau}^{\mathrm{CN}}(x)\delta_t & p_{2,\tau}^{\mathrm{St}}(x)\delta_t \\ u_{1,\tau}^{\mathrm{Si}}(x,t) & u_{2,\tau}^{\mathrm{Si}}(x,t) & p_\tau^{\mathrm{Si}}(x,t) \end{pmatrix}. \tag{8.81}$$

More precisely, we apply the differential operator on each row of G_τ (see (2.13)). The resulting tensor of the source scaling functions is denoted by

$$\boldsymbol{\Phi}_\tau(x,t) = \begin{pmatrix} \Phi_{11,\tau}(x)\delta_t & \Phi_{12,\tau}(x)\delta_t & \Phi_{13,\tau}^1(x)\delta_t' + \Phi_{13,\tau}^2(x)\delta_t \\ \Phi_{21,\tau}(x)\delta_t & \Phi_{22,\tau}(x)\delta_t & \Phi_{23,\tau}^1(x)\delta_t' + \Phi_{23,\tau}^2(x)\delta_t \\ \Phi_{31,\tau}(x,t) & \Phi_{32,\tau}(x,t) & \Phi_{33,\tau}(x,t) \end{pmatrix} \tag{8.82}$$

and we can figure out the several components. For our notation we have to say: With $\Phi_{ik,\tau}$, we denote the source scaling functions without the Delta distribution (if they contain such one) and $(\boldsymbol{\Phi}_\tau)_{ik}$ denotes the whole entry of the tensor, that means in the case of the first two rows the entry including the Delta distribution. For the third row, it is therefore $\Phi_{ik,\tau} = (\boldsymbol{\Phi}_\tau)_{ik}$. Please remember here how we constructed our regularized fundamental solutions: For $\|x\| \geq \tau$ we use the fundamental solutions themselves and for $\|x\| < \tau$, we use a Taylor mollification of the fundamental solutions. If we now apply the differential operator on $\boldsymbol{G}_\tau$, we only have support of the source scaling functions for $\|x\| \leq \tau$ for the spatial part because outside it is zero. Thus our derivations for the source scaling functions in the following have to be seen for the case $\|x\| \leq \tau$. We start with the first row

and calculate the several components that we need for the source scaling function tensor

$$\begin{aligned}(\Phi_{11,\tau}, \Phi_{12,\tau}, \Phi_{13,\tau}) &= L^{\mathrm{pe}}\left(u^{\mathrm{CN}}_{11,\tau}, u^{\mathrm{CN}}_{21,\tau}, p^{\mathrm{St}}_{1,\tau}\right) \\ &= \begin{pmatrix} -\frac{\lambda+\mu}{\mu}\nabla_x\left(\nabla_x \cdot \begin{pmatrix} u^{\mathrm{CN}}_{11,\tau} \\ u^{\mathrm{CN}}_{12,\tau}\end{pmatrix}\right) - \nabla_x^2 \begin{pmatrix} u^{\mathrm{CN}}_{11,\tau} \\ u^{\mathrm{CN}}_{12,\tau}\end{pmatrix} + \alpha\nabla_x p^{\mathrm{St}}_{1,\tau} \\ \partial_t\left(c_0\mu p^{\mathrm{St}}_{1,\tau} + \alpha\left(\nabla_x \cdot \begin{pmatrix} u^{\mathrm{CN}}_{11,\tau} \\ u^{\mathrm{CN}}_{12,\tau}\end{pmatrix}\right)\right) - \nabla_x^2 p^{\mathrm{St}}_{1,\tau}\end{pmatrix}^{\mathrm{T}}.\end{aligned} \tag{8.83}$$

For $\Phi_{11,\tau}$ and $\Phi_{12,\tau}$ we need for $\|x\| \leq \tau$ the following partial derivatives

$$\partial_{x_1} u^{\mathrm{CN}}_{11,\tau} = \frac{C_3}{2\pi}\left[-\frac{2x_1}{2\tau^2} + C_4 \cdot 2x_1 \cdot \left(\frac{2}{\tau^2} - \frac{\|x\|^2}{\tau^4}\right) + C_4 \cdot x_1^2 \cdot \left(-\frac{2x_1}{\tau^4}\right)\right], \tag{8.84}$$

$$\partial_{x_2} u^{\mathrm{CN}}_{11,\tau} = \frac{C_3}{2\pi}\left[-\frac{2x_2}{2\tau^2} + C_4 \cdot x_1^2 \cdot \left(-\frac{2x_2}{\tau^4}\right)\right], \tag{8.85}$$

$$\partial_{x_1^2} u^{\mathrm{CN}}_{11,\tau} = \frac{C_3}{2\pi}\left(-\frac{1}{\tau^2} + C_4 \cdot \left(\frac{4}{\tau^2} - \frac{12x_1^2 + 2x_2^2}{\tau^4}\right)\right), \tag{8.86}$$

$$\partial_{x_2^2} u^{\mathrm{CN}}_{11,\tau} = \frac{C_3}{2\pi}\left[-\frac{1}{\tau^2} + C_4 \cdot x_1^2 \cdot \left(-\frac{2}{\tau^4}\right)\right], \tag{8.87}$$

$$\partial_{x_1}\partial_{x_2} u^{\mathrm{CN}}_{11,\tau} = \frac{C_3 C_4}{2\pi}\left(-\frac{4x_1x_2}{\tau^4}\right), \tag{8.88}$$

$$\partial_{x_1} u^{\mathrm{CN}}_{12,\tau} = \frac{C_3 C_4}{2\pi}\left[x_2 \cdot \left(\frac{2}{\tau^2} - \frac{\|x\|^2}{\tau^4}\right) + x_1x_2 \cdot \left(-\frac{2x_1}{\tau^4}\right)\right], \tag{8.89}$$

$$\partial_{x_2} u^{\mathrm{CN}}_{12,\tau} = \frac{C_3 C_4}{2\pi}\left[x_1 \cdot \left(\frac{2}{\tau^2} - \frac{\|x\|^2}{\tau^4}\right) + x_1x_2 \cdot \left(-\frac{2x_2}{\tau^4}\right)\right], \tag{8.90}$$

$$\partial_{x_1^2} u^{\mathrm{CN}}_{12,\tau} = \frac{C_3 C_4}{2\pi}\left(-\frac{6x_1x_2}{\tau^4}\right), \tag{8.91}$$

$$\partial_{x_2^2} u^{\mathrm{CN}}_{12,\tau} = \frac{C_3 C_4}{2\pi}\left(-\frac{6x_1x_2}{\tau^4}\right), \tag{8.92}$$

$$\partial_{x_1}\partial_{x_2} u^{\mathrm{CN}}_{12,\tau} = \frac{C_3 C_4}{2\pi}\left(\frac{2}{\tau^2} - \frac{3\|x\|^2}{\tau^4}\right). \tag{8.93}$$

With these preliminary considerations, we can assemble the several components of our source scaling functions and obtain

$$\nabla_x p^{\mathrm{St}}_{1,\tau} = \frac{C_1}{2\pi}\frac{1}{\tau^2}\begin{pmatrix} 2 - \frac{3x_1^2 + x_2^2}{\tau^2} \\ -\frac{2x_1x_2}{\tau^2}\end{pmatrix}, \tag{8.94}$$

$$\begin{aligned}\nabla_x^2 u^{\mathrm{CN}}_{11,\tau} &= \frac{C_3}{2\pi}\left(-\frac{2}{\tau^2} + C_4 \cdot \left(-\frac{12x_1^2 + 2x_2^2 + 2x_1^2}{\tau^4} + \frac{4}{\tau^2}\right)\right) \\ &= \frac{C_3}{2\pi}\left(\frac{-2 + 4C_4}{\tau^2} + C_4 \cdot \left(-\frac{14x_1^2 + 2x_2^2}{\tau^4}\right)\right),\end{aligned} \tag{8.95}$$

$$\nabla_x^2 u_{12,\tau}^{\mathrm{CN}} = -\frac{C_3 C_4}{\pi}\frac{6x_1x_2}{\tau^4}, \tag{8.96}$$

$$\begin{aligned}\nabla_x\left(\nabla_x\cdot\begin{pmatrix}u_{11,\tau}^{\mathrm{CN}}\\ u_{12,\tau}^{\mathrm{CN}}\end{pmatrix}\right) &= \begin{pmatrix}\partial_{x_1^2}u_{11,\tau}^{\mathrm{CN}} + \partial_{x_1}\partial_{x_2}u_{12,\tau}^{\mathrm{CN}}\\ \partial_{x_2}\partial_{x_1}u_{11,\tau}^{\mathrm{CN}} + \partial_{x_2^2}u_{12,\tau}^{\mathrm{CN}}\end{pmatrix}\\ &= \begin{pmatrix}\frac{C_3}{2\pi}\left(-\frac{1}{\tau^2} + C_4\cdot\left(\frac{6}{\tau^2} - \frac{15x_1^2+5x_2^2}{\tau^4}\right)\right)\\ \frac{C_3C_4}{2\pi}\left(-\frac{10x_1x_2}{\tau^4}\right)\end{pmatrix}.\end{aligned} \tag{8.97}$$

Summarizing the components above, we get

$$\begin{aligned}\Phi_{11,\tau}(x) = &-\frac{\lambda+\mu}{\mu}\frac{C_3}{2\pi}\left(-\frac{1}{\tau^2} + C_4\cdot\left(\frac{6}{\tau^2} - \frac{15x_1^2+5x_2^2}{\tau^4}\right)\right)\\ &-\frac{C_3}{2\pi}\left(\frac{-2+4C_4}{\tau^2} + C_4\cdot\left(-\frac{14x_1^2+2x_2^2}{\tau^4}\right)\right) + \alpha\frac{C_1}{2\pi}\frac{1}{\tau^2}\left(2 - \frac{3x_1^2+x_2^2}{\tau^2}\right),\end{aligned} \tag{8.98}$$

$$\begin{aligned}\Phi_{12,\tau}(x) &= -\frac{\lambda+\mu}{\mu}\cdot\frac{C_3C_4}{2\pi}\left(-\frac{10x_1x_2}{\tau^4}\right) + \frac{C_3C_4}{\pi}\cdot\frac{6x_1x_2}{\tau^4} - \alpha\frac{C_1}{2\pi}\frac{2x_1x_2}{\tau^4}\\ &= \frac{x_1x_2}{\tau^4\pi}\left(\frac{\lambda+\mu}{\mu}\cdot 5C_3C_4 + 6C_3C_4 - \alpha C_1\right).\end{aligned} \tag{8.99}$$

For $\Phi_{13,\tau}$, we have to consider that the fundamental solutions $\boldsymbol{u}^{\mathrm{CN}}$ and p^{St} are not time-dependent but the whole entries in the fundamental solution tensor belonging to $\boldsymbol{u}^{\mathrm{CN}}$ and p^{St} are equipped with δ_t. Since the third equation contains a derivative with respect to t, we have to observe this. We get for the Laplacian of $p_{1,\tau}^{\mathrm{St}}$

$$\nabla_x^2 p_{1,\tau}^{\mathrm{St}} = -\frac{4x_1C_1}{\tau^4\pi} \tag{8.100}$$

and together with the derivatives above for the two components of $\Phi_{13,\tau}$

$$\Phi_{13,\tau}^1(x) = \left[\frac{c_0\mu C_1}{2\pi}\cdot\frac{x_1}{\tau^2}\left(2 - \frac{\|x\|^2}{\tau^2}\right) + \frac{\alpha C_3}{2\pi}\left(\frac{x_1(6C_4-1)}{\tau^2} - 5C_4\cdot x_1\cdot\frac{\|x\|^2}{\tau^4}\right)\right], \tag{8.101}$$

$$\Phi_{13,\tau}^2(x) = \frac{4x_1C_1}{\tau^4\pi}. \tag{8.102}$$

The first component is the part which has a δ_t' in the whole entry and the second one is equipped with δ_t, if we consider the whole entry of the source scaling function tensor. Please note here that it is necessary to do a little modification of $\Phi_{13,\tau}^2$ to ensure that the property of an approximate identity holds true (see Definition 4.1.3). From now on, we will change the τ^4 in the denominator to τ^3, which is a part of the regularization and necessary to obtain the theoretical requirements.

We continue with the second row of Φ_τ. In this case the calculations are similar to those above, because of the symmetry. We get

$$\begin{aligned}\left(\Phi_{21,\tau}, \Phi_{22,\tau}, \Phi_{23,\tau}\right) &= L^{\mathrm{pe}}\left(u_{21,\tau}^{\mathrm{CN}}, u_{22,\tau}^{\mathrm{CN}}, p_{2,\tau}^{\mathrm{St}}\right) \\ &= \begin{pmatrix} -\frac{\lambda+\mu}{\mu}\nabla_x\left(\nabla_x \cdot \begin{pmatrix} u_{21,\tau}^{\mathrm{CN}} \\ u_{22,\tau}^{\mathrm{CN}} \end{pmatrix}\right) - \nabla_x^2 \begin{pmatrix} u_{21,\tau}^{\mathrm{CN}} \\ u_{22,\tau}^{\mathrm{CN}} \end{pmatrix} + \alpha\nabla_x p_{2,\tau}^{\mathrm{St}} \\ \partial_t\left(c_0\mu p_{2,\tau}^{\mathrm{St}} + \alpha\left(\nabla_x \cdot \begin{pmatrix} u_{21,\tau}^{\mathrm{CN}} \\ u_{22,\tau}^{\mathrm{CN}} \end{pmatrix}\right)\right) - \nabla_x^2 p_{2,\tau}^{\mathrm{St}} \end{pmatrix}^{\mathrm{T}}.\end{aligned} \tag{8.103}$$

Furthermore, we have in analogy to above for $\|x\| < \tau$

$$\nabla_x p_{2,\tau}^{\mathrm{St}} = \frac{C_1}{2\pi}\frac{1}{\tau^2}\begin{pmatrix} -\frac{2x_1x_2}{\tau^2} \\ 2 - \frac{3x_2^2+x_1^2}{\tau^2} \end{pmatrix}, \tag{8.104}$$

$$\nabla_x^2 u_{21,\tau}^{\mathrm{CN}} = -\frac{C_3C_4}{\pi}\cdot\frac{6x_1x_2}{\tau^4}, \tag{8.105}$$

$$\nabla_x^2 u_{22,\tau}^{\mathrm{CN}} = \frac{C_3}{2\pi}\left(-\frac{2}{\tau^2} + C_4\cdot\left(-\frac{14x_2^2+2x_1^2-4}{\tau^4}\right)\right), \tag{8.106}$$

$$\nabla_x\left(\nabla_x \cdot \begin{pmatrix} u_{21,\tau}^{\mathrm{CN}} \\ u_{22,\tau}^{\mathrm{CN}} \end{pmatrix}\right) = \begin{pmatrix} \frac{C_3C_4}{2\pi}\left(-\frac{10x_1x_2}{\tau^4}\right) \\ \frac{C_3}{2\pi}\left(-\frac{1}{\tau^2} + C_4\cdot\left(\frac{6}{\tau^2} - \frac{5x_1^2+15x_2^2}{\tau^4}\right)\right) \end{pmatrix}. \tag{8.107}$$

We can see that $\Phi_{21,\tau}$ is exactly the same as $\Phi_{12,\tau}$ and $\Phi_{22,\tau}$ is the same as $\Phi_{11,\tau}$ with changed roles of x_1 and x_2. The same holds true for $\Phi_{23,\tau}$ compared with $\Phi_{13,\tau}$ (for both upper indices 1 and 2). Therefore, we do not write them down here separately but rather at the end of our calculations to have all source scaling functions at a look. Please note that we do the modification in the denominator of $\Phi_{23,\tau}^2$ in the same way as for $\Phi_{13,\tau}^2$. Let us continue with the third row. Here the functions are space and time dependent and we do not have to take care about the Delta distribution.

$$\begin{aligned}\left(\Phi_{31,\tau}, \Phi_{32,\tau}, \Phi_{33,\tau}\right) &= L^{\mathrm{pe}}\left(u_{1,\tau}^{\mathrm{Si}}, u_{2,\tau}^{\mathrm{Si}}, p_{\tau}^{\mathrm{Si}}\right) \\ &= \begin{pmatrix} -\frac{\lambda+\mu}{\mu}\nabla_x\left(\nabla_x \cdot \begin{pmatrix} u_{1,\tau}^{\mathrm{Si}} \\ u_{2,\tau}^{\mathrm{Si}} \end{pmatrix}\right) - \nabla_x^2 \begin{pmatrix} u_{1,\tau}^{\mathrm{Si}} \\ u_{2,\tau}^{\mathrm{Si}} \end{pmatrix} + \alpha\nabla_x p_{\tau}^{\mathrm{Si}} \\ \partial_t\left(c_0\mu p_{\tau}^{\mathrm{Si}} + \alpha\left(\nabla_x \cdot \begin{pmatrix} u_{1,\tau}^{\mathrm{Si}} \\ u_{2,\tau}^{\mathrm{Si}} \end{pmatrix}\right)\right) - \nabla_x^2 p_{\tau}^{\mathrm{Si}} \end{pmatrix}^{\mathrm{T}}.\end{aligned} \tag{8.108}$$

For the calculation of the several components regarding the first row of the differential operator, we can reduce therefore the relevant components for the derivative to the

$$\nabla_x \left(\nabla_x \cdot \begin{pmatrix} x_1 \|x\|^2 \\ x_2 \|x\|^2 \end{pmatrix} \right) = \nabla_x \left(\nabla_x \cdot \begin{pmatrix} x_1 (x_1^2 + x_2^2) \\ x_2 (x_1^2 + x_2^2) \end{pmatrix} \right) = \begin{pmatrix} 8x_1 \\ 8x_2 \end{pmatrix}, \tag{8.109}$$

$$\begin{aligned} \nabla_x \left(\nabla_x \cdot \begin{pmatrix} u_{1,\tau}^{\mathrm{Si}} \\ u_{2,\tau}^{\mathrm{Si}} \end{pmatrix} \right) = \frac{8C_1}{2\pi} \cdot 8 \cdot \begin{pmatrix} x_1 \\ x_2 \end{pmatrix} \left(-\frac{1}{\tau^4} + \exp\left(-\frac{\tau^2}{4C_2 t} \right) \frac{1}{4C_2 t} \frac{1}{\tau^2} \right. \\ \left. + \frac{1}{\tau^4} \exp\left(-\frac{\tau^2}{4C_2 t} \right) \right), \end{aligned} \tag{8.110}$$

$$\nabla_x^2 \begin{pmatrix} x_1 \|x\|^2 \\ x_2 \|x\|^2 \end{pmatrix} = \nabla_x^2 \begin{pmatrix} x_1 (x_1^2 + x_2^2) \\ x_2 (x_1^2 + x_2^2) \end{pmatrix} = \begin{pmatrix} 8x_1 \\ 8x_2 \end{pmatrix}, \tag{8.111}$$

$$\begin{aligned} \nabla_x^2 u_\tau^{\mathrm{Si}} = \frac{C_1}{2\pi} \cdot 8 \cdot \begin{pmatrix} x_1 \\ x_2 \end{pmatrix} \left(-\frac{1}{\tau^4} + \exp\left(-\frac{\tau^2}{4C_2 t} \right) \frac{1}{4C_2 t} \frac{1}{\tau^2} \right. \\ \left. + \frac{1}{\tau^4} \exp\left(-\frac{\tau^2}{4C_2 t} \right) \right), \end{aligned} \tag{8.112}$$

$$\begin{aligned} \nabla_x p_\tau^{\mathrm{Si}} &= \frac{1}{4\pi t} \exp\left(-\frac{\tau^2}{4C_2 t} \right) \cdot \left(-\frac{1}{4C_2 t} \right) \cdot \begin{pmatrix} 2x_1 \\ 2x_2 \end{pmatrix} \\ &= -\begin{pmatrix} x_1 \\ x_2 \end{pmatrix} \exp\left(-\frac{\tau^2}{4C_2 t} \right) \frac{1}{8\pi C_2 t^2}. \end{aligned} \tag{8.113}$$

In this case the $x\|x\|$-term is the only relevant term that remains if we consider derivatives of the second order. Now we can put together these derivatives to get the first two entries $\Phi_{31,\tau}$ and $\Phi_{32,\tau}$ of the last row of the source scaling function tensor, which are

$$\begin{aligned} \begin{pmatrix} \Phi_{31,\tau} \\ \Phi_{32,\tau} \end{pmatrix} &= \left[-\frac{\lambda + \mu}{\mu} - 1 \right] \frac{C_1}{2\pi} \cdot 8 \cdot \begin{pmatrix} x_1 \\ x_2 \end{pmatrix} \left(-\frac{1}{\tau^4} + \exp\left(-\frac{\tau^2}{4C_2 t} \right) \frac{1}{4C_2 t} \frac{1}{\tau^2} \right. \\ &\quad \left. + \frac{1}{\tau^4} \exp\left(-\frac{\tau^2}{4C_2 t} \right) \right) - \begin{pmatrix} x_1 \\ x_2 \end{pmatrix} \frac{\alpha}{8C_2 \pi t^2} \exp\left(-\frac{\tau^2}{4C_2 t} \right) \\ &= \begin{pmatrix} x_1 \\ x_2 \end{pmatrix} \frac{(-\lambda - 2\mu) 8C_1 \left(-4C_2 t^2 + t\tau^2 \exp\left(-\frac{\tau^2}{4C_2 t} \right) + 4C_2 t^2 \exp\left(-\frac{\tau^2}{4C_2 t} \right) \right)}{8C_2 \mu t^2 \tau^4 \pi} \\ &\quad - \begin{pmatrix} x_1 \\ x_2 \end{pmatrix} \frac{\alpha \mu \tau^4 \exp\left(-\frac{\tau^2}{4C_2 t} \right)}{8C_2 \mu t^2 \tau^4 \pi} \\ &= -\begin{pmatrix} x_1 \\ x_2 \end{pmatrix} \exp\left(-\frac{\tau^2}{4C_2 t} \right) \left(\frac{\alpha \mu \tau^4 + 8C_1 (\lambda + 2\mu) t \tau^2}{8C_2 \mu t^2 \tau^4 \pi} \right. \\ &\quad \left. + \frac{32 C_1 C_2 (\lambda + 2\mu) t^2 \left(1 - \exp\left(\frac{\tau^2}{4C_2 t} \right) \right)}{8C_2 \mu t^2 \tau^4 \pi} \right). \end{aligned} \tag{8.114}$$

The last function to figure out is $\Phi_{33,\tau}$. For the Laplacian of $p^{\mathrm{Si}}_{1,\tau}$, we can use the gradient from above and apply the divergence onto it. The several components that we need are given by

$$\begin{aligned}
\nabla_x^2 p_\tau^{\mathrm{Si}} &= \operatorname{div}\left((8.113)\right) \\
&= \frac{-1}{4\pi C_2 t^2}\exp\left(-\frac{\tau^2}{4C_2 t}\right), \qquad (8.115)\\
\partial_t p_\tau^{\mathrm{Si}} &= \frac{-1}{4\pi t^2}\exp\left(-\frac{\tau^2}{4C_2 t}\right)\left[1-\frac{1}{4C_2 t}(\|x\|^2-\tau^2)\right] \\
&\quad + \frac{1}{4\pi t}\exp\left(-\frac{\tau^2}{4C_2 t}\right)\cdot\frac{\tau^2}{4C_2 t^2}\left[1-\frac{1}{4C_2 t}(\|x\|^2-\tau^2)\right] \\
&\quad + \frac{1}{4\pi t}\exp\left(-\frac{\tau^2}{4C_2 t}\right)\cdot\frac{1}{4C_2 t^2}(\|x\|^2-\tau^2) \\
&= \exp\left(-\frac{\tau^2}{4C_2 t}\right)\left[-\frac{1}{4\pi t^2}+\frac{1}{16C_2 t^3\pi}(\|x\|^2-\tau^2)+\frac{\tau^2}{16C_2 t^3\pi}\right. \\
&\quad \left.-\frac{\tau^2}{64C_2^2 t^4\pi}(\|x\|^2-\tau^2)+\frac{1}{16C_2 t^3\pi}(\|x\|^2-\tau^2)\right] \\
&= \exp\left(-\frac{\tau^2}{4C_2 t}\right)\left[-\frac{1}{4\pi t^2}+\frac{1}{16C_2 t^3\pi}(2\|x\|^2-\tau^2)-\frac{\tau^2}{64C_2^2 t^4\pi}(\|x\|^2-\tau^2)\right], \\
&\qquad (8.116)\\
\partial_t(\nabla_x\cdot u^{\mathrm{Si}}) &= \partial_t\left(\frac{C_1}{2\pi}\left[2\cdot\left[\frac{1}{\tau^2}-\frac{1}{\tau^2}\exp\left(-\frac{\tau^2}{4C_2 t}\right)\right.\right.\right. \\
&\quad \left.+\left(\frac{-1}{\tau^4}+\frac{1}{4C_2 t}\exp\left(-\frac{\tau^2}{4C_2 t}\right)\cdot\frac{1}{\tau^2}+\frac{1}{\tau^4}\exp\left(-\frac{\tau^2}{4C_2 t}\right)\right)(\|x\|^2-\tau^2)\right] \\
&\quad \left.\left.+2\|x\|^2\left[\frac{-1}{\tau^4}+\frac{1}{4C_2 t}\frac{1}{\tau^2}\exp\left(-\frac{\tau^2}{4C_2 t}\right)+\frac{1}{\tau^4}\exp\left(-\frac{\tau^2}{4C_2 t}\right)\right]\right]\right) \\
&= \frac{C_1}{\pi}\left[-\frac{1}{\tau^2}\exp\left(-\frac{\tau^2}{4C_2 t}\right)\cdot\frac{\tau^2}{4C_2 t^2}+\left(-\frac{1}{4C_2 t^2}\exp\left(-\frac{\tau^2}{4C_2 t}\right)\cdot\frac{1}{\tau^2}\right.\right. \\
&\quad \left.+\frac{1}{4C_2 t}\exp\left(-\frac{\tau^2}{4C_2 t}\right)\cdot\frac{\tau^2}{4C_2 t^2}\cdot\frac{1}{\tau^2}+\frac{1}{\tau^4}\exp\left(-\frac{\tau^2}{4C_2 t}\right)\cdot\frac{\tau^2}{4C_2 t^2}\right) \\
&\quad \left.\cdot(2\|x\|^2-\tau^2)\right] \\
&= \frac{C_1}{\pi}\exp\left(-\frac{\tau^2}{4C_2 t}\right)\left[-\frac{1}{4C_2 t^2}+\frac{1}{16C_2^2 t^3}(2\|x\|^2-\tau^2)\right]. \qquad (8.117)
\end{aligned}$$

We put together the derivatives for the last component of our tensor $\mathbf{\Phi}_\tau$. Furthermore, the derived function can be a bit simplified by inserting the material constants for Berea sandstone given in (7.21) which is done in the next step and leads us to

$$\begin{aligned}
\Phi_{33,\tau} &= c_0\mu \exp\left(-\frac{\tau^2}{4C_2t}\right)\left[-\frac{1}{4\pi t^2}+\frac{1}{16C_2t^3\pi}(2\|x\|^2-\tau^2)-\frac{\tau^2}{64C_2^2t^4\pi}(\|x\|^2-\tau^2)\right] \\
&\quad+\frac{\alpha C_1}{\pi}\exp\left(-\frac{\tau^2}{4C_2t}\right)\left[-\frac{1}{4C_2t^2}+\frac{1}{16C_2^2t^3}(2\|x\|^2-\tau^2)\right] \\
&\quad+\exp\left(-\frac{\tau^2}{4C_2t}\right)\frac{1}{4C_2t^2\pi} \\
&= \exp\left(-\frac{\tau^2}{4C_2t}\right)\left[\overbrace{\frac{-C_2c_0\mu-C_1\alpha}{4C_2\pi t^2}}^{=-1}+\overbrace{\frac{C_2c_0\mu+C_1\alpha}{16C_2^2t^3\pi}}^{=1}(2\|x\|^2-\tau^2)\right. \\
&\quad\left.-\frac{c_0\mu\tau^2}{64C_2^2t^4\pi}(\|x\|^2-\tau^2)+\frac{1}{4C_2t^2\pi}\right] \\
&= \exp\left(-\frac{\tau^2}{4C_2t}\right)\frac{4t(2\|x\|^2-\tau^2)+c_0\mu\tau^2(\tau^2-\|x\|^2)}{64C_2^2t^4\pi}. \qquad (8.118)
\end{aligned}$$

We want to summarize the components of $\mathbf{\Phi}_\tau$ at a glance. Here we can see better the several symmetry relations of the source scaling function, for example $\Phi_{11,\tau}$ and $\Phi_{22,\tau}$, $\Phi_{13,\tau}$ and $\Phi_{23,\tau}$ and at last $\Phi_{31,\tau}$ and $\Phi_{32,\tau}$. The source scaling functions are given by

$$\begin{aligned}
\Phi_{11,\tau}(x) &= -\frac{\lambda+\mu}{\mu}\frac{C_3}{2\pi}\left(-\frac{1}{\tau^2}+C_4\cdot\left(\frac{6}{\tau^2}-\frac{15x_1^2+5x_2^2}{\tau^4}\right)\right) \\
&\quad-\frac{C_3}{2\pi}\left(\frac{-2+4C_4}{\tau^2}+C_4\cdot\left(-\frac{14x_1^2+2x_2^2}{\tau^4}\right)\right)+\alpha\frac{C_1}{2\pi}\frac{1}{\tau^2}\left(2-\frac{3x_1^2+x_2^2}{\tau^2}\right), \qquad (8.119)
\end{aligned}$$

$$\Phi_{12,\tau}(x) = \frac{x_1x_2}{\tau^4\pi}\left(\frac{\lambda+\mu}{\mu}\cdot 5C_3C_4+6C_3C_4-\alpha C_1\right), \qquad (8.120)$$

$$\Phi^1_{13,\tau}(x) = \left[\frac{c_0\mu C_1}{2\pi}\cdot\frac{x_1}{\tau^2}\left(2-\frac{\|x\|^2}{\tau^2}\right)+\frac{\alpha C_3}{2\pi}\left(\frac{x_1(6C_4-1)}{\tau^2}-5C_4\cdot x_1\cdot\frac{\|x\|^2}{\tau^4}\right)\right], \qquad (8.121)$$

$$\Phi^2_{13,\tau}(x) = \frac{4x_1C_1}{\tau^3\pi}, \qquad (8.122)$$

$$\Phi_{21,\tau}(x) = \frac{x_1 x_2}{\tau^4 \pi}\left(\frac{\lambda+\mu}{\mu}\cdot 5C_3C_4 + 6C_3C_4 - \alpha C_1\right), \tag{8.123}$$

$$\begin{aligned}\Phi_{22,\tau}(x) = &-\frac{\lambda+\mu}{\mu}\frac{C_3}{2\pi}\left(-\frac{1}{\tau^2} + C_4\cdot\left(\frac{6}{\tau^2} - \frac{15x_2^2+5x_1^2}{\tau^4}\right)\right)\\ &-\frac{C_3}{2\pi}\left(\frac{-2+4C_4}{\tau^2} + C_4\cdot\left(-\frac{14x_2^2+2x_1^2}{\tau^4}\right)\right) + \alpha\frac{C_1}{2\pi}\frac{1}{\tau^2}\left(2 - \frac{3x_2^2+x_1^2}{\tau^2}\right),\end{aligned} \tag{8.124}$$

$$\Phi^1_{23,\tau}(x) = \left[\frac{c_0\mu C_1}{2\pi}\cdot\frac{x_2}{\tau^2}\left(2 - \frac{\|x\|^2}{\tau^2}\right) + \frac{\alpha C_3}{2\pi}\left(\frac{x_2(6C_4-1)}{\tau^2} - 5C_4\cdot x_2\cdot\frac{\|x\|^2}{\tau^4}\right)\right], \tag{8.125}$$

$$\Phi^2_{23,\tau}(x) = \frac{4x_2C_1}{\tau^3\pi}, \tag{8.126}$$

$$\begin{aligned}\Phi_{31,\tau}(x,t) = &-x_1\exp\left(-\frac{\tau^2}{4C_2t}\right)\left(\frac{\alpha\mu\tau^4 + 8C_1(\lambda+2\mu)t\tau^2}{8C_2\mu t^2\tau^4\pi}\right.\\ &\left.+\frac{32C_1C_2(\lambda+2\mu)t^2\left(1-\exp\left(\frac{\tau^2}{4C_2t}\right)\right)}{8C_2\mu t^2\tau^4\pi}\right),\end{aligned} \tag{8.127}$$

$$\begin{aligned}\Phi_{32,\tau}(x,t) = &-x_2\exp\left(-\frac{\tau^2}{4C_2t}\right)\left(\frac{\alpha\mu\tau^4 + 8C_1(\lambda+2\mu)t\tau^2}{8C_2\mu t^2\tau^4\pi}\right.\\ &\left.+\frac{32C_1C_2(\lambda+2\mu)t^2\left(1-\exp\left(\frac{\tau^2}{4C_2t}\right)\right)}{8C_2\mu t^2\tau^4\pi}\right),\end{aligned} \tag{8.128}$$

$$\Phi_{33,\tau}(x,t) = \exp\left(-\frac{\tau^2}{4C_2t}\right)\frac{8\|x\|^2t - 4t\tau^2 + c_0\mu\tau^2(\tau^2-\|x\|^2)}{64C_2^2t^4\pi}. \tag{8.129}$$

The existence of the limit $\|x\| \to 0$ and $t \to 0+$ for $\Phi_{31,\tau}$, $\Phi_{32,\tau}$ and $\Phi_{33,\tau}$ can be obtained with the same considerations as for the existence of the limits for p^{Si}_τ and the components of u^{Si}_τ. After the theoretical calculations, we want to show some plots of the source scaling functions. Figure 8.19 shows the source scaling functions for the component $\Phi_{11,\tau}$ for several parameters j. We can see that the support gets smaller for larger j. Since the shrinking support is a character of all source scaling functions, Figure 8.20 shows $\Phi_{12,\tau}$, $\Phi^1_{13,\tau}$ and $\Phi^2_{13,\tau}$ together only for one parameter, namely for $j = 1$.
Please note that the source scaling function $\Phi_{21,\tau}$ is the same as $\Phi_{12,\tau}$. Due to the symmetry, $\Phi_{22,\tau}$ is the same as source scaling function $\Phi_{11,\tau}$ reflected at the line given by $x_1 = x_2$. Furthermore, $\Phi_{13,\tau}$ and $\Phi_{23,\tau}$ are similar, because $\Phi_{23,\tau}$ is the same as $\Phi_{13,\tau}$ also reflected at the line $x_1 = x_2$. This holds true for the function parts with upper index 1 and 2. Therefore, we do not show the components of $\Phi_{23,\tau}$ additionally. Figure 8.21 shows the source scaling functions for the component $\Phi_{31,\tau}$, where we have a spatial and time dependency to show.

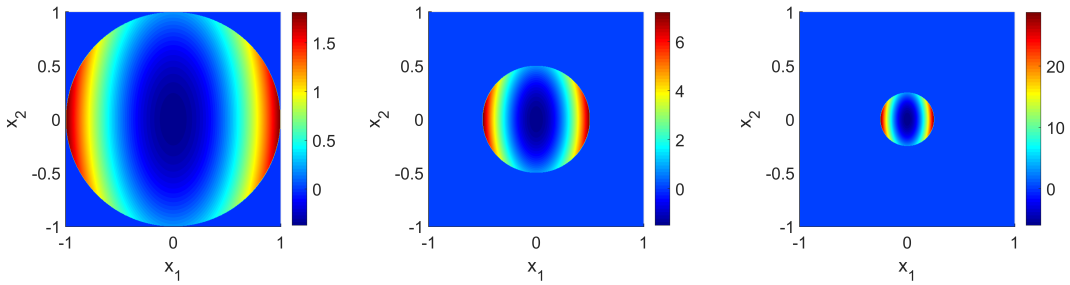

(a) $j = 0$ (b) $j = 1$ (c) $j = 2$

Figure 8.19.: The source scaling function $\Phi_{11,\tau}$ for several parameters j.

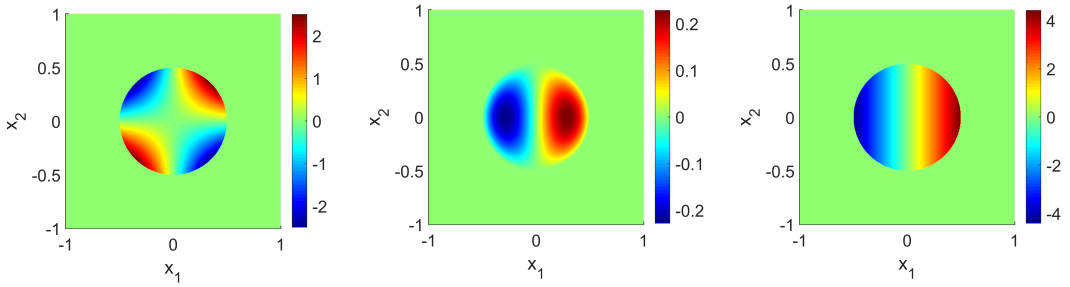

(a) $\Phi_{12,\tau},\ j = 1.$ (b) $\Phi^{(1)}_{13,\tau},\ j = 1.$ (c) $\Phi^{(2)}_{13,\tau},\ j = 1.$

Figure 8.20.: The source scaling functions $\Phi_{12,\tau}$, $\Phi^{(1)}_{13,\tau}$ and $\Phi^{(2)}_{13,\tau}$ for $j = 1$.

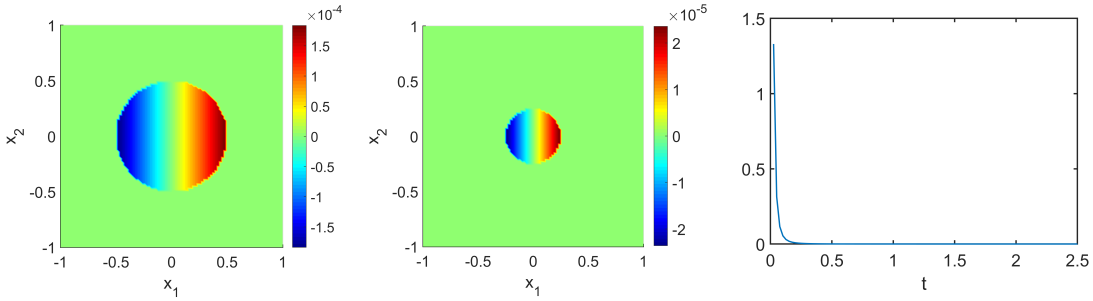

(a) $t = 1,\ j = 1.$ (b) $t = 1,\ j = 2.$ (c) $x = (0.2, 0.2),\ j = 1.$

Figure 8.21.: The source scaling function $\Phi_{31,\tau}$ for a fixed time over the space respectively for a fixed point over time for selected parameters j.

Since $\Phi_{32,\tau}$ does not differ from $\Phi_{31,\tau}$ evaluated at the point $(0.2, 0.2)$ due to the symmetry, this source scaling function is not shown here. Figure 8.22 shows the source scaling functions for the component $\Phi_{33,\tau}$ for selected parameters j in space and time.

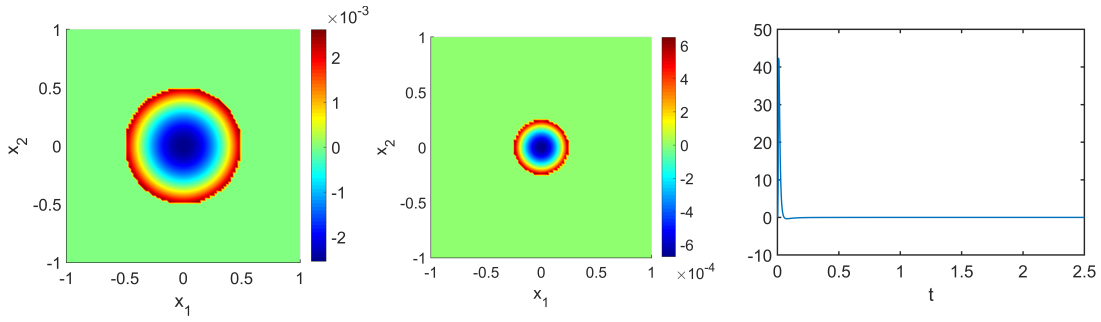

(a) $t = 1,\ j = 1.$ (b) $t = 1,\ j = 2.$ (c) $x = (0.2, 0.2),\ j = 1.$

Figure 8.22.: The source scaling function $\Phi_{33,\tau}$ for two fixed times in space respectively for a fixed point in space over the time for selected parameters j.

The wavelets (we state them as $\Psi_{ik,\tau}$) can be defined like above in the following way

$$\Psi_{ik,\tau_j} := \Phi_{ik,\tau_j} - \Phi_{ik,\tau_{j-1}}. \tag{8.130}$$

Some chosen wavelets are shown in the following figures to give a representative overview. Figure 8.23 shows the source wavelet for the component Ψ_{11} for several j.

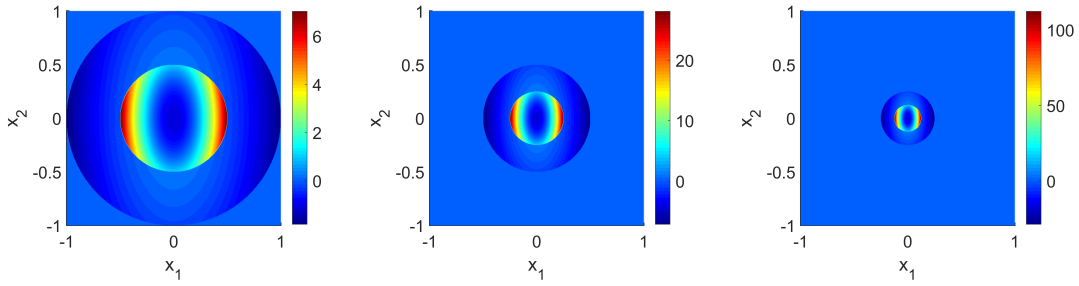

(a) $j = 1$ (b) $j = 2$ (c) $j = 3$

Figure 8.23.: The source wavelet function $\Psi_{11,\tau}$ for selected parameters j.

In this figure, we can see the behavior of the wavelets for increasing j. They are also getting smaller support for greater j. Therefore, we show in Figure 8.24 some of the wavelet functions together for $j = 1$.
Please note that the source wavelet Ψ_{12} is the same as Ψ_{21} and also the symmetry of Ψ_{31} and Ψ_{32} is the same as in the case of the source scaling functions and these functions are not depicted separately. Because of the symmetry of Ψ_{11} and Ψ_{22}, the latter is not shown here.

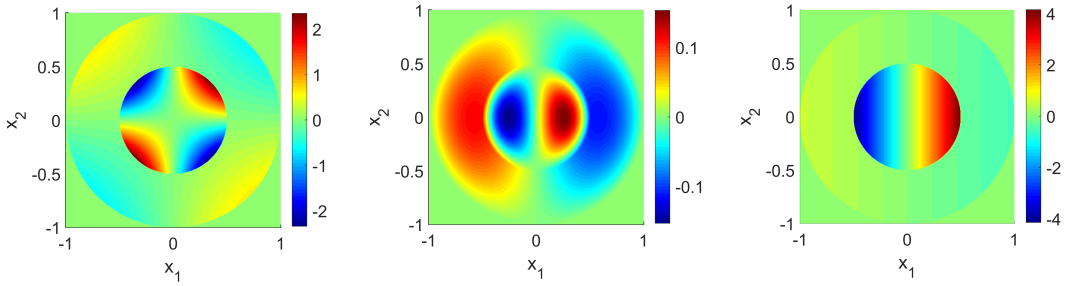

(a) $\Psi_{12,\tau},\ j=1.$ (b) $\Psi^{(1)}_{13,\tau},\ j=1.$ (c) $\Psi^{(2)}_{13,\tau},\ j=1.$

Figure 8.24.: The source wavelet functions $\Psi_{12,\tau}$, $\Psi^{(1)}_{13,\tau}$ and $\Psi^{(2)}_{13,\tau}$ for $j=1$.

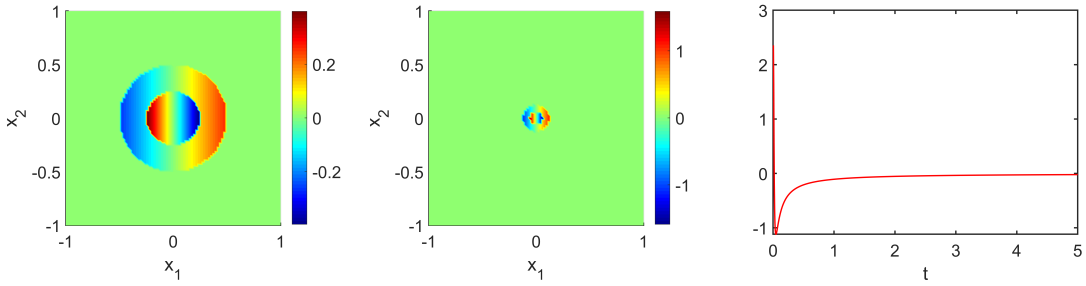

(a) $t=1,\ j=2.$ (b) $t=1,\ j=3.$ (c) $x=(0.2,0.2),\ j=1.$

Figure 8.25.: The source wavelet function $\Psi_{31,\tau}$ for two fixed times over space respectively for a fixed point in space over the time for selected parameters j.

Due to the symmetric aspects of Ψ_{31} and Ψ_{32}, we only show Ψ_{31} in Figure 8.25 for some space or time points and selected parameters j.
Figure 8.26 shows the source wavelet for the component $\Psi_{33,\tau}$ with the same parameters for space and time as $\Psi_{31,\tau}$ above.
Please note that the source scaling functions and corresponding wavelets all have compact support in space due to the construction. Remember how the mollified fundamental solutions were constructed: We used the fundamental solution for $\|x\| \geq \tau$ and the mollification for $\|x\| < \tau$. This has the consequence that the result of the application of the differential operator for $\|x\| \geq \tau$ vanishes. We get compact support for the spatial variable for our source scaling functions.

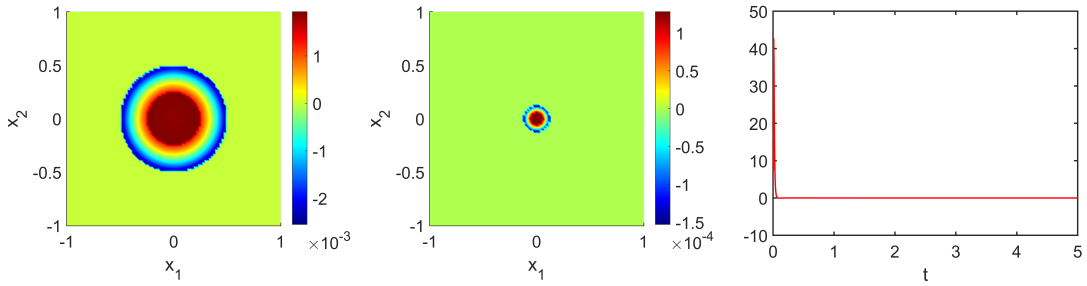

(a) $t = 1,\ j = 2.$ (b) $t = 1,\ j = 3.$ (c) $x = (0.2, 0.2),\ j = 1.$

Figure 8.26.: The source wavelet function $\Psi_{33,\tau}$ for two fixed times over space respectively for a fixed point in space over the time for selected parameters j.

8.4. Theoretical Aspects of the Decorrelation

For our source scaling functions, we want to show an important theorem, which provides the basis for our decorrelation. Here, we have to note that the space and time dependent source scaling functions $\Phi_{31,\tau}$, $\Phi_{32,\tau}$ and $\Phi_{33,\tau}$ have to be equipped with the Haar scaling function in time. This is necessary to achieve a compact support of the functions in space and time and to yield the theoretical results. We need the Haar saling function (see [117]) in time that has its support on the interval $[0, t_0]$, that means $\varphi(t/t_0)$, which we will denote by

$$\varphi_{t_0}(t) \coloneqq \varphi(t/t_0) = \mathcal{X}_{[0,1]}(t/t_0) = \begin{cases} 1, & 0 \leq t \leq t_0, \\ 0, & t > t_0. \end{cases} \tag{8.131}$$

That means, we modify the mentioned scaling functions by $\Phi_{\mathrm{new}}(x,t) = \Phi(x,t) \cdot \varphi_{t_0}(t)$ and omit the new, because we are only interested in these modified functions. Furthermore, we want to interconnect the parameter t_0 with τ in the following way: $t_0 = T \cdot \tau$, where T is the end point of our considered time interval. Before we go over to our main theoretical results and the corresponding theorem, we have a look at the following, which is also necessary for the proof of our main theorem.

Theorem 8.4.1. *We define the volume integral of the source scaling function tensor $\boldsymbol{\Phi}_\tau$ in the following way*

$$\boldsymbol{V}_{\boldsymbol{\Phi}_\tau} \coloneqq \int_{\mathbb{R}^2} \int_{\mathbb{R}} \boldsymbol{\Phi}_\tau(y,\theta) \, \mathrm{d}\theta \, \mathrm{d}y, \tag{8.132}$$

that means we want to calculate the volume integral of the several parts of the tensor $\boldsymbol{\Phi}_\tau$. Our source scaling functions satisfy

$$(\boldsymbol{V}_{\boldsymbol{\Phi}_\tau})_{11} = (\boldsymbol{V}_{\boldsymbol{\Phi}_\tau})_{22} = 1, \ \lim_{\tau \to 0+} (\boldsymbol{V}_{\boldsymbol{\Phi}_\tau})_{33} = C_2 c_0 \mu, \tag{8.133}$$

$$(\boldsymbol{V}_{\boldsymbol{\Phi}_\tau})_{12} = (\boldsymbol{V}_{\boldsymbol{\Phi}_\tau})_{21} = (\boldsymbol{V}_{\boldsymbol{\Phi}_\tau})_{13} = (\boldsymbol{V}_{\boldsymbol{\Phi}_\tau})_{23} = 0, \tag{8.134}$$

$$(\boldsymbol{V}_{\boldsymbol{\Phi}_\tau})_{31} = (\boldsymbol{V}_{\boldsymbol{\Phi}_\tau})_{32} = 0. \tag{8.135}$$

Proof. For the proof, we first need the volume integral $V_{\Phi_{ik,\tau}}$ over the several parts of Φ. We have three types of functions, namely entries of $\boldsymbol{\Phi}_\tau$ equipped with the Delta distribution δ_t, equipped with the derivative of the Delta distribution δ_t' and the spatial and time dependent functions from the last row. We start with the entry $(\boldsymbol{\Phi}_\tau)_{11}$ and use property (3.21) from Remark 3.3.3.

That means the time integral together with the delta distribution reduces to one and only the spatial integral with compact support is left. We obtain with polar coordinates

$$\begin{aligned}(\boldsymbol{V}_{\boldsymbol{\Phi}_\tau})_{11} &= \int_{\mathbb{B}_\tau(0)} -\frac{\lambda+\mu}{\mu}\frac{C_3}{2\pi}\left(-\frac{1}{\tau^2}+C_4\cdot\left(\frac{6}{\tau^2}-\frac{15x_1^2+5x_2^2}{\tau^4}\right)\right)\\ &\quad -\frac{C_3}{2\pi}\left(\frac{-2+4C_4}{\tau^2}+C_4\cdot\left(-\frac{14x_1^2+2x_2^2}{\tau^4}\right)\right)+\alpha\frac{C_1}{2\pi}\frac{1}{\tau^2}\left(2-\frac{3x_1^2+x_2^2}{\tau^2}\right)\,\mathrm{d}x\\ &= \int_0^\tau\int_0^{2\pi} -\frac{\lambda+\mu}{\mu}\frac{C_3}{2\pi}\left(\frac{6C_4-1}{\tau^2}\cdot r - C_4\cdot\frac{15r^2\cos^2\varphi+5r^2\sin^2\varphi}{\tau^4}\cdot r\right)\\ &\quad -\frac{C_3}{2\pi}\left(\frac{-2+4C_4}{\tau^2}\cdot r - C_4\cdot\frac{14r^2\cos^2\varphi+2r^2\sin^2\varphi}{\tau^4}\cdot r\right)\\ &\quad +\alpha\frac{C_1}{2\pi}\frac{1}{\tau^2}\left(2\cdot r-\frac{3r^2\cos^2\varphi+r^2\sin^2\varphi}{\tau^2}r\right)\,\mathrm{d}\varphi\,\mathrm{d}r. \end{aligned} \tag{8.136}$$

With $\int_0^{2\pi}\cos^2\varphi\,\mathrm{d}\varphi=\int_0^{2\pi}\sin^2\varphi\,\mathrm{d}\varphi=\pi$, we have

$$\begin{aligned}(\boldsymbol{V}_{\boldsymbol{\Phi}_\tau})_{11} &= -\frac{\lambda+\mu}{\mu}\frac{C_3}{2\pi}\left(\frac{6C_4-1}{\tau^2}\cdot 2\pi\cdot\frac{1}{2}\tau^2 - C_4\frac{20\pi}{\tau^4}\cdot\frac{1}{4}\tau^4\right)\\ &\quad -\frac{C_3}{2\pi}\left(\frac{4C_4-2}{\tau^2}\cdot 2\pi\cdot\frac{1}{2}\tau^2 - C_4\cdot\frac{16\pi}{\tau^4}\cdot\frac{1}{4}\tau^4\right)\\ &\quad +\frac{\alpha C_1}{2\pi}\left(\frac{2}{\tau^2}\cdot 2\pi\cdot\frac{1}{2}\tau^2-\frac{4\pi}{\tau^4}\cdot\frac{1}{4}\tau^4\right)\\ &= -\frac{\lambda+\mu}{\mu}\cdot\frac{C_3}{2}\left(6C_4-1-5C_4\right)-\frac{C_3}{2}\left(4C_4-2-4C_4\right)+\frac{\alpha C_1}{2}\\ &= -\frac{\lambda+\mu}{\mu}\cdot\frac{C_3}{2}\left(C_4-1\right)+C_3+\frac{\alpha C_1}{2}. \end{aligned} \tag{8.137}$$

Inserting the constants C_1, C_3 and C_4 from (7.21) and (7.22) leads us to

$$\begin{aligned}(\boldsymbol{V}_{\boldsymbol{\Phi}_\tau})_{11} &= -\frac{\lambda+\mu}{\mu}\cdot\frac{c_0(\lambda+3\mu)+\alpha^2}{4(c_0(\lambda+2\mu)+\alpha^2)}\cdot\left[\frac{c_0(\lambda+\mu)+\alpha^2}{c_0(\lambda+3\mu)+\alpha^2}-1\right]\\ &\quad +\frac{c_0(\lambda+3\mu)+\alpha^2}{2(c_0(\lambda+2\mu)+\alpha^2)}+\frac{\alpha^2}{2(c_0(\lambda+2\mu)+\alpha^2)}\\ &= -\frac{\lambda+\mu}{\mu}\frac{c_0(\lambda+\mu)+\alpha^2-c_0(\lambda+3\mu)-\alpha^2}{4(c_0(\lambda+2\mu)+\alpha^2)}+\frac{c_0(\lambda+3\mu)+2\alpha^2}{2(c_0(\lambda+2\mu)+\alpha^2)}\\ &= \frac{(-\lambda-\mu)\cdot(-2c_0\mu)+2\mu c_0(\lambda+3\mu)+4\mu\alpha^2}{4\mu(c_0(\lambda+2\mu)+\alpha^2)}\\ &= \frac{4\mu c_0\lambda+8c_0\mu^2+4\mu\alpha^2}{4\mu(c_0(\lambda+2\mu)+\alpha^2)}\\ &= 1. \end{aligned} \tag{8.138}$$

Due to the symmetry of $\Phi_{11,\tau}$ and $\Phi_{22,\tau}$, the volume integral $(\boldsymbol{V}_{\boldsymbol{\Phi}_\tau})_{22}$ is the same as $(\boldsymbol{V}_{\boldsymbol{\Phi}_\tau})_{11}$. Furthermore, for $(\boldsymbol{\Phi}_\tau)_{12}$, we get with the same argument for the Delta distribution as above, the integral over the spatial part

$$\begin{aligned}\int_{\mathcal{B}} \Phi_{12,\tau}(x)\,\mathrm{d}x &= \int_{\mathbb{B}_\tau(0)} \Phi_{12,\tau}(x)\,\mathrm{d}x \\ &= \int_{\mathbb{B}_\tau(0)} \frac{x_1 x_2}{\tau^4\pi}\left(\frac{\lambda+\mu}{\mu}\cdot 5C_3C_4 + 6C_3C_4 - \alpha C_1\right)\mathrm{d}x \\ &= \frac{1}{\tau^4\pi}\left(\frac{\lambda+\mu}{\mu}\cdot 5C_3C_4 + 6C_3C_4 - \alpha C_1\right)\int_0^{2\pi}\int_0^{\tau} r^3\sin(\varphi)\cos(\varphi)\,\mathrm{d}r\,\mathrm{d}\varphi \\ &= 0. \end{aligned} \tag{8.139}$$

Also due to the symmetry, we have $(\boldsymbol{V}_{\boldsymbol{\Phi}_\tau})_{21} = 0$. For the components $(\boldsymbol{\Phi}_\tau)_{13}$, we have to distinguish two cases (remember the part equipped with δ_t and the other one with δ_t'). For the case with δ_t, we can apply the same argument as above and get for the remaining integral over the spatial part with polar coordinates

$$\begin{aligned}\int_{\mathbb{B}_\tau(0)} \frac{4x_1C_1}{\tau^3\pi} &= \frac{4C_1}{\tau^3\pi}\int_0^{\tau}\int_0^{2\pi} r^2\cos\varphi\,\mathrm{d}\varphi\,\mathrm{d}r \\ &= 0. \end{aligned} \tag{8.140}$$

For the second part with δ_t', we have again a look at Remark 3.3.3 and (3.20) and get that this integral is zero. We get due to the similarity of $(\boldsymbol{\Phi}_\tau)_{23}$ and $(\boldsymbol{\Phi}_\tau)_{13}$, that the volume integrals of the two parts of $(\boldsymbol{\Phi}_\tau)_{23}$ are also zero with the same considerations as in the case of $(\boldsymbol{\Phi}_\tau)_{13}$.
So the last row of $\boldsymbol{\Phi}_\tau$ is left, where we now have a look at. We get for $(\boldsymbol{\Phi}_\tau)_{31}$ with some symmetric properties based on the factor x_1 the opportunity to separate the spatial from the time integral.

$$\begin{aligned}\int_{\mathcal{B}}\int_0^{t_0} \Phi_{31,\tau}\,\mathrm{d}t\,\mathrm{d}x = -\int_{\mathbb{B}_\tau(0)} x_1\,\mathrm{d}x \\ \times\int_0^{t_0}\exp\left(-\frac{\tau^2}{4C_2t}\right)\left(\frac{\alpha\mu\tau^4 + 8C_1(\lambda+2\mu)t\tau^2}{8C_2\mu t^2\tau^4\pi}\right. \\ \left.+\frac{32C_1C_2(\lambda+2\mu)t^2\left(1-\exp\left(\frac{\tau^2}{4C_2t}\right)\right)}{8C_2\mu t^2\tau^4\pi}\right)\mathrm{d}t\end{aligned}$$

$$
\begin{aligned}
&= -\int_0^{\tau}\int_0^{2\pi} r\cos(\varphi) r \,\mathrm{d}\varphi \,\mathrm{d}r \\
&\quad \int_0^{t_0} \exp\left(-\frac{\tau^2}{4C_2 t}\right)\left(\frac{\alpha\mu\tau^4 + 8C_1(\lambda+2\mu)t\tau^2}{8C_2\mu t^2\tau^4\pi}\right. \\
&\quad \left. + \frac{32C_1C_2(\lambda+2\mu)t^2\left(1-\exp\left(\frac{\tau^2}{4C_2t}\right)\right)}{8C_2\mu t^2\tau^4\pi}\right)\,\mathrm{d}t \\
&= 0\cdot\int_0^{t_0} \exp\left(-\frac{\tau^2}{4C_2 t}\right)\left(\frac{\alpha\mu\tau^4 + 8C_1(\lambda+2\mu)t\tau^2}{8C_2\mu t^2\tau^4\pi}\right. \\
&\quad \left. + \frac{32C_1C_2(\lambda+2\mu)t^2\left(1-\exp\left(\frac{\tau^2}{4C_2t}\right)\right)}{8C_2\mu t^2\tau^4\pi}\right)\,\mathrm{d}t \\
&= 0.
\end{aligned} \tag{8.141}
$$

We also get $(\boldsymbol{V}_{\boldsymbol{\Phi}_\tau})_{32} = 0$ due to the symmetry. Furthermore, we need the following integrals over $\mathbb{B}_\tau(0)$ for $(\boldsymbol{V}_{\boldsymbol{\Phi}_\tau})_{33}$

$$
\int_{\mathbb{B}_\tau(0)} \|x\|^2 \,\mathrm{d}x = \int_0^{2\pi}\int_0^{\tau} r^2\cdot r \,\mathrm{d}r\,\mathrm{d}\varphi = 2\pi\cdot\frac{1}{4}r^4\big|_0^{\tau} = \frac{\pi}{2}\tau^4, \tag{8.142}
$$

$$
\int_{\mathbb{B}_\tau(0)} 1 \,\mathrm{d}x = \pi\tau^2. \tag{8.143}
$$

With this, let us now have a look at $(\boldsymbol{\Phi}_\tau)_{33}$. Please remember Remark 2.2.4 for the time integral.

$$
\begin{aligned}
&\int_{\mathcal{B}}\int_0^{t_0} \Phi_{33,\tau}\,\mathrm{d}t\,\mathrm{d}x \\
&\quad = \int_0^{t_0}\int_{\mathbb{B}_\tau(0)} \exp\left(-\frac{\tau^2}{4C_2t}\right)\frac{4t(2\|x\|^2-\tau^2)+c_0\mu\tau^2(\tau^2-\|x\|^2)}{64C_2^2t^4\pi}\,\mathrm{d}x\,\mathrm{d}t \\
&\quad = \int_0^{t_0} \exp\left(-\frac{\tau^2}{4C_2t}\right)\frac{4t\,(\tau^4\pi-\pi\tau^4)+c_0\mu\tau^2(\pi\tau^4-\frac{1}{2}\tau^4\pi)}{64C_2^2t^4\pi}\,\mathrm{d}t \\
&\quad = \frac{1}{64C_2^2}\frac{c_0\mu\tau^6}{2}\int_0^{t_0}\exp\left(-\frac{\tau^2}{4C_2t}\right)\frac{1}{t^4}\,\mathrm{d}t \\
&\quad = \frac{1}{64C_2^2}\frac{c_0\mu\tau^6}{2}\cdot\frac{4C_2\exp\left(-\frac{\tau^2}{4C_2t_0}\right)(32C_2^2t_0^2+8C_2t_0\tau^2+\tau^4)}{t_0^2\tau^6}.
\end{aligned} \tag{8.144}
$$

Now we have to take into account the coupling between τ and t_0. We obtain for a constant $T > 0$ (which is the length of our considered time interval) and $t_0 = T\tau$

$$\begin{aligned}\lim_{\tau \to 0+} V_{\Phi_{33,\tau}} &= \frac{1}{64C_2^2}\frac{c_0\mu}{2} \cdot 4C_2 \cdot 32C_2^2 \\ &= C_2 c_0 \mu \end{aligned} \tag{8.145}$$

that means the volume integral converges to a constant for $t \to 0+$. □

Remark 8.4.2. *In the case of Berea sandstone, we obtain for the limit of the volume integral of $\Phi_{33,\tau}$ the following (see [135])*

$$C_2 c_0 \mu \approx 0.6205. \tag{8.146}$$

For a better comparison of the convolution results later, it is better to modify $\Phi_{33,\tau}$ in such a way that the volume integral is 1. Therefore, we define the new function $\Phi_{33,\tau}^{\text{new}}$ with the help of the volume integral in the following way

$$\Phi_{33,\tau}^{\text{new}} = \frac{1}{(\boldsymbol{V}_{\boldsymbol{\Phi}_\tau})_{33}} \Phi_{33,\tau}. \tag{8.147}$$

Please note that this is necessary on the one hand to prove Theorem 8.4.4 and on the other hand for a better comparison of the decorrelation for different j. In the further considerations we omit the "new" for the sake of readability but consider always the newly defined function. For the decorrelation of given data for u and p, we have to show that our constructed source scaling functions fulfill the properties of scaling functions in the sense of Definition 4.1.3.
Before we go over to this theorem, we have to prove another lemma, which we need for the main theorem.

Lemma 8.4.3. *The positive part of $\Phi_{11,\tau}$ achieves its maximum at $(\tau, 0)$ or $(-\tau, 0)$.*

Proof. We can rearrange $\Phi_{11,\tau}$ in the following way

$$\begin{aligned}\Phi_{11,\tau} &= \left(-\frac{\lambda+\mu}{\mu}\frac{C_3}{2\pi}\frac{1}{\tau^2}(6C_4 - 1) - \frac{C_3}{2\pi}\frac{1}{\tau^2}(4C_4 - 2) + \frac{\alpha C_1}{2\pi}\frac{2}{\tau^2}\right) \\ &\quad + x_1^2\left(\frac{\lambda+\mu}{\mu}\frac{C_3 \cdot C_4}{2\pi\tau^4} \cdot 15 + \frac{C_3 \cdot C_4}{2\pi\tau^4} \cdot 14 - \frac{\alpha C_1}{2\pi\tau^4} \cdot 3\right) \\ &\quad + x_2^2\left(\frac{\lambda+\mu}{\mu}\frac{C_3 \cdot C_4}{2\pi\tau^4} \cdot 5 + \frac{C_3 \cdot C_4}{2\pi\tau^4} \cdot 2 - \frac{\alpha C_1}{2\pi\tau^4}\right) \\ &=: D_0 + x_1^2 D_1 + x_2^2 D_2. \end{aligned} \tag{8.148}$$

We write $D_0 =: \frac{1}{\tau^2} d_0$, $D_1 =: \frac{1}{\tau^4} d_1$ and $D_2 =: \frac{1}{\tau^4} d_2$ and have a closer look at d_0, d_1 and d_2 and want to show that $d_0 < 0$ and $d_1,\ d_2 > 0$ holds true by inserting the constants (see (7.21) and (7.22)):

$$
\begin{aligned}
d_0 &= -\frac{\lambda+\mu}{\mu}\frac{C_3}{2\pi}(6C_4-1) - \frac{C_3}{2\pi}(4C_4-2) + \frac{\alpha C_1}{\pi} \\
&= \frac{C_3C_4}{2\pi}\left(-\frac{\lambda+\mu}{\mu}\cdot 6 - 4\right) + \frac{C_3}{2\pi}\left(\frac{\lambda+\mu}{\mu}+2\right) + \frac{\alpha C_1}{\pi} \\
&= \frac{1}{2\pi}\frac{c_0(\lambda+\mu)+\alpha^2}{2(c_0(\lambda+2\mu)+\alpha^2)}\cdot\frac{-6\lambda-10\mu}{\mu} + \frac{1}{2\pi}\frac{c_0(\lambda+3\mu)+\alpha^2}{2(c_0(\lambda+2\mu)+\alpha^2)}\cdot\frac{\lambda+3\mu}{\mu} \\
&\quad + \frac{1}{\pi}\frac{\alpha^2}{c_0(\lambda+2\mu)+\alpha^2} \\
&= \frac{1}{2\pi}\frac{(c_0(\lambda+\mu)+\alpha^2)(-6\lambda-10\mu)+(c_0(\lambda+3\mu)+\alpha^2)(\lambda+3\mu)+4\alpha^2\mu}{2\mu(c_0(\lambda+2\mu)+\alpha^2)} \\
&= \frac{1}{2\pi}\frac{-5c_0\lambda^2-10c_0\lambda\mu-c_0\mu^2-5\lambda\alpha^2-3\mu\alpha^2}{2\mu(c_0(\lambda+2\mu)+\alpha^2)} < 0. \qquad (8.149)
\end{aligned}
$$

With the same steps, we get for d_1 and d_2

$$
\begin{aligned}
d_1 &= \frac{1}{2\pi}\left(\frac{15\lambda+29\mu}{\mu}\cdot C_3C_4 - 3\alpha C_1\right) \\
&= \frac{1}{2\pi}\frac{(c_0(\lambda+\mu)+\alpha^2)\cdot 15\lambda + 29\mu c_0(\lambda+\mu)+23\mu\alpha^2}{2\mu(c_0(\lambda+2\mu)+\alpha^2)} > 0, \qquad (8.150) \\
d_2 &= \frac{1}{2\pi}\left(\frac{5\lambda+7\mu}{\mu}\cdot C_3C_4 - \alpha C_1\right) \\
&= \frac{1}{2\pi}\frac{(c_0(\lambda+\mu)+\alpha^2)\cdot 5\lambda + c_0(\lambda+\mu)\cdot 7\mu + 5\mu\alpha^2}{2\mu(c_0(\lambda+2\mu)+\alpha^2)} > 0. \qquad (8.151)
\end{aligned}
$$

Please note that also $d_1 > d_2$ holds true. That means we want to find the maximum of the function $\Phi_{11,\tau}(x) = D_0 + x_1^2 D_1 + x_2^2 D_2$ under the given constraint $g(x) \coloneqq x_1^2 + x_2^2 - \tau^2 \leq 0$. We want to do this by determining the Karush-Kuhn-Tucker points. Therefore, we have to minimize $F(x) = -\Phi_{11,\tau}$ under the constraint above. We get the following equations

$$
\begin{aligned}
& \nabla F(x) + u\nabla g(x) \stackrel{!}{=} 0 && (8.152) \\
\Leftrightarrow\ & -2x_1D_1 + u2x_1 = 0 && (8.153) \\
& -2x_2D_2 + u2x_2 = 0 && (8.154) \\
\text{and}\quad & u(x_1^2 + x_2^2 - \tau^2) = 0 && (8.155) \\
\text{and}\quad & u \geq 0 && (8.156) \\
\text{and}\quad & g(x) \leq 0. && (8.157)
\end{aligned}
$$

That means we have from the first equation $x_1 = 0 \ \vee \ u = D_1$ and from the second equation $x_2 = 0 \ \vee \ u = D_2$. Combining the conditions and inserting them in (8.155)-(8.157), we get

a) $\underline{x_1 = 0 \ \wedge \ x_2 = 0}$: With (8.155), we get $u = 0$ and (8.156) and (8.157) are fulfilled. We get the point $(0, 0, 0)$.

b) $\underline{x_1 = 0 \ \wedge \ u = D_2}$: With (8.155) $u(x_2^2 - \tau^2) = 0$ and therefore $u = 0$ (contradiction to $u = D_2$) or $x_2 = \pm\tau$. (8.156) and (8.157) are fulfilled. We have the points $(0, \pm\tau, D_2)$.

c) $\underline{x_2 = 0 \ \wedge \ u = D_1}$: With (8.155), we get $u(x_1^2 - \tau^2) = 0$ and therefore $u = 0$ (contradiction to $u = D_1$) or $x_1 = \pm\tau$. (8.156) and (8.157) are fulfilled and we have the points $(\pm\tau, 0, D_1)$.

We insert the KKT-points in the functions F and $\Phi_{11,\tau}$ and get

$$F(0,0) = -D_0, \quad F(0,\pm\tau) = -D_0 - \tau^2 D_2, \quad F(\pm\tau,0) = -D_0 - \tau^2 D_1, \tag{8.158}$$

$$\Phi_{11,\tau}(0,0) = D_0, \quad \Phi_{11,\tau}(0,\pm\tau) = D_0 + \tau^2 D_2, \quad \Phi_{11,\tau}(\pm\tau,0) = D_0 + \tau^2 D_1. \tag{8.159}$$

Since $D_1 > D_2 > 0$, the function achieves its maximum at the points $(\tau, 0)$ and $(-\tau, 0)$. More precisely: The side condition describes a compact disc and the function $\Phi_{11,\tau}$ is continuous, that means we have the existence of minimum and maximum. Therefore, one of the KKT-points yields a maximum. □

After this preparatory work, we can state the following theorem for our calculated source scaling function tensor $\mathbf{\Phi}_\tau$ from (8.82).

Theorem 8.4.4. *Let $\mathcal{B}$ be a regular region in $\mathbb{R}^2$ and $f : \overline{\mathcal{B}} \times \mathbb{R} \to \mathbb{R}^3$ continuously differentiable. Then*

$$\lim_{\substack{\tau\to 0\\ \tau>0}} \int_{\mathcal{B}} \int_{\mathbb{R}} \mathbf{\Phi}_\tau(x - y, t - \theta) f(y, \theta) \, \mathrm{d}\theta \, \mathrm{d}y = f(x, t) \tag{8.160}$$

holds true for all $x \in \mathcal{B}$, $t \in \mathbb{R}$ and our constructed $\mathbf{\Phi}_\tau$ is a scaling function in the sense of Definition 4.1.3.

Proof. In detail we have to show (see the deduced source scaling functions above)

$$\begin{aligned}\lim_{\substack{\tau\to 0\\ \tau>0}} \int_{\mathcal{B}} \int_{\mathbb{R}} &\Phi_{11,\tau}(x - y)\delta_t f_1(y, \theta) + \Phi_{12,\tau}(x - y)\delta_t f_2(y, \theta) \\ &+ \left(\Phi^1_{13,\tau}(x - y)\delta'_t + \Phi^2_{13,\tau}(x - y)\delta_t\right) f_3(y, \theta) \, \mathrm{d}\theta \, \mathrm{d}y = f_1(x, t),\end{aligned} \tag{8.161}$$

$$\begin{aligned}\lim_{\substack{\tau\to 0\\ \tau>0}} \int_{\mathcal{B}} \int_{\mathbb{R}} &\Phi_{21,\tau}(x - y)\delta_t f_1(y, \theta) + \Phi_{22,\tau}(x - y)\delta_t f_2(y, \theta) \\ &+ \left(\Phi^1_{23,\tau}(x - y)\delta'_t + \Phi^2_{23,\tau}(x - y)\delta_t\right) f_3(y, \theta) \, \mathrm{d}\theta \, \mathrm{d}y = f_2(x, t),\end{aligned} \tag{8.162}$$

$$\begin{aligned}\lim_{\substack{\tau\to 0\\ \tau>0}} \int_{\mathcal{B}} \int_{\mathbb{R}} &\Phi_{31,\tau}(x - y, t - \theta) f_1(y, \theta) + \Phi_{32,\tau}(x - y, t - \theta) f_2(y, \theta) \\ &+ \Phi_{33,\tau}(x - y, t - \theta) f_3(y, \theta) \, \mathrm{d}\theta \, \mathrm{d}y = f_3(x, t).\end{aligned} \tag{8.163}$$

Together with Remark 3.3.3, the equations above simplify to the following that has to be shown

$$\lim_{\substack{\tau\to 0\\ \tau>0}} \int_{\mathcal{B}} \Phi_{11,\tau}(x-y) f_1(y,t) + \Phi_{12,\tau}(x-y) f_2(y,t) - \Phi^1_{13,\tau}(x-y)\frac{\partial}{\partial t} f_3(y,t) + \Phi^2_{13,\tau}(x-y) f_3(y,t)\,\mathrm{d}y = f_1(x,t), \tag{8.164}$$

$$\lim_{\substack{\tau\to 0\\ \tau>0}} \int_{\mathcal{B}} \Phi_{21,\tau}(x-y) f_1(y,t) + \Phi_{22,\tau}(x-y) f_2(y,t) - \Phi^1_{23,\tau}(x-y)\frac{\partial}{\partial t} f_3(y,t) + \Phi^2_{23,\tau}(x-y) f_3(y,t)\,\mathrm{d}y = f_2(x,t), \tag{8.165}$$

$$\lim_{\substack{\tau\to 0\\ \tau>0}} \int_{\mathcal{B}} \int_{\mathbb{R}} \Phi_{31,\tau}(x-y,t-\theta) f_1(y,\theta) + \Phi_{32,\tau}(x-y,t-\theta) f_2(y,\theta) + \Phi_{33,\tau}(x-y,t-\theta) f_3(y,\theta)\,\mathrm{d}y\,\mathrm{d}\theta = f_3(x,t). \tag{8.166}$$

We start with the several parts of (8.161) and are guided by the technique in [22]. We have $x \in \mathcal{B}$ and $\mathcal{B}$ is open. Then there exists a τ_0 such that $\mathcal{B} \cap \mathbb{B}_\tau(x) = \mathbb{B}_\tau(x)$ for all $0 < \tau \leq \tau_0$. We can write the equation for the approximate identity with time dependence and the compact support of the functions as

$$\begin{aligned}\int_{\mathcal{B}}\int_{\mathbb{R}} \boldsymbol{\Phi}_\tau(x-y,t-\theta) f(y,\theta)\,\mathrm{d}\theta\,\mathrm{d}y &= \int_{\mathbb{B}_\tau(x)}\int_{t-t_0}^{t} \boldsymbol{\Phi}_\tau(x-y,t-\theta) f(y,\theta)\,\mathrm{d}\theta\,\mathrm{d}y \\ &= \left(\sum_{j=1}^{3}\int_{\mathbb{B}_\tau(x)}\int_{t-t_0}^{t} \left(\boldsymbol{\Phi}_\tau\right)_{ij}(x-y,t-\theta) f_j(y,\theta)\,\mathrm{d}\theta\,\mathrm{d}y\right)_{i=1,2,3}.\end{aligned} \tag{8.167}$$

We split $(\boldsymbol{\Phi}_\tau)_{ij}$ into its positive and negative parts, that means we have

$$(\boldsymbol{\Phi}_\tau)^+_{ij}(x,t) = \begin{cases} (\boldsymbol{\Phi}_\tau)_{ij}(x,t), & (\boldsymbol{\Phi}_\tau)_{ij}(x,t) \geq 0 \\ 0, & (\boldsymbol{\Phi}_\tau)_{ij}(x,t) < 0 \end{cases}, \tag{8.168}$$

$$(\boldsymbol{\Phi}_\tau)^-_{ij}(x,t) = \begin{cases} (\boldsymbol{\Phi}_\tau)_{ij}(x,t), & (\boldsymbol{\Phi}_\tau)_{ij}(x,t) \leq 0 \\ 0, & (\boldsymbol{\Phi}_\tau)_{ij}(x,t) > 0 \end{cases}. \tag{8.169}$$

Then we have

$$\begin{aligned}\int_{\mathbb{B}_\tau(x)} \int_{t-t_0}^{t} (\mathbf{\Phi}_\tau)_{ij}(x-y,t-\theta) f_j(y,\theta)\,\mathrm{d}\theta\,\mathrm{d}y \\ = \int_{\mathbb{B}_\tau(x)} \int_{t-t_0}^{t} (\mathbf{\Phi}_\tau)^+_{ij}(x-y,t-\theta) f_j(y,\theta)\,\mathrm{d}\theta\,\mathrm{d}y \\ + \int_{\mathbb{B}_\tau(x)} \int_{t-t_0}^{t} (\mathbf{\Phi}_\tau)^-_{ij}(x-y,t-\theta) f_j(y,\theta)\,\mathrm{d}\theta\,\mathrm{d}y.\end{aligned} \tag{8.170}$$

Due to the continuity of f and the integrability of $(\mathbf{\Phi}_\tau)^+_{ij}$ and $(\mathbf{\Phi}_\tau)^-_{ij}$ and the fact that the positive and negative part do not change their sign in $\mathbb{B}_\tau(x) \times [t-t_0, t]$, we want to apply the mean value theorem of integration. Here we have to distinguish two cases, the parts of Φ_τ with δ_t or δ_t' and the spatial and time dependent functions. We start with the first case, that means we apply the mean value theorem only for the spatial part and consider (8.164) and (8.165). The mean value theorem guarantees the existence of $\xi_1, \xi_2 \in \mathbb{B}_\tau(x)$ such that

$$\begin{aligned}\int_{\mathbb{B}_\tau(x)} \Phi_{ij,\tau}(x-y) f_j(y,t)\,\mathrm{d}y = f_j(\xi_1,t) \int_{\mathbb{B}_\tau(x)} \Phi^+_{ij,\tau}(x-y)\,\mathrm{d}y \\ + f_j(\xi_2,t) \int_{\mathbb{B}_\tau(x)} \Phi^-_{ij,\tau}(x-y)\,\mathrm{d}y,\ i=1,2,\ j=1,2,3.\end{aligned} \tag{8.171}$$

Remembering Theorem 8.4.1, we have

$$\int_{\mathbb{B}_\tau(x)} \Phi^+_{ij,\tau}(x-y)\,\mathrm{d}y + \int_{\mathbb{B}_\tau(x)} \Phi^-_{ij,\tau}(x-y)\,\mathrm{d}y = \delta_{ij}. \tag{8.172}$$

We can rearrange this equation to

$$\int_{\mathbb{B}_\tau(x)} \Phi^-_{ij,\tau}(x-y)\,\mathrm{d}y = \delta_{ij} - \int_{\mathbb{B}_\tau(x)} \Phi^+_{ij,\tau}(x-y)\,\mathrm{d}y. \tag{8.173}$$

Furthermore, substituting this equation into (8.171), we get

$$\begin{aligned}\int_{\mathbb{B}_\tau(x)} \Phi_{ij,\tau}(x-y) f_j(y,t)\,\mathrm{d}y \\ = f_j(\xi_2,t)\delta_{ij} + (f_j(\xi_1,t) - f_j(\xi_2,t)) \int_{\mathbb{B}_\tau(x)} \Phi^+_{ij,\tau}(x-y)\,\mathrm{d}y.\end{aligned} \tag{8.174}$$

In a last step, we have to estimate

$$\int_{\mathbb{B}_\tau(x)} \Phi^+_{ij,\tau}(x-y,t-\theta)\,\mathrm{d}y \le C \tag{8.175}$$

for a positive constant C independent of τ. With this we get

$$\lim_{\substack{\tau\to 0\\ \tau>0}} \int_{\mathbb{B}_\tau(x)} \Phi_{ij,\tau}(x-y) f_j(y,t)\,\mathrm{d}y = \delta_{ij} f_j(x,t) \tag{8.176}$$

since $\xi_1, \xi_2 \in \mathbb{B}_\tau(x)$ and f_j is continuous. This shows our theorem for the functions with δ_t-part, because the difference $(f_j(\xi_1,t) - f_j(\xi_2,t))$ shrinks to 0 for $\tau \to 0+$, because for $\tau \to 0+$ it holds true that $\xi_1, \xi_2 \to x$. Together with the boundedness of the integral over the positive part, the second term in (8.174) gets 0 and the first term gets $f_j(x,t)\delta_{ij}$. This goes in analogy for the parts with δ_t' but in this case we have the derivative with respect to t for f_j instead of f_j. The same technique can be applied for the spatial and time dependent functions from the last row of $\mathbf{\Phi}_\tau$, which we will also depict here. Since the beginning of the proof was worded in general terms, we do not have to reproduce this part for the spatial and time dependent functions again. We continue with the application of the mean value theorem, which we now apply for the spatial and time integral.
This guarantees the existence of $(\xi_1,\eta_1),\ (\xi_2,\eta_2) \in \mathbb{B}_\tau(x)\times[0,t_0]$, such that

$$\begin{aligned}\int_{\mathbb{B}_\tau(x)} \int_{t-t_0}^{t} (\mathbf{\Phi}_\tau)_{ij}(x-y,t-\theta) f_j(y,\theta)\,\mathrm{d}\theta\,\mathrm{d}y \\ = f_j(\xi_1,\eta_1) \int_{\mathbb{B}_\tau(x)} \int_{t-t_0}^{t} (\mathbf{\Phi}_\tau)^+_{ij}(x-y,t-\theta)\,\mathrm{d}\theta\,\mathrm{d}y \\ + f_j(\xi_2,\eta_2) \int_{\mathbb{B}_\tau(x)} \int_{t-t_0}^{t} (\mathbf{\Phi}_\tau)^-_{ij}(x-y,t-\theta)\,\mathrm{d}\theta\,\mathrm{d}y.\end{aligned} \tag{8.177}$$

Remembering Theorem 8.4.1 and (8.147), we have

$$\int_{\mathbb{B}_\tau(x)} \int_{t-t_0}^{t} (\mathbf{\Phi}_\tau)^+_{ij}(x-y,t-\theta)\,\mathrm{d}\theta\,\mathrm{d}y + \int_{\mathbb{B}_\tau(x)} \int_{t-t_0}^{t} (\mathbf{\Phi}_\tau)^-_{ij}(x-y,t-\theta)\,\mathrm{d}\theta\,\mathrm{d}y = \delta_{ij}. \tag{8.178}$$

We can rearrange this equation to

$$\int_{\mathbb{B}_\tau(x)} \int_{t-t_0}^{t} (\mathbf{\Phi}_\tau)^-_{ij}(x-y,t-\theta)\,\mathrm{d}\theta\,\mathrm{d}y = \delta_{ij} - \int_{\mathbb{B}_\tau(x)} \int_{t-t_0}^{t} (\mathbf{\Phi}_\tau)^+_{ij}(x-y,t-\theta)\,\mathrm{d}\theta\,\mathrm{d}y. \tag{8.179}$$

Moreover, substituting this equation into (8.177), we get

$$\begin{aligned}\int_{\mathbb{B}_\tau(x)} \int_{t-t_0}^{t} (\mathbf{\Phi}_\tau)_{ij}(x-y,t-\theta) f_j(y,\theta)\,\mathrm{d}\theta\,\mathrm{d}y \\ = f_j(\xi_2,\eta_2)\delta_{ij} + (f_j(\xi_1,\eta_1) - f_j(\xi_2,\eta_2)) \int_{\mathbb{B}_\tau(x)} \int_{t-t_0}^{t} (\mathbf{\Phi}_\tau)^+_{ij}(x-y,t-\theta)\,\mathrm{d}\theta\,\mathrm{d}y.\end{aligned} \tag{8.180}$$

In a last step, we have to estimate again

$$\int_{\mathbb{B}_\tau(x)} \int_{t-t_0}^{t} (\mathbf{\Phi}_\tau)_{ij}^{+} (x-y, t-\theta) \, \mathrm{d}\theta \, \mathrm{d}y \leq C \tag{8.181}$$

for a positive constant C independent of τ. With this we get

$$\lim_{\substack{\tau \to 0 \\ \tau > 0}} \int_{\mathbb{B}_\tau(x)} \int_{t-t_0}^{t} (\mathbf{\Phi}_\tau)_{ij} (x-y, t-\theta) f_j(y, \theta) \, \mathrm{d}\theta \, \mathrm{d}y = \delta_{ij} f_j(x, t) \tag{8.182}$$

since (ξ_1, η_1),$(\xi_2, \eta_2) \in \mathbb{B}_\tau(x) \times [t-t_0, t]$, f_j is continuous and we have the coupling between τ and t_0 that means t_0 goes to zero likewise as τ. Together with (8.167), we get

$$\lim_{\substack{\tau \to 0 \\ \tau > 0}} \int_{\mathcal{B}} \int_{\mathbb{R}} \mathbf{\Phi}_\tau (x-y, t-\theta) f(y, \theta) \, \mathrm{d}\theta \, \mathrm{d}y = f(x, t). \tag{8.183}$$

That means, we are left to show that the positive part of each source scaling function is restricted by a positive constant C independent of τ. We show this for each function separately. Let us start with the source scaling functions with δ_t and δ_t' dependency and take Remark 3.3.3 into account. That means we start with $\Phi_{11,\tau}$ because we do not have to consider the δ_t any more and want to show that the positive part is limited by a constant. We estimate

$$\int_{\mathbb{B}_\tau(x)} (\Phi_{11,\tau})^{+} (x-y) \, \mathrm{d}y \leq \max_{y \in \mathbb{B}_\tau(x)} \left| (\Phi_{11,\tau})^{+} (x-y) \right| \underbrace{\int_{\mathbb{B}_\tau(x)} 1 \, \mathrm{d}y}_{=\pi\tau^2} \tag{8.184}$$

From Lemma 8.4.3 we know that $\Phi_{11,\tau}$ achieves its maximum at $(\pm\tau, 0)$ and we insert it and get

$$\begin{aligned} \Phi_{11,\tau}(\pm\tau, 0) = &-\frac{\lambda+\mu}{\mu} \frac{C_3}{2\pi} \left(\frac{(6C_4 - 1)}{\tau^2} - C_4 \frac{15\tau^2}{\tau^4} \right) \\ &- \frac{C_3}{2\pi} \left(\frac{(4C_4 - 2)}{\tau^2} - C_4 \frac{14\tau^2}{\tau^4} \right) + \frac{\alpha C_1}{2\pi} \left(\frac{2}{\tau^2} - \frac{3\tau^2}{\tau^4} \right) \\ &= \mathcal{O}(\tau^{-2}) \text{ as } \tau \to 0 + . \end{aligned} \tag{8.185}$$

Hence it follows that the integral over the positive part can be estimated by a constant. We continue with the positive part of $\Phi_{12,\tau}$

$$\int_{\mathbb{B}_\tau(x)} (\Phi_{12,\tau})^{+} (x-y) \, \mathrm{d}y = \int_{\mathbb{B}_\tau(0)} (\Phi_{12,\tau})^{+} (y) \, \mathrm{d}y \tag{8.186}$$

and get for the constants

$$\begin{aligned}
&\frac{\lambda+\mu}{\mu}\frac{C_3C_4}{\pi}\cdot 5+\frac{C_3C_4}{\pi}\cdot 6-\alpha\frac{C_1}{\pi}\\
&\qquad=\frac{C_3C_4}{\pi}\left(5\frac{\lambda+\mu}{\mu}+6\right)-\frac{\alpha C_1}{\pi}\\
&\qquad=\frac{1}{\pi}\left(C_3C_4\frac{5\lambda+11\mu}{\mu}-\alpha C_1\right)\\
&\qquad=\frac{1}{\pi}\left(\frac{c_0(\lambda+\mu)+\alpha^2}{2(c_0(\lambda+2\mu)+\alpha^2)}\cdot\frac{5\lambda+11\mu}{\mu}-\frac{\alpha^2}{c_0(\lambda+2\mu)+\alpha^2}\right)\\
&\qquad>0. \qquad (8.187)
\end{aligned}$$

Due to the fact that the combination of constants above is >0 and the symmetry, we get for $\Phi_{12,\tau}$ (for the part with $y_1, y_2>0$) and the usage of polar coordinates.

$$\begin{aligned}
&\int_{\substack{\mathbb{B}_\tau(0)\\ y_1,y_2>0}}\left(\Phi_{12,\tau}\right)^+(y)\,\mathrm{d}y\\
&\qquad=\left(5\frac{\lambda+\mu}{\mu}\frac{C_3C_4}{\pi\tau^4}+6\frac{C_3C_4}{\pi\tau^4}-\frac{\alpha C_1}{\pi\tau^4}\right)\int_0^{\pi/2}\int_0^{\tau}\left(r^2\sin\varphi\cos\varphi\right)\cdot r\,\mathrm{d}r\,\mathrm{d}\varphi\\
&\qquad=\left(5\frac{\lambda+\mu}{\mu}\frac{C_3C_4}{\pi\tau^4}+6\frac{C_3C_4}{\pi\tau^4}-\frac{\alpha C_1}{\pi\tau^4}\right)\cdot\frac{1}{2}\cdot\frac{1}{4}\tau^4 \qquad (8.188)
\end{aligned}$$

which implies that the positive part can also be estimated by a constant. Let us continue with the two components of $\Phi_{13,\tau}$. We can show that the function $\Phi^1_{13,\tau}$ without the x_1 is >0. We show that the combination of constants is >0 and have

$$\begin{aligned}
&\frac{c_0\mu C_1}{2\pi}\frac{1}{\tau^2}\left(2-\frac{\|x\|^2}{\tau^2}\right)+\frac{\alpha C_3}{2\pi}\frac{1}{\tau^2}\left(6C_4-1-5C_4\frac{\|x\|^2}{\tau^2}\right)\\
&>\frac{c_0\mu C_1}{2\pi}\frac{1}{\tau^2}\left(2-\frac{\tau^2}{\tau^2}\right)+\frac{\alpha C_3}{2\pi}\frac{1}{\tau^2}\left(6C_4-1-5C_4\frac{\tau^2}{\tau^2}\right)\\
&=\frac{1}{2\pi\tau^2}\left(c_0\mu C_1+\alpha C_3(C_4-1)\right)\\
&=\frac{1}{2\pi\tau^2}\left(c_0\mu\frac{\alpha}{c_0(\lambda+2\mu)+\alpha^2}+\alpha\frac{c_0(\lambda+3\mu)+\alpha^2}{2(c_0(\lambda+2\mu)+\alpha^2)}\cdot\left(\frac{c_0(\lambda+\mu)+\alpha^2}{c_0(\lambda+3\mu)+\alpha^2}-1\right)\right)\\
&=\frac{1}{2\pi\tau^2}\left(c_0\mu\frac{\alpha}{c_0(\lambda+2\mu)+\alpha^2}-\alpha\cdot\frac{c_0\mu}{c_0(\lambda+2\mu)+\alpha^2}\right)\\
&=0. \qquad (8.189)
\end{aligned}$$

With this knowledge, let us continue and have a look at the integral

$$\begin{aligned}
&\int_{\substack{\mathbb{B}_\tau(0)\\ y_1,y_2>0}} \frac{C_1 c_0 \mu}{2\pi} \cdot \frac{y_1}{\tau^2}\left(2-\frac{\|y\|^2}{\tau^2}\right) + \frac{\alpha C_3}{2\pi}\left(\frac{y_1(6C_4-1)}{\tau^2} - 5C_4 \cdot y_1 \frac{\|y\|^2}{\tau^4}\right) \mathrm{d}y \\
&= \frac{c_0\mu C_1}{2\pi}\frac{1}{\tau^2}\int_0^{\pi/2}\int_0^{\tau} r\cos\varphi\left(2-\frac{r^2}{\tau^2}\right)\cdot r \,\mathrm{d}r\,\mathrm{d}\varphi \\
&\quad + \frac{\alpha C_3}{2\pi}\int_0^{\pi/2}\int_0^{\tau}\left(\frac{r\cos\varphi(6C_4-1)}{\tau^2} - 5C_4 r\cos\varphi\cdot\frac{r^2}{\tau^4}\right)\cdot r\,\mathrm{d}r\,\mathrm{d}\varphi \\
&= \frac{c_0\mu C_1}{2\pi}\frac{1}{\tau^2}\left(\frac{2}{3}\tau^3 - \frac{1}{5}\frac{\tau^5}{\tau^2}\right) + \frac{\alpha C_3}{2\pi}\left(\frac{1}{3}\frac{\tau^3}{\tau^2}(6C_4-1) - 5C_4\cdot\frac{1}{5}\frac{\tau^5}{\tau^4}\right) \\
&\to 0 \ (\tau\to 0+),
\end{aligned} \tag{8.190}$$

that means the integral can also be estimated by a constant. Due to the symmetry it is for $\Phi^2_{13,\tau}$ sufficient to have a look at the part with $y_1, y_2 > 0$

$$\begin{aligned}
\int_{\substack{\mathbb{B}_\tau(0)\\ y_1,y_2>0}} \frac{4y_1 C_1}{\tau^3\pi}\,\mathrm{d}y &= \frac{4C_1}{\tau^3\pi}\int_0^{\pi/2}\int_0^{\tau} r^2\cos\varphi\,\mathrm{d}r\,\mathrm{d}\varphi \\
&= \frac{4C_1}{\pi}\frac{\tau^3}{3\tau^3} \\
&= \frac{4C_1}{3\pi}.
\end{aligned} \tag{8.191}$$

This integral is also bounded. Now we have a look at the positive part of $\Phi_{31,\tau}$. If we have a look at the function without the y_1-term, we see that the remaining part contains no y-dependent term. Therefore, the sign of this term is independent of the spatial variable. We consider an arbitrary time interval and a half circle with polar coordinates and also Remark 2.2.4. We can separate the spatial and the time integral to obtain

$$\begin{aligned}
&\int_0^{\tau}\int_{t_1}^{t_2}\int_{-\pi/2}^{\pi/2} \Phi_{31,\tau}\,\mathrm{d}\varphi\,\mathrm{d}t\,\mathrm{d}r \\
&\qquad = \int_0^{\tau}\int_{t_1}^{t_2}\int_{-\pi/2}^{\pi/2} -r^2\cos\varphi\,\mathrm{d}\varphi \\
&\qquad\quad \times \exp\left(-\frac{\tau^2}{4C_2 t}\right)\left(\frac{\alpha\mu\tau^4 + 8C_1(\lambda+2\mu)t\tau^2}{8C_2\mu t^2\tau^4\pi}\right. \\
&\qquad\quad \left. + \frac{32C_1C_2(\lambda+2\mu)t^2\left(1-\exp\left(\frac{\tau^2}{4C_2t}\right)\right)}{8C_2\mu t^2\tau^4\pi}\right)\,\mathrm{d}t\,\mathrm{d}r
\end{aligned}$$

$$
\begin{aligned}
&= -2\frac{\tau^3}{3}\frac{1}{8C_2\mu\tau^4\pi}\cdot\Bigg[\alpha\mu\tau^4\left(\frac{4C_2\exp\left(-\frac{\tau^2}{4C_2t_2}\right)}{\tau^2}-\frac{4C_2\exp\left(-\frac{\tau^2}{4C_2t_1}\right)}{\tau^2}\right)\\
&-8C_1(\lambda+2\mu)\tau^2\left(\mathrm{Ei}\left(-\frac{\tau^2}{4C_2t_2}\right)-\mathrm{Ei}\left(-\frac{\tau^2}{4C_2t_1}\right)\right)\\
&+32C_1C_2(\lambda+2\mu)\left(\frac{\tau^2}{4C_2}\left(\mathrm{Ei}\left(-\frac{\tau^2}{4C_2t_2}\right)-\mathrm{Ei}\left(-\frac{\tau^2}{4C_2t_1}\right)\right)\right.\\
&\left.+\left(t_2\exp\left(-\frac{\tau^2}{4C_2t_2}\right)-t_1\exp\left(-\frac{\tau^2}{4C_2t_1}\right)\right)-(t_2-t_1)\right)\Bigg].
\end{aligned}
\tag{8.192}
$$

For the limit $\tau\to 0+$, it is obvious that the first three lines vanish. We only have to look at the last line more precisely and get

$$
\underbrace{\frac{t_2}{\tau}\left(\exp\left(-\frac{\tau^2}{4C_2t_2}\right)-1\right)}_{\to 0\ (\tau\to 0+)}-\underbrace{\frac{t_1}{\tau}\left(\exp\left(-\frac{\tau^2}{4C_2t_1}\right)-1\right)}_{\to 0\ (\tau\to 0+)}
\tag{8.193}
$$

due to L'Hospital's rule

$$
\lim_{\tau\to 0+}\frac{\exp\left(-\frac{\tau^2}{4C_2t_1}\right)-1}{\tau}=\lim_{\tau\to 0+}\frac{\exp\left(-\frac{\tau^2}{4C_2t_1}\right)\cdot\frac{-2\tau}{4C_2t_1}}{1}=0.
\tag{8.194}
$$

Please note that we have a quadratic term for t in the numerator, that means we have a maximum of 3 intervals, where the function is only positive or negative. For $\Phi_{33,\tau}$, our aim is to estimate the function for the space-dependent part with its maximum. Therefore, we have a look at the derivative with respect to $\|x\|^2$ and get for the numerator (because the numerator is sufficient to get the roots of the derivative)

$$
8t-c_0\mu\tau^2\begin{cases}>0,\ t>\frac{1}{8}c_0\mu\tau^2,\\ <0,\ t<\frac{1}{8}c_0\mu\tau^2.\end{cases}
\tag{8.195}
$$

We start with the first case $t>\frac{1}{8}c_0\mu\tau^2$, that means the function is monotonically increasing for $\|x\|$ and achieves its maximum at the boundary for $\|x\|=\tau$. Inserting this maximum into the numerator of the function (here it is sufficient to have a look at the numerator for the sign of the function) leads us to $4t\tau^2$ which is positive and the maximum therefore too. In the second case we have a monotonically decreasing function and its maximum in the point $(0,0)$. We have to check for the case $t<1/8c_0\mu\tau^2$ that the numerator of the function is actually positive again. This can be done by insertion of $(0,0)$ in the numerator and a simple estimate:

$$
-4t\tau^2+c_0\mu\tau^4>-\frac{1}{2}c_0\mu\tau^4+c_0\mu\tau^4=\frac{1}{2}c_0\mu\tau^4>0.
\tag{8.196}
$$

We can now go over to the estimation of the integrals for both cases and split the integral over the positive part of $\Phi_{33,\tau}$ into two cases (remember Remark 2.2.4). We start with the second case and the following integral, where the maximum is estimated by $\|x\| = 0$ and get (do not forget the area of $\mathbb{B}_\tau(0)$ multiplied with the integral)

$$\begin{aligned}
&\pi\tau^2 \int_0^{1/8 c_0\mu\tau^2} \exp\left(-\frac{\tau^2}{4C_2 t}\right) \frac{-4t\tau^2 + c_0\mu\tau^4}{64C_2^2 t^4 \pi}\,\mathrm{d}t \\
&= \tau^2 \left[-4\tau^2 \frac{4C_2 \exp\left(-\frac{\tau^2}{4C_2\left(\frac{1}{8}c_0\mu\tau^2\right)}\right)\left(\tau^2 + 4\left(\frac{1}{8}c_0\mu\tau^2\right)C_2\right)}{64C_2^2\left(\frac{1}{8}c_0\mu\tau^2\right)\tau^4} \right. \\
&\quad \left. + c_0\mu\tau^4 \frac{4C_2 \exp\left(-\frac{\tau^2}{4C_2\left(\frac{1}{8}c_0\mu\tau^2\right)}\right)\left(32C_2^2\left(\frac{1}{8}c_0\mu\tau^2\right)^2 + 8C_2\left(\frac{1}{8}c_0\mu\tau^2\right)\tau^2 + \tau^4\right)}{\left(\frac{1}{8}c_0\mu\tau^2\right)^2 \tau^6 \cdot 64C_2^2} \right],
\end{aligned} \tag{8.197}$$

where the integral converges to a constant for $\tau \to 0+$ and is therefore bounded. We continue with the integral in the first case given by $t > 1/8\ c_0\mu\tau^2$ and the maximum for $\|x\| = \tau$.

$$\begin{aligned}
&\pi\tau^2 \int_{\frac{1}{8}c_0\mu\tau^2}^{t_0} \exp\left(-\frac{\tau^2}{4C_2 t}\right) \frac{t\tau^2}{16C_2^2 t^4 \pi}\,\mathrm{d}t \\
&\qquad = \frac{\tau^2}{16C_2^2} \cdot \tau^2 \cdot \left[\frac{4C_2 \exp\left(-\frac{\tau^2}{4C_2 t_0}\right)\left(\tau^2 + 4t_0 C_2\right)}{t_0\tau^4} \right. \\
&\qquad\quad \left. - \frac{4C_2 \exp\left(-\frac{\tau^2}{4C_2\left(\frac{1}{8}c_0\mu\tau^2\right)}\right)\left(\tau^2 + 4\left(\frac{1}{8}c_0\mu\tau^2\right)C_2\right)}{\left(\frac{1}{8}c_0\mu\tau^2\right)\tau^4} \right],
\end{aligned} \tag{8.198}$$

where this integral is also bounded for $\tau \to 0+$. Please note that t_0 is linked with τ by a constant T in the way that $t_0 = T \cdot \tau$ holds true. In our case T is the length of our considered time interval. □

This finishes our proof. We showed that our constructed source scaling functions fulfill the property of a scaling function and the approximate identity. This theoretical result builds the basis for our upcoming numerical part. We can now go over to the numerical details of the decorrelation.

9. Numerical Experiments

In this section, we want to introduce suitable cubature formulas for our source scaling functions and show the numerical results. For the cubature formulas, we implement the numerical method from [21].

9.1. Cubature Formulas for Scaling Functions

Our next step is now, to have a look at the situation of our given data. This is the following: We have given data sets on a fixed grid. That implies for increasing τ the support of the source scaling function gets smaller and the Poisson summation formula gets less points to evaluate. This goes on up to the point that the source scaling function covers only one point for increasing j. The problem is that the soure scaling function has to cover a sufficient number of integration nodes for good convolution results. Therefore, it is necessary to modify the Poisson summation formula. We do this in the same way as it was done in [21], that means we introduce a particular weight, which is multiplied to the summation formula and is related to the source scaling functions.
We start with the procedure of a decomposition at a scale j_0 and have the data given on a lattice Λ, that means we calculate the convolution integrals with $\mathbf{\Phi}_{t_{j_0}}$ on a coarse grid $\Lambda_{j_0} \subset \Lambda$. This grid Λ_{j_0} has to be chosen such that there are enough data points and integration nodes such that the integration method (which is in our case the Poisson summation formula) yields good results. In this case it is not necessarily required that we use the whole lattice Λ for the convolution. This has the advantage that the convolution integral can be calculated faster than with the whole lattice Λ. Proceeding with this principle, we can use a lattice Λ_{j_1} for the convolution $\Phi_{\tau_{j_1}}$ and so on with the property that the grids are nested like this

$$\Lambda_{j_0} \subset \Lambda_{j_1} \subset \Lambda_{j_2} \subset \cdots \subset \Lambda_{J-1} \subset \Lambda_J = \Lambda. \tag{9.1}$$

With this we have for a convolution $\mathbf{\Phi}_{\tau_j}$ against the data the associated grid Λ and it is desired that the error of the numerical integration is small. For this purpose it is very important that the support of the respective source scaling function covers enough integration nodes. But here is another thing to mention if we are at step J, where we use the originally given lattice $\Lambda = \Lambda_J$: If we want to do a convolution for $j > J$, we are confronted with the problem that we do not have more integration nodes as in the case for J, since we used in this case the whole lattice. If we now increase $j > J$, we come to the point again that the support of

the source scaling function tends to a single point and therefore our summation formula results in infinity or zero. This is dependent on the single point itself, if it is a node of the numerical integration method or not. One solution for this problem would be to interpolate the given data and get nodes on lattices like

$$\Lambda = \Lambda_J \subset \Lambda_{J+1} \subset \Lambda_{J+2} \subset \dots. \tag{9.2}$$

But this would also increase the computational effort because of the additional task to compute the interpolation. Due to these reasons, we want to introduce cubature formulas that are suited for our singular integrals. For the construction, we follow the same way as it was done in [21], that means we equip the original summation formula (5.34) with an additional weight on the right-hand side. This weight is connected with the source scaling function due to the construction. For a short overview, we first show the choice of the additional weight for the Laplace case. Here the weight is chosen such that

$$w^{\mathrm{L}}(\tau; x) = \frac{\int_{\mathcal{B}} \Phi_\tau(\|x-y\|)\,\mathrm{d}y}{\|\mathcal{F}_\Lambda\| \sum\limits_{g\in\Lambda\cap\overline{\mathcal{B}}} \alpha(g)\Phi_\tau(\|x-g\|)}. \tag{9.3}$$

Due to the construction, the weight reflects how precisely the integral of Φ_τ is approximated by the Poisson summation formula. If we now define

$$I(x) \coloneqq \int_{\mathcal{B}} \Phi_\tau(\|x-y\|)\,\mathrm{d}y \tag{9.4}$$

with $I(x) = 1$ for the case $\mathbb{B}_\tau(x) \subset \mathcal{B}$, we see the following property of the weight:

$$w^L(\tau; x) \begin{cases} > 1, & \text{shows that the approximation of } I(x) \text{ by Corollary 5.2.6 is too small,} \\ = 1, & \text{shows that the approximation of } I(x) \text{ by Corollary 5.2.6 is exact,} \\ < 1, & \text{shows that the approximation of } I(x) \text{ by Corollary 5.2.6 is too large.} \end{cases} \tag{9.5}$$

That means the weight provides information about the quality of the approximation. With the help of the Poisson summation formula, it is shown that the modified cubature formula

$$w^L(\tau; x)\,\|\mathcal{F}_\Lambda\| \sum_{g\in\Lambda\cap\overline{\mathcal{B}}} \alpha(g)\Phi_\tau(\|x-g\|)\rho(g) \tag{9.6}$$

tends to $\alpha(x)\rho(x)$ in the limit $\tau \to 0+$, which is in the Laplace case also the result in the limit $\tau \to 0+$ of the convolution integral (see Definition 4.1.1) given by

$$\int_{\mathcal{B}} \Phi_\tau(\|x-y\|)\rho(y)\,\mathrm{d}y. \tag{9.7}$$

That means summarizing the results, we get

$$\lim_{\substack{\tau\to 0\\ \tau>0}} \left(w^{\mathrm{L}}(\tau;x)\,\|\mathcal{F}_{\Lambda}\| \sum_{g\in\Lambda\cap\overline{\mathcal{B}}} \alpha(g)\Phi_{\tau}(\|x-g\|)\rho(g) \right) = \alpha(x)\rho(x)$$
$$= \lim_{\substack{\tau\to 0\\ \tau>0}} \int_{\mathcal{B}} \Phi_{\tau}(\|x-y\|)\rho(y)\,\mathrm{d}y. \tag{9.8}$$

With these preliminary considerations, we want to switch over to our source scaling functions in the case of poroelasticity. Please note here that we have a source scaling function tensor (in contrast to [21], where there is a single source scaling function). Due to the construction and the properties of the source scaling function tensor (see Theorem 8.4.1), it is only for the diagonal elements possible to compute such specific weights in analogy to the weight in the Laplace case. For the functions on the minor diagonal, we use the same weights as for the main diagonal. For the functions $\Phi_{11,\tau}$ and $\Phi_{22,\tau}$, we introduce the following weights in analogy to [21]

$$w^{1}(\tau;x) \coloneqq \frac{\int_{\mathfrak{B}_{\tau}(x)} \Phi_{11,\tau}(x-y)\,\mathrm{d}y}{\|\mathcal{F}_{\Lambda_x}\| \sum\limits_{g\in\Lambda_x\cap\mathfrak{B}_{\tau}(x)} \alpha(g)\Phi_{11,\tau}(x-g)}, \tag{9.9}$$

$$w^{2}(\tau;x) \coloneqq \frac{\int_{\mathfrak{B}_{\tau}(x)} \Phi_{22,\tau}(x-y)\,\mathrm{d}y}{\|\mathcal{F}_{\Lambda_x}\| \sum\limits_{g\in\Lambda_x\cap\mathfrak{B}_{\tau}(x)} \alpha(g)\Phi_{22,\tau}(x-g)}, \tag{9.10}$$

where we used the abbreviation $\mathfrak{B}_{\tau}(x) \coloneqq \mathbb{B}_{\tau}(x)\cap\mathcal{B}$ to consider the compact support of the source scaling functions. For the weights belonging to $\Phi_{33,\tau}$, we have the drawback that the function tends to zero for $(x,t)\to(0,0)$. Therefore, we have to define the auxiliary function

$$\Phi'_{33,\tau}(x,t) = \begin{cases} \Phi_{33,\tau}(x,t), & t\geq\sigma,\\ \Phi_{33,\tau}(x,\sigma), & t<\sigma, \end{cases} \tag{9.11}$$

where σ is sufficiently small enough. For an estimation, how small this σ should be, we have a short look at $\Phi_{33,\tau}(x,\sigma)$

$$\Phi_{33,\tau}(x,\sigma) = \exp\left(-\frac{\tau^2}{4C_2\sigma}\right) \frac{8\|x\|^2\sigma - 4\sigma\tau^2 + c_0\mu\tau^2(\tau^2-\|x\|^2)}{64C_2^2\sigma^4\pi}. \tag{9.12}$$

Neither the expression with the exponential function nor the denominator can get zero.

Let us have a look at the numerator more precisely and solve the equation with respect to $\|x\|$

$$\begin{aligned} & 8\|x\|^2\sigma - 4\sigma\tau^2 + c_0\mu\tau^4 - c_0\mu\tau^2\|x\|^2 = 0 \\ \Leftrightarrow\ & \|x\|^2(8\sigma - c_0\mu\tau^2) = 4\sigma\tau^2 - c_0\mu\tau^4 \\ \Leftrightarrow\ & \|x\|^2 = \frac{4\sigma\tau^2 - c_0\mu\tau^4}{8\sigma - c_0\mu\tau^2}, \end{aligned} \tag{9.13}$$

where the denominator is unlike zero for $\sigma \neq \frac{1}{8}c_0\mu\tau^2$. The numerator gets zero for $\sigma = \frac{1}{4}c_0\mu\tau^2$, that means if we, for example, take care that $\sigma < \frac{1}{8}c_0\mu\tau^2$ holds true, because σ should be chosen sufficiently small, both requirements are fulfilled. Therefore it seems useful to couple the parameter σ with the parameter τ, that means σ should decrease with decreasing τ. With this we can state the weight belonging to the function Φ_τ. Furthermore, we have to introduce the originally solid angle $\alpha(x)$ now with respect to domain and time as a combination. That means, we understand the space and the time as a three-dimensional space and define $\alpha(x,t)$ as the following (in the setting of a rectangular prism $\mathcal{B}\times[0,T] = (-1,1)^2\times[0,T]$ for our numerical setting, where T is the end point of our considered time interval)

$$\alpha(x,t) = \begin{cases} 0, & \text{if } x \text{ is not an element of the cube } \mathcal{B} \text{ or the boundary } \partial\mathcal{B} \\ & \text{and } t \text{ is not an element of the closed interval } [0,T], \\ \frac{1}{8}, & \text{if } x \text{ is one of the four corner points of } \partial\mathcal{B} \text{ and } t \in \{0,T\} \\ \frac{1}{4}, & \text{if } x \text{ is on one of the four edges of } \partial\mathcal{B} \text{ and } t \in \{0,T\} \\ & \text{or } x \text{ is one of the four corner points of } \partial\mathcal{B} \text{ and } t \in (0,T), \\ \frac{1}{2}, & \text{if } x \text{ is in the open square } \mathcal{B} \text{ and } t \in \{0,T\} \\ & \text{or } x \text{ is on one of the four edges of } \partial\mathcal{B} \text{ and } t \in (0,T), \\ 1, & \text{if } x \text{ is in the open square } \mathcal{B} \text{ and } t \in (0,T). \end{cases} \tag{9.14}$$

With this definition, we go over and set the last weight as

$$w^3(\tau;x,t) := \frac{\int_{\mathfrak{B}_\tau(x)}\int_{\mathfrak{T}_{t_0}(t)} \Phi_{33,\tau}(x-y,t-\theta)\,\mathrm{d}\theta\,\mathrm{d}y}{\|\mathcal{F}_{\Lambda_x}\|\|\mathcal{F}_{\Lambda_t}\| \sum\limits_{g\in\Lambda_x\cap\mathfrak{B}_\tau(x)}\ \sum\limits_{s\in\Lambda_t\cap\mathfrak{T}_{t_0}(t)} \alpha(g,s)\Phi'_{33,\tau}(x-g,t-s)}, \tag{9.15}$$

where we used the abbreviation $\mathfrak{T}_{t_0}(t) := [0,T]\cap[t-t_0,t]$. Here, Λ_x is a lattice in $\mathbb{R}^2$ referring to the spatial component and Λ_t is a lattice in $\mathbb{R}$ regarding the time component. Especially for the construction in the time-dependent case of $w^3(\tau;x,t)$, we refer to the d'Alembert case in [21]. These weights reflect also how precisely the integrals of $\Phi_{11,\tau}$, $\Phi_{22,\tau}$ and $\Phi_{33,\tau}$ are approximated by the classical Poisson summation formula. For a more detailed comparison of the classical Poisson summation formula to its modified version in the Laplace, Helmholtz and d'Alembert case, we refer to [21]. In this thesis the behavior of both summation formulas is shown for some numerical examples (test functions for the

data functions that are convolved). More precisely, the exact solution, the corresponding approximation and the relative error are shown for some $n \in \mathbb{N}$. Now we want to show that our constructed weights and the corresponding summation formulas also fulfill the necessary results to approximate our convolution integrals like in (9.8) in the following theorem.

Theorem 9.1.1. *Let a regular region $\mathcal{B}$ in $\mathbb{R}^2$ be given. We have $\alpha(x)$ as the solid angle in x subtended by the boundary $\partial\mathcal{B}$ or $\alpha(x,t)$ for the time dependent case as defined above. Furthermore, we have fixed lattices Λ_x in $\mathbb{R}^2$ and Λ_t in $\mathbb{R}$ with the respective fundamental cells $\mathcal{F}_{\Lambda_x}$ and $\mathcal{F}_{\Lambda_t}$. Let $x \in \Lambda_x \cap \mathcal{B}$, $t \in \Lambda_t \cap [0,T]$ and $\mathfrak{B}_\tau(x) \coloneqq \mathbb{B}_\tau(x) \cap \overline{\mathcal{B}}$ and $\mathfrak{T}_{t_0}(t) \coloneqq [0,T] \cap [t-t_0, t]$ and $f : \overline{\mathcal{B}} \times [0,T] \to \mathbb{R}^3$ be continuously differentiable. We obtain*

$$\begin{aligned}
&w^j(\tau;x)\,\|\mathcal{F}_{\Lambda_x}\| \sum_{g\in\Lambda_x\cap\mathfrak{B}_\tau(x)} \alpha(g)\Phi_{ji,\tau}(x-g)f_i(g,t) \\
&\quad= \int_{\mathfrak{B}_\tau(x)} \Phi_{ji,\tau}(x-y)f_i(y,t)\,\mathrm{d}y + \big(w^j(\tau;x)-1\big)\int_{\mathfrak{B}_\tau(x)} \Phi_{ji,\tau}(x-y)f_i(y,t)\,\mathrm{d}y \\
&\quad+w^j(\tau;x)\lim_{\substack{\varepsilon\to 0\\ \varepsilon>0}} \sum_{\substack{h_x\in\Lambda_x^{-1}\\ h_x\neq 0}} \exp(-\varepsilon\pi^2\,\|h\|^2)\int_{\mathfrak{B}_\tau(x)} \Phi_{ji,\tau}(x-y)f_i(y,t)\exp(-2\pi i h\cdot y)\,\mathrm{d}y, \\
&\quad \textit{for } j=1,2,\ i=1,2,3
\end{aligned} \tag{9.16}$$

and for the case with the additional time component

$$\begin{aligned}
&w^3(\tau;x,t)\,\|\mathcal{F}_{\Lambda_x}\|\,\|\mathcal{F}_{\Lambda_t}\| \sum_{g\in\Lambda_x\cap\mathfrak{B}_\tau(x)}\sum_{s\in\Lambda_t\cap\mathfrak{T}_{t_0}(t)} \alpha(g,s)\Phi'_{3i,\tau}(x-g,t-s)f_i(g,s) \\
&\quad= \int_{\mathfrak{B}_\tau(x)}\int_{\mathfrak{T}_{t_0}(t)} \Phi_{3i,\tau}(x-y,t-\theta)f_i(y,\theta)\,\mathrm{d}\theta\,\mathrm{d}y \\
&\quad+ \big(w^3(\tau;x,t)-1\big)\int_{\mathfrak{B}_\tau(x)}\int_{\mathfrak{T}_{t_0}(t)} \Phi'_{3i,\tau}(x-y,t-\theta)f_i(y,\theta)\,\mathrm{d}\theta\,\mathrm{d}y \\
&\quad+\int_{\mathfrak{B}_\tau(x)}\int_{\mathfrak{T}_{t_0}(t)} \big(\Phi'_{3i,\tau}(x-y,t-\theta)-\Phi_{3i,\tau}(x-y,t-\theta)\big)f_i(y,\theta)\,\mathrm{d}\theta\,\mathrm{d}y \\
&\quad+w^3(\tau;x,t)\lim_{\substack{\varepsilon\to 0\\ \varepsilon>0}} \sum_{\substack{h_x\in\Lambda_x^{-1}\\ h_x\neq 0}}\sum_{\substack{h_t\in\Lambda_t^{-1}\\ h_t\neq 0}} \exp(-\varepsilon\pi^2(\|h_x\|^2+h_t^2)) \\
&\qquad\times\int_{\mathfrak{B}_\tau(x)}\int_{\mathfrak{T}_{t_0}(t)} \Phi'_{3i,\tau}(x-y,t-\theta)f_i(y,\theta)\exp(-2\pi i(h_x\cdot y+h_t\cdot\theta))\,\mathrm{d}\theta\,\mathrm{d}y, \\
&\quad \textit{for } i=1,2,3,
\end{aligned} \tag{9.17}$$

where we have

$$\Phi'_{3i,\tau} \coloneqq \begin{cases} \Phi_{3i,\tau}, & i=1,2, \\ \Phi'_{33,\tau}, & i=3, \end{cases} \tag{9.18}$$

and the introduced weights $w^1(\tau;x)$, $w^2(\tau;x)$ *and* $w^3(\tau;x,t)$ *from* (9.9),(9.10) *and* (9.15). *Additionally, we obtain*

$$\begin{aligned}
&\lim_{\substack{\tau\to 0\\ \tau>0}} \begin{pmatrix} w^1(\tau;x)\,\|\mathcal{F}_{\Lambda_x}\| \sum_{g\in\Lambda_x\cap\mathfrak{B}_\tau(x)} \sum_{i=1}^3 \alpha(g)\Phi_{1i,\tau}(x-g)f_i(g,t) \\ w^2(\tau;x)\,\|\mathcal{F}_{\Lambda_x}\| \sum_{g\in\Lambda_x\cap\mathfrak{B}_\tau(x)} \sum_{i=1}^3 \alpha(g)\Phi_{2i,\tau}(x-g)f_i(g,t) \\ w^3(\tau;x,t)\,\|\mathcal{F}_{\Lambda_x}\|\,\|\mathcal{F}_{\Lambda_t}\| \sum_{g\in\Lambda_x\cap\mathfrak{B}_\tau(x)} \sum_{s\in\Lambda_t\cap\mathfrak{T}_{t_0}(t)} \sum_{i=1}^3 \\ \qquad\qquad \alpha(g,s)\Phi'_{3i,\tau}(x-g,t-s)f_i(g,s) \end{pmatrix} \\
&= f(x,t) = \lim_{\substack{\tau\to 0\\ \tau>0}} \int_{\mathcal{B}} \int_0^T \mathbf{\Phi}_\tau(x-y,t-\theta) f(y,\theta)\,\mathrm{d}\theta\,\mathrm{d}y, \qquad (9.19)
\end{aligned}$$

that means

$$\begin{aligned}
&\lim_{\substack{\tau\to 0\\ \tau>0}} \Bigg(\big(w^j(\tau;x)-1\big) \int_{\mathfrak{B}_\tau(x)} \Phi_{ji,\tau}(x-y) f_i(y,t)\,\mathrm{d}y + w^j(\tau;x) \\
&\quad \times \lim_{\substack{\varepsilon\to 0\\ \varepsilon>0}} \sum_{\substack{h_x\in\Lambda_x^{-1}\\ h_x\neq 0}} \exp(-\varepsilon\pi^2\,\|h\|^2) \int_{\mathfrak{B}_\tau(x)} \Phi_{ji,\tau}(x-y) f_i(y,t) \exp(-2\pi i h\cdot y)\,\mathrm{d}y \Bigg) \\
&\quad = 0 \qquad (9.20)
\end{aligned}$$

and

$$\begin{aligned}
&\lim_{\substack{\tau\to 0\\ \tau>0}} \Bigg(\big(w^3(\tau;x,t)-1\big) \int_{\mathfrak{B}_\tau(x)} \int_{\mathfrak{T}_{t_0}(t)} \Phi'_{3i,\tau}(x-y,t-\theta) f_i(y,\theta)\,\mathrm{d}\theta\,\mathrm{d}y \\
&\quad + \int_{\mathfrak{B}_\tau(x)} \int_{\mathfrak{T}_{t_0}(t)} \big(\Phi'_{3i,\tau}(x-y,t-\theta) - \Phi_{33,\tau}(x-y,t-\theta)\big) f_i(y,\theta)\,\mathrm{d}\theta\,\mathrm{d}y \\
&\quad + w^3(\tau;x,t) \lim_{\substack{\varepsilon\to 0\\ \varepsilon>0}} \sum_{\substack{h_x\in\Lambda_x^{-1}\\ h_x\neq 0}} \sum_{\substack{h_t\in\Lambda_t^{-1}\\ h_t\neq 0}} \exp(-\varepsilon\pi^2(\|h_x\|^2 + h_t^2)) \\
&\qquad \times \int_{\mathfrak{B}_\tau(x)} \int_{\mathfrak{T}_{t_0}(t)} \Phi'_{3i,\tau}(x-y,t-\theta) f_i(y,\theta) \exp(-2\pi i(h_x\cdot y + h_t\cdot\theta))\,\mathrm{d}\theta\,\mathrm{d}y \Bigg) \\
&\qquad = 0. \qquad (9.21)
\end{aligned}$$

Proof. For the proof, we have a look at each convolution integral separately. We start with the convolution integrals given by (8.164) and the convolution $\Phi_{11,\tau} * f_1$. We apply the same technique for the proof as given in [21].

With the help of the defined weight $w^1(\tau;x)$ and the Poisson summation formula (see Theorem 5.2.5 and the resulting Corollary 5.2.6), we find

$$\begin{aligned}
&w^1(\tau;x)\,\|\mathcal{F}_{\Lambda_x}\| \sum_{g\in\Lambda_x\cap\mathfrak{B}_\tau(x)} \alpha(g)\Phi_{11,\tau}(x-g)f_1(g,t)\\
&\quad= w^1(\tau;x)\int_{\mathfrak{B}_\tau(x)} \Phi_{11,\tau}(x-y)f_1(y,t)\,\mathrm{d}y + w^1(\tau;x)\\
&\qquad\times \lim_{\substack{\varepsilon\to 0\\ \varepsilon>0}} \sum_{\substack{h_x\in\Lambda_x^{-1}\\ h_x\neq 0}} \exp(-\varepsilon\pi^2\,\|h\|^2)\int_{\mathfrak{B}_\tau(x)} \Phi_{11,\tau}(x-y)f_1(y,t)\exp(-2\pi i h\cdot y)\,\mathrm{d}y\\
&\quad= \int_{\mathfrak{B}_\tau(x)} \Phi_{11,\tau}(x-y)f_1(y,t)\,\mathrm{d}y\\
&\qquad+ \big(w^1(\tau;x)-1\big)\int_{\mathfrak{B}_\tau(x)} \Phi_{11,\tau}(x-y)f_1(y,t)\,\mathrm{d}y\\
&\qquad+ w^1(\tau;x)\lim_{\substack{\varepsilon\to 0\\ \varepsilon>0}} \sum_{\substack{h_x\in\Lambda_x^{-1}\\ h_x\neq 0}} \exp(-\varepsilon\pi^2\,\|h\|^2)\\
&\qquad\times \int_{\mathfrak{B}_\tau(x)} \Phi_{11,\tau}(x-y)f_1(y,t)\exp(-2\pi i h\cdot y)\,\mathrm{d}y. \qquad (9.22)
\end{aligned}$$

For the limit relation, we consider the following: Because $x\in\Lambda_x\cap\mathcal{B}$, we find a τ_0 such that $\{g|g\in\Lambda_x\cap\mathfrak{B}_\tau(x)\}=\{x\}$ for all $0<\tau\leq\tau_0$. We insert this and the weight into the modified cubature formula and get

$$\begin{aligned}
&w^1(\tau;x)\,\|\mathcal{F}_{\Lambda_x}\| \sum_{g\in\Lambda_x\cap\mathfrak{B}_\tau(x)} \alpha(g)\Phi_{11,\tau}(x-g)f_1(g,t)\\
&\qquad= \frac{\int_{\mathfrak{B}_\tau(x)}\Phi_{11,\tau}(x-y)\,\mathrm{d}y}{\alpha(x)\Phi_{11,\tau}(0)}\alpha(x)\Phi_{11,\tau}(0)f_1(x,t). \qquad (9.23)
\end{aligned}$$

Now taking the limit $\tau\to 0+$, we obtain

$$\lim_{\substack{\tau\to 0\\ \tau>0}} w^1(\tau;x)\,\|\mathcal{F}_{\Lambda_x}\| \sum_{g\in\Lambda_x\cap\mathfrak{B}_\tau(x)} \alpha(g)\Phi_{11,\tau}(x-g)f_1(g,t) = f_1(x,t). \qquad (9.24)$$

For the second and third term on the right-hand side of (9.22), it follows from the limit relation above and the fact that the first term on the right-hand side tends to $f_1(x,t)$ for $\tau\to 0+$ that this part tends to zero in the limit $\tau\to 0+$, that means

$$\lim_{\substack{\tau\to 0\\ \tau>0}} \Bigg(\big(w^1(\tau;x)-1\big) \int_{\mathfrak{B}_\tau(x)} \Phi_{11,\tau}(x-y) f_1(y,t)\,\mathrm{d}y + w^1(\tau;x) \lim_{\substack{\varepsilon\to 0\\ \varepsilon>0}} \sum_{\substack{h_x\in\Lambda_x^{-1}\\ h_x\neq 0}} \exp(-\varepsilon\pi^2\,\|h\|^2) \times \int_{\mathfrak{B}_\tau(x)} \Phi_{11,\tau}(x-y) f_1(y,t)\exp(-2\pi i h\cdot y)\,\mathrm{d}y \Bigg) = 0. \tag{9.25}$$

If we now follow the same procedure for the remaining convolution integrals in (8.164), that means for the functions $\Phi_{12,\tau}$, $\Phi^1_{13,\tau}$ and $\Phi^2_{13,\tau}$ with the modified weight $w^1(\tau;x)$, we can do the same steps as before and obtain instead of (9.23), for example for $\Phi_{12,\tau}$,

$$w^1(\tau;x)\,\|\mathcal{F}_{\Lambda_x}\| \sum_{g\in\Lambda_x\cap\mathfrak{B}_\tau(x)} \alpha(g)\Phi_{12,\tau}(x-g) f_2(g,t) = \frac{\int_{\mathfrak{B}_\tau(x)} \Phi_{11,\tau}(x-y)\,\mathrm{d}y}{\alpha(x)\Phi_{11,\tau}(0)} \alpha(x)\Phi_{12,\tau}(0) f_2(x,t). \tag{9.26}$$

Since $\Phi_{12,\tau}(0) = 0$ and also $\Phi^1_{13,\tau}(0) = \Phi^2_{13,\tau}(0) = 0$, we get altogether for the convolution integrals of (8.164) the result $f_1(x,t)$ in the limit, which is also the first line of the convolution integral

$$f(x,t) = \lim_{\substack{\tau\to 0\\ \tau>0}} \int_{\mathcal{B}} \int_{\mathbb{R}} \mathbf{\Phi}_\tau(x-y,t-\theta) f(y,\theta)\,\mathrm{d}\theta\,\mathrm{d}y. \tag{9.27}$$

The same thoughts and steps can be applied to the second line of our convolution integrals (see (8.165)) with the weight $w^2(\tau;x)$. For the third line (see (8.166)), the technique is the same with the weight $w^3(\tau;x,t)$ but we want to show it more detailed here again because of the time dependency. We have a look at the third convolution integral $\Phi_{33,\tau} * f_3$.

With the help of the Poisson summation formula and the defined weight $w^3(\tau;x,t)$, we get for the auxiliary function $\Phi'_{33,\tau}$ defined above

$$\begin{aligned}
&w^3(\tau;x,t)\,\|\mathcal{F}_{\Lambda_x}\|\,\|\mathcal{F}_{\Lambda_t}\| \sum_{g\in\Lambda_x\cap\mathfrak{B}_\tau(x)}\sum_{s\in\Lambda_t\cap\mathfrak{T}_{t_0}(t)} \alpha(g,s)\Phi'_{33,\tau}(x-g,t-s)f_3(g,s)\\
&\quad= w^3(\tau;x,t)\int_{\mathfrak{B}_\tau(x)}\int_{\mathfrak{T}_{t_0}(t)} \Phi'_{33,\tau}(x-y,t-\theta)f_3(y,\theta)\,\mathrm{d}\theta\,\mathrm{d}y\\
&\quad+w^3(\tau;x,t)\lim_{\substack{\varepsilon\to 0\\ \varepsilon>0}}\sum_{\substack{h_x\in\Lambda_x^{-1}\\ h_x\neq 0}}\sum_{\substack{h_t\in\Lambda_t^{-1}\\ h_t\neq 0}} \exp(-\varepsilon\pi^2(\|h_x\|^2+h_t^2))\\
&\qquad\times\int_{\mathfrak{B}_\tau(x)}\int_{\mathfrak{T}_{t_0}(t)} \Phi'_{33,\tau}(x-y,t-\theta)f_3(y,\theta)\exp(-2\pi i(h_x\cdot y+h_t\cdot\theta))\,\mathrm{d}\theta\,\mathrm{d}y\\
&\qquad=\int_{\mathfrak{B}_\tau(x)}\int_{\mathfrak{T}_{t_0}(t)} \Phi'_{33,\tau}(x-y,t-\theta)f_3(y,\theta)\,\mathrm{d}\theta\,\mathrm{d}y\\
&\qquad+\big(w^3(\tau;x,t)-1\big)\int_{\mathfrak{B}_\tau(x)}\int_{\mathfrak{T}_{t_0}(t)} \Phi'_{33,\tau}(x-y,t-\theta)f_3(y,\theta)\,\mathrm{d}\theta\,\mathrm{d}y\\
&\quad+w^3(\tau;x,t)\lim_{\substack{\varepsilon\to 0\\ \varepsilon>0}}\sum_{\substack{h_x\in\Lambda_x^{-1}\\ h_x\neq 0}}\sum_{\substack{h_t\in\Lambda_t^{-1}\\ h_t\neq 0}} \exp(-\varepsilon\pi^2(\|h_x\|^2+h_t^2))\\
&\qquad\times\int_{\mathfrak{B}_\tau(x)}\int_{\mathfrak{T}_{t_0}(t)} \Phi'_{33,\tau}(x-y,t-\theta)f_3(y,\theta)\exp(-2\pi i(h_x\cdot y+h_t\cdot\theta))\,\mathrm{d}\theta\,\mathrm{d}y.
\end{aligned}\tag{9.28}$$

Proceeding, we get

$$\begin{aligned}
&w^3(\tau;x,t)\,\|\mathcal{F}_{\Lambda_x}\|\,\|\mathcal{F}_{\Lambda_t}\| \sum_{g\in\Lambda_x\cap\mathfrak{B}_\tau(x)}\sum_{s\in\Lambda_t\cap\mathfrak{T}_{t_0}(t)} \alpha(g,s)\Phi'_{33,\tau}(x-g,t-s)f_3(g,s)\\
&\quad=\int_{\mathfrak{B}_\tau(x)}\int_{\mathfrak{T}_{t_0}(t)} \Phi_{33,\tau}(x-y,t-\theta)f_3(y,\theta)\,\mathrm{d}\theta\,\mathrm{d}y\\
&\quad+\big(w^3(\tau;x,t)-1\big)\int_{\mathfrak{B}_\tau(x)}\int_{\mathfrak{T}_{t_0}(t)} \Phi'_{33,\tau}(x-y,t-\theta)f_3(y,\theta)\,\mathrm{d}\theta\,\mathrm{d}y\\
&\quad+\int_{\mathfrak{B}_\tau(x)}\int_{\mathfrak{T}_{t_0}(t)} \big(\Phi'_{33,\tau}(x-y,t-\theta)-\Phi_{33,\tau}(x-y,t-\theta)\big)f_3(y,\theta)\,\mathrm{d}\theta\,\mathrm{d}y\\
&\quad+w^3(\tau;x,t)\lim_{\substack{\varepsilon\to 0\\ \varepsilon>0}}\sum_{\substack{h_x\in\Lambda_x^{-1}\\ h_x\neq 0}}\sum_{\substack{h_t\in\Lambda_t^{-1}\\ h_t\neq 0}} \exp(-\varepsilon\pi^2(\|h_x\|^2+h_t^2))\\
&\qquad\times\int_{\mathfrak{B}_\tau(x)}\int_{\mathfrak{T}_{t_0}(t)} \Phi'_{33,\tau}(x-y,t-\theta)f_3(y,\theta)\exp(-2\pi i(h_x\cdot y+h_t\cdot\theta))\,\mathrm{d}\theta\,\mathrm{d}y.
\end{aligned}\tag{9.29}$$

For the limit relation, we consider again the following: Because $x \in \Lambda_x \cap \mathcal{B}$ and $t \in \Lambda_t \cap [0,T]$, we find a τ_0 such that

$$\left\{g \in \Lambda_x \cap \mathfrak{B}_\tau(x),\ s \in \Lambda_t \cap \mathfrak{T}_{t_0}(t) | \Phi'_{33,\tau}(x-g,t-s) \neq 0\right\} = \{(x,t)\} \tag{9.30}$$

for all $0 < \tau \leq \tau_0$. We insert the weight and get

$$\begin{aligned} & w^3(\tau;x,t)\,\|\mathcal{F}_{\Lambda_x}\|\,\|\mathcal{F}_{\Lambda_t}\| \sum_{g\in\Lambda_x\cap\mathfrak{B}_\tau(x)} \sum_{s\in\Lambda_t\cap\mathfrak{T}_{t_0}(t)} \alpha(g,s)\Phi'_{33,\tau}(x-g,t-s)f_3(g,s) \\ &= \frac{\int_{\mathfrak{B}_\tau(x)}\int_{\mathfrak{T}_{t_0}(t)} \Phi_{33,\tau}(x-y,t-\theta)\,\mathrm{d}\theta\mathrm{d}y}{\alpha(x,t)\Phi'_{33,\tau}(0,0)}\alpha(x,t)\Phi'_{33,\tau}(0,0)f_3(x,t). \end{aligned} \tag{9.31}$$

Now taking the limit $\tau \to 0+$, we obtain

$$\begin{aligned} & \lim_{\substack{\tau\to 0\\ \tau>0}} \left(w^3(\tau;x,t)\,\|\mathcal{F}_{\Lambda_x}\|\,\|\mathcal{F}_{\Lambda_t}\| \sum_{g\in\Lambda_x\cap\mathfrak{B}_\tau(x)} \sum_{s\in\Lambda_t\cap\mathfrak{T}_{t_0}(t)} \alpha(g,s)\Phi'_{33,\tau}(x-g,t-s)f_3(g,s) \right) \\ &= f_3(x,t). \end{aligned} \tag{9.32}$$

The last four lines of (9.29) tend to zero for $\tau \to 0+$ due to the limit relation proven above and the fact that the first line tends to $f_3(x,t)$ for $\tau \to 0+$, that means we have

$$\begin{aligned} & \lim_{\substack{\tau\to 0\\ \tau>0}} \Bigg(\left(w^3(\tau;x,t)-1\right) \int_{\mathfrak{B}_\tau(x)}\int_{\mathfrak{T}_{t_0}(t)} \Phi'_{33,\tau}(x-y,t-\theta)f_3(y,\theta)\,\mathrm{d}\theta\,\mathrm{d}y \\ &\qquad + \int_{\mathfrak{B}_\tau(x)}\int_{\mathfrak{T}_{t_0}(t)} \left(\Phi'_{33,\tau}(x-y,t-\theta) - \Phi_{33,\tau}(x-y,t-\theta)\right) f_3(y,\theta)\,\mathrm{d}\theta\,\mathrm{d}y \\ &\qquad + w^3(\tau;x,t) \lim_{\substack{\varepsilon\to 0\\ \varepsilon>0}} \sum_{\substack{h_x\in\Lambda_x^{-1}\\ h_x\neq 0}} \sum_{\substack{h_t\in\Lambda_t^{-1}\\ h_t\neq 0}} \exp(-\varepsilon\pi^2(\|h_x\|^2+h_t^2)) \\ &\qquad \times \int_{\mathfrak{B}_\tau(x)}\int_{\mathfrak{T}_{t_0}(t)} \Phi'_{33,\tau}(x-y,t-\theta)f_3(y,\theta)\exp(-2\pi i(h_x\cdot y + h_t\cdot\theta))\,\mathrm{d}\theta\,\mathrm{d}y \Bigg) \\ &= 0. \end{aligned} \tag{9.33}$$

If we now follow the same procedure for the remaining convolution integrals in (8.166), that means for the functions $\Phi_{31,\tau}$ and $\Phi_{32,\tau}$ with the modified weight $w^3(\tau;x,t)$, we can do the same steps as before and obtain instead of (9.31), for example for $\Phi_{31,\tau}$,

$$\begin{aligned} & w^3(\tau;x,t)\,\|\mathcal{F}_{\Lambda_x}\|\,\|\mathcal{F}_{\Lambda_t}\| \sum_{g\in\Lambda_x\cap\mathfrak{B}_\tau(x)} \sum_{s\in\Lambda_t\cap\mathfrak{T}_{t_0}(t)} \alpha(g,s)\Phi_{31,\tau}(x-g,t-s)f_1(g,s) \\ &= \frac{\int_{\mathfrak{B}_\tau(x)}\int_{\mathfrak{T}_{t_0}(t)} \Phi_{33,\tau}(x-y,t-\theta)\,\mathrm{d}\theta\mathrm{d}y}{\alpha(x,t)\Phi'_{33,\tau}(0,0)}\alpha(x,t)\Phi_{31,\tau}(0,0)f_1(x,t). \end{aligned} \tag{9.34}$$

Since $\Phi_{31,\tau}(0,0) = 0$ and also $\Phi_{32,\tau}(0,0) = 0$, we get altogether for the convolution integrals of (8.166) the result $f_3(x,t)$ in the limit $\tau \to 0+$, which is also the third line of the convolution integral

$$f(x,t) = \lim_{\substack{\tau \to 0 \\ \tau > 0}} \int_{\mathcal{B}} \int_0^T \mathbf{\Phi}_\tau(x-y, t-\theta) f(y,\theta) \, \mathrm{d}\theta \, \mathrm{d}y. \tag{9.35}$$

□

Summarizing, we can say that the constructed weights together with the modified cubature formulas correspond to the right-hand side of the approximate identity given in Theorem 8.4.4 in the limit $\tau \to 0+$. In other words, we can rewrite Theorem 9.1.1 as a cubature formula in the following way.

Corollary 9.1.2. *Under the assumptions of Theorem 9.1.1, we have the cubature formulas*

$$\int_{\mathfrak{B}_\tau(x)} \Phi_{1i,\tau}(x-y) f_i(y,t) \, \mathrm{d}y \approx w^1(\tau;x) \, \|\mathcal{F}_{\Lambda_x}\| \sum_{g \in \Lambda_x \cap \mathfrak{B}_\tau(x)} \alpha(g) \Phi_{1i,\tau}(x-y) f_i(y,t),$$

for $i = 1,2,3$ (9.36)

$$\int_{\mathfrak{B}_\tau(x)} \Phi_{2i,\tau}(x-y) f_i(y,t) \, \mathrm{d}y \approx w^2(\tau;x) \, \|\mathcal{F}_{\Lambda_x}\| \sum_{g \in \Lambda_x \cap \mathfrak{B}_\tau(x)} \alpha(g) \Phi_{2i,\tau}(x-y) f_i(y,t),$$

for $i = 1,2,3$ (9.37)

$$\begin{aligned} &\int_{\mathfrak{B}_\tau(x)} \int_{t-t_0}^t \Phi_{3i,\tau}(x-y, t-\theta) f_i(y,\theta) \, \mathrm{d}\theta \, \mathrm{d}y \\ &\approx w^3(\tau;x,t) \, \|\mathcal{F}_{\Lambda_x}\| \, \|\mathcal{F}_{\Lambda_t}\| \sum_{g \in \Lambda_x \cap \mathfrak{B}_\tau(x)} \sum_{s \in \Lambda_t \cap \mathfrak{T}_{t_0}(t)} \alpha(g,s) \Phi'_{3i,\tau}(x-y, t-\theta) f_i(y,\theta), \end{aligned}$$

for $i = 1,2,3$ (9.38)

Please note that we have to use the auxiliary function in (9.38) *instead of* $\Phi_{33,\tau}$ *on the right-hand side. The cubature formulas also hold true for the cases* $\Phi^1_{13,\tau}$ *and* $\Phi^1_{23,\tau}$*, where we have the derivative of the data with respect to the time instead of the data itself at the time* t*.*

9.2. Test Datasets

We introduce the data sets that we want to decompose with the help of our source scaling functions and the appropriate cubature formulas from Section 9.1. We have to draw on synthetic data, which we generate with the help of the fundamental solutions.
This is done in the following way: We take the fundamental solutions u^{Si} and p^{Si} and shift them such that the singularity is outside of our considered area (this

is also done in [10] for testing the method of fundamental solutions). Then we evaluate these fundamental solutions on a fixed grid and take them (in analogy to [10]) as our given input data. In our case this means that we take the square $[-1,1]^2$, the time interval $[0,5]$ and shift the fundamental solutions by $(2,2)$ in the space and -1 in the domain. More precisely, we evaluate $u^{\mathrm{Si}}(x_1-2, x_2-2, t+1)$ and $p^{\mathrm{Si}}(x_1-2, x_2-2, t+1)$ for $N = 100$ points in the spatial direction and $M = 200$ points in the time direction. For the last scale $j = 6$, we use $N = 200$ points as an exception.
In Figure 9.1 the plots of the generated datasets for u_1, u_2 and p for the fixed point of time $t = 1$ are shown. We see that we have very smooth data in contrast to the used data in [21–23, 61]. Unfortunately, we do not have access to real data or data models in poroelasticity.

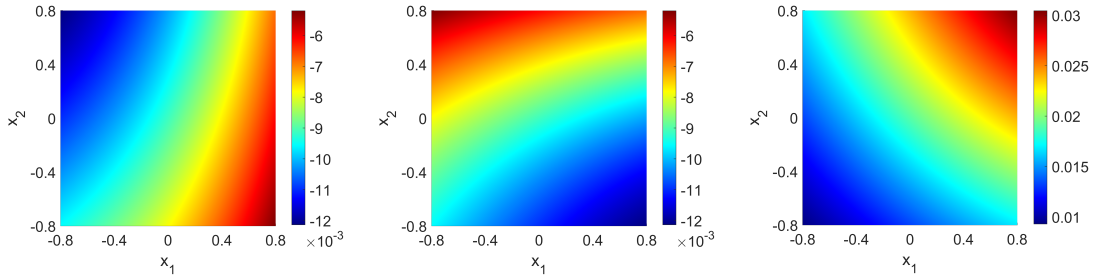

(a) Component $u_1,\ t = 1$ (b) Component $u_2,\ t = 1$ (c) Component $p,\ t = 1$

Figure 9.1.: Data sets for the displacement component and the pore pressure given for the multiscale modeling for the fixed time $t = 1$.

One thing is to mention here about the image section of the data before we go over to the convolution results.

Remark 9.2.1. *Since we have some boundary effects in our convolutions (see further considerations in Remark 9.3.3 and Figure 9.14), we cut off a fixed part of the boundary in the spatial component because these boundary effects should not superimpose the overall structure of the convolutions. This is also done here in the case of the given data for a better comparability between the data and the convolutions in the next section.*

In the following, we summarize the data set consisting of u_1, u_2 and p sometimes by the data vector f that means $f = (u_1, u_2, p)^{\mathrm{T}}$.

9.3. Pictures

In this section, we show the decomposition ability of our source scaling function tensor $\{\mathbf{\Phi}_{\tau,j}\}_{j\in\mathbb{N}}$ and the corresponding wavelet tensor $\{\mathbf{\Psi}_{\tau,j}\}_{j\in\mathbb{N}}$ by showing the decorrelation for several parameters τ_j of the data. We choose the monotonically decreasing sequence $\tau_j = 2^{-j}$. For a better clarity, we show the convolutions for a time cut that means the spatial part for a fixed time.

Remark 9.3.1. *Please note that we do not use the σ-distinction (see* (9.11)*) for $\Phi_{33,\tau}$ because our numerical tests show that σ can be chosen arbitrarily small. For the numerical tests we do not let the support of $\Phi_{33,\tau}$ shrink so small that it shrinks to a single point because this is not useful for a numerical integration. It is necessary that a sufficient number of points is covered by the source scaling function.*

The convolutions and numerical tests are implemented in Matlab (see [111] and [112]) and the computations are performed on the OMNI cluster (University of Siegen). We have a look at the convolution results of the data u_1 and u_2 together because due to the symmetry of the data, the fundamental solutions and the constructed source scaling functions, they behave very similarly. Please remember here that we have the situation of a source scaling function tensor (see Section 8.3). First we have a look at the convolutions of (8.164) respectively (8.165) together that means the several components of the convolution are added in the pictures for a better comparability with the input data. Later, we show the several components of (8.164) as an example individually for some parameters.
Figures 9.2-9.7 show the multiscale approximation of the data u_1 respectively u_2 by convolution of the source scaling function (tensor) $\left\{\Phi_{\tau_j}\right\}_{j\in\mathbb{N}}$ (scale-space) and the source wavelet (tensor) $\left\{\Psi_{\tau_j}\right\}_{j\in\mathbb{N}}$ (detail-space) with the data. Here we use the parameters $j = 0,\ldots,6$ for the source scaling function (results depicted in the left column of the mentioned figures) and $j = 1,\ldots,6$ for the source wavelet function (resulting pictures in the right column of the figures). Remembering the definition of the wavelet function, we obtain the convolution of the source scaling function at scale j if we add the convolution at scale $j-1$ and the appropriate wavelet convolution at scale j. In our case the last two mentioned components are shown in one row that means the pictures of one row have to be added to obtain the convolution in the next row on the left-hand side. For example Figure 9.2a and Figure 9.2b are added to obtain Figure 9.2c.
Especially in Figure 9.2 and 9.5 we can see that the main difference of two convolutions happens near to the boundary (see Figures 9.2b, 9.2d and 9.2f for u_1 and Figures 9.5b, 9.5d and 9.5f for u_2). The convolutions with the source scaling function tensor for $j = 0$ (see Figure 9.2a for u_1 and Figure 9.5a for u_2) and $j = 1$ (see Figure 9.2c for u_1 and Figure 9.5c for u_2) have a scale with a positive and negative range. This changes with the parameter $j = 2$ (see Figure 9.2e for u_1 and Figure 9.5e for u_2) and we see a clear similarity between the scale of the data and of the convolution. Furthermore, there is a rough correspondence in the structure. Although, we have big variations on the boundary for the convolution with the source wavelet tensor for $j = 3$ (see Figure 9.2f for u_1 and Figure 9.5f for u_2), we can recognize the structure inside compared to the convolution with wavelets of a higher scale (see Figures 9.3 and 9.4).
In Figures 9.3, 9.4, 9.6 and 9.7 we can see that there is no obvious difference between the low-pass filtered versions (see Figures 9.3a, 9.3c, 9.4a and 9.4c for u_1 and Figures 9.6a, 9.6c, 9.7a and 9.7c for u_2) because the magnitude is 10^{-3}, whereas the magnitude of the band-pass filtered information is between 10^{-4} and

10^{-5} (see Figures 9.3b, 9.3d and 9.4b for u_1 and Figures 9.6b, 9.6d and 9.7b for u_2). The magnitude of the band-pass filtered information decreases with increasing parameter j. That means the detail information gets consecutively finer and that is what we expected from the convolution. In our case of smooth data a lower scale j would be sufficient to do a coarse approximation of the data.
Although we do not see differences between the convolutions with the source scaling functions of a higher scale, we consider later some kind of computational difference between the convolutions and the given data. That means we compute a root mean square error and show that there is improvement for increasing scale j.
We mentioned above that the shown pictures represent the sum of the convolution integrals in (8.164) respectively (8.165). Now we want to show the several components of the composited pictures, that means the convolutions of the several elements of the tensor with the appropriate data. We do this, as an example, for the parameters $j = 1$ and $j = 3$ in Figure 9.8 respectively Figure 9.9 for (8.164). We can see that the convolution with $\Phi_{11,\tau}$ for $j = 1$ (see Figure 9.8a) is a very rough approximation of the data and the convolutions with the other functions have major effects on the boundary (see Figures Figure 9.8b-9.8d). For $j = 3$ we can see more clearly that the convolution with $\Phi_{11,\tau}$ (see Figure 9.9a) tends to the data (here the magnitude is also better than in the case $j = 1$). The effect of the convolutions with the elements on the minor diagonal on the boundary decreased respectively vanishes (see Figures 9.9b-9.9d). Furthermore, the magnitude of the convolution with the minor diagonal elements gets smaller that means we have for $j = 1$ a range from 10^{-2} to 10^{-4} and in the case of $j = 3$ the range decreases from 10^{-4} to 10^{-6}. In both cases the convolution with $\Phi^2_{13,\tau}$ (see Figures 9.8d and 9.9d) has the most impact among the minor diagonal convolutions. All in all, the contributions of the elements of the minor diagonal to the whole convolution in (8.164) get smaller and in the limit the convolution with $\Phi_{11,\tau}$ tends to the data. Let us continue with the multiscale approximation of the data given for p.
Figures 9.10 and 9.11 show the sum of the convolutions of the source scaling functions and the wavelets represented in (8.166). In the multiscale approximation in Figure 9.10, we can see that we have again effects near the boundary for the wavelets (especially see Figures 9.10d and 9.10f) which get smaller with increasing j.
The magnitude of the convolution for $j = 0$ (see Figure 9.10a) is quite good and improves with increasing j. Here Figure 9.10b does not have boundary effects and contributes an important part for the improvement of the convolution. In the picture with the convolution with the source scaling function for $j = 2$ (see Figure 9.10e), we can already see a good approximation of the data but with effects on the boundary.
In Figure 9.11 we can see no difference between the convolutions with the source scaling functions (see Figures 9.11a, 9.11c and 9.11e), whereas we can see that something on the detail-space happens (see Figures 9.11b and 9.11d). Here the

magnitude of the convolutions in the left column is about 10^{-2} and the magnitude of the convolution with the wavelet falls from 10^{-4} to 10^{-5}. The calculation of the difference between the data and the convolutions later shows still an improvement at the higher scale.
In the case of the multiscale approximation of p, we only have the decorrelation up to scale $j = 5$, because for $j = 6$, we need $N = 200$ points and the computational effort is very big due to the fact that the functions are space and time dependent. For a consideration of some of the results with an uncut boundary, we refer to Remark 9.3.3. For a more computational difference (not only based on the pictures) between the different scales, we have a look at the so-called relative root mean square error (RMSE) given by

$$E_{\text{rms}}^{\text{rel}} h = \left(\frac{\sum_{x \in \Lambda_x \cap \mathcal{B}} \sum_{t \in \Lambda_t \cap [0,T]} |h(x,t) - h^{\text{num}}(x,t)|^2}{\sum_{x \in \Lambda_x \cap \mathcal{B}} \sum_{t \in \Lambda_t \cap [0,T]} |h(x,t)|^2} \right)^{\frac{1}{2}}. \tag{9.39}$$

Here x and t represent the points at which we calculated our convolutions, which are the same as the points of our data grid (see also Remark 9.3.2). The function h represents one of the components u_1, u_2 or p and $h(x,t)$ is the evaluation of h on our given data grid. By h^{num} we denote the results of the convolution given on the data grid. Here this error is not to be understood in the classical sense of an error but rather as a measure how large the difference between the convolutional data and given data is and how well the convolution approximates the data.

Remark 9.3.2. *Please note that we use the given data grid also for the calculation of the convolutions. Due to the construction of the cubature formulas, this is a fact that we have to accept here. Therefore, the RMSE can also only be computed on this fixed grid. For evaluating the convolutional results and the RMSE on a different grid as the data grid, we have to interpolate the data on the new desired grid and then calculate the convolutions on this new grid. Our intention here is to show that the approach with these scaling functions and wavelets basically works.*

First we have a look at Table 9.1 which shows the RMSE evaluated on the same sector as our given plots above for the spatial part. For the time dependent part, we did only cut off the end points $\{0, 5\}$ of our considered time interval, because in Theorem 8.4.4 we assumed $t \in (0, T)$ without the boundary.
We see that the RMSE decreases rapidly with increasing j. Also in the most cases of u_1 and u_2, the RMSE is slightly better if we choose more points (parameter N) in the spatial domain. For $j = 5$ it is conversely but in this case the source scaling function might not cover enough data points for $N = 100$ and the RMSE is not that convincing. For p the RMSE is only up to $j = 5$ reasonable to calculate, because the combination of $N = 100$ points with the parameter $j = 6$ only covers one point in the spatial domain and a few points in the time domain. This is not justifiable for a meaningful result.

Another thing to mention is that the RMSE is in the case of p smaller in general in the beginning in comparison to u_1 and u_2. Remember that we have only spatial-dependent functions in the case of u_1 and u_2 and in the case of p the functions are space and time dependent. In Table 9.2, the RMSE for the several convolutions

Parameter j	N	M	$E_{\text{rms}}^{\text{rel}}\, u_1$	$E_{\text{rms}}^{\text{rel}}\, u_2$	$E_{\text{rms}}^{\text{rel}}\, p$
0	100	200	0.8012	0.8012	0.1585
0	200	200	0.7900	0.7900	
1	100	200	0.4187	0.4187	0.0396
1	200	200	0.4018	0.4018	
2	100	200	0.0812	0.0812	0.0101
2	200	200	0.0787	0.0787	
3	100	200	0.0391	0.0391	0.0061
3	200	200	0.0387	0.0387	
4	100	200	0.0207	0.0207	0.0082
4	200	200	0.0200	0.0200	
5	100	200	0.0091	0.0091	0.0062
5	200	200	0.0105	0.0105	
6	100	200			0.0060
6	200	200	0.0046	0.0046	

Table 9.1.: RMSE for the plot area.

is shown for the whole domain $(-1,1)^2 \times (0,T)$ without the boundary points. In contrast to Table 9.1, we can see that the RMSE is greater in general from which we can conclude that there are effects on the boundary. All in all, the RMSE also decreases in the case of u_1 and u_2 for increasing j. The RMSE for p is also decreasing but has an outlier for $j = 2$ which we can explain with some high peaks in the convolution near to the boundary (they cannot be seen in the convolution pictures because of the outcut boundary) because the RMSE in the case of the cut boundary is small. For a reflection in greater detail for the case $j = 2$, we refer to Remark 9.3.4. Again the value for $j = 6$ is not very convincing because of the small coverage of integration points.

Remark 9.3.3. *In our pictures we cut off some part of the boundary due to boundary effects that influence the general structure of the picture. Here we want to show what the pictures look like without the clipped off boundary. We do this, as an example, for the first line of the convolution integral (see* (8.164)*) in Figures 9.12 and 9.13.*
There are some things to mention. We can see that the boundary effects for the convolution with the source scaling functions on the minor diagonal get smaller due to the magnitude and the area they influence (see Figures 9.12b-9.12d compared to Figures 9.13b-9.13d).

Parameter j	N	M	$E^{\text{rel}}_{\text{rms}}\ u_1$	$E^{\text{rel}}_{\text{rms}}\ u_2$	$E^{\text{rel}}_{\text{rms}}\ p$
0	100	200	0.9402	0.9402	0.1895
0	200	200	0.9357	0.9357	
1	100	200	0.7605	0.7605	0.0693
1	200	200	0.7562	0.7562	
2	100	200	0.5541	0.5541	1.3359
2	200	200	0.5744	0.5744	
3	100	200	0.3862	0.3862	0.0540
3	200	200	0.4055	0.4055	
4	100	200	0.2548	0.2548	0.0107
4	200	200	0.2777	0.2777	
5	100	200	0.0708	0.0708	0.0072
5	200	200	0.1815	0.1815	
6	100	200			0.0066
6	200	200	0.0501	0.0501	

Table 9.2.: RMSE for the whole area without the boundary.

Here the convolution with $\Phi^2_{13,\tau}$ decreases very slowly such that it has a big influence on the overall image on the boundary (see Figures 9.12d and 9.13d). We can see in both cases that the boundary influences the overall image so much that we cannot detect the main structure of the data in both cases (see Figures 9.12e and 9.13e) in contrast to the picture where we cut off the boundary (see Figures 9.2c and 9.3a). So it is necessary to find a suitable parameter for the boundary cut off.

Remark 9.3.4. *We have a look at the multiscale approximation of p at scale $j = 2$ with the whole boundary, because in Table 9.2 there is an outlier for the RMSE in this case. Figure 9.14a shows the approximation, where we can see that there are some high peaks near the edges which influence the RMSE so much that it seems that the approximation is not that good. Therefore we have a look at Figure 9.14b, where we can see the absolute difference of the approximation minus the given data. Furthermore, we restricted the colorbar axis to the interval $[0, 0.02]$. Here we can see that the problem of the big RMSE is a boundary problem. The approximation of the remaining part without a boundary is quite good. For the further detection of the reasons for these boundary effects, more data sets have to be tested and more numerical experiments need to be done.*

Remark 9.3.5. *In our case we have fairly smooth synthetic data in contrast to the Laplace case in [21] with the data model. That means in our case we cannot see the decorrelation so good and the detail spaces because of our smooth data.*

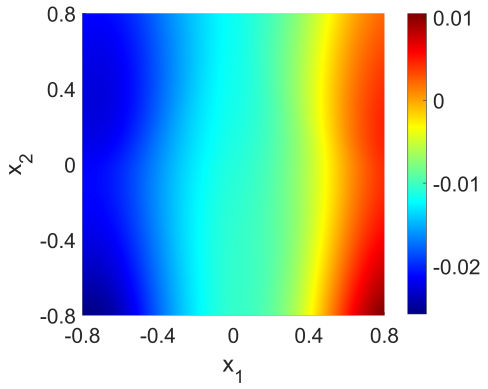

(a) Application of the low-pass filter $\left(\mathcal{P}_{\Phi_{\tau_j}}[f]\right)_1$ at scale $j = 0$.

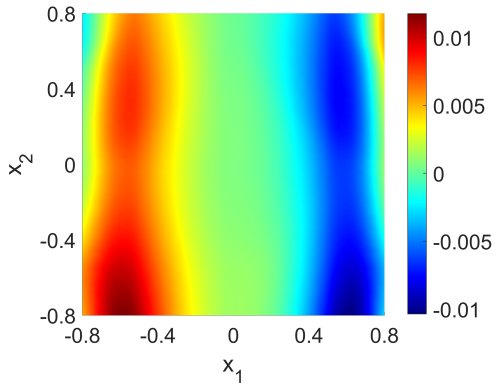

(b) Application of the band-pass filter $\left(\mathcal{R}_{\Phi_{\tau_j}}[f]\right)_1$ at scale $j = 1$.

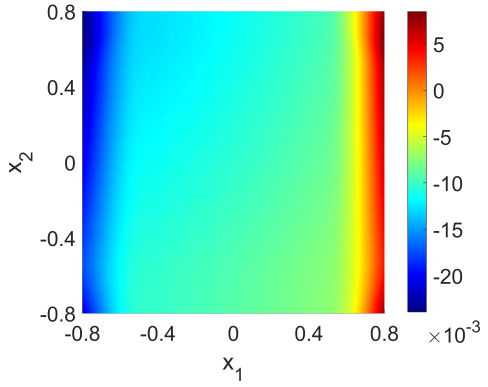

(c) Application of the low-pass filter $\left(\mathcal{P}_{\Phi_{\tau_j}}[f]\right)_1$ at scale $j = 1$.

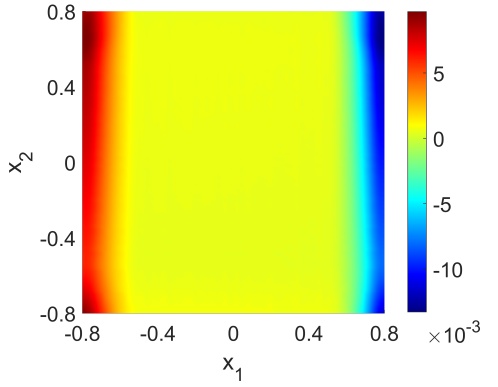

(d) Application of the band-pass filter $\left(\mathcal{R}_{\Phi_{\tau_j}}[f]\right)_1$ at scale $j = 2$.

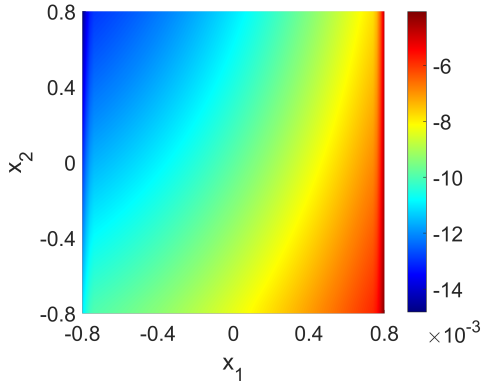

(e) Application of the low-pass filter $\left(\mathcal{P}_{\Phi_{\tau_j}}[f]\right)_1$ at scale $j = 2$.

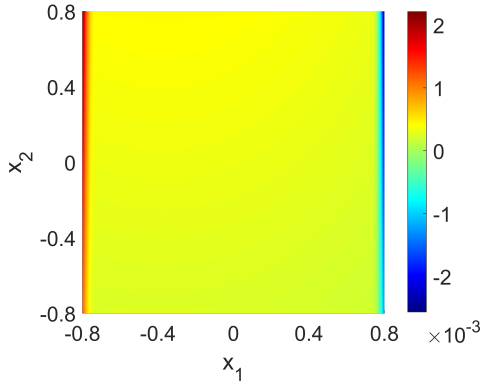

(f) Application of the band-pass filter $\left(\mathcal{R}_{\Phi_{\tau_j}}[f]\right)_1$ at scale $j = 3$.

Figure 9.2.: Multiscale approximation of the data u_1 by convolution of the source scaling function (tensor) $\left\{\Phi_{\tau_j}\right\}_{j\in\mathbb{N}}$ (scale-space) and the source wavelet (tensor) $\left\{\Psi_{\tau_j}\right\}_{j\in\mathbb{N}}$ (detail-space) with the data f.

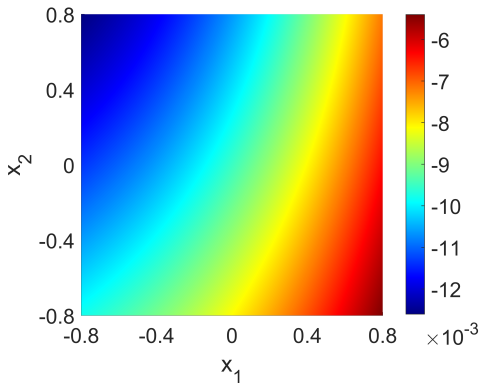

(a) Application of the low-pass filter $\left(\mathcal{P}_{\Phi_{\tau_j}}[f]\right)_1$ at scale $j = 3$.

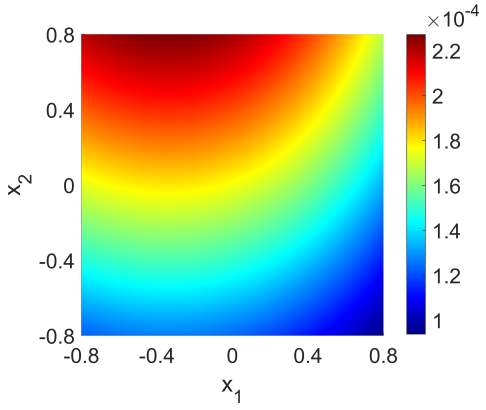

(b) Application of the band-pass filter $\left(\mathcal{R}_{\Phi_{\tau_j}}[f]\right)_1$ at scale $j = 4$.

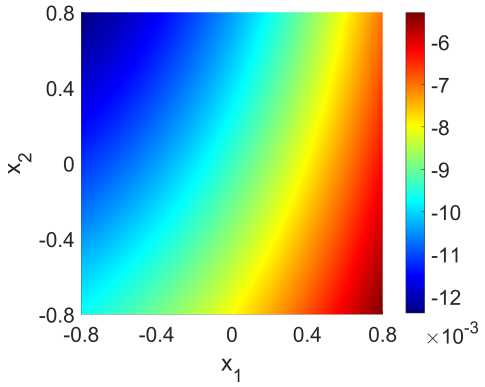

(c) Application of the low-pass filter $\left(\mathcal{P}_{\Phi_{\tau_j}}[f]\right)_1$ at scale $j = 4$.

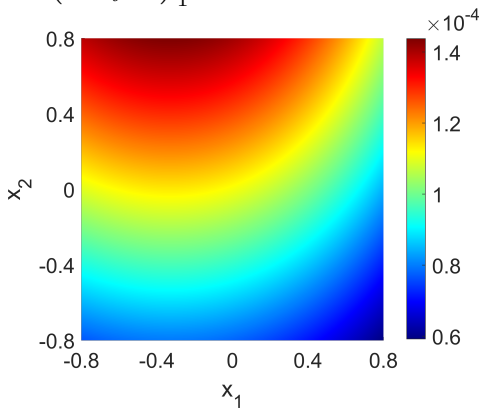

(d) Application of the band-pass filter $\left(\mathcal{R}_{\Phi_{\tau_j}}[f]\right)_1$ at scale $j = 5$.

Figure 9.3.: Multiscale approximation of the data u_1 by convolution of the source scaling function (tensor) $\left\{\Phi_{\tau_j}\right\}_{j\in\mathbb{N}}$ (scale-space) and the source wavelet (tensor) $\left\{\Psi_{\tau_j}\right\}_{j\in\mathbb{N}}$ (detail-space) with the data f.

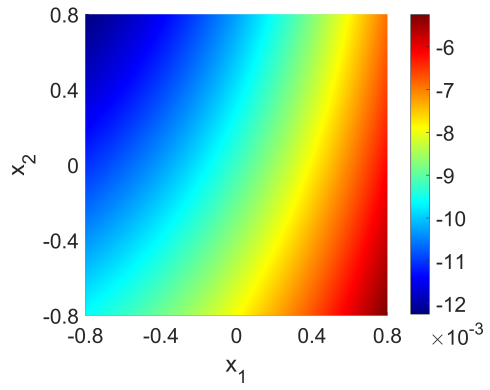

(a) Application of the low-pass filter $\left(\mathcal{P}_{\Phi_{\tau_j}}[f]\right)_1$ at scale $j = 5$.

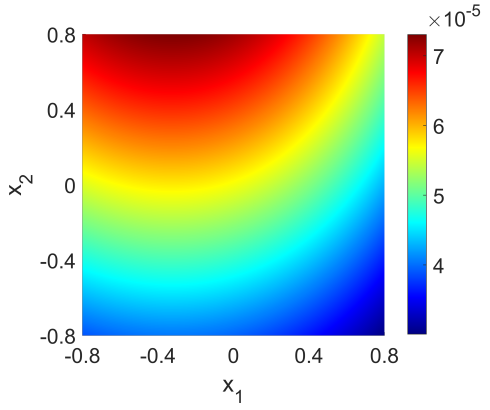

(b) Application of the band-pass filter $\left(\mathcal{R}_{\Phi_{\tau_j}}[f]\right)_1$ at scale $j = 6$.

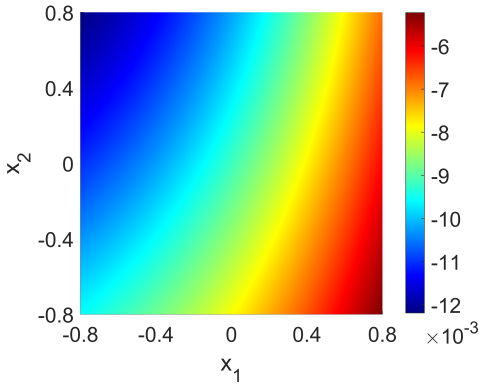

(c) Application of the low-pass filter $\left(\mathcal{P}_{\Phi_{\tau_j}}[f]\right)_1$ at scale $j = 6$.

Figure 9.4.: Multiscale approximation of the data u_1 by convolution of the source scaling function (tensor) $\left\{\Phi_{\tau_j}\right\}_{j\in\mathbb{N}}$ (scale-space) and the source wavelet (tensor) $\left\{\Psi_{\tau_j}\right\}_{j\in\mathbb{N}}$ (detail-space) with the data f.

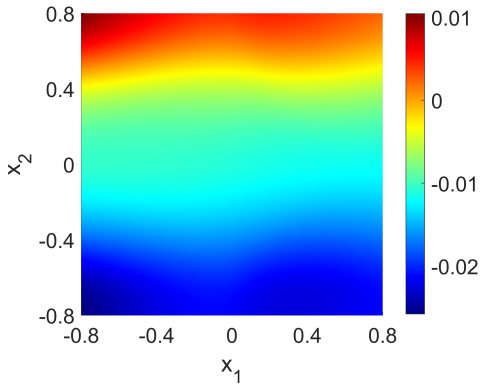

(a) Application of the low-pass filter $\left(\mathcal{P}_{\Phi_{\tau_j}}[f]\right)_2$ at scale $j = 0$.

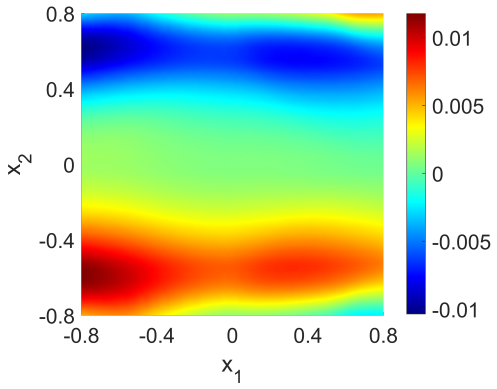

(b) Application of the band-pass filter $\left(\mathcal{R}_{\Phi_{\tau_j}}[f]\right)_2$ at scale $j = 1$.

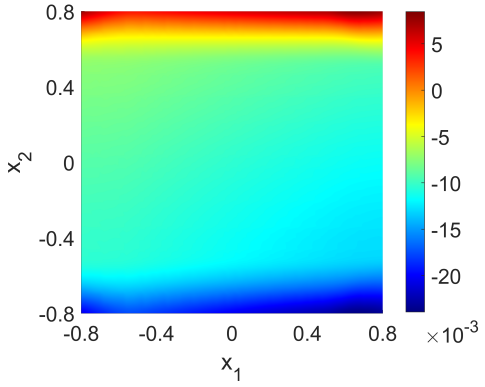

(c) Application of the low-pass filter $\left(\mathcal{P}_{\Phi_{\tau_j}}[f]\right)_2$ at scale $j = 1$.

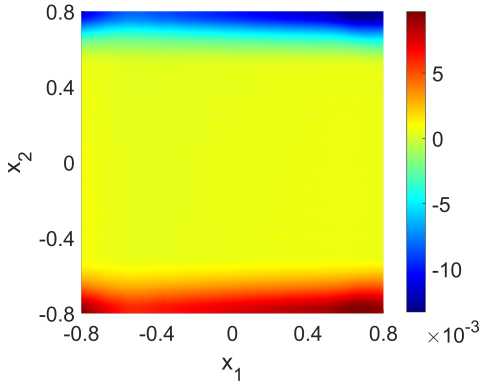

(d) Application of the band-pass filter $\left(\mathcal{R}_{\Phi_{\tau_j}}[f]\right)_2$ at scale $j = 2$.

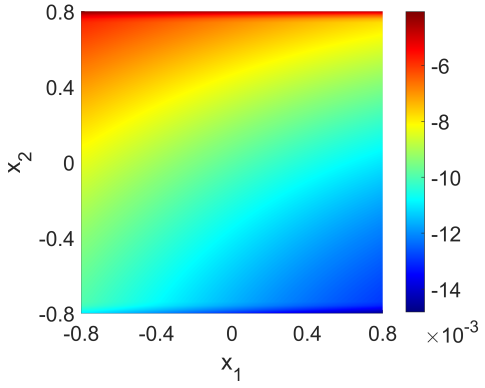

(e) Application of the low-pass filter $\left(\mathcal{P}_{\Phi_{\tau_j}}[f]\right)_2$ at scale $j = 2$.

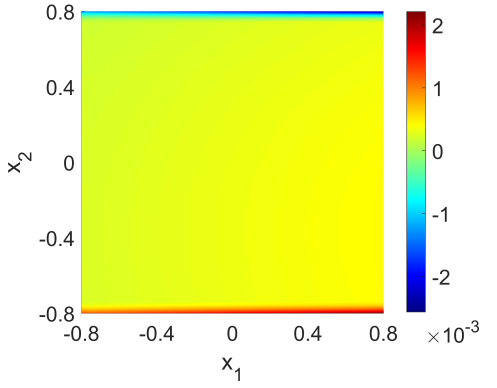

(f) Application of the band-pass filter $\left(\mathcal{R}_{\Phi_{\tau_j}}[f]\right)_2$ at scale $j = 3$.

Figure 9.5.: Multiscale approximation of the data u_2 by convolution of the source scaling function (tensor) $\left\{\Phi_{\tau_j}\right\}_{j\in\mathbb{N}}$ (scale-space) and the source wavelet (tensor) $\left\{\Psi_{\tau_j}\right\}_{j\in\mathbb{N}}$ (detail-space) with the data f.

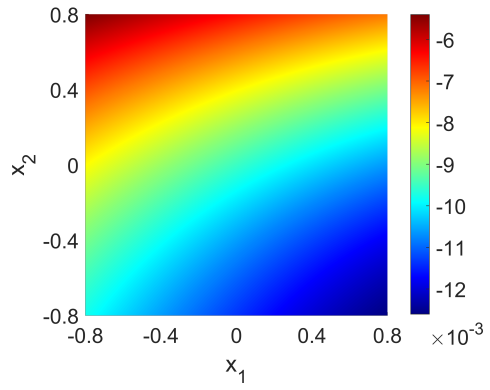

(a) Application of the low-pass filter $\left(\mathcal{P}_{\Phi_{\tau_j}}[f]\right)_2$ at scale $j = 3$.

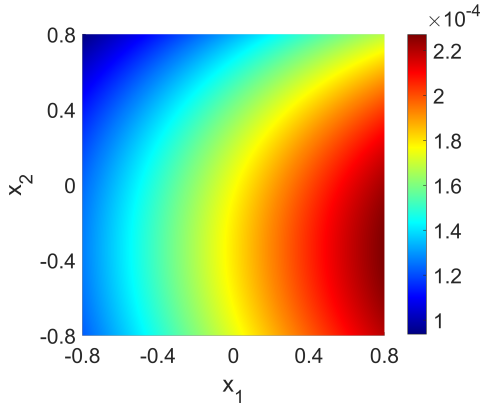

(b) Application of the band-pass filter $\left(\mathcal{R}_{\Phi_{\tau_j}}[f]\right)_2$ at scale $j = 4$.

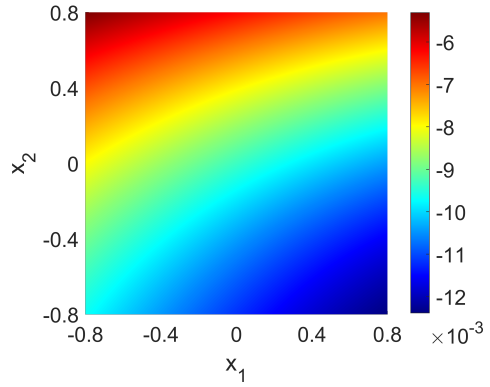

(c) Application of the low-pass filter $\left(\mathcal{P}_{\Phi_{\tau_j}}[f]\right)_2$ at scale $j = 4$.

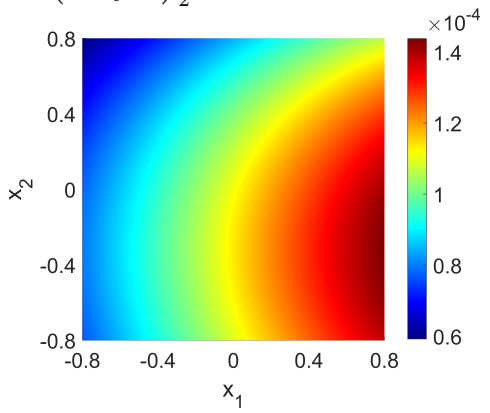

(d) Application of the band-pass filter $\left(\mathcal{R}_{\Phi_{\tau_j}}[f]\right)_2$ at scale $j = 5$.

Figure 9.6.: Multiscale approximation of the data u_2 by convolution of the source scaling function (tensor) $\left\{\Phi_{\tau_j}\right\}_{j\in\mathbb{N}}$ (scale-space) and the source wavelet (tensor) $\left\{\Psi_{\tau_j}\right\}_{j\in\mathbb{N}}$ (detail-space) with the data f.

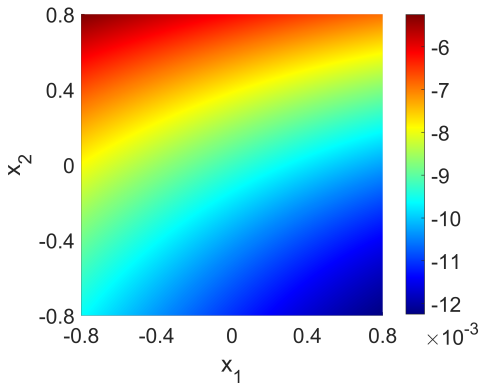

(a) Application of the low-pass filter $\left(\mathcal{P}_{\Phi_{\tau_j}}[f]\right)_2$ at scale $j = 5$.

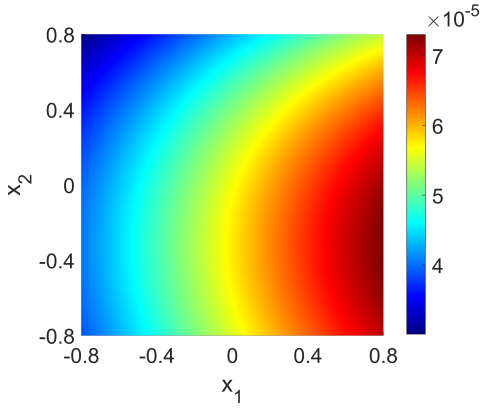

(b) Application of the band-pass filter $\left(\mathcal{R}_{\Phi_{\tau_j}}[f]\right)_2$ at scale $j = 6$.

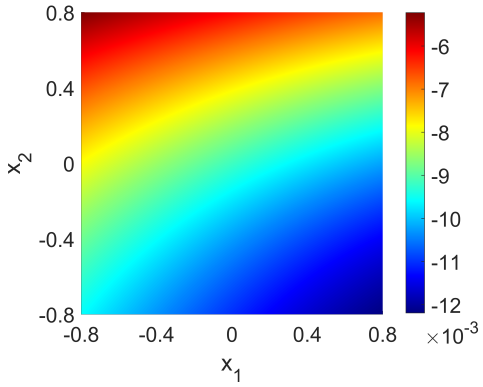

(c) Application of the low-pass filter $\left(\mathcal{P}_{\Phi_{\tau_j}}[f]\right)_2$ at scale $j = 6$.

Figure 9.7.: Multiscale approximation of the data u_2 by convolution of the source scaling function (tensor) $\left\{\Phi_{\tau_j}\right\}_{j\in\mathbb{N}}$ (scale-space) and the source wavelet (tensor) $\left\{\Psi_{\tau_j}\right\}_{j\in\mathbb{N}}$ (detail-space) with the data f.

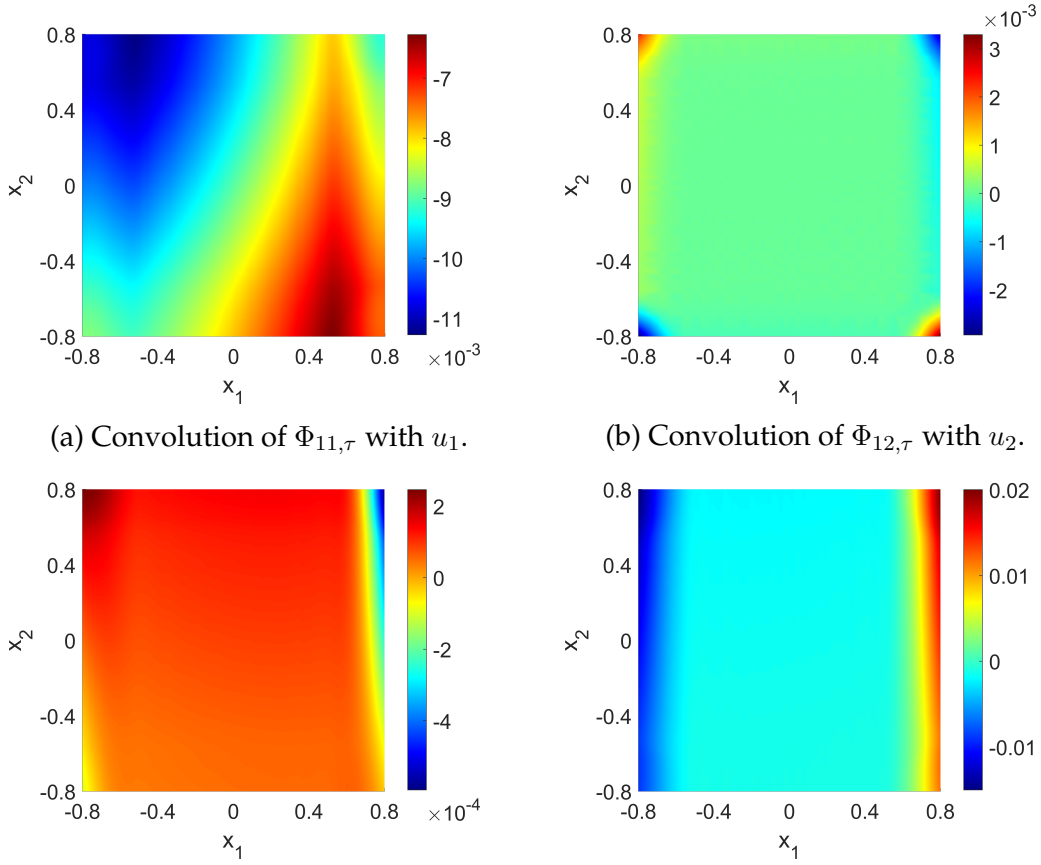

(a) Convolution of $\Phi_{11,\tau}$ with u_1.

(b) Convolution of $\Phi_{12,\tau}$ with u_2.

(c) Convolution of $\Phi^1_{13,\tau}$ with $\partial_t p$.

(d) Convolution of $\Phi^2_{13,\tau}$ with p.

Figure 9.8.: Single parts of the application of the low-pass filter $\left(\mathcal{P}_{\Phi_{\tau_j}}[f]\right)_1$ at scale $j = 1$.

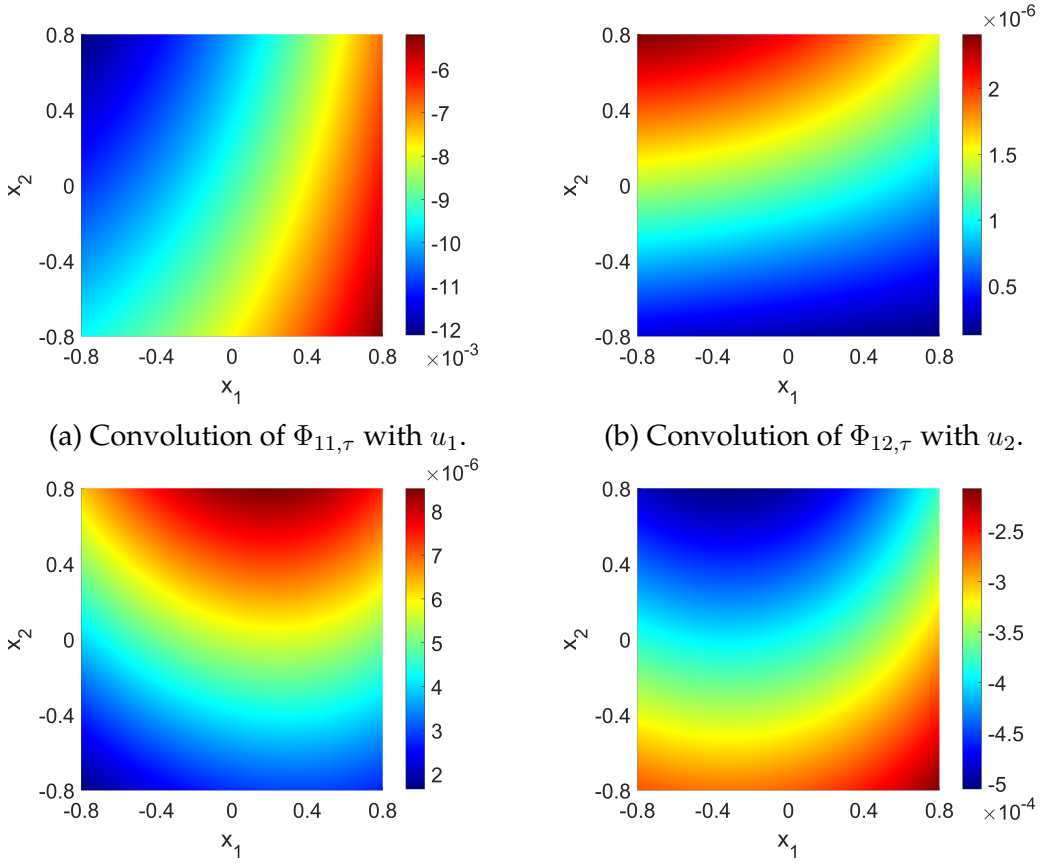

(a) Convolution of $\Phi_{11,\tau}$ with u_1.

(b) Convolution of $\Phi_{12,\tau}$ with u_2.

(c) Convolution of $\Phi^1_{13,\tau}$ with $\partial_t p$.

(d) Convolution of $\Phi^2_{13,\tau}$ with p.

Figure 9.9.: Single parts of the application of the low-pass filter $\left(\mathcal{P}_{\Phi_{\tau_j}}[f]\right)_1$ at scale $j = 3$.

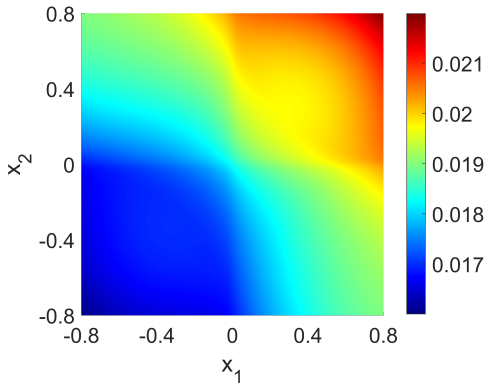

(a) Application of the low-pass filter $\left(\mathcal{P}_{\Phi_{\tau_j}}[f]\right)_3$ at scale $j = 0$.

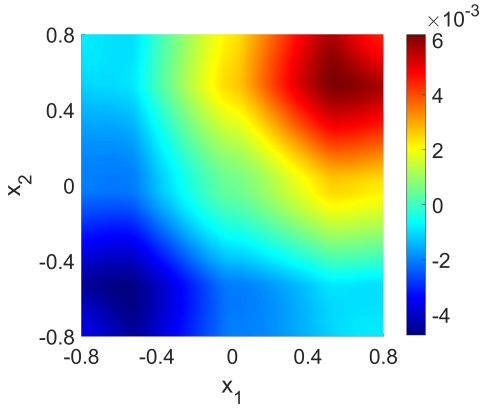

(b) Application of the band-pass filter $\left(\mathcal{R}_{\Phi_{\tau_j}}[f]\right)_3$ at scale $j = 1$.

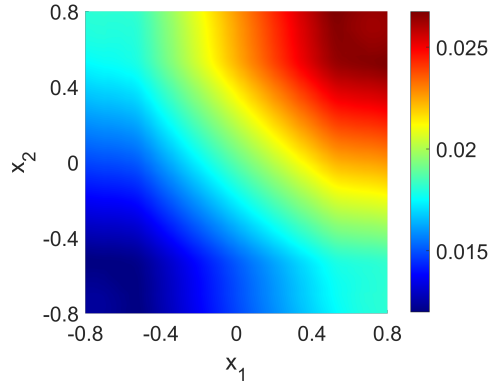

(c) Application of the low-pass filter $\left(\mathcal{P}_{\Phi_{\tau_j}}[f]\right)_3$ at scale $j = 1$.

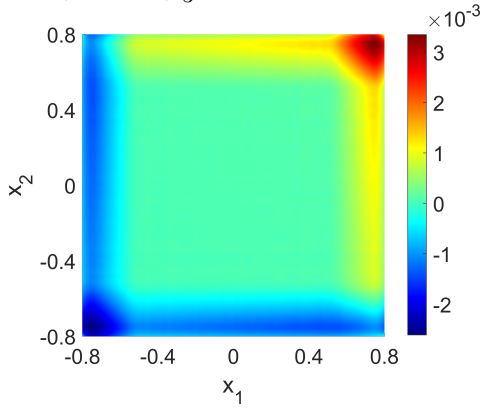

(d) Application of the band-pass filter $\left(\mathcal{R}_{\Phi_{\tau_j}}[f]\right)_3$ at scale $j = 2$.

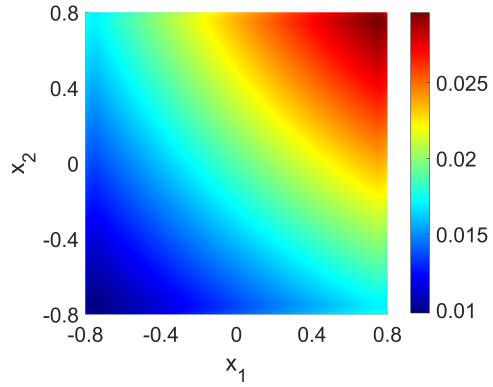

(e) Application of the low-pass filter $\left(\mathcal{P}_{\Phi_{\tau_j}}[f]\right)_3$ at scale $j = 2$.

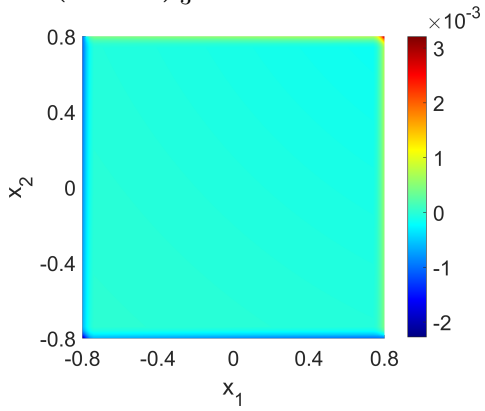

(f) Application of the band-pass filter $\left(\mathcal{R}_{\Phi_{\tau_j}}[f]\right)_3$ at scale $j = 3$.

Figure 9.10.: Multiscale approximation of the data p by convolution of the source scaling function (tensor) $\left\{\Phi_{\tau_j}\right\}_{j\in\mathbb{N}}$ (scale-space) and the source wavelet (tensor) $\left\{\Psi_{\tau_j}\right\}_{j\in\mathbb{N}}$ (detail-space) with the data f.

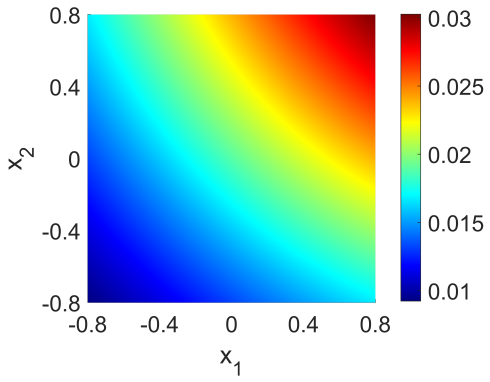

(a) Application of the low-pass filter $\left(\mathcal{P}_{\Phi_{\tau_j}}[f]\right)_3$ at scale $j = 3$.

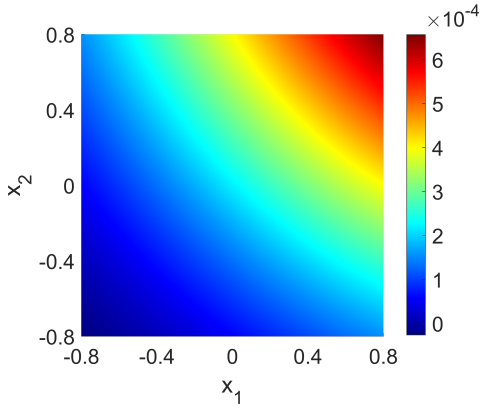

(b) Application of the band-pass filter $\left(\mathcal{R}_{\Phi_{\tau_j}}[f]\right)_3$ at scale $j = 4$.

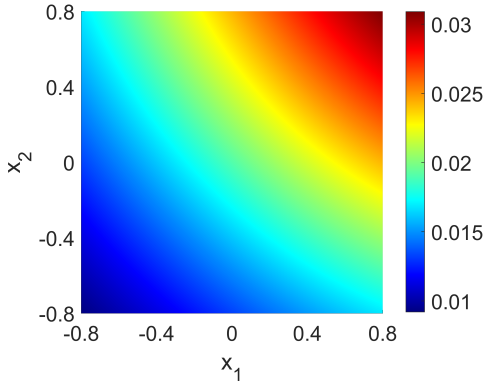

(c) Application of the low-pass filter $\left(\mathcal{P}_{\Phi_{\tau_j}}[f]\right)_3$ at scale $j = 4$.

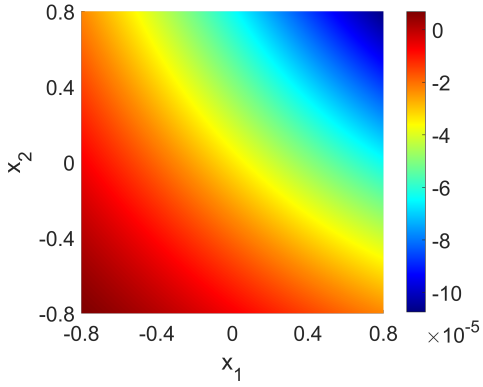

(d) Application of the band-pass filter $\left(\mathcal{R}_{\Phi_{\tau_j}}[f]\right)_3$ at scale $j = 5$.

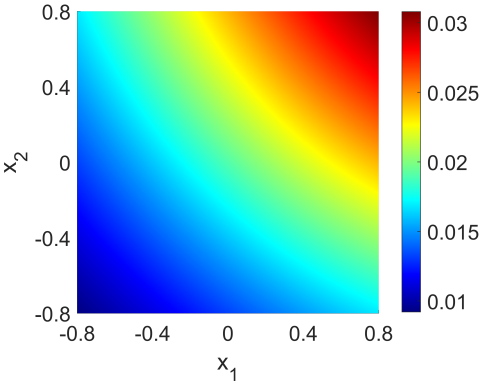

(e) Application of the low-pass filter $\left(\mathcal{P}_{\Phi_{\tau_j}}[f]\right)_3$ at scale $j = 5$.

Figure 9.11.: Multiscale approximation of the data p by convolution of the source scaling function (tensor) $\left\{\Phi_{\tau_j}\right\}_{j\in\mathbb{N}}$ (scale-space) and the source wavelet (tensor) $\left\{\Psi_{\tau_j}\right\}_{j\in\mathbb{N}}$ (detail-space) with the data f.

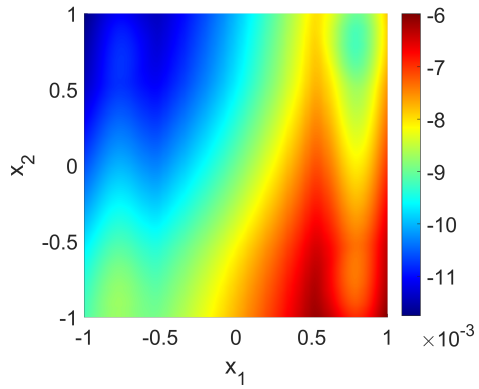

(a) Convolution of $\Phi_{11,\tau}$ with u_1.

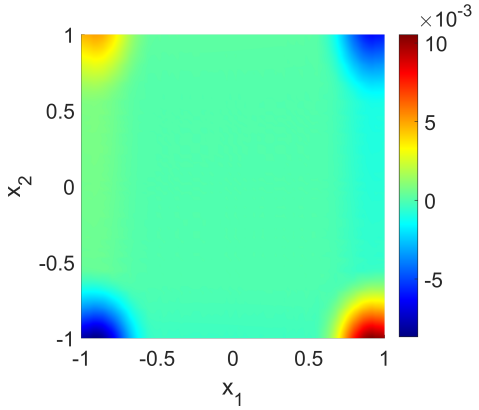

(b) Convolution of $\Phi_{12,\tau}$ with u_2.

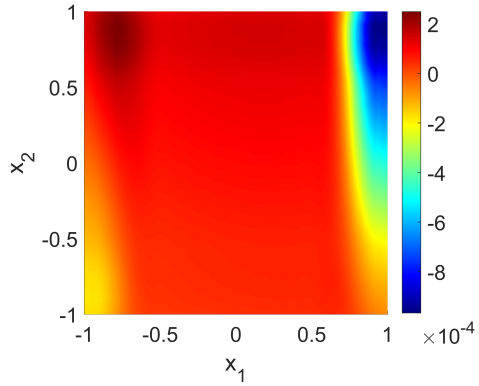

(c) Convolution of $\Phi^1_{13,\tau}$ with $\partial_t p$.

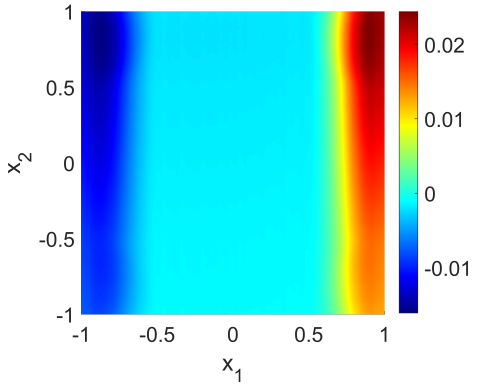

(d) Convolution of $\Phi^2_{13,\tau}$ with p.

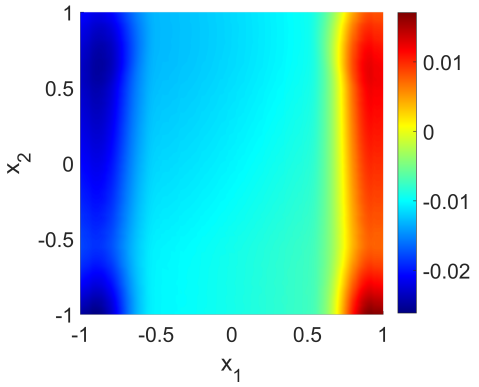

(e) Application of the low-pass filter $\left(\mathcal{P}_{\Phi_{\tau_j}}[f]\right)_1$ at scale $j = 1$.

Figure 9.12.: Single parts of the application of the low-pass filter $\left(\mathcal{P}_{\Phi_{\tau_j}}[f]\right)_1$ at scale $j = 1$ without cutting off the boundary.

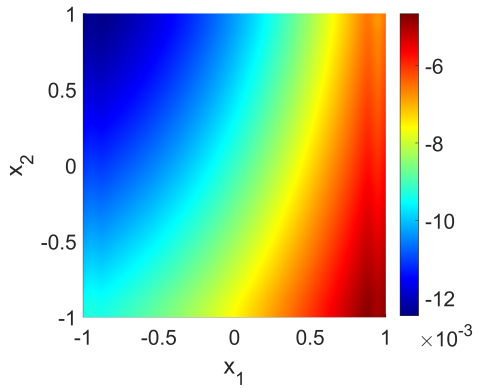

(a) Convolution of $\Phi_{11,\tau}$ with u_1.

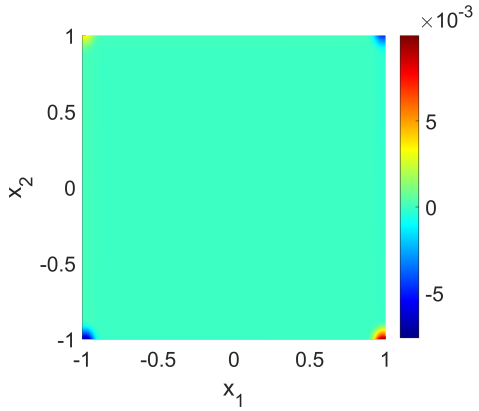

(b) Convolution of $\Phi_{12,\tau}$ with u_2.

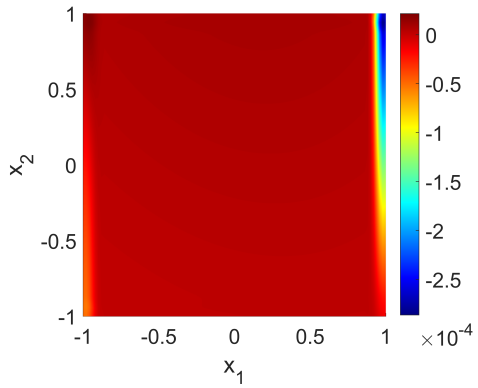

(c) Convolution of $\Phi^1_{13,\tau}$ with $\partial_t p$.

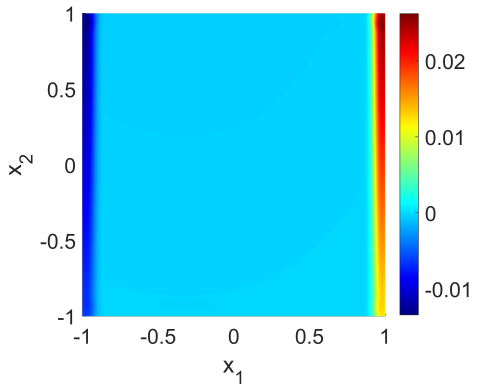

(d) Convolution of $\Phi^2_{13,\tau}$ with p.

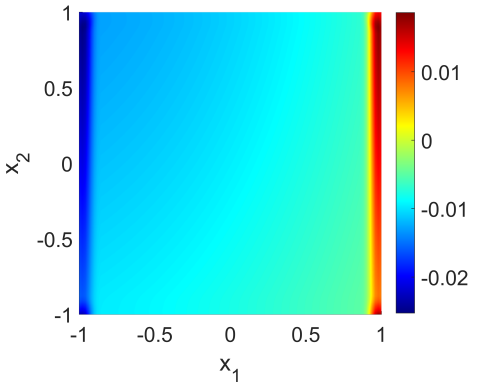

(e) Application of the low-pass filter $\left(\mathcal{P}_{\Phi_{\tau_j}}[f]\right)_1$ at scale $j = 3$.

Figure 9.13.: Single parts of the application of the low-pass filter $\left(\mathcal{P}_{\Phi_{\tau_j}}[f]\right)_1$ at scale $j = 3$ without cutting off the boundary.

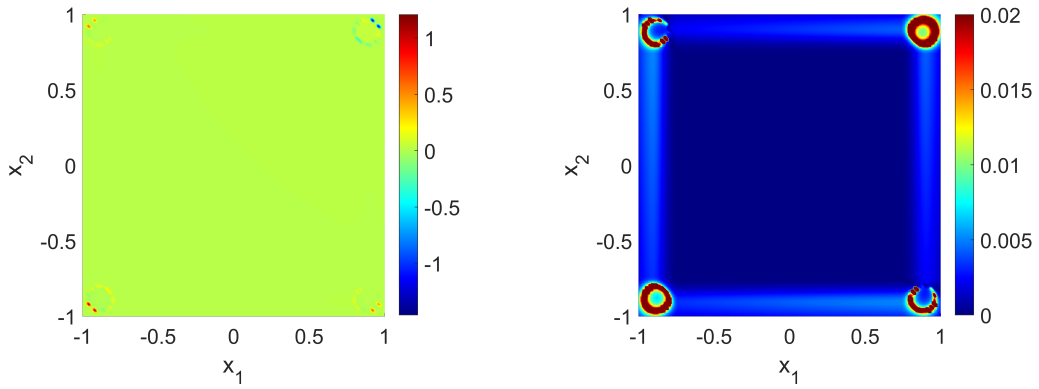

(a) Application of the low-pass filter $\left(\mathcal{P}_{\Phi_{\tau_j}}[f]\right)_3$ at scale $j = 2$ with the whole boundary.

(b) Absolute difference of the application of the band-pass filter $\left(\mathcal{R}_{\Phi_{\tau_j}}[f]\right)_3$ at scale $j = 2$ to the given data.

Figure 9.14.: Multiscale approximation of the data p by convolution of the source scaling function (tensor) $\left\{\Phi_{\tau_j}\right\}_{j\in\mathbb{N}}$ (scale-space) and the source wavelet (tensor) $\left\{\Psi_{\tau_j}\right\}_{j\in\mathbb{N}}$ (detail-space) with the data f.

Part IV.

Summary

10. Conclusion and Outlook

Our main aim in this thesis was to develop a multiscale mollifier technique in poroelasticity that means the construction of physically motivated scaling functions and wavelets for the decomposition of given poroelastic data. The approach extracts and visualizes underlying structures that cannot be seen in the whole data. We started in a more general setting, the thermoporoelasticity, that means poroelastic effects including thermal influences. There are three main model types: the complete, the coupled and the uncoupled model, where we focused on the coupled model and showed how to get the uncoupled model from this. In a first step, we derived the main equations (partial differential equations with time and spatial dependency) in thermoporoelasticity with their related physical laws. Afterwards, the fundamental solutions were derived with the help of a scheme, called the Biot decomposition. The fundamental solutions themselves can be arranged in a tensor. The nondimensionalization of the equations completed the aspect of this physical model.
We went over to a simplification of the model by ignoring the thermal effects in the following, that means we concentrated on poroelasticity. Here we were interested in the fundamental solutions because they build the basis for the construction of the scaling functions and wavelets with the mollifier technique. For that reason, we constructed a mollification of the fundamental solutions by applying a Taylor expansion up to the first order regarding a parameter τ. With this step, we avoid the singularities of the fundamental solutions. It was sufficient to do this regarding the spatial variable (also for the space and time dependent functions). The last step in construction was to apply the poroelastic differential operator (obtained by the equations of poroelasticity) on these mollifier functions. The so-called source scaling functions are the result of this last step. They are used for the decomposition in the sense that we convolve them with the given poroelastic data for different parameters τ. We considered a monotonically decreasing sequence for our parameter τ and the differences of two consecutive source scaling functions are the source wavelet functions.
The next step was to check the theoretical requirements and necessary properties that the source scaling functions have to satisfy. These considerations showed that we have to do little modifications on some of our source scaling functions, which did not change the character of the functions. This allowed us to state and prove the property of an approximate identity, which is our main result in theory. This theorem builds the fundament for our numerical experiments.
Before we could go over to the numerical implementation of the convolutions, we had to think about a suitable cubature formula. Here we used the Poisson

summation formula in Gauß-Weierstraß summability as a starting point. Due to the compact support of the source scaling functions and the fact that this support shrinks with decreasing τ, it was necessary to define modified weights depending on the source scaling functions to control the case that the support of the source scaling function covers only a few integration points. These cubature formulae guarantee the convergence of the convolutional data to the given data. With these ingredients, we performed the convolutions with synthetic data and showed the appropriate convolution pictures. For a rough approximation of the data, a lower scale would be sufficient. But there is still improvement for higher scales, which can be seen more clearly in the convolutions with the wavelets. Some of the convolutions were considered additionally in view of the effects that occur on the boundary. In a last step, we computed a relative root mean square error to show how big the difference between the multiscale approximation of the data compared to the given data is. All in all, the results showed that our source scaling functions and wavelets provide a good decomposition of the given data.
There are some things which may be considered in future research work. One point is to test the decomposition ability with more data sets. In general it would be interesting to see how the boundary effects behave in these cases and especially in the case, where we had some high peaks near the boundary (see Remark 9.3.4). In this context, we have to mention again that our synthetic data are very smooth due to the way we constructed them via the fundamental solutions. Data that are not that smooth would show the decomposition ability of our source scaling functions maybe much better. It would be more interesting for the decorrelation technique of the source scaling functions in general, if we had access to data from another source, maybe more realistic data or data models would be great. Laboratory experiments and measurement data may be the next step to more realistic data. More concrete, measurement data of experiments that are designed to determine the poroelastic material constants are meant in this case. This would also be more challenging due to noisy data because of measuring errors. In the case of realistic and probably not so smooth data, a higher scale for convolutions may be necessary, which includes the use of more data points. In this case, the performance of the algorithm has to be further improved, maybe also transferred in another coding language. The last point to mention is the integration method, which is in its fundamental structure like a trapezoidal rule. Maybe there is a possibility to use another cubature formula or improve the existing one such that less integration points are needed. One more drawback with the cubature formula is the fact that we have to calculate the result of the convolutions on the given data grid due to the construction. One possibility would be to check if another integration method can avoid this problem that we can calculate the convolutions on a different grid. This would also be better for the calculation of the RMSE.
One can also think of long term goals: We started with thermoporoelasticity and reduced to poroelasticity due to the complexity of the fundamental solutions. The inclusion of thermal effects in the process of decorrelation would be interesting to

investigate the injection of cold water for example in the reservoir. A more realistic setting would also be the consideration for example of heterogeneous media, fractured media, prediction and prevention of seismic events. For this future research it is necessary to check if for more complicated cases, it is still possible to do a mollifier regularization and obtain the required theoretical properties.

Bibliography

[1] M. Abramowitz and I.A. Stegun. *Handbook of Mathematical Functions With Formulas, Graphs, and Mathematical Tables.* Dover Publ., Inc., New York, 1972.

[2] K. Aki and P. Richards. *Quantitative Seismology.* 2nd edition. University Science Books, Mill Valley, 2002.

[3] M. Aliyu. *Thermoelastic analysis of enhanced geothermal systems using a fully coupled thermo-hydro-mechanical model.* In: ed. by E. Oñate, M. Papadrakakis, and B. Schrefler. IX International Conference on Computational Methods for Coupled Problems in Science and Engineering COUPLED PROBLEMS, Online, 2021, doi: 10.23967/coupled.2021.057.

[4] T.L. Anderson. *Fracture Mechanics Fundamentals and Applications*. 3rd edition. Taylot & Francis, Boca Raton, 2005.

[5] J.P. Antoine, L. Demanet, L. Jacques, and P. Vandergheynst. *Wavelets on the sphere: implementations and approximations. Appl. Comput. Harm. Anal.* **13** (2002), 177–200.

[6] J.P. Antoine and P. Vandergheynst. *Wavelets on the 2-sphere: A group-theoretic approach. Appl. Comput. Harm. Anal.* **7** (1999), 1–30.

[7] S. Arnórsson, A. Stefánsson, and J. Bjarnason. *Fluid-fluid interactions in geothermal systems. Rev. Mineral Geochem.* **65** (2007), 259–312.

[8] B.K. Atkinson. *Fracture Mechanics of Rock.* Academic Press Inc., San Diego, 1987.

[9] M. Augustin. *On the role of poroelasticity for modeling of stress fields in geothermal reservoirs. Int. J. Geomath.* **3** (2012), 67–93.

[10] M. Augustin. *A Method of Fundamental Solutions in Poroelasticity to Model the Stress Field in Geothermal Reservoirs.* PhD thesis. Geomathematics Group, Department of Mathematics, University of Kaiserslautern, 2015, Birkhäuser, New York, 2015.

[11] M. Augustin, M. Bauer, C. Blick, S. Eberle, W. Freeden, C. Gerhards, M. Ilyasov, R. Kahnt, M. Klug, S. Möhringer, T. Neu, H. Nutz, I. Ostermann, and A. Punzi. *Modeling deep geothermal reservoirs: recent advances and future perspectives.* In: *Handbook of Geomathematics*. Ed. by W. Freeden, M.Z. Nashed, and T. Sonar. 2nd edition. Springer Berlin Heidelberg, 2014, 1547–1629.

[12] D. Bächler and T. Kohl. *Coupled thermal–hydraulic–chemical modelling of enhanced geothermal systems. Geophys. J. Int.* **161** (2005), 533–548.

[13] M. Bai and A. Bouhroum. *Equivalent thermoelastic coupling in fractured geothermal reservoirs. Erdöl und Kohle, Erdgas, Petrochemie* **48** (1995), 72–78.

[14] E.A. Bergkamp, C.V. Verhoosel, J.J.C. Remmers, and D.M.J. Smeulders. *A dimensionally-reduced fracture flow model for poroelastic media with fluid entry resistance and fluid slip. J. Comput. Phys.* **455** (2022), article 110972.

[15] M.A. Biot. *Le problème de la consolidation des matières argileuses sous une charge. Ann. Soc. Sci. Brux.* **B55** (1935), 110–113.

[16] M.A. Biot. *General theory of three-dimensional consolidation. J Appl. Phys.* **12** (1941), 151–164.

[17] M.A. Biot. *Theory of elasticity and consolidation for a porous anisotropic solid. J Appl. Phys.* **26** (1955), 182–185.

[18] M.A. Biot. *General solutions of the equations of elasticity and consolidation for a porous material. J Appl. Mech.* **78** (1956), 91–96.

[19] M.A. Biot. *Thermoelasticity and irreversible thermodynamics. J Appl. Phys.* **27** (1956), 240–253.

[20] M.A. Biot. *Mechanics of deformation and acoustic propagation in porous media. J Appl. Phys.* **33** (1962), 1482–1498.

[21] C. Blick. *Multiscale Potential Methods in Geothermal Research: Decorrelation Reflected Post-Processing and Locally Based Inversion.* PhD thesis. Geomathematics Group, Department of Mathematics, University of Kaiserslautern, 2015, Verlag Dr. Hut Munich, 2015.

[22] C. Blick and S. Eberle. *Multiscale density decorrelation by Cauchy–Navier wavelets. Int. J. Geomath.* **10** (2019), article 24.

[23] C. Blick and S. Eberle. *A survey on multiscale mollifier decorrelation of seismic data*. *Int. J. Geomath.* **12** (2021), article 16.

[24] C. Blick, W. Freeden, M. Nashed, H. Nutz, and M. Schreiner. *Inverse Magnetometry: Mollifier Magnetization Distribution from Geomagnetic Field Data*. Lecture Notes in Geosystems Mathematics and Computing. Springer, Cham, 2021.

[25] C. Blick, W. Freeden, and H. Nutz. *Feature extraction of geological signatures by multiscale gravimetry. Int. J. Geomath.* **8** (2017), 57–83.

[26] C. Blick, W. Freeden, and H. Nutz. *Gravimetry and exploration.* In: *Handbook of Mathematical Geodesy, Geosystems Mathematics*. Ed. by W. Freeden and M.Z. Nashed. Birkhäuser, Cham, 2018, 687–751.

[27] C. Blick, W. Freeden, and H. Nutz. *Innovative Explorationsmethoden in der Gravimetrie und Reflexionsseismik.* In: *Handbuch Oberflächennahe Geothermie*. Ed. by M. Bauer, W. Freeden, H. Jacobi, and T. Neu. Springer Spektrum, Berlin, 2018, 221–256.

[28] G. Blöcher, G. Zimmermann, and H. Milsch. *Impact of poroelastic response of sandstones on geothermal power production. Pure Appl. Geophys.* **166** (2009), 1107–1123.

[29] L. Bodri. *Three-dimensional modelling of deep temperature and heat flow anomalies with applications to geothermics of the Pannonian basin. Tectonophysics* **79** (1981), 225–236.

[30] Bundesverband Geothermie e.V. *https://www.geothermie.de/bibliothek/lexikon-der-geothermie/r/reservoirmanagement.html, last accessed June 12, 2022*.

[31] W. Cao, S. Durucan, J.Q. Shi, W. Cai, A. Korre, and T. Ratouis. *Induced seismicity associated with geothermal fluids re-injection: Poroelastic stressing, thermoelastic stressing, or transient cooling-induced permeability enhancement? Geothermics* **102** (2022), article 102404.

[32] Z.R. Chen. *Poroelastic model for induced stresses and deformations in hydrocarbon and geothermal reservoirs. J. Pet. Sci. Eng.* **80** (2011), 41–52.

[33] A.H.D. Cheng. *Poroelasticity.* Springer, Switzerland, 2016.

[34] A.H.D. Cheng and E. Detournay. *On singular integral equations and fundamental solutions of poroelasticity. Int. J. Solid. Struct.* **35** (1998), 4521–4555.

[35] C.K. Chui. *An Introduction to Wavelets.* Academic, San Diego, 1992.

[36] C. Clauser. *Grundlagen der angewandten Geophysik – Seismik, Gravimetrie*. Springer Spektrum, Berlin, 2018.

[37] M. Conrad and J. Prestin. *Multiresolution on the sphere.* In: *Summer School Lecture Notes on Principles of Multiresolution in Geometric Moedlling*. Ed. by A. Iske, E. Quak, and M.S. Floater. Munich, 2001, 165–202.

[38] F.A. Coutelieris and J.M.P.Q. Delgado. *Transport Processes in Porous Media.* Springer, Berlin Heidelberg, 2012.

[39] S. Dahlke, W. Dahmen, E. Schmitt, and I. Weinreich. *Multiresolution analysis and wavelets on S^2 and S^3. Numer. Func. Anal. Opt.* **16** (1995), 19–41.

[40] S. Dahlke and P. Maaß. *Continuous wavelet transforms with application to analyzing functions on spheres. J. Fourier Anal. Appl.* **2** (1996), 379–396.

[41] S. Dahlke, G. Steidl, and G. Teschke. *Frames and coorbit theory on homogeneous spaces with a special guidance on the sphere. J. Fourier Anal. Appl.* **13** (2007), 387–403.

[42] B. Das. *Problems and Solutions in Thermoelasticity and Magneto-thermoelasticity.* Springer International Publishing, Cham, 2017.

[43] I. Daubechies. *Ten Lectures on Wavelets.* SIAM, Philadelphia, 1992.

[44] P.J. Davis. *Interpolation and Approximation.* Introductions to higher mathematics. Blaisdell Publishing Company, Waltham, MA, 1963.

[45] V. Dicken and P. Maaß. *Wavelet-Galerkin methods for ill-posed problems. J. Inv. and Ill-posed Probl.* **24** (1996), 203–222.

[46] D.L. Donoho. *Nonlinear solution of linear inverse problems by wavelet-vaguelette decomposition. Appl. Comp. Harm. Anal.* **2** (1995), 101–126.

[47] B.C. Dyer, U. Schanz, F. Ladner, M.O. Häring, and T. Spillman. *Microseismic imaging of a geothermal reservoir stimulation. Lead. Edge* **27** (2008), 856–869.

[48] H. Engl, M. Hanke, and A. Neubauer. *Regularization of Inverse Problems.* Kluwer, Dordrecht, 1996.

[49] H. Engl, A. Louis, and W. Rundell, eds. *Inverse Problems in Geophysical Applications.* SIAM, Philadelphia, 1997.

[50] L.C. Evans. *Partial Differential Equations.* Graduate Studies in Mathematics. AMS, Providence, Rhode Island, 1998.

[51] B. Farina, F. Poletto, and J. Carcione. *Seismic wave propagation in geothermal hot rocks: a review of simulation analysis and results based on Burgers models.* In: 79th EAGE Conference and Exhibition, Workshop, Paris, 2017, doi: 10.3997/2214–4609.201701769.

[52] E. Febrianto, M. Ortiz, and F. Cirak. *Mollified finite element approximants of arbitrary order and smoothness. Comput. Methods Appl. Mech. Eng.* **373** (2021), article 113513.

[53] R. Feng, N. Balling, and D. Grana. *Lithofacies classification of a geothermal reservoir in Denmark and its facies-dependent porosity estimation from seismic inversion. Geothermics* **87** (2020), article 101854.

[54] J. Folesky, J. Kummerow, S.A. Shapiro, M. Häring, and H. Asanuma. *Rupture directivity of fluid-induced microseismic events: Observations from an enhanced geothermal system. J. Geophys. Res. Solid Earth* **121** (2016), 8034–8047.

[55] G. Foulger. *Geothermal exploration and reservoir monitoring using earthquakes and the passive seismic method. Geothermics* **11** (1982), 259–268.

[56] H. Franzson, R. Zierenberg, and P. Schiffmann. *Chemical transport in geothermal systems in Iceland: Evidence from hydrothermal alteration. J. Volcan. Geotherm. Res.* **173** (2008), 217–229.

[57] W. Freeden. *Multiscale Modelling of Spaceborne Geodata.* B.G. Teubner, Stuttgart, Leipzig, 1999.

[58] W. Freeden. *Metaharmonic Lattice Point Theory*. Chapman & Hall Pure and Applied Mathematics. CRC Press, Taylor & Francis Group, Boca Raton, 2011.

[59] W. Freeden. *Decorrelative Mollifier Gravimetry: Basics, Ideas, Concepts, and Examples.* Geosystems Mathematics Series. Birkhäuser, Cham, 2021.

[60] W. Freeden and M. Bauer. *Dekorrelative Gravimetrie: Ein innovativer Zugang für Geowissenschaften und Exploration*. Springer Spektrum, Berlin, 2020.

[61] W. Freeden and C. Blick. *Signal decorrelation by means of multiscale methods. World Min. Surf. Undergr.* **65** (2013), 304–317.

[62] W. Freeden and C. Gerhards. *Poloidal and toroidal field modeling in terms of locally supported vector wavelets. Math. Geosci.* **42** (2010), 817–838.

[63] W. Freeden and C. Gerhards. *Geomathematically Oriented Potential Theory.* Chapman & Hall/CRC Pure and Applied Mathematics. CRC Press, Taylor & Francis Group, Boca Raton, 2012.

[64] W. Freeden, T. Gervens, and M. Schreiner. *Constructive Approximation on the Sphere. With Applications to Geomathematics.* Oxford University Press, Oxford, 1998.

[65] W. Freeden and M. Gutting. *Special Functions of Mathematical (Geo-) physics.* Birkhäuser, Basel, 2013.

[66] W. Freeden and M. Gutting. *Integration and Cubature Methods: A Geomathematically Oriented Course*. Chapman & Hall/CRC Monographs and Research Notes in Mathematics. CRC Press, Taylor & Francis Group, Boca Raton, 2018.

[67] W. Freeden and C. Mayer. *Wavelets generated by layer potentials. Appl. Comput. Harm. Anal.* **14** (2003), 195–237.

[68] W. Freeden and C. Mayer. *Multiscale solution for the Molodensky problem on regular telluroidal surfaces. Acta Geod. Geophys. Hung.* **41** (2006), 55–86.

[69] W. Freeden and V. Michel. *Multiscale Potential Theory. With Applications to Geoscience.* Birkhäuser, Boston, 2004.

[70] W. Freeden and V. Michel. *Orthogonal zonal, tesseral and sectorial wavelets on the sphere for the analysis of satellite data. Adv. Comput. Math.* **21** (2004), 181–217.

[71] W. Freeden and M.Z. Nashed. *Inverse gravimetry: background material and multiscale mollifier approaches. Int. J. Geomath.* **9** (2018), 199–264.

[72] W. Freeden and H. Nutz. *Mathematik als Schlüsseltechnologie zum Verständnis des Systems "Tiefe Geothermie". DMV Jahresbericht* **117** (2015), 45–84.

[73] W. Freeden and R. Rummel, eds. *Mathematische Geodäsie/Mathematical Geodesy: Handbuch der Geodäsie*. Springer Reference Naturwissenschaften. Springer Berlin Heidelberg, 2020.

[74] W. Freeden and M. Schreiner. *Orthogonal and non-orthogonal multiresolution analysis, scale discrete and fully discrete wavelet transform on the sphere. Constr. Appr.* **14** (1998), 493–515.

[75] W. Freeden and M. Schreiner. *Local multiscale modelling of geoid undulations from deflections of the vertical. J. Geod.* **79** (2006), 641–651.

[76] W. Freeden and M. Schreiner. *Spherical Functions of Mathematical Geosciences: A Scalar, Vectorial, and Tensorial Setup.* Advances in Geophysical and Environmental Mechanics and Mathematics. Springer Berlin Heidelberg, 2008.

[77] W. Freeden, M. Schreiner, and R. Franke. *A survey on spherical spline approximation. Surv. Math. Ind.* **7** (1996), 29–85.

[78] W. Freeden and U. Windheuser. *Spherical wavelet transform and its discretization. Adv. Comput. Math.* **5** (1996), 51–94.

[79] K.O. Friedrichs. *Die Identität schwacher und starker Erweiterungen von Differentialoperatoren. Transact. American Math. Soc.* **55** (1944), 132–151.

[80] Q. Gao and A. Ghassemi. *Three-dimensional thermo-poroelastic modeling and analysis of flow, heat transport and deformation in fractured rock with applications to a lab-scale geothermal system. Rock. Mech. Rock. Eng.* **53** (2020), 1565–1586.

[81] C. Geiger and C. Kanzow. *Theorie und Numerik restringierter Optimierungsaufgaben.* Springer-Lehrbuch Masterclass. Springer Berlin Heidelberg, 2002.

[82] C. Gerhards. *Spherical Multiscale Methods in Terms of Locally Supported Wavelets: Theory and Application to Geomagnetic Modeling.* PhD thesis. Geomathematics Group, Department of Mathematics, University of Kaiserslautern, 2011.

[83] A. Ghassemi and Q. Tao. *Thermo-poroelastic effects on reservoir seismicity and permeability change. Geothermics* **63** (2016), 210–224.

[84] E. Gómez-Díaz, S. Scott, T. Ratouis, and J. Newson. *Numerical modeling of reinjection and tracer transport in a shallow aquifer, Nesjavellir Geothermal System, Iceland. Geotherm. Energy* **10** (2022), article 7.

[85] J. Göttelmann. *Locally supported wavelets on the sphere. Z. Angew. Math. Mech.* **78** (1998), 919–920.

[86] I. Gradshtein and I. Ryshik. *Summen-, Produkt- und Integraltafeln.* Vol. 1. Harri Deutsch, Thun, 1981.

[87] D. Gross. *Bruchmechanik*. Springer, Berlin Heidelberg, 2007.

[88] M. Grothaus and T. Raskop. *Limit formulae and jump relations of potential theory in Sobolev spaces. Int. J. Geomath.* **1** (2010), 51–100.

[89] A. Haar. *Zur Theorie der orthogonalen Funktionen-Systeme. Math. Ann.* **69** (1910), 331–371.

[90] H. Harbrecht and R. Schneider. *Wavelet Galerkin schemes for boundary integral equations – implementation and quadrature. SIAM J. Sci. Comput.* **27** (2006), 1347–1370.

[91] R. Hielscher and M. Quellmalz. *Optimal mollifiers for spherical deconvolution. Inverse Probl.* **31** (2015), article 085001.

[92] J. Hinderer, M. Calvo, Y. Abdelfettah, B. Hector, U. Riccardi, G. Ferhat, and J.D. Bernard. *Monitoring of a geothermal reservoir by hybrid gravimetry; feasibility study applied to the Soultz-sous-Forêts and Rittershoffen sites in the Rhine graben. Geotherm. Energy* **3** (2015), article 16.

[93] M. Holschneider. *Continuous wavelet transforms on the sphere. J. Math. Phys.* **37** (1996), 4156–4165.

[94] L. Hörmander. *The Analysis of Linear Partial Differential Operators.* I. Springer, Berlin, Heidelberg, New York, 1990.

[95] M. Ilyasov. *A Tree Algorithm for Helmholtz Potential Wavelets on Non-smooth Surfaces: Theoretical Background and Application to Seismic Data Postprocessing.* PhD thesis. Geomathematics Group, Department of Mathematics, University of Kaiserslautern, 2011.

[96] A.B. Jacquey, M. Cacace, G. Blöcher, N. Watanabe, E. Huenges, and M. Scheck-Wenderoth. *Thermo-poroelastic numerical modelling for enhanced geothermal system performance: Case study of the Groß Schönebeck reservoir. Tectonophysics* **684** (2016), 119–130.

[97] L. Jantscher. *Distributionen.* De Gruyter Lehrbuch. De Gruyter, Berlin, New York, 2014.

[98] H.T. Jongen and O. Stein. *Smoothing by mollifiers. Part II: nonlinear optimization. J. Glob. Optim.* **41** (2008), 335–350.

[99] J. Koh, H. Roshan, and S.H. Rahman. *A numerical study on the long term thermo-poroelastic effects of cold water injection into naturally fractured geothermal reservoirs. Comput. Geotech.* **38** (2011), 669–682.

[100] C.M. Krawczyk, M. Stiller, K. Bauer, B. Norden, J. Henninges, A. Ivanoca, and E. Huenges. *3-D seismic exploration across the deep geothermal research platform Groß Schönebeck north of Berlin/Germany. Geotherm. Energy* **7** (2019), 15.

[101] A. Kunoth and J. Sahner. *Wavelets on manifolds: an optimized construction. Math. Comput.* **75** (2006), 1319–1349.

[102] V.D. Kupradze. *Three-Dimensional Problems of the Mathematical Theory of Elasticity and Thermoelasticity.* North Holland, Amsterdam, 1979.

[103] P.K. Kythe. *Fundamental Solutions for Differential Operators and Applications.* Birkhäuser, Boston, Basel, Berlin, 1996.

[104] N. Laín Fernández. *Polynomial bases on the sphere.* PhD thesis. University of Lübeck, Logos, Berlin, 2003.

[105] N. Laín Fernández. *Optimally space-localized band-limited wavelets on* $\mathbb{S}^{q-1}$. *J. Comput. Appl. Math.* **199** (2007), 68–79.

[106] A.K. Louis. *Inverse und schlecht gestellte Probleme.* Teubner Studienbücher, Stuttgart, 1989.

[107] A.K. Louis and P. Maaß. *A mollifier method for linear equations of the first kind. Inverse Probl.* **6** (1990), 427–440.

[108] A.K. Louis, P. Maaß, and A. Rieder. *Wavelets: Theory and Applications.* Wiley, Chichester, 1997.

[109] Y. Luchko and A. Punzi. *Modeling anomalous heat transport in geothermal reservoirs via fractional diffusion equations. Int. J. Geomath.* **1** (2011), 257–276.

[110] S. Mallat. *A Wavelet Tour of Signal Processing.* 3rd edition. Academic, Berlin, 2009.

[111] MATLAB. *R2020b*. Natick, Massachusetts: The MathWorks Inc., 2020.

[112] MATLAB. *R2021b*. Natick, Massachusetts: The MathWorks Inc., 2021.

[113] T. Megies and J. Wassermann. *Microseismicity observed at a non-pressure-stimulated geothermal power plant. Geothermics* **52** (2014), 36–49.

[114] T. Meidav. *Application of electrical resistivity and gravimetry in deep geothermal exploration. Geothermics* **2** (1970), 303–310.

[115] Y. Meyer. *Orthonormal Wavelets.* In: *Wavelets: Time-Frequency Methods and Phase Spaces*. Ed. by J.M. Comlees, A. Grossnan, and P. Tchamitchian. Springer, Heidelberg, 1989, 21–37.

[116] V. Michel. *Optimally localized approximate identities on the 2-sphere. Numeric. Func. Anal. Opt.* **32** (2011), 877–903.

[117] V. Michel. *Lectures on Constructive Approximation – Fourier, Spline, and Wavelet Methods on the Real Line, the Sphere, and the Ball.* Birkhäuser, New York, 2013.

[118] V. Michel. *Geomathematics: Modelling and Solving Mathematical Problems in Geodesy and Geophysics.* Cambridge University Press, Cambridge, 2022.

[119] S. Möhringer. *Decorrelation of Gravimetric Data.* PhD thesis. Geomathematics Group, Department of Mathematics, University of Kaiserslautern, 2014, Verlag Dr. Hut, Munich, 2014.

[120] C. Müller. *Spherical Harmonics.* Springer, Berlin, Heidelberg, 1966.

[121] C. Müller. *Foundations of the Mathematical Theory of Electromagnetic Waves.* Springer, Berlin, 1969.

[122] G. Muñoz, K. Bauer, I. Moeck, A. Schulze, and O. Ritter. *Exploring the Groß Schönebeck (Germany) geothermal site using a statistical joint interpretation of magnetotelluric and seismic tomography models. Geothermics* **39** (2010), 35–45.

[123] F.J. Narcowich and J.D. Ward. *Nonstationary wavelets on the m-sphere for scattered data. Appl. Comput. Harm.* **3** (1996), 324–336.

[124] W. Nowacki. *Thermoelasticity.* 2nd edition. Pergamon Press, Oxford, New York, 1986.

[125] R. Ortiz, A. E., R. Jung, and J. Renner. *Two-dimensional numerical investigations on the termination of bilinear flow in fractures. Solid Earth* **4** (2013), 331–345.

[126] I. Ostermann. *Three-dimensional modeling of heat transport in deep hydrothermal reservoirs. Int. J. Geomath.* **2** (2011), 37–68.

[127] J. Pogacnik, D. Elsworth, M. O'Sullivan, and J. O'Sullivan. *A damage mechanics approach to the simulation of hydraulic fracturing/shearing around a geothermal injection well. Comput. Geotech.* **71** (2016), 338–351.

[128] D. Potts and M. Tasche. *Interpolatory wavelets on the sphere.* In: *Approximation Theory VIII*. Ed. by C.K. Chui and L.L. Schumaker. Vol. 2. World Scientific, Singapore, 1995, 335–342.

[129] R.M. Prol-Ledesma and D.J. Morán-Zenteno. *Heat flow and geothermal provinces in Mexico. Geothermics* **78** (2019), 183–200.

[130] K. Pruess. *Numerical simulation of 'multiphase tracer transport in fractured geothermal reservoirs. Geothermics* **31** (2002), 475–499.

[131] W. Rabbel, M. Thorwart, R. Behrendt, N. Holzrichter, J. Niederau, A. Ebigo, G. Marquart, I. Dini, and S. Ciuffi. *A stochastic assessment of geothermal potential based on seismic and potential field analysis and hydro-thermal forward modeling – an example from Tuscany (Italy).* In: Proceedings World Geothermal Congress, Melbourne, 2015, https://pangea.stanford.edu/ERE/db/WGC/papers/WGC/2015/13078.pdf, last accessed June 12, 2022.

[132] C. Rawal and A. Ghassemi. *A reactive thermo-poroelastic analysis of water injection into an enhanced geothermal reservoir. Geothermics* **50** (2014), 10–23.

[133] J. Rutqvist and O. Stephansson. *The role of hydromechanical coupling in fractured rock engineering. Hydrogeol.* **11** (2003), 7–40.

[134] R. Safari and A. Ghassemi. *3D thermo-poroelastic analysis of fracture network deformation and induced micro-seismicity in enhanced geothermal systems. Geothermics* **58** (2015), 1–14.

[135] M. Schanz. *Application of 3D time domain boundary element formulation to wave propagation in poroelastic solids. Eng. Anal. Bound. Elem.* **25** (2001), 363–376.

[136] T. Schuster. *An efficient mollifier method for three-dimensional vector tomography: convergence analysis and implementation. Inverse Probl.* **17** (2001), 739–766.

[137] T. Schuster. *A novel mollifier inversion scheme for the Laplace transform.* In: Proc. Appl. Math. Mech., 2002, 422–423.

[138] S.W. Scott, C. Covell, E. Júliússon, Á. Wavfells, J. Newson, B. Hrafnkelsson, H. Pálsson, and M. Gudjónsdóttir. *A probabilistic geologic model of the Krafla geothermal system constrained by gravimetric data. Geotherm. Energy* **7** (2019), 29.

[139] A.P.S. Selvadurai and A.P. Suvorov. *Thermo-Poroelasticity and Geomechanics.* Cambridge University Press, Cambridge, 2017.

[140] D. Smith and J. Booker. *Green's functions for a fully coupled thermo-poroelastic material. Int. J. Numer. Anal. Methods Geomech.* **17** (1993), 139–163.

[141] M. Sugihara and T. Ishido. *Geothermal reservoir monitoring with a combination of absolute and relative gravimetry. Geophysics* **73** (2008), WA37–WA47.

[142] W. Sweldens. *The lifting scheme: a construction of second generation wavelets. SIAM J. Math. Anal.* **29** (1997), 511–546.

[143] A. Tanaka, M. Yamano, Y. Yano, and M. Sasada. *Geothermal gradient and heat flow data in and around Japan (I): Appraisal of heat flow from geothermal gradient data. Earth Planets Space* **56** (2004), 1191–1194.

[144] J. Tanner. *Optimal filter and mollifier for piecewise smooth spectral data. Math. Comput.* **75** (2006), 767–790.

[145] J. Taron and D. Elsworth. *Thermal–hydrologic–mechanical–chemical processes in the evolution of engineered geothermal reservoirs. Int. J. Rock Mech. Min. Sci.* **46** (2009), 855–864.

[146] C. Vinci, J. Renner, and H. Steeb. *On attenuation of seismic waves associated with flow in fractures. Geophys. Res. Lett.* **41** (2014), 7515–7523.

[147] H.F. Wang. *Theory of Linear Poroelasticity with Applications to Geomechanics and Hydrogeology.* Princeton University Press, Princeton, 2000.

[148] X. Wang and A. Ghassemi. *A 3D thermal-poroelastic model for naturally fractured geothermal reservoir stimulation. GRC Transactions* **36** (2012), 575–582.

[149] Y. Wang and M. Oberguggenberger. *Nonlinear parabolic equations with regularized derivatives. J. Math. Anal. Appl.* **233** (1999), 644–658.

[150] I. Weinreich. *A construction of C^1-wavelets on the two-dimensional sphere. Appl. Comput. Harm. Anal.* **10** (2001), 1–26.

[151] Y. Wiaux, J.D. McEwen, P. Vandergheynst, and O. Blanc. *Exact reconstruction with directional wavelets on the sphere. Mon. Not. R. Astron. Soc.* **388** (2008), 770–788.

[152] U. Windheuser. *Sphärische Wavelets: Theorie und Anwendung in der Physikalischen Geodäsie.* PhD thesis. Geomathematics Group, Department of Mathematics, University of Kaiserslautern, 1995.

[153] Y.S. Wu and K. Pruess. *A 3-D hydrodynamic dispersion model for modeling tracer transport in geothermal reservoirs.* In: Proc. 23rd Workshop on Geoth. Res. Eng., Stanford University, 1998, 139–146.

[154] A. Zang, V. Oye, P. Jousset, N. Deichmann, R. Gritto, A. MCGarr, E. Maher, and D. Bruhn. *Analysis of induced seismicity in geothermal reservoirs – An overview. Geothermics* **52** (2014), 6–21.

[155] X.X. Zhou, A. Ghassemi, and A.H.D. Cheng. *A three-dimensional integral equation model for calculating poro- and thermoelastic stresses induced by cold water injection into a geothermal reservoir. Int. J. Numer. Anal. Methods Geomech.* **33** (2009), 1613–1640.

[156] R.W. Zimmerman. *Coupling in poroelasticity and thermoelasticity*. *Int. J. Rock Mech. Min. Sci.* **37** (2000), 79–87.

[157] V.V. Zubkov, V.F. Koshelev, and A.M. Lin'kov. *Numerical modeling of hydraulic fracture initiation and development. J. Min. Sci.* **43** (2007), 40–56.

Index

α, 39
$\alpha(x)$, 25
$\alpha(x,t)$, 124
$\mathbb{B}_r^n(x)$, 9
$\mathcal{B}$, 10
$\mathfrak{B}_\tau(x)$, 123
C_3, 60
C_1, 60
$\mathrm{C}^{(k)}(X)$, 14
$\mathrm{C}_0^{(k)}(X)$, 14
$\mathrm{C}_\Lambda^{(k)}(\mathbb{R}^q)$, 32
c_0, 58
$\mathbb{C}$, 9
$*$, 15
$\mathrm{CP}_1^{(2m)}(\lambda,\mathbb{R}^q)$, 33
$\mathrm{CP}_2^{(2m)}(\varepsilon,\lambda,\mathbb{R}^q)$, 33
C_4, 60
C_2, 60
Δ, 11
δ_{nm}, 11
$\Delta^\wedge(h)$, 32
δ_a, 22
$\mathcal{D}'(X)$, 22
D^ν, 19
E_0, 12
E_1, 11
Ei, 11
erf, 12
$.^{\mathrm{Fc}}$, 50
$\mathcal{F}_\Lambda$, 29
$F_\Lambda^\wedge(h)$, 33
$.^{\mathrm{fpc}}$, 50
$.^{\mathrm{fsc}}$, 49
$\boldsymbol{G}(x,t)$, 93
Γ, 10
$\boldsymbol{G}_\tau$, 93
$.^{\mathrm{hpc}}$, 50
$.^{\mathrm{hsc}}$, 46
$\langle\cdot,\cdot\rangle_{\mathrm{L}^2(\mathcal{B})}$, 15
$\mathrm{L}_\Lambda^p(\mathbb{R}^q)$, 32
Λ, 29
Λ^{-1}, 31
$\lambda,\ \mu$, 39
$\mathcal{L}_\Lambda^p(\mathbb{R}^q)$, 32
$\mathcal{L}^p(\mathcal{B})$, 14
$\mathrm{L}^p(\mathcal{B})$, 15
L^{pe}, 60
∇, 10
$\mathbb{N}$, 9
$\mathcal{N}_\Lambda^p(\mathbb{R}^q)$, 32
$\|\cdot\|_{\mathrm{L}^p(\mathcal{B})}$, 15
$\|\ \mathcal{F}_\Lambda\ \|$, 29
$\|\cdot\|_{\mathrm{L}_\Lambda^p(\mathbb{R}^q)}$, 32
$\|\cdot\|_\infty$, 15
$\mathcal{N}^p(\mathcal{B})$, 15
ν_y, 25
ω_n, 23
$\varphi_{t_0}(t)$, 105
Φ_τ, 67
$\boldsymbol{\Phi}_\tau$, 93
$\mathcal{P}_{\boldsymbol{\Phi}_{\tau_j}}[\cdot]$, 28
Ψ_{ik,τ_j}, 102
$\mathbb{R}$, 9
$\mathcal{R}_{\boldsymbol{\Phi}_{\tau_j}}[\cdot]$, 28
s, 41
σ_{ij}, 41
$\mathbb{S}_r^{n-1}(x)$, 9
$\vartheta^{(q)}$, 34

$\mathcal{T}_{\mathrm{lin}}(x)$, 17
$\mathfrak{T}_{t_0}(t)$, 124
$\mathcal{T}_X$, 17
$\mathrm{vol}(\mathcal{B})$, 10
$\mathcal{V}_{\mathbf{\Phi}_{\tau_j}}$, 28
$\boldsymbol{V}_{\mathbf{\Phi}_\tau}$, 105
$\mathcal{W}_{\mathbf{\Phi}_{\tau_j}}$, 28
$\mathbb{Z}$, 9
ζ, 41, 60

approximate identity
  definition, 26
  poroelasticity, 111

ball, 9
band-pass filter, 28
Biot decomposition
  thermoporoelasticity, 45
Biot-Willis constant, 39

Cauchy-Navier equations, *see* linear elasticity equations
compact support, 14
constraint qualification
  Abadie, 17
convolution, 15
  with distribution, 23
cubature formula, 35
  poroelasticity, 131

data sets, 131
decomposition, 27
Delta distribution, *see* Dirac distribution
detail-space, 28
diffusion equation, *see* heat equation
Dirac distribution, 22
distribution, 21
  convolution with, 23
  regular, 22
  singular, 22
divergence, 10
dual lattice, *see* inverse lattice

eigenfunction, 32
eigenvalue, 32
error function, 12
exponential integral, 11

filter
  band-pass filter, 28
  low-pass filter, 28
fluid content change, 60
Fourier coefficients, 33
fundamental cell, 29
  volume, 29
fundamental solution
  definition, 22
  heat, 23
  Laplace, 23
  linear elasticity, 23
  poroelasticity
    homogeneous, 62
    inhomogeneous, 61
  Stokes, 23
  thermoporoelasticity, 44
    continuous fluid and heat dipole, 50
    continuous fluid source, 49
    continuous force, 50
    continuous heat source, 46

Gamma function, 10
Gauss error function, *see* error function
gradient, 10

Haar scaling function, 105
heat equation, 21

inverse lattice, 31

Karush-Kuhn-Tucker conditions, 16
Kronecker delta, 11

Lagrange
  function, 16
  multiplier, 16
Λ-periodic function, 31
Lamé constants, 21
Laplace operator, 11

Laplace's equation, 21
lattice, 29
linear elasticity equations, 21
low-pass filter, 28

material constants, 60
mollification
  p^{Si}, 81
  p^{St}, 72
  u^{CN}, 76
  u^{Si}, 85
  general function, 69
  Laplace, 66
  radially symmetric function, 68
multiscale representation, 28

optimization problem, 16

partial differential equation
  definition, 19
  elliptic, 19
  heat, 21
  hyperbolic, 20
  Laplace, 21
  linear elasticity, 21
  parabolic, 20
  poroelasticity
    dimensionless, 58
  Stokes, 21
  thermoporoelasticity
    coupled, 40
    dimensionless, 58
    uncoupled, 44
PDE, *see* partial differential equation
Poisson summation formula, 33
poroelastic differential operator, 60

region, 10
regular region, 10
RMSE, *see* root mean square error
root mean square error
  definition, 135
  plot area, 136
  whole area, 136

scale-space, 28
scaling function, 25
  with time component, 26
solid angle
  3-dim. cube, 26
  definition, 25
  with time component, 124
source scaling function
  Laplace, 67
  poroelasticity, 99
sphere, 9
Stokes equations, 21
summation formula, 35

Theta function
  definition, 34
  functional equation, 35

unit normal vector, 25

volume, 10
  fundamental cell, 29

wavelet function, 27
wavelets
  poroelasticity, 102